Regulation of Hepcidin and Hemojuvelin Expression and Their Role in Iron Homeostasis

Thesis submitted by

Mohamed Fouda Ibrahim Salama

For the Degree of

Doctor of Philosophy in Biochemistry and Molecular Biology

Research Department of Structural and Molecular Biology

University College London

Gower Street, London, WC1E 6BT, UK

London
2010

Declaration

I, **Mohamed Fouda Ibrahim Salama**, declare that all work presented in this thesis is the result of my own work. Where information has been derived from other sources, I confirm that this has been indicated in the thesis. The work herein was carried out while I was a graduate student at the University College London, Research Department of Structural and Molecular Biology under the supervision of Professor Kaila Srai.

Abstract

Hepcidin is the key regulator of iron homeostasis acting as a negative regulator of intestinal iron absorption. Several proteins have recently been identified to act as upstream regulators of hepcidin expression, such as HFE and hemojuvelin (HJV). Although hepcidin is regulated by iron, the molecules involved in this regulation and whether HFE is involved in this regulation remain to be clarified. The aims of this study were to investigate the molecules involved in hepcidin regulation by iron and the role played by HFE in this regulation, to understand the regulation of *hepcidin* and *HJV* expression during inflammation, and finally to investigate the possible role of upstream stimulatory factors (USFs) in the regulation of *HJV* expression.

Wild type and *HFE* KO animal models were used to investigate the regulation of *hepcidin* by iron *in vivo*; the same animal models and *in vitro* studies were conducted to study the regulation of *hepcidin* and *HJV* expression during inflammation. A possible regulation of *HJV* by USFs was also examined *in vitro* and *in vivo* using ChIP assay.

In this study, it was found that iron regulates the expression of *BMP-6*, for which *HJV* acts as a co-receptor, and phosphorylation of SMADs 1/5/8 in the liver which in turn may regulate *hepcidin* gene expression in response to different iron status. Moreover, HFE seems to be involved in the regulation of downstream signalling of BMP-6 that regulates *hepcidin* expression in response to iron loading.

It was also found that the pro-inflammatory cytokines regulate *hepcidin* and *HJV* expression differently during inflammation. TNF-alpha seems to act directly on HJV to suppress its transcription possibly via a TNFRE within the *HJV* promoter, while IL-6 induces *hepcidin* expression via STAT3 signalling. In addition, acute inflammation studies in mice showed that although *hepcidin* expression is upregulated as a result of inflammation, *HJV* and *BMP* expression is selectively repressed in the liver suggesting a crucial requirement for the downregulation of

these genes in order to induce *hepcidin* during inflammation *in vivo*. However, this response seems to be HFE-independent.

Finally, the study showed an interaction between USFs and the *HJV* promoter both *in vitro* and *in vivo* suggesting that USFs are important for the regulation of *hemojuvelin* expression, and further strengthen the link between these transcription factors and iron metabolism.

For

My parents, Amira, Omar, and Faris

Acknowledgements

The work presented in this thesis was carried out in the Department of Structural and Molecular Biology, University College London, London, UK. I am indebted to the Egyptian Cultural and Educational Bureau (ECEB) in London for their generous financial support that allowed me to undertake my PhD studies and without which this work could not have been performed.

First, I would like to express my sincere gratitude to Prof. Kaila Srai for his supervision, continuous support, and advice during the course of my thesis. It was great pleasure for me to work with Kaila and I have learnt a lot from him. I would also like to thank Dr. Jill Norman, my subsidiary supervisor for her help and advice during my studies.

I would also like to thank all members of our research group. In particular, I would like to thank Dr. Henry Bayele and Dr. Sara Balesaria for their support, advice, and help in learning of techniques at the beginning of my research. I would also like to thank Rumeza Hanif for her friendly support and good company over the past four years.

I would like to express my deep gratitude to my parents to whom I owe all what I have learnt in my life.

Last but by no means least, I would like to thank my wife, Amira and my lovely kids, Omar & Faris for their love, support, and the help they have given me. Thanks Amira for your patience, support, positive attitude at all times, and for always being there.

Results shown in this thesis were presented in the following meetings:

Salama MFI, Bayele HK, Srai SK. Regulation of hemojuvelin (HJV) during inflammation. European Iron Club, Saint Gallen, Switzerland, 17-19 September 2008. Poster presentation.

Salama MFI, Bayele HK, Srai SK. Upstream stimulatory factors (usf-1/usf-2) regulate human hemojuvelin gene expression. International BioIron Conference, Porto, Portugal, 7-11 June 2009. Poster presentation.

Salama MFI, Bayele HK, Srai SK. Upstream stimulatory factors (usf-1/usf-2) regulate human hemojuvelin gene expression. Physiological Society Meeting, University of Newcastle, UK, 6-8 September 2009. Poster presentation.

Contents

Index of Figures and Tables

Abbreviations

aa	Amino acid
AdML	Adenovirus major late promoter
AI	Anaemia of inflammation
apo TF	Apotransferrin
APS	Ammonium persulphate
ATP	Adenosine triphosphate
BCA	Bicinchoninic acid
b-HLH-LZ	Basic helix-loop-helix leucine zipper
BMP	Bone morphogenic proteins*
BMP-RE	BMP-responsive element
bp	Base pair
BPS-T	Phosphate buffered saline containing 0.05% Tween-20
BSA	Bovine serum albumin
Caco-2	Human intestinal epithelial cells
cDNA	Complementary DNA
ChIP	Chromatin-immunoprecipitation
Cp	Ceruloplasmin*
Ct	Cycle threshold
C-terminal	Carboxyl terminal
Dcytb	Duodenal cytochrome b*
DEPC	Diethylpyrocarbonate
DMEM	Dulbecco's Modified Eagle's Medium
DMT1	Divalent Metal Transporter 1*
DMT1+IRE	Divalent Metal Transporter 1 with an iron response element
DMT1-IRE	Divalent Metal Transporter 1 without an iron response element
DNA	Deoxyribonucleic acid
dNTP	Deoxyribonucleotide 5'-triphosphate
dsDNA	Double stranded deoxyribonucleic acid
DTT	Dithiothreitol
ECL	Enhanced chemiluminescence system
EDTA	Ethylenediaminetetraacetic acid
EMSA	Electrophoretic mobility shift assay
EPO	Erythropoietin
ER	Endoplasmic reticulum
ERK1/ERK2	Signal-regulated kinases 1/2
FBS	Foetal bovine serum

FBXL5	F-box and leucine-rich repeat protein 5
Fe	Iron
Fe^{2+}	Ferrous iron
Fe^{3+}	Ferric iron
GDF15	Growth differentiation factor 15
GPI	Glycosylphosphatidylinositol
HAMP	The hepcidin gene
Hamp1$^{-/-}$	*Hamp1* knockout
H-chain (ferritin)	Heavy chain
HCP1	Haem carrier protein 1
HEK 293	Human embryonic kidney cells
HFE	Haemochromatosis protein*
HFE$^{-/-}$	*HFE* knockout
HH	Hereditary haemochromatosis
HIF	Hypoxia inducible factor
HJV	Hemojuvelin*
HJV$^{-/-}$	*HJV* knockout
HL	Hepatic lipase
HO1	Haem oxygenase 1
Hp	Hephaestin*
HRP	Horseradish peroxidase
IgG	Immuno globulin
IL-1	Interleukin 1
IL-6	Interleukin 6*
IPTG	Isopropyl β-D-1-thiogalactopyranoside
IRE	Iron response element
IREG1	Iron-regulated transporter-1*
IRP	Iron- regulatory protein
JAK	Janus kinase
JH	Juvenile haemochromatosis
kb	Kilo base
kDa	Kilo Dalton
Kg	Kilogram
L	Litre
LB	Luria broth
L-chain (ferritin)	Light chain
LEAP-1	Liver Expressed Antimicrobial Peptide-1
LPS	Lipopolysaccharide

M	Molar
mA	Milli amps
MAPK	Mitogen-activated protein kinase
mg	Milligrams
MHC	Major histo compatability
m-HJV	Membrane-bound hemojuvelin
min	Minute
mL	Millilitre
mRNA	Messenger ribonucleic acid
MTP1	Metal Transporter Protein-1
n	Sample size
ng	Nanogram
nm	Nanometre
nM	Nanomolar
Nramp2	Natural resistance-associated macrophage protein 2
NTBI	Non transferrin bound iron
N-terminal	Amino terminal
ORF	Open reading frame
PBS	Phosphate buffered saline
PCR	Polymerase chain reaction
PHD	Prolyl hydroxylase
PHZ	Phenyl hydrazine
pmol	Pico mole
ppm	Part per million
PVDF	Polyvinylidene Fluoride
RE	Reticulo endocyte
RGM	Repulsive guidance molecules
RIPA buffer	Radioimmunoprecipitation assay buffer
RNA	Ribonucelic acid
rpm	Revolutions per minute
R-Smads	Receptor-activated Smads
SDS	Sodium deoxycholate
SDS-PAGE	Sodium dedocyl sulphate Polyacrylamide Gel Electrophoresis
SEM	Standard error of the mean
s-HJV	Soluble hemojuvelin
sla	Sex-linked anaemia
SMAD	Mothers against decapentaplegic
SMAD4	Common mediator SMAD*

SP	Signal peptide
ssDNA	Single stranded deoxyribonucleic acid
STAT	Signal transducer and activator of transcription
STEAP	Six-transmembrane epithelial antigen of prostate protein
STEAP3	The epithelial antigen of prostate 3
sTFR	Soluble TFR
TAE	Tris-acetate-EDTA
TBI	Transferrin bound iron
TE	Tris-EDTA
TEMED	3,3',5,5'-tetramethyl-ethylenediamine
TF	Transferrin*
TFR1	Transferrin receptor 1*
TFR2	Transferrin receptor 2*
TFR2$^{-/-}$	*TFR2* knockout
TGF-β	Transforming growth factor-β*
TIBC	Total iron binding capacity
TM	Transmembrane domain
TNF-α	Tumour necrosis factor- α*
UIBC	Unsaturated Iron-Binding Capacity
USF	Upstream stimulatory factor*
UTR	Untranslated region of an mRNA transcript
UV	Ultra violet
VHL	von Hippel-Lindau tumour suppressor
VWF	von Willebrand factor
ZIP14	Zrt-Irt-like protein 14*
β_2m	β_2-microglobulin*
μg	Microgram
μM	Micromolar
3'	3 prime terminal
3D	Three dimensional
5'	5 prime terminal

*if written in *italics* name refers to the gene.

Chapter 1: General Introduction

1.1 Importance of iron

Following oxygen, silicon, and aluminium, iron is the fourth most bountiful constituent in the Earth's crust. Iron is renowned to be an indispensable element for all living organisms apart from a few bacterial species (Neilands 1974; Stubbe 1990). Iron is fundamental for different biological processes such as the synthesis of DNA, RNA, and proteins, electron transport, cellular respiration, cell proliferation and differentiation, and regulation of gene expression (Andrews1999; Boldt 1999; Conrad et al. 1999; Gerlach et al. 1994; Wessling-Resnick 1999). It also forms the active centre of important enzymes, including aconitase (Jordanov et al. 1992) and ribonucleotide reductase (Uppsten et al. 2004). Moreover, it acts as a co-factor for haem-containing enzymes (Lieu et al. 2001), and cytochromes of the electron transport chain as well as oxygen transport to tissues through haemoglobin (Winfield, 1965).

Iron exists in two forms, ferrous (Fe^{2+}) and ferric (Fe^{3+}) states. The redox potential of iron makes it able to generate highly toxic free radicals in the presence of oxygen derivatives from Fe^{2+} and Fe^{3+} via Fenton's reaction (Imlay and Linn 1988; Halliwell 1994; Stadtman and Wittenberger 1985). To abrogate the toxic effects of free iron, iron is usually bound to Fe-binding proteins, such as transferrin (TF) and ferritin (Richardson and Ponka 1997; Sahlstedt et al. 2002).

1.2 Iron Distribution

The body iron content depends on nutrition, gender, and general health condition. Iron represents approximately 35 and 45 mg/kg of body weight in adult women and men, respectively (Andrews 1999; Bothwell et al. 1995). About 60-70% of total body iron (~ 1800 mg) is integrated into haemoglobin of circulating red blood cells and about 300 mg in erythroid precursor cells in the bone marrow (Figure 1.1). In

addition, about 30% of body iron is stored as ferritins and haemosidrins in liver cells (~ 1000 mg) and reticuloendothelial macrophages (~ 600 mg). Another 10% of essential body iron (~ 300 mg) is incorporated into myoglobins, cytochromes, and iron-containing enzymes, amounting to no more than 4–8 mg of iron (Conrad et al. 1999).

In the balanced physiological state, 1-2 mg of dietary iron is absorbed each day, which is adequate to reimburse the daily losses (Cook et al. 1973) (Figure1.1). The amount of dietary iron absorption is tightly regulated, as there is no iron excretory mechanism in humans and only a very small amount of iron is excreted in faeces and urine (Green et al. 1968; Miret et al. 2003). In addition, approximately 1-2 mg/day of iron is lost from the body by skin sloughing, and menstruation (Demaeyer 1980). Iron homeostasis is maintained by a firm control at the sites of iron uptake (duodenum), storage (liver), recycling (reticuloendothelial macrophages), and use (erythroid precursor).

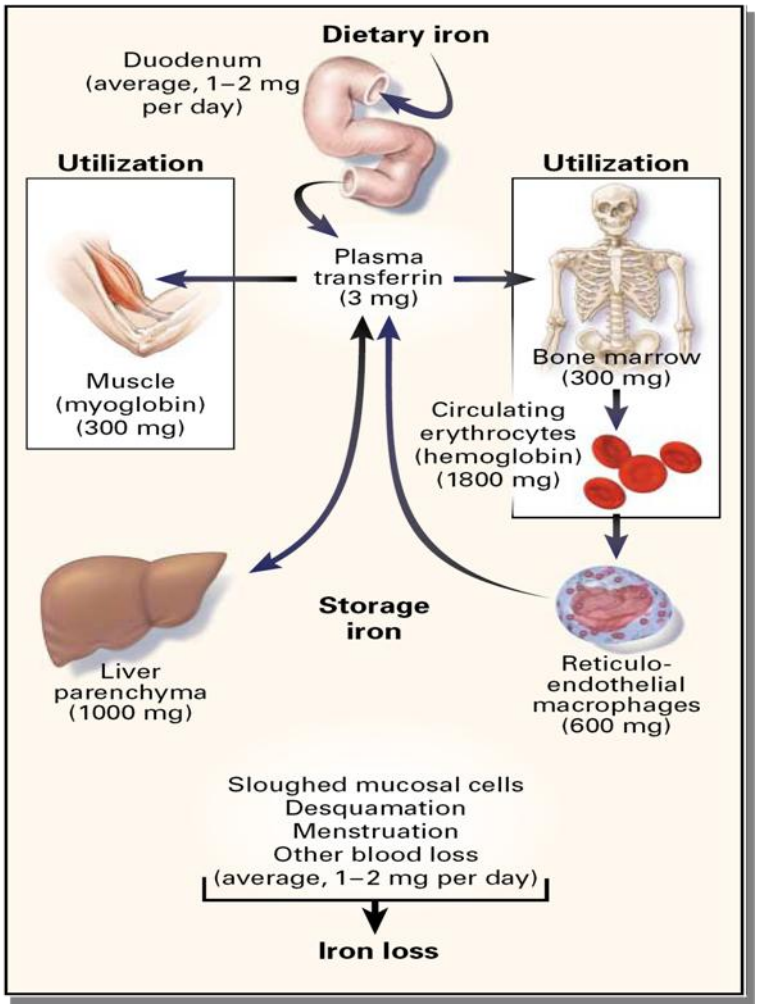

Figure 1.1 Distribution of iron in adults.

Dietary iron is absorbed by duodenum into the plasma. Most of the iron is incorporated into haemoglobin of the red blood cells in the bone marrow, which are then released into the circulation. Senescent red blood cells are engulfed by macrophages, which recycle iron into the circulation. Iron is stored in parenchymal cells of the liver and reticuloendothelial macrophages. Adapted from (Andrews, 1999).

1.3 Duodenal Iron absorption

The duodenum is the primary site of iron uptake in mammals (Duthie 1964; Johnson et al. 1983; Wheby et al. 1964). The duodenal lumen is covered by finger-like projections (villi) that increase the absorptive surface area of the duodenum (brush border).

Unlike in other nucleated cells, there are no transferrin receptors (TFRs) in the lumenal surface of absorptive enterocytes (Parmley et al. 1985; Pietrangelo et al. 1992). Thus, iron must enter these cells via a mechanism that is dissimilar to the conventional transferrin (TF)-TFR pathway.

Dietary iron exists in two forms, haem (from meat) and non-haem (from plant and dairy products). In humans, haem iron is more efficiently absorbed than non-haem iron and accounting for 20-30% of the absorbed iron (Bothwell and Charlton 1979); though haem iron represents a lesser fraction of dietary iron (~10-15%) (Carpenter and Mahoney 1992). The duodenal iron uptake of haem and non-haem iron occurs by different mechanisms (Siah et al. 2005), being different in the initial uptake step. Once inside the enterocyte, iron from each source then enters low molecular weight iron pools and is transferred across the basolateral border of the enterocyte to the blood via a common pathway (Forth and Rummel 1973; Peters et al. 1988).

Haem iron enters the cell as an intact iron-protoporphyrin complex (Conrad et al. 1966; Wyllie and Kaufman 1982; Parmley et al. 1981), possibly by endocytosis or by a recently identified haem receptor on the brush border of enterocytes, haem carrier protein 1 (HCP1) (Shayeghi et al. 2005). Then it is likely to be cleaved by intracellular microsomal enzyme, haem-oxygenase 1 (HO1) to release ferrous iron and form biliverdin (Raffin et al. 1974).

Non-haem iron exists in the forms of Fe^{2+} and Fe^{3+} salts. Most Fe^{2+} iron remains soluble even at pH7 and Fe^{3+} iron becomes insoluble at physiological pH (values above 3) (Moore et al. 1944; Brise and Hallberg 1962); consequently, absorption of

Fe^{2+} iron salts is more efficient than absorption of Fe^{3+} iron salts. However, most dietary non-haem iron is in the form of Fe^{3+} iron, thus the reduction of Fe^{3+} iron becomes compulsory for competent dietary iron absorption (Conrad et al. 1999).

1.3.1 Molecular mechanisms of duodenal iron uptake (Figure 1.2)

Different molecules involved in duodenal non-haem iron uptake are described in detail below.

1.3.1.1 Dcytb

In the intestinal lumen, the reduction of Fe^{3+} is mediated by a mucosal ferrireductase Duodenal cytochrome b (Dcytb) that is present on the apical surface of the duodenum (Raja et al. 1992; Riedel et al. 1995). This role of Dcytb is supported by its high expression levels at the apical surface of enterocytes and its reductase property (McKie et al. 2001). Both Dcytb mRNA and protein levels are reduced in iron overload, and are increased in iron deficiency and hypoxia when iron absorption increases (Collins et al. 2005, McKie et al. 2001).

The inhibition of ferrireductase activity in intestinal cells has been shown to diminish iron absorption (Han et al. 1995; Nunez et al. 1994). On the other hand, it was recently shown that disruption of mouse Dcytb had no effect on intestinal iron absorption (Gunshin et al. 2005), suggesting the existence of an alternative ferrireductase. Ohgami et al. (2006) showed that members of six-transmembrane epithelial antigen of prostate protein (STEAP) have ferrireductase activity and could be a surrogate for Dcytb.

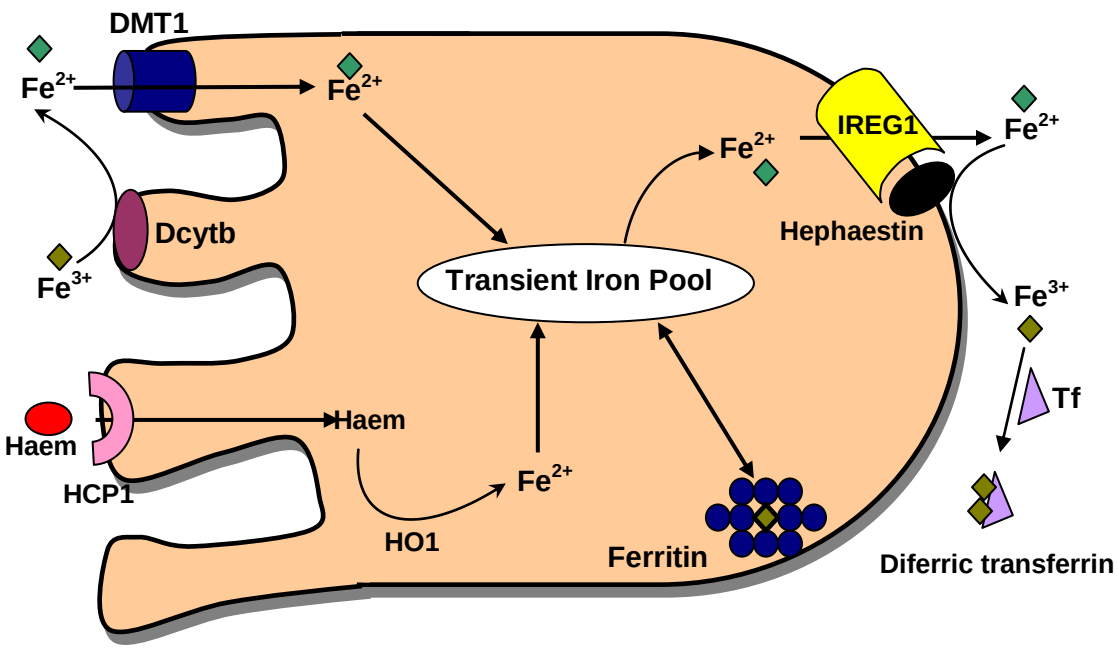

Figure 1.2 Iron absorption by the enterocyte.

Non-haem iron is transported across the brush border via divalent metal transporter 1 (DMT1) after being reduced into Fe^{+2} by duodenal cytochrome b (Dcytb). Haem carrier protein 1 (HCP1) mediates haem iron uptake into the cells, iron is then released by haem oxygenase-1 (HO1). Inside the cell, iron can either be stored as ferritin or be exported through the basolateral membrane to the blood by IREG1. In the blood, iron is oxidised by hephaestin then circulates in the blood bound to transferrin (TF). Modified from (Chua et al. 2007).

1.3.1.2 DMT1

Following reduction by Dcytb, Fe^{2+} iron transport across the brush border is mediated by a divalent cation transporter, termed natural resistance-associated macrophage protein 2 (Nramp2) or divalent metal transporter 1 (DMT1) (Fleming et al. 1997; Gunshin et al. 1997, Tandy et al. 2000). DMT1 mRNA is ubiquitously expressed in most tissues and cell types, being higher in brain, proximal intestine and thymus, kidney, and bone marrow (Gunshin et al. 1997). Furthermore, its hepatic expression has been also reported (Trinder et al. 2000). There are two splice isoforms of DMT1 which differ at their C-terminal end. One contains an iron responsive element (IRE) within its 3'-UTR (DMT1+IRE), while the other isoform lacks this element (DMT1-IRE) (Fleming et al. 1997; Gunshin et al. 1997; Tabuchi et al. 2000). Only DMT1+IRE is regulated by iron levels in human cell culture and in the intestine (Zoller et al. 1999; Canonne-Hergaux et al. 1999; Byrnes et al. 2002). Two additional splice variants of exon 1 have recently been reported that differ at their N-terminal end (Hubert and Hentze 2002); however, these isoforms are not well characterised.

The role of DMT1 in iron uptake was underscored by the effects observed with DMT1 mutations in two rodent models of iron deficiency anaemia, namely the microcytic anaemia mouse and the Belgrade rat (Fleming et al. 1997; 1998). Both rodent models are characterised by iron deficiency due to impaired iron uptake by the intestine and other tissues (Edwards and Hoke 1972; Fleming et al. 1998). The DMT1 mutation in microcytic anaemia mice leads to incorrect localisation of the protein to the plasma membrane (Canonne-Hergaux et al. 2000).

Gunshin and coworkers (2001) showed that in hepatic (Hep3B) and intestinal (CaCo2) cell culture, increased cellular iron was associated with a decrease in DMT1 mRNA levels while expression levels increased when cells were iron deficient. This regulation occurs through binding of iron response proteins (IRPs) to

the IRE which protects the mRNA from endocytic cleavage, increasing mRNA half-life and consequently translated protein (Casey et al. 1988).

On the contrary, the expression of DMT1-IRE is not regulated by cellular iron (Canonne-Hergaux et al. 1999, Gunshin et al. 2001).

1.3.1.3 Ferritin

In the enterocyte, surplus Intracellular iron can either be stored as ferritin (Torti and Torti 2002), or transferred across the basolateral membrane of the enterocyte to the plasma. Ferritin is ubiquitously expressed and its main function is to store and sequester excess iron in a soluble, non-toxic form (Theil 1983; Theil 1990).

Ferritin is composed of a spherical protein shell of 24 subunits of two types, light (L) and heavy (H) chains with a central cavity able to store up to 4500 iron atoms in the form of hydrous ferric oxide phosphate (Mann et al. 1986; Theil, 1983; Thiel, 1990). Both chains have the same 3D structure and share 50% sequence identity; however, they have different surface charges which give them different properties (Arosio et al. 1978; Harrison and Arosio 1996). L-chain is important for core iron binding, while H-chains confer ferroxidase activity required for iron incorporation (Levi et al. 1988; Levi et al. 1992).

The 5' UTR of ferritin mRNA contains an IRE (Huang et al. 1999). During iron deficiency, IRPs bind to IRE and block translation; therefore increasing cellular iron availability. Ferritin is also regulated by cytokines, such as interleukin (IL)-6 and -1 as well as interferon-γ (Wei et al. 1990; Fahmy and Young 1993). Due to its iron sequestering capacity, ferritin seems to have an anti-oxidant function (Theil 2003). Ferritin has been also detected in the plasma; however, Linder et al. (1996) recognized a number of differences between tissue and plasma ferritin, suggesting that they might be encoded by different genes. Serum ferritin is commonly used to

diagnose iron deficiency anaemia and hereditary haemochromatosis (iron overload) (Beutler et al. 2003).

1.3.1.4 IREG1

IREG1 (Iron-regulated transporter-1), also known as ferroportin1, Slc40a1, and MTP1 (Metal Transporter Protein-1) was shown by three laboratories to be the putative basolateral iron exporter (Donovan et al. 2000; McKie et al. 2000; Abboud and Haile 2000).

IREG1 was found to be expressed in basolateral membrane of the duodenal enterocyte where it mediates iron efflux to the circulation (Abboud and Haile 2000). It was also found to be expressed in placental syncytiotrophoblast, liver, spleen, and reticuloendothelial macrophages (Donovan et al. 2000; McKie et al. 2000). IREG1 is highly conserved among species with 90-95% sequence homology between human, rat, and mouse (Abboud and Haile 2000).

IREG1 mRNA contains a functional IRE in its 5' UTR (McKie et al. 2000; Abboud and Haile 2000), thus it is regulated by iron. Duodenal IREG1 mRNA and protein expression is decreased in iron loading and increased in iron deficiency (Anderson et al. 2002; Chen et al. 2003; Zoller et al. 2001). On the other hand, IREG1 protein expression is repressed in the liver of iron-deficient mice (Abboud and Haile 2000) and is increased in haemochromatosis liver due to iron overload (Adams et al. 2003). These findings suggest the existence of regulatory mechanisms other than iron. Recently, a novel isoform of IREG1 was identified in intestinal cells (Zhang et al. 2009). This isoform lacks IRE and is believed to allow intestinal iron export during iron deficiency.

Inflammation also affects IREG1 expression levels by repressing its expression in the lipopolysaccharide (LPS) model of the acute inflammation in the mouse (Yang et al. 2002). IREG1 is also post-transcriptionally regulated by hepcidin (as will be

discussed later), which binds to IREG1 inducing its internalisation and lysosomal degradation (Nemeth et al. 2004b).

IREG1 gene mutations are associated with Ferroportin disease, an autosomal dominant form of hereditary haemochromatosis (HH), which is characterised by iron accumulation in reticuloendothelial macrophages (Pietrangelo 2004). This effect highlights the role of IREG1 in iron release from reticuloendothelial macrophages.

Recently, selective inactivation of the murine IREG1 gene in intestinal cells documented that IREG1 is the key, if not only, intestinal iron exporter (Donovan et al. 2005).

1.3.1.5 Hephaestin

Hephaestin (Hp) is a membrane-bound multi-copper oxidase. It has high sequence homology to ceruloplasmin (Cp), a serum multi-copper oxidase, which has ferroxidase activity (Syed et al. 2002). The role of Hp in iron homeostasis was identified in the studies of sex-linked anaemia (sla) in mice. These mice have a mutation in the *Hp* gene (Bannerman et al. 1973; Vulpe et al. 1999) and showed normal iron absorption, yet suffered from impaired iron export to the circulation resulting in microcytic anaemia (Manis 1971; Vulpe et al. 1999).

Unlike Cp, Hp is highly expressed in intestinal villi and to a lesser extent in the lung, kidney, and brain (Vulpe et al. 1999; Klomp et al. 1996).

Functional studies of IREG1 revealed that IREG1-mediated iron efflux requires an auxiliary ferroxidase activity (Donovan et al. 2000; McKie et al. 2000). However, the mechanisms by which IREG1 mediates iron efflux across the basolateral membrane and by which it interacts with Hp and Cp, remain to be clarified. Oxidation of Fe^{+2} to Fe^{+3} by Hp is important for iron to bind to circulating plasma transferrin (Vulpe et al.1999).

1.3.2 Regulation of duodenal iron uptake

As mentioned earlier, humans do not have the machinery to excrete excess iron; therefore, the process of iron absorption must be under a tight control to avoid pathological conditions associated with iron overload and deficiency. The control of duodenal iron absorption depends on body iron needs. In studies conducted in recent years, it was shown that the control of intestinal iron absorption is achieved by controlling the expression of key iron transport proteins including DMT1, Dcytb, and IREG1.

1.3.2.1 Regulation by hypoxia-inducible factor (HIF)

Hypoxia-inducible factor (HIF) is a transcription factor that exists as a heterodimer composed of alpha subunits (HIF-1α and HIF-2α) and beta subunit (HIF-1β), which is also known as aryl hydrocarbon nuclear translocator (ARNT) (Semenza and Wang, 1992; Wang and Semenza 1993; Wang et al. 1995). Under normal oxygen conditions, the prolyl hydroxylase domain (PHD) family of proteins (PHD1, 2, and 3) hydroxylates HIF-1α and HIF-2α followed by their ubiquitination by the E3 ubiquitin ligase, von Hippel-Lindau (VHL) tumour suppressor protein, and subsequent proteasomal degradation (Jaakkola et al. 2001; Ivan et al. 2001).

Two recent studies showed that iron deficiency stimulates duodenal HIF-2α signalling that induces DMT1 and Dcytb expression, and accordingly increases iron absorption (Shah et al. 2009; Mastrogiannaki et al. 2009). Moreover, this response was not observed in mice lacking HIF-2α.

1.3.2.2 Regulation by iron regulatory proteins (IRPs) (Figure 1.3)

Many proteins of iron metabolism are post-transcriptionally regulated by cellular iron levels. This regulation involves the cytoplasmic iron regulatory proteins (IRPs) binding to the iron-response element (IRE). IRE is a palindromic sequence of mRNA that forms a stem-loop structure (Hentze et al. 1987; Casey et al. 1988). DMT1 and TFR1 mRNA have IREs in their 3'-UTR that are stabilised upon IRP binding (Gunshin et al. 1997; Casey et al. 1988). In contrast, ferritin and IREG1 mRNA have IREs in their 5'UTR and IRP binding decreases protein synthesis (Huang et al. 1999; McKie et al. 2000; Abboud and Haile 2000).

Two IRPs exist in the mammalian cytoplasm (IRP1 and IRP2). IRP1 contains a 4Fe-4S cluster and possesses aconitase activity (Rouault et al. 1991). When cellular iron levels are low, IRP1 loses its Fe-S cluster and, hence, becomes able to bind IREs (Schalinske et al. 1997). Although IRP1 and IRP2 share 60% amino acid identity, IRP2 does not possess aconitase activity and is regulated by cellular iron as it is degraded when cellular iron levels are high and preserved in iron deficiency due to *de novo* synthesis (Guo et al. 1995). However, it is likely that iron-sensing by IRP2 is mediated by F-box and leucine-rich repeat protein 5 (FBXL5) (Salahudeen et al. 2009; Vashisht et al. 2009). FBXL5 possesses ubiquitin ligase E3 activity, which targets IRP2 for proteasomal degradation. The role of IRP2 in regulation of IREG1 translation/DMT1 stability remains to be determined. However, it appears to be important for intestinal expression of ferritin, as selective disruption of IRP2 increased duodenal ferritin and non-haem iron levels (Ferring-Appel et al. 2009).

During iron overload states, IRPs fail to bind IREs of ferritin, DMT1, TFR1, and IREG1. Therefore, the protein expression of ferritin and IREG1 increase, while that of TFR1 and DMT1 decrease to limit further iron uptake (Casey et al. 1988; Hentze et al. 1988; Guo et al. 1995; Gunshin et al. 2001). Intestinal disruption of IRP1 and

IRP2 in the mouse increases IREG1 and decreases DMT1 expression (Galy et al. 2008). In addition, these mice presented malabsorption and dehydration and died at the age of 4 weeks.

Recently, HIF-2α mRNA was shown to possess an IRE within its 5'-UTR (Sanchez et al. 2007). During iron deficiency and hypoxia, HIF-2α expression is repressed via IRP1-mediated transcriptional suppression (Sanchez et al. 2009; Zimmer et al. 2008). Moreover, HIF-2α–deficient mice showed hypoferremia, decreased hepatic iron and hepcidin expression levels (Mastrogiannaki et al. 2009).

IREG1 mRNA contains an IRE in its 5'-UTR. However, duodenal IREG1 expression increased in iron deficiency and decreased in iron overload *in vivo* (Abboud and Haile 2000; McKie et al. 2000).These findings are inconsistent with the regulation of genes with 5'-UTR IRE by IRPs. Recently, a novel IREG1 isoform lacking IRE was identified in intestinal cells (Zhang et al. 2009). This isoform is proposed to allow intestinal iron export during iron deficiency.

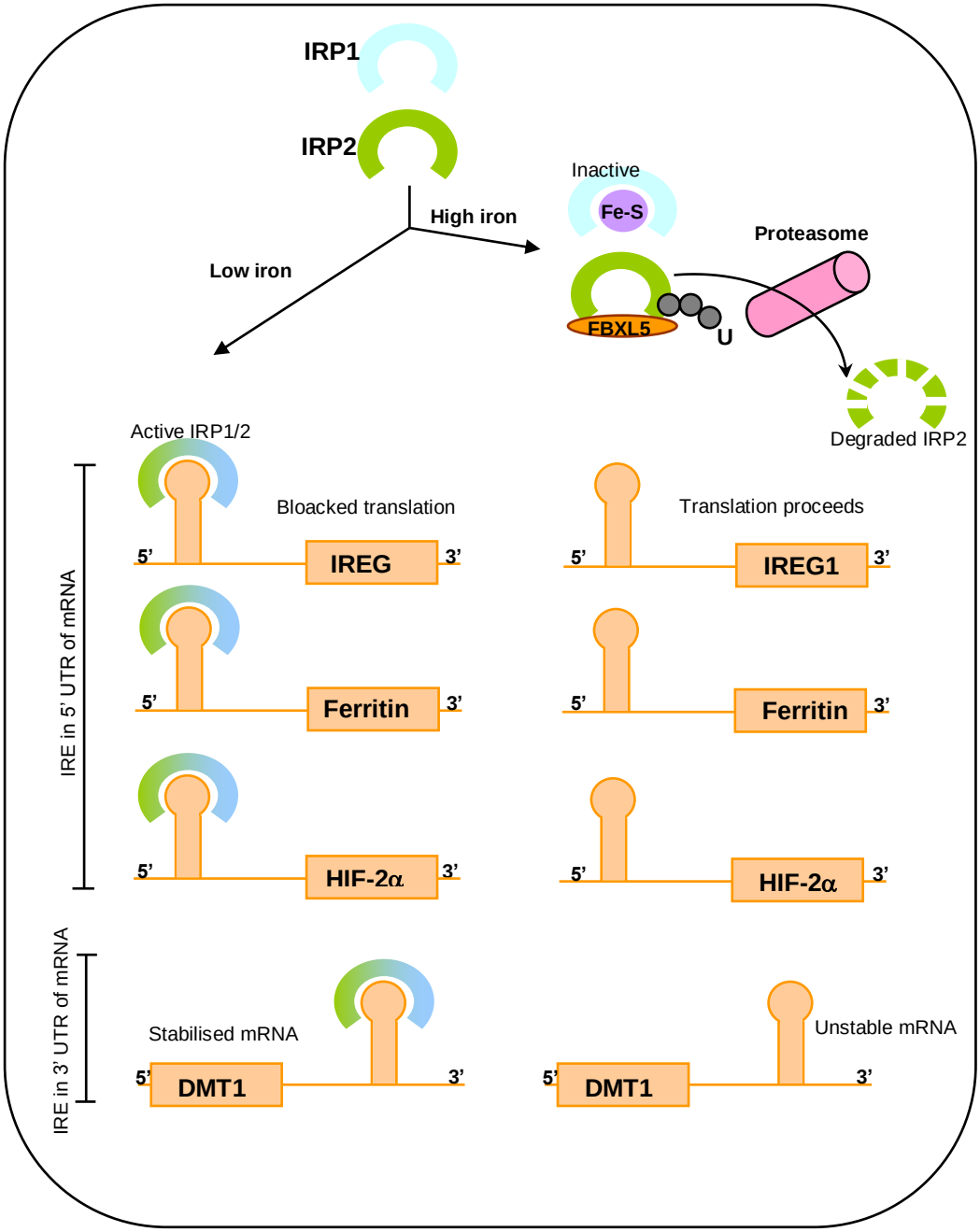

Figure 1.3 Regulation of iron transport genes by IRP-IRE pathway.
Post-transcriptional control of IRE-containing mRNAs is mediated by IRP1 and IRP2. In high iron states, iron is sensed by FBXL5 that targets IRP2 for proteasomal degradation. On the other hand, IRP1 forms a cluster (Fe-S) that interferes with its binding to IRE. Unbinding of IRPs to IREs permits translation of IREG1, ferritin, and HIF-2α while it unstabilises DMT1 mRNA. In low iron conditions, binding of IRPs to IREs results in translational repression of ferritin, IREG1, and HIF-2α while it stabilises DMT1 mRNA. Modified from (Knuston, 2010).

1.3.2.3 Regulation by hepcidin

IREG1 protein expression is negatively regulated by hepcidin, which is sensitive to systemic iron changes. Binding of hepcidin to IREG1 results in its internalisation and degradation in the lysosomes. The decreased intestinal iron export causes iron deficiency (Nemeth et al. 2004b). The role of hepcidin in the regulation of iron homeostasis will be discussed later in more detail.

1.4 Iron circulation in the body

1.4.1 Transferrin (TF)

The main function of transferrin is iron transportation between sites of absorption, storage, and usage. It is an 80 kDa monomeric glycoprotein mainly produced by the liver (Morgan, 1981), and to a lesser extent by the mammary gland, testis, and the brain (Anderson et al. 1987; Bailey et al. 1988). Transferrin contains two globular domains; each domain contains a high-affinity binding site for one Fe^{3+} iron molecule (Yang et al. 1984). . Both domains bind iron with high affinity (Yang et al. 1984); they also bind copper, cobalt, manganese, and cadmium but with lower affinity (Aisen et al. 1969; Davidson et al. 1989). A simultaneous binding of bicarbonate or carbonate to arginine and threonine residues is a requisite for iron binding to TF (Baker and Lindley, 1992).

The affinity of TF for iron is pH-dependent. At pH lower than 6.5, iron is released from TF; while at physiological pH7.4, iron is strongly bound to TF. This is an important property as it plays a vital role in the mechanism of iron release from TF.

In the plasma, TF exists as a mixture of iron-free apotransferrin, monoferric, and diferric transferrin which depends on TF and iron concentrations in the blood. In the normal physiological state, about 20-50% of TF is saturated by iron (Morgan 1996).

This incomplete saturation provides a shield against a sudden increase in plasma iron levels in certain diseases.

1.4.2. Transferrin receptor 1 (TFR1)

TFR1 is ubiquitously expressed in most cells apart from mature red blood cells (Davies et al. 1981; Enns et al. 1982), with the highest expression being in placenta, erythroid marrow, and liver (Ponka and Lok 1999). It is a disulfide-linked homodimeric glycoprotein of two 90 kDa subunits (Jing and Trowbridge 1987). Each TFR1 homodimer is able to bind two TF molecules (Enns and Sussman 1981; Sheth and Brittenham 2000).

The affinity of TFR1 to diferric-TF is pH-dependent, at the physiological pH of 7.4, the affinity of TFR1 to diferric TF is about 2000 times higher than that of apotransferrin. On the other hand, at the endosomal pH of 5.5, the affinity for apotransferrin is higher than diferric transferrin (Tsunoo and Sussman 1983).

TFR1 expression is regulated by iron, where it is up-regulated by iron deficiency and down-regulated by iron overload (Casey et al. 1988; Hentze et al. 1988). Its expression is also altered by hydrogen peroxide and nitric oxide generated by oxidative stress through Iron-regulatory protein (IRP) (Cairo and Pietrangelo 1995).

1.4.3 TFR1 mediated iron uptake (Figure 1.4)

The TRF1-mediated iron uptake occurs by receptor-mediated endocytosis. Following the binding of TF to TFR1, the complex is internalised into endosomes through clathrin-coated pits. The vesicles are acidified by ATP-dependent proton pumps (Paterson et al. 1984), which decreases the affinity of TF for Fe^{3+}, while apoTF remains bound to TFR1 (Morgan 1983). Iron is then transported into the

cytoplasm by DMT1 (Su et al. 1998). It is believed that Fe^{3+} is reduced to Fe^{2+} before being transported by DMT1. The epithelial antigen of prostate 3 (STEAP3), an erythroid reductase, has recently been identified to act as a ferrireductase (Ohgami et al. 2005). Inside the cytoplasm, iron is either utilised or stored inside the cell. ApoTF-TRF1 complex is then returned to the cell surface (Morgan 1981). At physiological pH, apoTF dissociates from TFR1 and circulates in the blood where it can bind to iron and the cycle is repeated (Dautry-Varsat et al. 1983; Morgan 1983). Haemochromatosis protein (HFE) (which will be discussed later) is another factor that affects TF-bound iron uptake. It has been shown to bind to TFR1 to compete with TF for binding in placenta, enterocytes and transfected cells (Pakkila et al. 1997; Feder et al. 1998; Lebron and Bjorkman 1999). However, the precise role of HFE in TFR1-mediated iron uptake is not clearly understood.

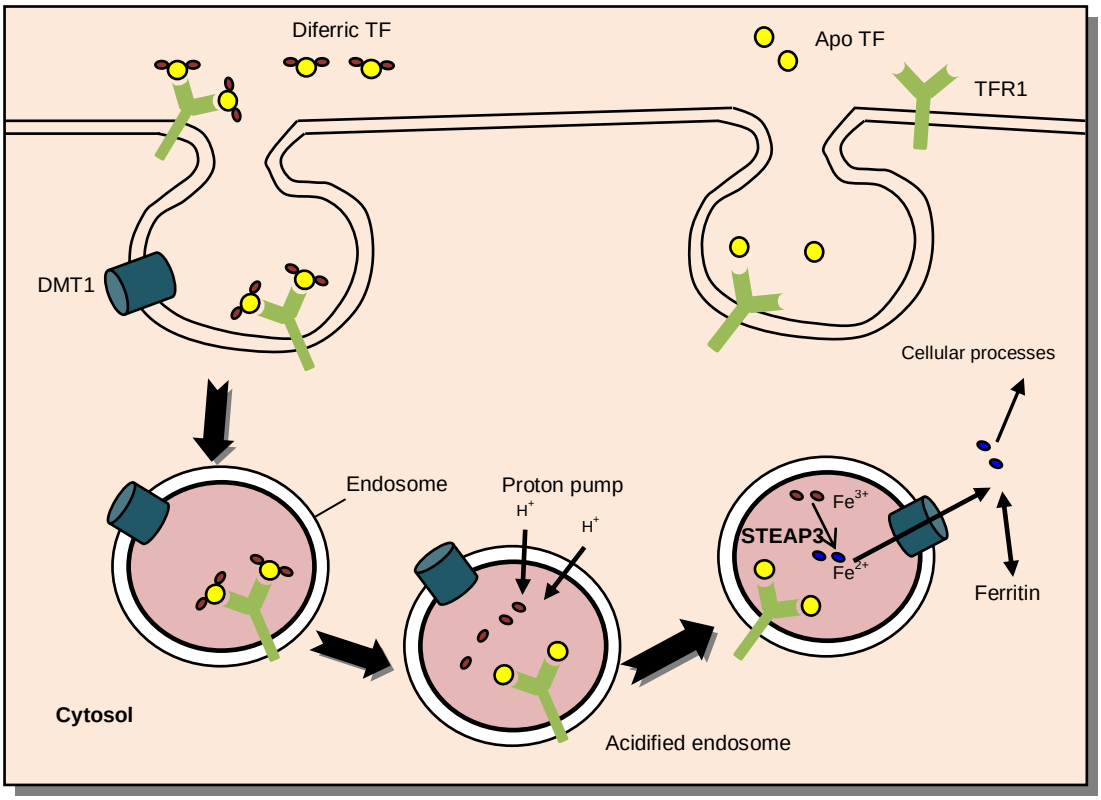

Figure 1.4 Transferrin mediated iron uptake.

Diferric TF binds to TFR1 on the cell membrane, followed by internalisation of the complex via clathrin-coated pits into endosomes. The endosome is acidified by ATP-dependent proton pump which decreases pH within the lumen. Acidic pH causes dissociation of iron from the TF-TFR1 complex. Iron is then reduced by STEAP3 followed by its transport across the endosomal membrane by DMT1 to the cytosol. In the cytoplasm iron is either utilised or stored within the cell in ferritin. The TF-TFR1 complex is then recycled to the cell membrane, and the higher pH dissociate TF from TFR1 and both can be used for additional cycles of iron uptake. Modified from (Andrews, 1999).

1.4.4 Transferrin receptor 2 (TFR2)

In 1999, Kawabata et al. identified a second human TFR gene, named TFR2. It has two splice variants: the alpha (α) form which is 2.9 kb and beta (β) form which is 2.5 kb (Kawabata et al. 1999). TFR2-α is highly expressed in the liver; it is type 2 transmembrane glycoprotein with high structural similarity to TFR1 (about 66% sequence homology) (Kawabata et al. 1999). On the other hand, TFR2-β lacks the transmembrane domain and part of the extracellular domain, suggesting that it is an intracellular protein (Kawabata et al. 1999).

TFR2 is highly expressed in the liver (Merle et al. 2007); low expression levels have also been reported in spleen, heart, small intestine, kidney, and testicles (Kabawata et al. 1999; Fleming et al. 2000).

Unlike TFR1, TFR2 mRNA does not have any IREs in its UTR (Kabawata et al. 1999); therefore TFR2 is not transcriptionally regulated by iron (Fleming et al. 2000; Kawabata et al. 2000). TFR2 protein expression is decreased with iron deficiency and increased with iron overload, suggesting post-transcriptional regulation of TFR2 (Robb and Wessling-Resnick 2004). TFR2 protein expression has been shown to increase in response to diferric TF in a time and dose-dependent manner in cultured hepatocytes, with no effect of non-transferrin-bound iron (NTBI) or apo TF (Johnson and Enns 2004).

Like TFR1, TFR2 can bind TF-bound iron (TBI) in a pH-dependent manner (Kawabata et al. 2000). Yet, the affinity of TFR2 for TBI is 25-30 times lower than that of TFR1 (Kawabata et al. 2000; West et al. 2000). Moreover, the embryonic mortality of mice with genetic disruption of TFR1 (Levy et al. 1999) suggests that TFR2 can not compensate for the loss of TFR1.

Regarding HFE-TFR2 interaction, an early study using soluble forms of both proteins did not show any interaction (West et al. 2000). Subsequently, co-

localisation between the two proteins has been reported in enterocytes (Griffiths and Cox 2003). In addition, co-immunoprecipitation of HFE and TFR2 has recently been reported in liver cells over-expressing TFR2 and HFE (Goswami and Andrews 2006).

Both of *TFR2* and *HFE* gene mutations lead to adult-onset forms of hereditary hamochromatosis (Feder et al. 1996; Camaschella et al. 2000).

1.5 Liver and iron metabolism

The liver plays an imperative role in iron homeostasis: it takes up TBI and NTBI from the blood, stores surplus iron, and produces hepcidin (to be discussed later) which modulates intestinal iron absorption. In addition, it has RE macrophages that deliver iron to the blood TF through phagocytosis of effete erythrocytes. Liver also expresses proteins important for iron metabolism such as TF (Ponka et al. 1998), ceruloplasmin (Hellman and Gitlin 2002), haptoglobin (Wassel 2000), and haemopexin (Tolosano and Altruda 2002). Excess iron in conditions of iron overload is stored in the liver as ferritin (Loreal et al. 2000; Philpott 2002). On the other hand, under conditions of iron deficiency, iron mobilisation from the liver takes place to provide iron to different cells.

In a normal human adult, about 40% of the stored iron (which represents about 10% of total body iron) is stored in the liver (Bacon and Tavill 1984; Searle et al. 1994) with most of it found in hepatic parenchymal cells (Van Wyk et al. 1971).

1.5.1 Iron uptake by hepatocytes (Figure 1.5)

The liver can take up both TBI (Trinder et al. 1996) and NTBI (Craven et al. 1987; Parkes et al. 1995; Randell et al. 1994; Thorstensen and Romslo 1988). As mentioned in section (1.4.3), TBI uptake occurs by receptor-mediated endocytosis

of diferric TF. During iron overload, TF saturation may reach up to 100% which is accompanied by increased plasma NTBI levels, in which case the liver is able to take up NTBI to protect cells from its harmful effects. The liver can also take up other forms of iron including: ferritin (Adams et al. 1988; Osterloh and Aisen 1989), haem-haemopexin complex (Smith and Morgan 1981; Smith and Hunt 1990), and haemoglobin-haptoglobin (Kristiansen et al. 2001).

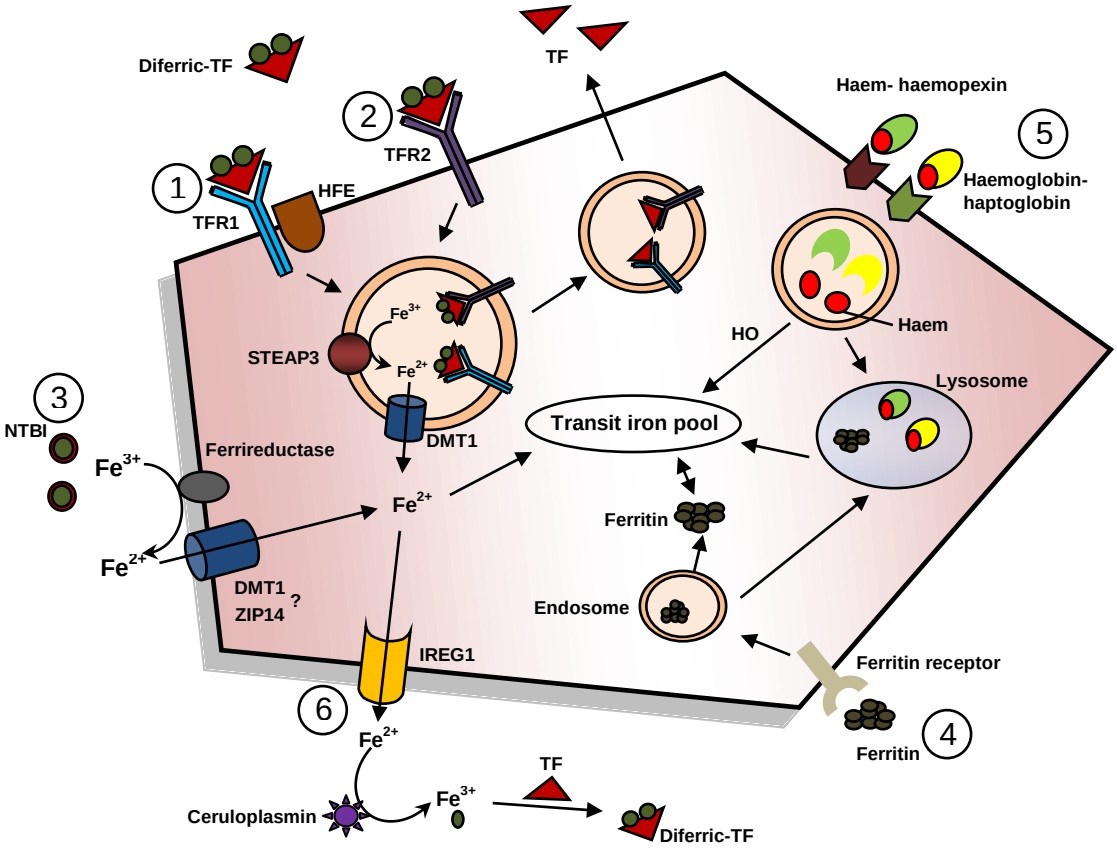

Figure 1.5 Iron uptake by hepatocytes.

(1) TFR1 pathway: Diferric TF binds to TFR1 and is endocytosed into endosomes. Acidified endosome releases iron via DMT1 after being reduced to Fe^{2+} by STEAP3. Apo TF is recycled. (2) TFR2 pathway: similar to the TFR1 pathway. (3) NTBI uptake: Iron is reduced by ferrireductase and transported inside the cytosol by the iron carrier. (4) Ferritin uptake: Ferritin is endocytosed after binding to its membrane receptor. The endosome is then transferred to the lysosomal compartment and iron is then either directed to intracellular ferritin or to the transient iron pool. (5) Uptake of haem-haemopexin and haemoglobin-haptoglobin complexes: Complexes bind their receptors (CD91 for haem-haemopexin and CD163 for haemoglobin-haptoglobin) and are endocytosed and moved to lysosomes. Haem is then removed and oxidised by HO1 and moved to transient iron pool. (6) Hepatic iron efflux: Iron is released from the hepatocytes by IREG1 and oxidised by Cp before binding to TF. Modified from (Chua et al. 2007).

1.5.1.1 Uptake of TBI

TFR1 expression has been well known since 1977 (Grohlich et al. 1977). As described in section 1.4.3, TBI uptake occurs by receptor-mediated endocytosis of the TFR1-TBI complex, release of iron from acidic endosomes, and return of the TFR1-TF complex to the cell membrane (Figure 1.5). In hepatocytes, each cycle takes around 4-15 min (Morgan and Baker 1986; Bacon and Tavill 1984). Iron is reduced possibly by STEAP3, and transferred to the cytoplasm by DMT1 (Fleming et al. 1998; Trinder et al. 2000). Inside the cytosol, iron is either stored as ferritin or incorporated into haem synthesis in the mitochondria.

Hepatic iron levels affect TBI uptake, as it is decreased in dietary iron-loading subsequent to decreased TFR1 expression (Chua et al. 2006a). On the other hand, TBI uptake is increased in iron-deficient liver cells owing to increased TFR1 expression (Morton and Tavill 1978; Trinder et al. 1990).

However, at least two mechanisms have been documented for TFR1-independent TBI uptake. The first mechanism involves binding of iron-TF to low affinity sites on the cell membrane with subsequent endocytosis and iron release from the endosomes via DMT1 (Trinder et al. 1986, Morgan et al. 1986). The second mechanism involves iron release from TF at the cell membrane which is then transferred inside the cell via a transporter. However, this pathway seems to require reduction of Fe^{3+} to Fe^{2+}, as iron uptake by hepatocytes is inhibited by ferrous chelators (Thorstensen and Ramslo 1988; Thorstensen 1988). The transporter-mediated step in the second iron uptake mechanism seems to transport both TBI and NTBI, since TBI uptake by hepatoma cells is inhibited by NTBI (Trinder and Morga 1997) and vice versa (Chua et al. 2004; Graham et al. 1998b). Trinder and Morgan (1997) showed that NTBI specifically interferes with the uptake of iron released from TF on the cell membrane.

TFR2 can also transport TBI; however, it has lower affinity for TF than TFR1 (Kawabata et al. 2000; West et al. 2000). It has been shown to mediate TBI uptake in TRF2 over-expressing CHO cells (Kawabata et al. 1999).

1.5.1.2 Uptake of NTBI

In the normal state, NTBI levels are less than 1μM, while in cases of iron overload, levels can reach up to 10 μM (Breuer et al. 2000, al-Refaie et al. 1992). Elevated plasma levels of NTBI have been reported in HH patients (Grootveld et al. 1989) and in a murine model of HFE HH (Chua et al. 2004) Liver NTBI uptake is inhibited by divalent metals as zinc, manganese, and cobalt (Wright et al. 1986; Wright et al. 1988). The mechanism of NTBI uptake by the liver has been studied in both hepatoma cells (Randell et al. 1994; Trinder and Morgan 1998) and isolated rat hepatocytes (Parkes et al. 1995; Richardson et al. 1999). Iron dissociates from its ligand at the cell membrane which probably involves reduction of Fe^{3+} to Fe^{2+} by ferrireductase, and subsequently transported inside the cell by a carrier (Trinder and Morgan 1998; Graham et al. 1998a). Several NTBI transporters have been hypothesised, among them DMT1, calcium channels, and Zrt-Irt-like protein 14 (ZIP14). The role of DMT1 in NTBI uptake was supported by the reduction of Fe^{3+} to Fe^{2+} before being transported (Chua et al. 2004; Trinder and Morgan 1998); however, it is not known whether STEAP3 has a membrane ferrireductase activity similar to that reported in the endosomal membrane (Ohgami et al. 2005). The repression of hepatocyte NTBI uptake by divalent metals, suggests that both iron and divalent metals are taken up by the same transporter (Chua et al. 2004; Baker et al. 1998). Moreover, *HFE* knockout mouse hepatocytes showed an increase in NTBI uptake as well as an increase in DMT1 expression (Chua et al. 2004). The role of HFE in NTBI uptake is supported by a recent finding of Gao et al. (2008)

who showed that HFE expression in HepG2 cells inhibited NTBI uptake and decreased ZIP14 protein levels. Nevertheless, the lack of DMT1 does not eliminate NTBI uptake by the liver, suggesting the existence of different carriers in liver cells (Gunshin et al. 2005).

L-type calcium channels have been shown to mediate NTBI uptake by cardiac muscle cells; however, it is not known if these are required for NTBI uptake by the liver (Oudit at al. 2003). ZIP14, a zinc transporter, has also been shown to mediate NTBI uptake by mouse liver cells (Liuzzi et al. 2006).

1.5.1.3 Uptake of other forms of iron (Figure 1.5)

Other iron complexes can be taken up by the liver; however, it is likely to be a scavenging mechanism rather than iron uptake. These forms include: ferritin, haemoglobin-haptoglobin complex, and haem-haemopexin complex. As it contains small amount of iron (Arosio et al. 1977; Pootrakul et al. 1988; Worwood et al. 1976), ferritin is not regarded as a main source of iron in humans. Liver scavenges ferritin via receptor-mediated endocytosis after binding to a specific ferritin receptor (Adams et al. 1988; Mack et al. 1983; Osterloh and Aisen 1989). Once endocytosed, ferritin can either be catabolised within lysosomes or directed to the cellular ferritin pool (Sibille et al. 1989; Unger and Hershko 1974).

Uptake of haem-haemopexin complexes is mediated by receptor-mediated endocytosis after binding to its specific receptor, CD91 (Hvidberg et al. 2005). Inside the endosome, haem is degraded by haem oxygenase. Originally, like TF, it was believed that haemopexin was recycled back (Smith and Hunt 1990; Smith and Morgan 1978; 1979). However, recent findings have suggested that lysosomal degradation might antagonise this hypothesis (Hvidberg et al. 2005).

Haemoglobin-haptoglobin complexes bind to their receptor, CD163, and are taken up by receptor-mediated endocytosis. The complex is then degraded in the

lysosomes to release haem, which is further degraded by HO1 to release iron (Higa et al. 1981).

1.5.2 Iron efflux from hepatocytes

Unlike iron uptake, little is known about hepatic iron release. Even in the presence of external chelators, hepatocytes have limited capacity to release iron. The released iron is approximately 20% of iron taken up (Baker et al. 1985; Chua et al. 2003; 2006). The molecular mechanism of hepatic iron efflux is believed to be mediated via IREG1 (Abboud et al. 2000; McKie et al. 2000; Donovan et al. 2000). Expression of IREG1 in mouse hepatocytes is correlated with iron efflux (Chua et al. 2006b). Moreover, selective disruption of the IREG1 gene resulted in increased cellular iron accumulation (Donovan et al. 2005). IREG1 is expressed at quite high levels in hepatocytes and hepatic stellate cells, and to a lesser extent in sinusoidal endothelial cells (Zhang et al. 2004). Before binding to TF, released Fe^{2+} has to be oxidised to Fe^{3+}. Ceruloplasmin (Cp) is believed to be the ferroxidase, which promotes iron efflux by hepatocytes (Young et al. 1997). It is a liver-derived glycoprotein that contains more than 95% of circulating copper (Hellman and Giltin, 2002). Cp expression has also been reported in brain, spleen, testicles, and lungs (Yang et al. 1986; Koschinsky et al. 1986; Aldred et al. 1987; Klomp and Giltin 1996; Yang et al. 1996). In addition, in mice lacking Cp and patients with *Cp* gene mutations, hepatocellular iron efflux is impaired (Harris et al. 1999; Miyajima et al. 1987; Yoshida et al. 1995). However, the exact role of Cp and IREG1 in hepatic iron release remains to be fully clarified.

Hepcidin is the other hepatocyte-derived protein (to be discussed later) believed to play a vital role in iron release. It has been shown to inhibit iron release from different cell types, such as macrophages, enterocytes, and liver cells (Ganz 2005;

Rivera et al. 2005) possibly via binding to IREG1, facilitating its internalisation so that it is unable to participate in iron efflux (Nemeth et al. 2004b).

1.5.3 Hepcidin

Two groups investigating small antimicrobial peptides in body fluids independently identified hepcidin in the urine (Park et al. 2001) and plasma (Krause et al. 2000). It was named Liver Expressed Antimicrobial Peptide-1 (LEAP-1) (Kraus et al. 2000) and Hepcidin “hep” for hepatocyte and “idin” for its antimicrobial activity (Park et al. 2001). Despite being initially isolated from blood and urine, hepcidin is highly expressed in human and mouse liver and to a lesser extent in intestine, lung, heart, brain, and kidney (Pigeon et al. 2001; Kulaksiz et al. 2005).

The human hepcidin gene (*HAMP*) was mapped to the chromosome 19 (Park et al. 2001) and encodes an 84 aminoacid prepropeptide that possesses a cleavage site. This is then modified to give 20 and 25-aminoacid peptides with eight cysteine residues forming four intra-chain disulfide bonds (Figure 1.6) that are conserved across hepcidin-producing species (Hunter et al. 2002). The hepcidin disulfide bonds were recently revised (Jordan et al. 2009). Two of them are required to stabilise the anti-parallel sheets while the other bonds are required to maintain the bending of the peptide (Nemeth and Ganz 2009). Hepcidin has been shown to be a member of the cysteine-rich antimicrobial peptide family that includes defensin, so called because of its antibacterial and antifungal properties (Park et al. 2001; Klaus et al. 2000). Consistent with its role in immunity, hepcidin has been shown to be a type II acute-phase protein (Nemeth et al. 2003).

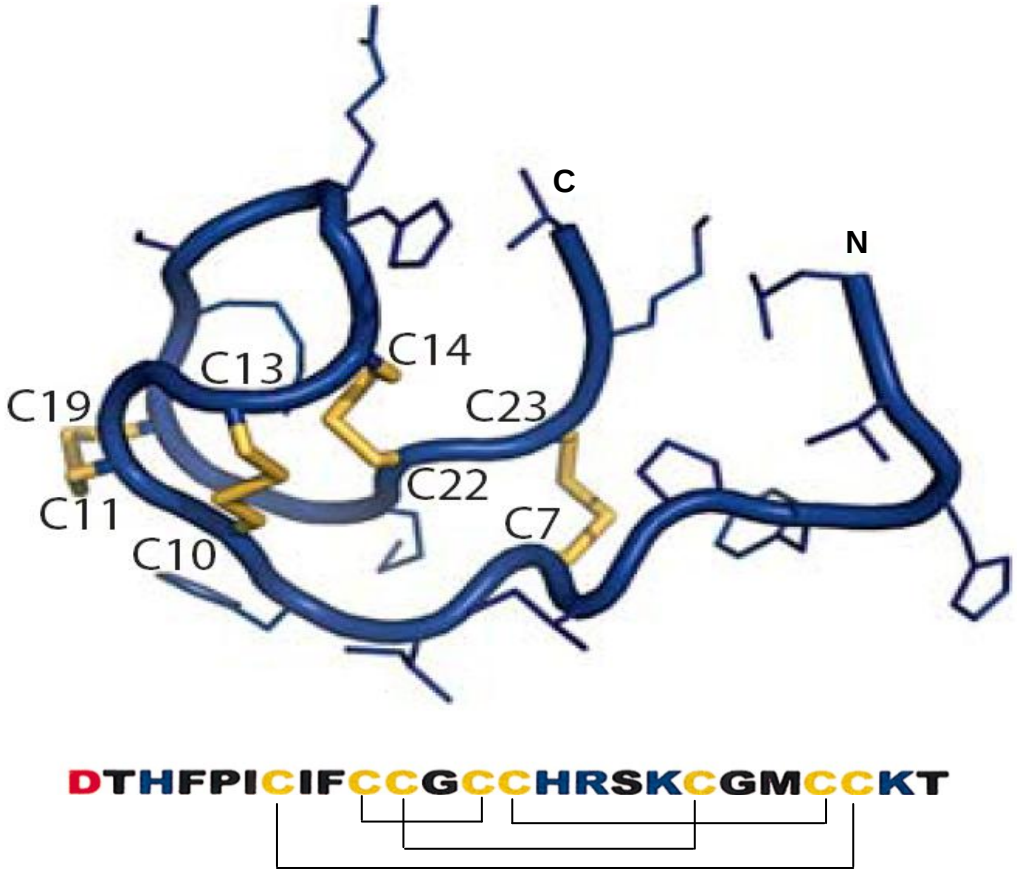

Figure 1.6 A schematic model of the major form of human hepcidin and its amino acid sequence.

This schematic model shows the main 25 amino acid form of human hepcidin with its amino (N) and carboxy (C) termini. Acidic amino acids are shown in red, basic amino acids in blue. Recently revised disulfide bonds are in yellow and are also shown in the amino acid sequence. Adapted from (Nemeth and Ganz 2009).

1.5.3.1 Role of hepcidin in iron metabolism

The role of hepcidin in iron homeostasis was independently recognized by two groups working on mice (Pigeon et al. 2001; Nicolas et al. 2001). During their search for genes that were up-regulated in iron-loaded mice, Pigeon et al. (2001) identified hepcidin among the induced genes. Furthermore, they reported a decrease in hepcidin mRNA expression when animals were fed a low iron diet, suggesting that iron regulates hepcidin gene expression.

The group of Nicolas (Nicolas et al. 2001) generated a mouse strain lacking functional Upstream stimulatory factor -2 (USF2) and accidentally removed the neighbouring hepcidin gene. These mice showed a severe iron-overload phenotype similar to that observed in HH. Subsequently, it was shown that disruption of the hepcidin gene *per se* resulted in iron overload in mice (Lesbordes-Brion et al. 2006). In humans, hepcidin gene mutations were shown to be associated with a severe form of haemochromatosis, called Juvenile haemochromatosis (JH) (Roetto et al. 2003). In addition, mice lacking the hepcidin gene develop iron loading in the liver, heart, and pancreas due to increased duodenal iron uptake (Nicolas et al. 2001). On the other hand, mice over-expressing hepcidin showed profound iron deficiency anaemia due to decreased duodenal iron uptake (Nicolas et al. 2002a).

Unlike humans, two hepcidin genes were found in mice (*HAMP-1* and *HAMP-2*) (Nicolas et al. 2001; Pigeon et al. 2001). While the role of *HAMP-1* (*hepcidin 1*) in iron homeostasis is established, the precise functions of *HAMP2* (*hepcidin 2*) remain to be fully clarified. In addition, no iron deficiency was observed in mice over-expressing *HAMP-2* (Lou et al. 2004). Therefore, in the thesis only the expression of *hepcidin1* is studied.

1.5.3.2 Mechanism of hepcidin action

Circulating hepcidin acts by adjusting iron efflux to the blood via binding to its receptor, IREG1. This binding triggers internalisation and degradation of the complex in lysosomes (De Domenico et al. 2007; Nemeth et al. 2004b), and consequently cellular iron export stops. It is believed that binding involves an exchange of a disulfide bond between hepcidin and the ferroportin thiol residue Cys326, as patients with C326S mutations show early-onset iron overload phenotype, and mutant IREG1 lost its hepcidin-binding ability *in vitro* (Fernandes et al. 2009). The shorter 20 aminoacid form of hepcidin can not repress IREG1, suggesting that the five N-terminal amino acids of the mature protein are the most critical regions for IREG1 binding (Nemeth et al. 2006). Moreover, neither mutations to remove any of the disulfide bridges nor removal of the two C-terminal amino acids of hepcidin affected its biological activity (Nemeth et al. 2006).

Loss of IREG1 function in macrophages leads to iron retention and hypoferraemia; likewise, loss of IREG1 from enterocytes results in reduced iron absorption. *In vivo*, hepcidin injection inhibited intestinal iron absorption in mice (Laftah et al. 2004). On the other hand, reduced hepcidin expression in iron-deficient rodent models increased *IREG1* expression in duodenal enterocytes (Frazer et al. 2002; Weinstein et al. 2002), and subsequently increased iron absorption. In addition, hepcidin has been shown to repress iron uptake in human intestinal epithelial cells (Caco-2) by down-regulating *DMT1* expression (Yamaji et al. 2004).

1.5.3.3 Regulation of hepcidin expression by hereditary iron storage diseases

HH includes a diverse group of disorders that are accompanied by hepcidin deficiency and subsequent iron overload and organ damage. Most HH cases are associated with mutations in the *HFE* gene (type I). In others, the mutations occur in genes encoding proteins that are important for iron homeostasis (non-HFE haemochromatosis; Pietrangelo, 2004). In type II (juvenile) haemochromatosis, mutations occur in the *hemojuvelin* (*HJV*) or *hepcidin* genes is the most severe form of haemochromatosis with maximum hepcidin deficiency. In type III haemochromatosis, mutations affect *TFR2* gene, and in type IV mutations occur in *SLC40A1* gene encoding IREG1. These genes and their mutations will be discussed in detail below.

1.5.3.3.1 *HFE* haemochromatosis (Type I HH)

The *HFE* gene, identified by Feder et al. (1996) belongs to the major histocompatability complex I family (MHC 1). The gene is located on chromosome 6 and encodes a 343 amino acid protein with a 22 amino acid signal peptide, extracellular (α1, α2, and α3), transmembrane, and cytoplasmic domains (Figure 1.7). Beta-2-microglobulin (β2m) interacts with α3 domain which is important for surface expression of HFE (Cardoso and de Sousa 2003; Waheed et al. 1997; Feder et al. 1997). In addition, a lack of the *β2m* gene in mice alters the expression of HFE and causes iron overload similar to that of HH (Santos et al. 1996).

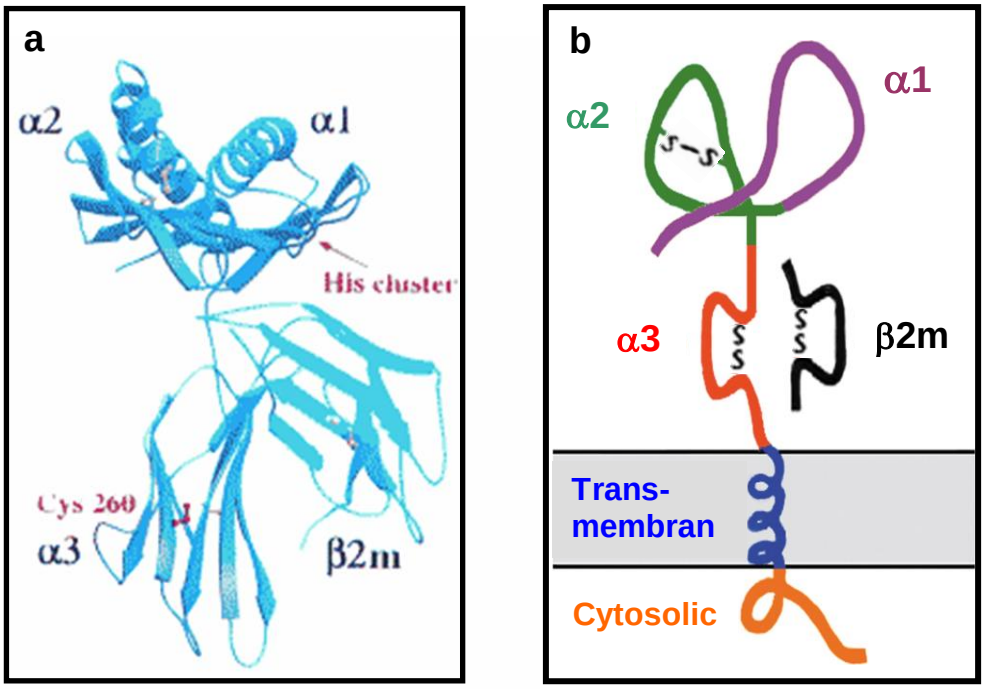

Figure 1.7 The HFE structure.

Ribbon diagram (a) and a cartoon (b) showing HFE with its three-loop extracellular domain (α1, α2, and α3), transmembrane domain, and a cytosolic tail. Like other MHC1 molecules, HFE associates with β2 microglobulin (β2m) via its α3 domain. Adapted from (Lebron et al. 1999; Fleming and Sly 2002).

Several gene mutations in HFE have been linked to HH. The most common mutation is a tyrosine for cysteine substitution at position 282 (C282Y), which interferes with α3 domain folding, interaction with β2m, and surface expression of the protein (Feder et al. 1997; Waheed et al. 1997). This mutation is most common in people of Northern European origin; however, it can also occur in Asian and African people albeit less frequently (Rochette et al. 1999; Acton et al. 2006). A second mutation in *HFE* was characterised in HH patients, resulting in substitution of an aspartate for a histidine at position 63 (H63D). This mutation, unlike C282Y, has no effect on the interaction between β2m and HFE and surface expression of

the protein (Feder et al. 1997). However, the contribution of the H63D mutation to HH has been controversial.

The role of HFE mutations C282Y and H63D were studied in mouse models with analogous mutations C294Y and H67D, respectively (Tomatsu et al. 2003). They showed that mice homozygous for C294Y had higher levels of liver iron followed by compound heterozygous for C282Y and H63D and then mice homozygous for H63D.

C282Y homozygotes show inconsistent penetrance of iron overload (Beutler et al. 2002). In addition, the estimated frequency of the C282Y mutation in patients of Northern European origin is 1 in 150 (Feder et al. 1996). This lead to a belief that this mutation has low penetrance and there are many asymptomatic cases of haemochromatosis (Bomford 2002). Although many modulator genes have been tested (Lee et al. 2002) and it has been suggested that hepcidin gene mutation may affect the expression of HFE mutation (Merryweather-Clarke et al. 2003; Jacolot et al. 2004), the reasons of inconsistent HFE penetrance in humans have yet to be determined. On the other hand, different gene modifiers for the *HFE* mutation phenotype have been characterised in mice of different backgrounds with genetic disruption of *HFE. Rag1* is believed to be one of the modifiers, as *HFERag1*$^{-/-}$ double mutant mice showed more iron overload than *HFE*$^{-/-}$ mice (Miranda et al. 2004). *Smad4* has also been shown to be differently expressed in high iron absorbing DBA and low iron absorbing C57Bl/6 mouse strains (Coppin et al. 2007). When crossed with hepcidin transgenic mice, *HFE*$^{-/-}$ mice showed no hepatic iron accumulation, suggesting a role of hepcidin in the prevention iron overload in *HFE*$^{-/-}$ mice (Nicolas et al. 2003).

Patients homozygous for C282Y have been shown to have less urinary hepcidin and less hepcidin mRNA expression than control subjects (Bozzini et al. 2007; Bridle et al. 2003). Moreover, these patients showed less hepcidin in response to

iron depletion and failed to upregulate hepcidin in response to oral iron (Piperno et al. 2007).

1.5.3.3.2 Juvenile haemochromatosis (Type II HH)

Juvenile haemochromatosis (JH) is an early-onset hereditary recessive disorder characterised by severe iron deposition in parenchymal cells and organ damage, which usually develops before the age of 30 years (De Gobbi et al. 2002). JH is caused by mutations in genes encoding HJV (Type IIA JH) (Lanzara et al. 2004; Papanikolaou et al. 2004) or hepcidin (type IIB) (Roetto et al. 2003)

1.5.3.3.2.1 Hemojuvelin haemochromatosis (Type IIA JH)

Hemojuvelin (HJV; RGMc) is a member of the repulsive guidance molecules (RGM) family. The *HJV* gene was first identified by Papanikolaou et al. (2004). Similar to hepcidin, in mouse the expression of HJV is detected in the liver, skeletal muscle, and heart (Papanikolaou et al. 2004). On the other hand, the expression of RGMa and RGMb is confined to the developing and adult central nervous system. *HJV* has five splice isoforms encoding proteins of 200, 313, and 426 amino acids with three isoforms generating the same protein (Papanikolaou et al. 2004) (Figure 1.8)

The full-length (426 amino acid) protein is characterized by multiple domains, including an N-terminal signal peptide, a RGD integrin-binding motif, a partial von Willebrand factor (VWF) type D domain, and a C-terminal glycosilphosphatidylinositol (GPI) anchor domain. All RGM proteins possess a Gly-Asp-Pro-His (GDPH) sequence (Monnier et al. 2002). The full-length protein undergoes a partial autocatalytic cleavage (Lin et al. 2005) to reach the plasma membrane (m-HJV) as a cleaved heterodimer (Kuninger et al. 2006; Silvestri et al. 2007).

It has been recently shown that HJV can bind bone morphogenic proteins (BMP) (Babitt et al. 2006), members of the transforming growth factor (TGF)-β superfamily of cytokines that play a crucial role in the development of tissues, in regulating cell proliferation, cell differentiation, and in apoptosis (Chen et al. 2004; Gambaro et al. 2006; Varga and Wrana 2005). The mechanism of BMP-SMAD signalling will be discussed later.

HJV is retained in the outer layer of the plasma membrane through the GPI anchor motif (m-HJV); however, it can also be found as a soluble form (s-HJV) both *in vitro* and *in vivo* (Lin et al. 2005; Kuninger et al. 2006). S-HJV was detected in cell culture supernatants of transfected human hepatoma cells (Hep3B) and human embryonic kidney cells (HEK 293) as well as in human and rat blood (Lin et al. 2005; Zhang et al. 2007).

Treatment of HJV-transfected Hep3B or HEK 293 with organic iron or holotransferrin reduced the amount of s-HJV in the culture medium. Moreover, recombinant s-HJV suppressed hepcidin expression in human primary hepatocytes in a dose-dependent manner (Lin et al. 2005). The inverse correlation between iron loading and s-HJV concentration *in vitro* lead to the hypothesis that s-HJV could be a negative regulator of hepcidin. The authors proposed a model in which s-HJV and m-HJV reciprocally regulate hepcidin expression in response to iron-load (Lin et al. 2005). However, it is not clearly known whether s-HJV only originates from m-HJV or whether it has different origin, possibly heart or skeletal muscle.

Silvestri et al. (2007) showed that HJV mutants defective in plasma membrane presentation could still release s-HJV. They suggested that s-HJV does not originate from m-HJV, but is independently secreted by the cell. However, robust evidence supporting the secretion model is lacking. In contrast, a recent study provided evidence that s-HJV can originate from cell surface m-HJV (Kuninger et al. 2006). Lin et al. (2007) reported that s-HJV is generated by a proprotein convertase through the cleavage at a conserved polybasic RNRR site. Furthermore, Silvestri et

al. (2008a) showed that s-HJV originates from furin cleavage at the C terminus at position 332-335 of the protein in the ER. They also showed that this cleavage was induced by iron deficiency and hypoxia and that release of s-HJV might be a tissue-specific mechanism signalling the local iron requirement of skeletal muscles independently of the oxygen status of the liver (Silvestri et al. 2008a).

s-HJV has been shown to hinder BMP-2 and BMP-4 signalling both *in vitro* (Lin et al. 2005) and *in vivo* (Babitt et al. 2007). BMP-2 administration increases hepcidin expression and decreases serum iron levels *in vivo*; moreover, s-HJV administration decreases hepcidin expression, increases IREG1 expression, mobilizes splenic iron stores, and increases serum iron levels *in vivo* (Babitt et al. 2007).

HJV and other members of the RGM family have been shown to bind to the receptor neogenin (Matsunaga et al. 2004; Rajagopalan et al. 2004). Moreover, Zhang et al. (2005) showed that HJV-mediated iron accumulation is enhanced by neogenin *in vitro* suggesting a link between HJV, neogenin, and iron homeostasis. In addition, Zhang et al. (2007) demonstrated that HJV shedding *in vitro* could be mediated by neogenin. However, whether HJV-neogenin interaction plays a role in hepcidin regulation by HJV remains unclear. Recently, Xia et al. (2008) showed that HJV-induced BMP signalling *in vitro* was not altered either by inhibition of endogenous neogenin or by neogenin over-expression. Therefore, the hepcidin regulation via HJV-BMP signalling occurs independently of neogenin.

HJV haemochromatosis is characterised by severe iron overload at a young age. The age of onset has been reported to be as young as five years; however, it mostly occurs when patients are in their twenties. Patients with *HJV* mutations show high serum ferritin and transferrin saturation, cardiomyopathy, hypogonadism, and diabetes (Papanikolaou et al. 2005).

HJV$^{-/-}$ mice showed low hepcidin expression and hepcidin was not responsive to high iron, but responsive to inflammation by lipopolysaccharide (LPS). Unlike

human patients, *HJV*$^{-/-}$ mice do not show diabetes or cardiomyopathy (Niederkofler et al. 2005); on the other hand, they show high iron loading in the liver, heart, and pancreas and decreased splenic iron as seen in the human disease (Huang et al. 2005; Niederkofler et al. 2005).

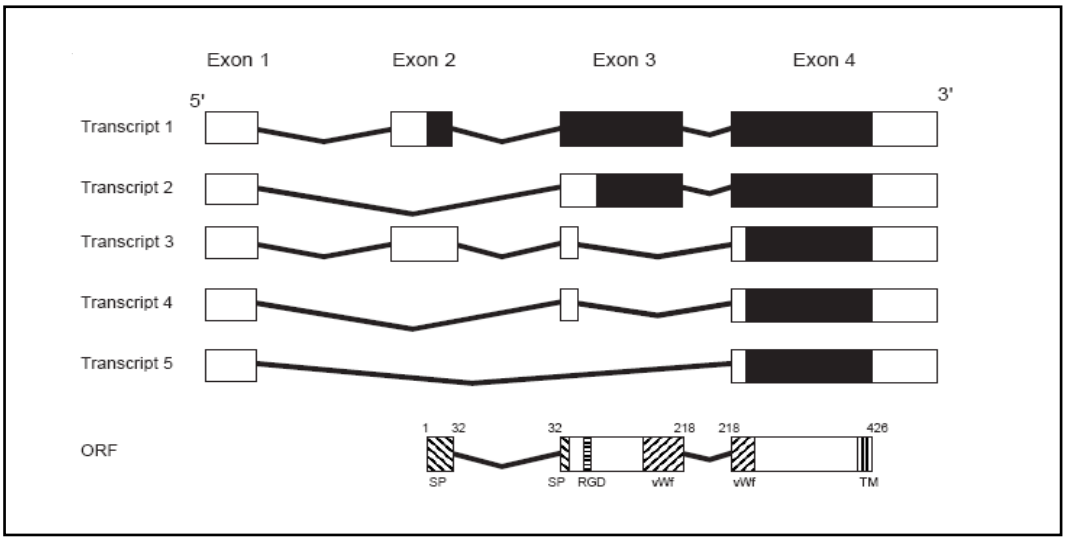

Figure 1.8 Structure of the *HJV* gene.

A diagram showing five different *HJV* transcripts. Each of these transcripts may be translated into a polypeptide. Transcripts 3, 4 and 5 generate the same protein; therefore, there are three HJV isoforms of 426, 313 or 200 amino acids. Untranslated sequence is coloured white, translated sequence black. The longest open reading frame (ORF) is shown below transcripts. (SP, signal peptide; RGD, tri-amino acid motif; vWf, partial von Willebrand domain; TM, transmembrane domain). Adapted from (Papanikolaou et al. 2004).

1.5.3.3.2.2 Hepcidin haemochromatosis (Type IIB JH)

This type of haemochromatosis is caused by mutations in the *HAMP* gene encoding hepcidin; however, this type of haemochromatosis is less frequent than *HJV* haemochromatosis (Lanzara et al. 2004; Papanikolaou et al. 2005). Patients with Type IIB JH have the same characteristics of Type IIA JH such as progressive iron overload, hypogonadism, diabetes, and cardiomyopathy (Rideau et al. 2007; Matthes et al. 2004; Delatycki et al. 2004).

Hamp1$^{-/-}$ mice show excessive iron loading in the liver but they show less iron loading in macrophages and spleen (Nicolas et al. 2001; Lesbordes-Brion et al. 2006). Unlike human disease, *Hamp1*$^{-/-}$ mice did not manifest diabetes or reduced insulin production despite excessive iron loading in pancreatic β cells (Ramey et al. 2007).

1.5.3.3.3 Haemochromatosis type III (TFR2 haemochromatosis)

This was the second type of HH to be identified after the cloning of *HFE* gene (Camaschella et al. 2000). Mutations in *TFR2,* as with *HFE* mutations*,* are associated with high serum ferritin and transferrin saturation, as well as hepatic iron loading (Camaschella et al. 2000; Roetto et al. 2001; Le Gac et al. 2004). Many patients with *TFR2* haemochromatosis show low hepcidin expression levels that is not proportional to the degree of iron loading (Nemeth et al. 2005).

TFR2$^{-/-}$ mice manifest hepatic iron overload and low splenic iron content (Fleming et al. 2002; Kawabata et al. 2005). In these mice, hepcidin expression is not induced in response to iron (Kawabata et al. 2005; Wallace et al. 2005), while it is induced by inflammatory stimuli (Lee et al. 2004).

1.5.3.3.4 Haemochromatosis type IV (ferroportin disease)

Haemochromatosis associated with *IREG1* mutation is inherited as an autosomal dominant disorder. It is clinically different from other iron-storage diseases and it is also known as ferroportin disease (Pietrangelo, 2004). Most *IREG1* mutations fall in two categories: (a) Loss of iron export activity due to loss of IREG1 function or loss of IREG1 surface localisation, which is characterised by high blood ferritin levels but without a rise in transferrin saturation, and iron accumulation mainly in macrophages (Montosi et al. 2001; Njajou et al. 2001; De Domenico et al. 2006; Drakesmith et al. 2005); (b) *IREG1* mutations that cause loss of hepcidin binding activity without affecting iron export activity. It is characterised by elevated blood ferritin and transferrin saturation levels and hepatic iron loading (Drakesmith et al. 2005; Sham et al. 2005).

1.5.3.4 Regulation of hepcidin expression

1.5.3.4.1 Regulation by inflammation, infection, and obesity

Hepcidin expression is induced by inflammation and infection. In animal models and human subjects, injection of LPS or Freund's adjuvant increased hepatic hepcidin mRNA expression (Pigeon et al. 2001; Frazer et al. 2004; Kemna et al. 2005; Nemeth et al. 2004b). Despite the fact that the increase in hepcidin expression is favourable for the organism during the course of an infection as it limits the iron availability for the pathogen, prolonged increase has a harmful effect as it leads to the development of anaemia of inflammation (AI). Increased hepcidin causes internalisation and degradation of IREG1 that inhibits iron release from macrophages causing hypoferremia characteristic of AI (Ganz 2006). The same response of hepcidin and anaemia has been shown in turpentine oil-injected mice

(Nicolas et al. 2002b; Weinstein et al. 2002). However, the anaemia was absent in mice lacking USF2/hepcidin, indicating that hepcidin mediates anaemia observed in treated mice. The inflammatory cytokines, mostly interleukin (IL)-6, induce activation of STAT-3 that binds to the hepcidin promoter region to activate transcription (Wrighting and Andrews 2006; Truksa et al. 2007; Verga Falzacappa et al. 2007).

IL-6 binds to its receptor on the surface of hepatocytes. The receptor complex is composed of a α (80 kDa) subunit and two β (13kDa) subunits (Figure 1.9). Binding of IL-6 to α–subunit induces dimerisation of the β-subunits, which in turn are phosphorylated by the cytosolic JAK (janus kinase) proteins (Heinrich et al. 2003). The phosphorylation of the β-subunits stimulates the STAT (signal transducer and activator of transcription) pathway. STAT3 proteins bind to the β-subunits and after phosphorylation, detach from β subunit, and then translocate to the nucleus as dimers where they bind to a response element within the hepcidin gene promoter inducing its transcription (Wrighting and Andrews 2006; Truksa et al. 2007; Verga Falzacappa et al. 2007).

IL-6 induces *hepcidin* mRNA expression *in vivo* and *in vitro* (Nemeth et al. 2003; 2004). Hepcidin expression in hepatocytes is induced by conditioned medium from LPS-treated macrophages, and this response is blocked by anti-IL-6 antibodies (Nemeth et al. 2003; Lee et al. 2005). However, mice with genetic disruption of the *IL-6* gene are able to regulate hepcidin in response to endotoxin, suggesting the existence of other factors that regulate hepcidin expression (Lee et al. 2004). Interestingly, the treatment of primary mouse hepatocytes with IL-1α and IL-1β strongly increases hepcidin mRNA expression (Lee et al. 2005), suggesting possible regulation of hepcidin by different cytokines such as IL-1.

Obesity is characterised by low-grade inflammation (Wellen et al. 2003; Greenberg and Obin 2006). Adipose tissue secretes different cytokines and adipokines (Iago et

al. 2007) that can affect iron metabolism through induction of hepcidin expression causing hypoferremia. Recently, leptin, the first discovered adipokine (Zhang et al. 1994), has been shown to induce hepcidin expression *in vitro* via JAK2-STAT3 signalling pathway in a time- and dose-dependent manner (Chung et al. 2007). Therefore, leptin in conjunction with other pro-inflammatory cytokines can contribute to hypoferremia observed in obese subjects. Recently, Aeberli and coworkers (2009) showed that overweight children have higher hepcidin levels and hypoferremia despite normal dietary iron intake and bioavailability. They concluded that the reduced iron availability for erythropoiesis in overweight children is likely due to hepcidin-mediated reduced iron absorption and/or increased iron sequestration.

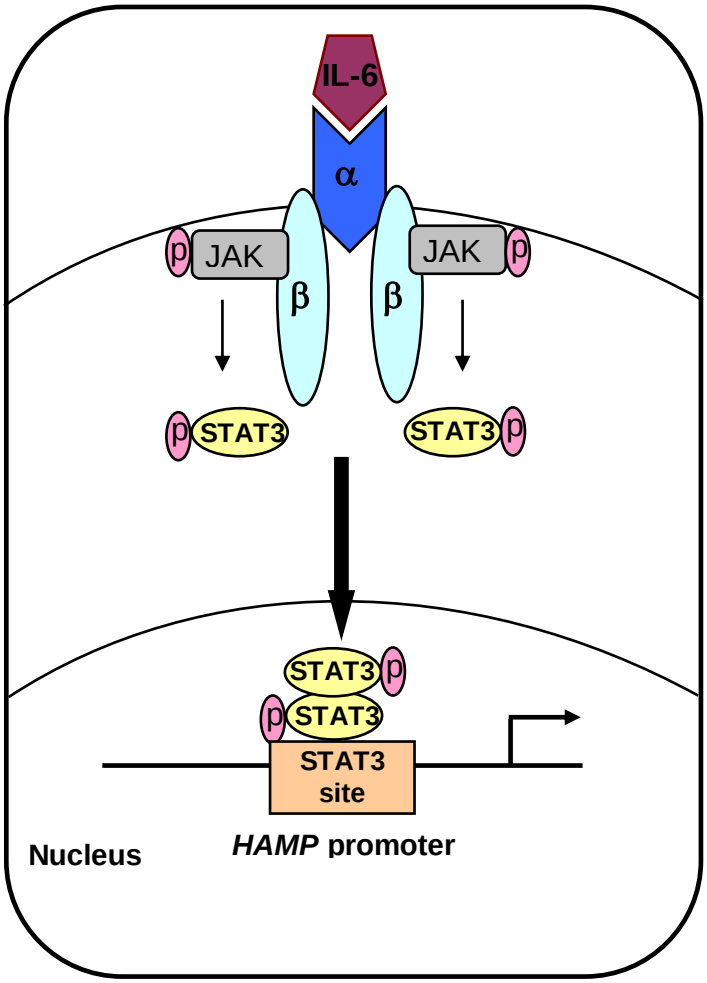

Figure 1.9 Mechanism of IL-6 induction of hepcidin expression.

Binding of IL-6 to the α subunit of the receptor induces dimerisation of the β subunits, which in turn are phosphorylated by the cytosolic JAK (janus kinase) proteins. The phosphorylation of β subunit stimulates the STAT pathway. STAT3 proteins are then phosphorylated, detach from the β subunit, and then translocate to the nucleus as dimers where it binds to response element within the hepcidin gene promoter inducing its transcription. Modified from (Fleming, 2007)

1.5.3.4.2 Regulation of hepcidin by hemojuvelin, BMPs, and Smads

Membrane expression of HJV leads to increased hepcidin expression; similarly, lack of HJV expression as in JH, is accompanied by reduced hepcidin expression (Babitt et al. 2006; Niederkofler et al. 2005). Babitt et al. (2006) showed that m-HJV binds to the type I BMP receptor and enhance the signal produced by the binding of BMP-2 and BMP-4. However, this signalling pathway is inhibited by s-HJV (Babitt et al. 2007). BMP-7 and BMP-9 have been also shown to be potent activators of hepcidin expression (Babitt et al. 2007; Truksa et al. 2006); however, their activity does not require HJV as they are not inhibited by s-HJV (Babitt et al. 2007).

BMPs bind to combinations of type I and type II serine/threonine kinase receptors (Babitt et al. 2006). The binding of BMPs to their receptors results in phosphorylation of type I by type II receptors that in turn phosphorylate a subset of receptor-activated Smads (R-Smads; Smad1, 5 and 8), which then bind to a common mediator Smad4. This complex then translocates to the nucleus where it binds to specific DNA motifs and regulates hepcidin gene transcription as shown in Figure 1.10. The importance of Smads in hepcidin regulation was shown in mice with liver-specific Smad4 deficiency, these mice showed very low hepcidin expression levels with iron deposition in the liver, pancreas, and kidney (Wang et al. 2005). Moreover, these mice lost their ability to regulate hepcidin in response to IL-6 suggesting a possible interaction between IL-6 and the Smad signalling pathway.

A recent study by Verga Falzacappa et al. (2008) demonstrated that a BMP-responsive element (BMP-RE) within the *hepcidin* promoter is important for HJV-dependent hepcidin gene expression. Moreover, the mutation of that BMP-RE abolishes hepcidin induction by IL-6 suggesting a possible crosstalk between the IL-6 and BMP-Smad pathways at the level of the hepcidin promoter.

Smad7 is a naturally occurring inhibitor of TGF-β signaling. It interacts and forms a complex with activated TGF-β type I receptors, thus blocking the phosphorylation and activation of receptor-Smads and subsequent downstream signals (Nakao et al. 1997, Hayashi et al. 1997, Imamura et al. 1997). Smad7 expression is induced by TGF-β1 in hepatic stellate cells (HSCs) (Stopa et al. 2000), which leads to a negative feed-back loop of signal transduction.

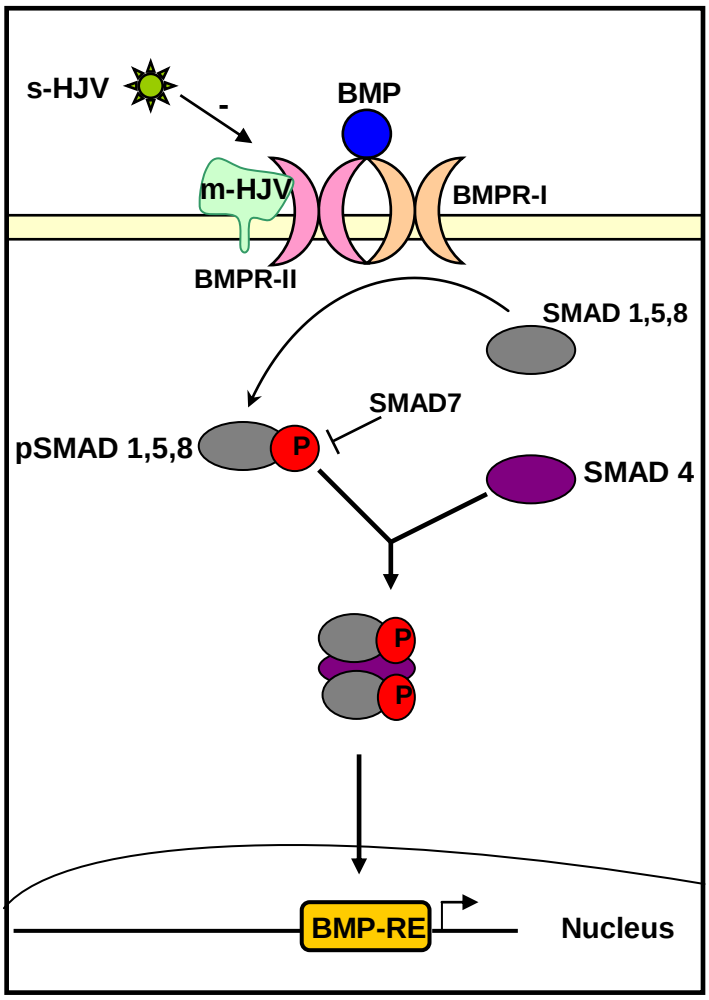

Figure 1.10 Schematic diagram representing the role of hemojuvelin in the BMP signaling pathway and hepcidin regulation.

Membrane HJV (m-HJV) interacts with BMPs and type I (BMPR-I) and type II (BMPR-II) receptors to form an active signalling complex. BMPR-II then phosphorylates BMPR-I which in turn phosphorylates Smad1, 5, and 8. Phosphorylated Smads then binds to Smad4, which translocates to the nucleus, where it binds to BMP responsive elements within the *hepcidin* promoter and induces its transcription. Soluble HJV (s-HJV) is able to interfere with BMP-SMAD signalling. Smad7 inhibits signalling pathway at the level of Smad phosphorylation by the activated receptor complex.

1.5.3.4.3 Regulation hepcidin by HFE and TFR2

Both HFE and hepcidin are expressed in hepatocytes (Holmstorm et al. 2003; Zhang et al. 2004). The role of hepatocyte-specific expression of *HFE* in regulation of iron homeostasis was confirmed by a recent study by Vujic spasic et al. (2008) conducted on *HFE*$^{-/-}$ mice. They found that hepatocyte-specific expression of *HFE* in these mice restores normal iron homeostasis. Therefore, HFE seems to function upstream of hepcidin to control iron homeostasis. In addition, mice with HFE disruption have low hepcidin expression (Ahmad et al. 2002; Bridle et al. 2003); moreover, when these mice were crossed with mice over-expressing hepcidin their iron overload was normalised (Nicolas et al. 2003). These findings suggest that HFE participates in the regulation of iron absorption via regulation of hepcidin expression; yet through an unknown mechanism.

HFE has been shown to interact with TFR1 (Feder et al. 1998; Waheed et al. 1999) via its α1 and α2 domains (Bennett et al. 2000). This binding lowers the affinity of TFR1 for Fe-TF by competing for iron-binding sites (Feder et al. 1998; Waheed et al. 1999). After the identification of TFR2 and its implication in type III haemochromatosis (Camaschella et al. 2000), an interaction between HFE and TFR2 was hypothesised similar to TFR1. However, this interaction could not be shown using soluble forms of both proteins *in vitro* (West, Jr et al. 2000). Recently, co-immunoprecipitation studies have demonstrated an interaction between HFE and TFR2 (Chen et al. 2007; Goswami and Andrews 2006). In addition, it was found that TFR2 competes with TFR1 for HFE binding.

TFR2 mutations are associated with low hepcidin expression levels (Nemeth et al. 2005), suggesting that this molecule is involved in hepcidin regulation and both TFR2 and HFE may be a part of the same pathway (Ganz and Nemeth 2006; Nemeth et al. 2005). It is hypothesised that the TFR2-HFE complex acts as an iron sensor, which regulates hepcidin expression in response to Fe-TF; however, this

remains to be confirmed. Recently, hepcidin induction by holotransferrin was associated with an interaction between TFR2 and HFE (Gao et al. 2009) suggesting the formation of a signalling complex composed of holotransferrin, TFR2, and HFE that stimulates hepcidin expression. On the other hand, holotransferrin failed to induce hepcidin expression in primary mouse hepatocytes lacking either HFE or TFR2 (Gao et al. 2009). However, a recent report showed that holotransferrin induced hepcidin expression in HFE-deficient primary mouse hepatocytes (Ramey et al. 2009). *In vitro*, the binding of TFR2 to holotransferrin resulted in stimulation of the mitogen-activated protein kinase (MAPK) pathway that was accompanied by increased phosphorylation of p38 and extracellular signal-regulated kinases 1/2 (ERK1/ERK2) (Calzolari et al. 2006). A similar response to holotransferrin was recently reported in isolated primary mouse hepatocytes which was blocked by an ERK inhibitor, implicating ERK1/2 in hepcidin expression in response to holotransferrin (Ramey et al. 2009).

1.5.3.4.4 Regulation of hepcidin by iron

The investigation of the mechanism of hepcidin expression by iron has been very difficult. In mouse models, both short-term and chronic iron administration result in increased hepatic hepcidin mRNA expression (Nemeth et al. 2004a; Pigeon et al. 2001). In human studies, oral iron administration increased urinary hepcidin excretion (Nemeth et al. 2004a); likewise, phlebotomy-induced iron deficiency in mice reduced hepcidin expression (Nicolas et al. 2002b).

In spite of the huge hepcidin response to iron *in vivo*, only a moderate response to holotransferrin has been reported in isolated primary hepatocytes and HepG2 cells (Lin et al. 2007; Gehrke et al. 2003). In addition, NTBI treatment of hepatocytes and HepG2 cells suppresses hepcidin expression (Nemeth et al. 2003; Gehrke et al. 2003). In primary hepatocytes, hepcidin induction by holotransferrin is blocked by s-

HJV and noggin, an inhibitor of BMP signalling (Lin et al. 2007). These findings are in agreement with the hypothesis that release of s-HJV is regulated by holotransferrin, where its release is inhibited by holotransferrin, resulting in m-HJV-mediated enhanced responsiveness to BMPs.

However, the mechanism of iron sensing in hepatocytes is not clearly understood. HFE and TFR2 are thought to be iron sensors by hepatocytes (Johnson and Enns 2004; Robb and Wessling-Resnick 2004; Goswami and Andrews 2006). TFR2 protein expression is modulated by Fe-TF in a time- and dose-dependent manner (Johnson and Enns 2004; Robb and Wessling-Resnick 2004); moreover, HFE can increase TFR2 levels independently of Fe-TF (Chen et al. 2007). These data suggest that HFE indirectly regulates hepcidin expression via modulation of TFR2 expression (Chen et al. 2007).

1.5.3.4.5 Regulation of hepcidin by anaemia, erythropoietic drive, and hypoxia

In humans, iron absorption is mainly synchronised by the rate of erythropoiesis and iron stores. Erythropoiesis regulates iron absorption regardless of iron stores to provide adequate iron for the production of red blood cells. In mice models, phenylhydrazine- or phlebotomy- induced anaemia are associated with low hepcidin expression (Nicolas et al. 2002b; c). They also showed that hypoxia and erythropoietin (EPO) suppress hepcidin expression. Therefore, anaemia may suppress hepcidin expression through tissue hypoxia, EPO, or increased erythropoiesis. Pak et al. (2006) showed that erythropoiesis is the main driving force to suppress hepcidin expression. They showed that blockage of erythropoiesis by chemicals, by EPO neutralising antibodies, or by irradiation eliminates the hepcidin-suppressive effect of anaemia (Pak et al. 2006; Vokurka et al. 2006).

Cases of anaemia with ineffective erythropoiesis, such as β-thalassemia major are characterised by increased iron absorption and subsequent iron overload (Nemeth and Ganz 2006; Origa et al. 2007) suggesting that erythropoietic drive dominates over iron overload in hepcidin regulation.

Increased erythropoiesis is also associated with increased levels of EPO and soluble TFR (sTFR), both of which are associated with low hepcidin expression (Kattamis et al. 2006). sTFR is produced by proteolytic cleavage of TFR, and circulates in the blood in the form of a monomer bound to TF. sTFR levels increase when less iron is available or when erythropoitic drive is stimulated (Beguin 2003; Nemeth et al. 2005). However, no alteration in hepcidin expression was found in mice overexpressing sTFR (Flanagan et al. 2006), a finding that remains to be justified. These findings support the hypothesis that the erythron creates a novel mediator that is transported to hepatocytes to regulate hepcidin expression. One possible candidate is growth differentiation factor 15 (GDF15), a member of the TGF-β superfamily isolated from thalassemia patients' sera that has been shown to suppress hepcidin expression *in vitro* (Tanno et al. 2007). However, it remains to be clarified whether GDF15 is the modulator of hepcidin expression in thalassemia and/or whether there are additional candidates. Recently, twisted gastrulation protein (TWSG1) has been suggested to mediate hepcidin suppression in anaemias with ineffective erythropoiesis. In addition, high TWSG1 expression levels were reported in a mouse model of thalassemia (Tanno et al. 2009). TWSG1, a BMP-binding protein, is produced by developing erythroblasts and was shown to suppress hepcidin mRNA *in vitro* by interfering with BMP-mediated hepcidin regulation (Tanno et al. 2009).

Hypoxia is associated with a reduction in hepcidin gene expression *in vivo* and *in vitro* (Nicolas et al. 2002b; Choi et al. 2007). Hypoxia may exert its effect on hepcidin expression via different pathways. As mentioned earlier, hypoxia induces

furin expression that in turns cleaves HJV (Silvestri et al. 2008a). Alternatively, hypoxia can induce the hepatic expression of the hypoxia-inducible factor-1 alpha (HIF1α) subunit (Semenza 2007) that associates with the human and murine hepcidin promoter (Peyssonnaux et al. 2007). Mice with hepatic disruption of the Hippel-Lindau gene causing increased HIF1α expression present a marked suppression in hepcidin expression. Moreover, IL-6 induction of hepcidin was abrogated by stabilisation of HIF1α, suggesting that the hypoxia signal overrides the inflammatory one (Peyssonnaux et al. 2007).

1.5.3.4.6 Regulation of hepcidin by TMPRSS6

TMPRSS6, also known as *matriptase-2*, encodes a type II plasma serine protease (Velasco et al. 2002). The protein is mainly expressed in the liver of mice and humans and is highly conserved in mammals (Ramsay et al. 2008). Mice with genetic disruption in the serine protease domain of matriptase2 (Mask) and *TMPRSS6*$^{-/-}$ mice have truncal alopecia and microcytic anaemia because of decreased intestinal iron absorption owing to increased hepcidin expression (Du et al. 2008; Folgueras et al. 2008). In addition, TMPRSS6 was shown to abrogate hepcidin induction by IL-6, BMPs, and HJV *in vitro* (Du et al. 2008).

Patients with mutations in *TMPRSS6* have iron-refractory iron deficiency anaemia (IRIDA). These patients show high hepcidin expression despite iron deficiency (Finberg et al. 2008; Guillem et al. 2008; Melis et al. 2008; Silvestri et al. 2009). These findings from mice and humans imply that matriptase2 is important to sense iron deficiency in mammals and acts as a potent inhibitor of hepcidin mRNA expression (Du et al. 2008).

Recently, Silvestri et al. (2008b) identified HJV as a substrate for matriptase-2, a finding that might provide an explanation for the anaemia observed with *TMPRSS6*

mutations. They demonstrated a physical interaction between matriptase-2 and HJV by immunoprecipitation. Moreover, they showed that over-expression of wild-type matriptase-2 and HJV *in vitro* induced a cleavage of HJV, which was absent in cells over-expressing mutant matriptase-2 lacking the proteolytic domain.

Truska et al. (2009) examined the relationship between HJV and matriptase-2 *in vivo* by crossing mice lacking HJV with mice lacking the protease domain of matriptase-2. This mouse model presented iron overload, high plasma iron and TF saturation, and low hepcidin levels. Moreover, these mice retain the ability to induce hepcidin in response to BMP-2, BMP-4, BMP-9, and IL-6, but not to dietary iron. The similarity between the phenotype of these mice and *HJV*$^{-/-}$ mice supports the hypothesis that matriptase-2 acts on HJV rather than another substrate downstream (Truska et al. 2009). *In vitro*, matriptase-2 cleaves m-HJV and generates multiple cleavage products and loss of m-HJV (Silvestri et al. 2008b). However, whether these cleavage products generated by matriptase2 are able to antagonise the binding of BMPs to cognate receptors, similar to s-HJV, remains to be determined.

In contrast, the s-HJV generated in response to iron deficiency or hypoxia *in vitro* has no effect on the surface expression of m-HJV (Silvestri et al. 2008a) suggesting that these stimuli act mainly by generating s-HJV, which acts as an antagonist for BMP-induced hepcidin expression. Lee (2009) suggested that the main function of matriptase-2 is to degrade m-HJV removing its positive effect on hepcidin expression rather than generate soluble antagonists. However, it remains to be determined how matriptase-2 is regulated and whether it is regulated by iron.

1.5.3.4.7 Regulation of hepcidin by upstream stimulatory factors (USFs)

The upstream stimulatory factors (USFs) are members of the basic helix-loop-helix leucine zipper (b-HLH-LZ) family of transcription factors. Their highly conserved C-

terminal domain is important for their DNA binding and dimerisation (Littlewood and Evan 1995). Sawadogo (1988) was first to explain USFs, he showed that adenovirus major late promoter (AdML) was transactivated by HeLa cell nuclear components through binding to the E-box motif with the canonical sequence CANNTG. In human, rat, and mouse, USFs has been shown to exist in two different forms, USF1 and USF2, encoded by two distinct genes (Henrion et al. 1995; 1996; Aperlo et al. 1996; Lin et al. 1994). Although they are ubiquitously expressed expressed in mammalian cells, the 43 kDa USF1 and 44 kDa USF2 proteins are expressed in different mammalian cells to different extents (Sirito et al. 1994; Viollet et al. 1996). USF1 and USF2 have been shown to bind DNA as homodimers and heterodimers and have comparable DNA binding abilities (Viollet et al. 1996; Sirito et al. 1992). However, Viollet et al. (1996) showed that the USF1-USF2 heterodimer is the main DNA binding species *in vivo*. These transcription factors control a broad range of genes including glucose-responsive genes, genes for glycoprotein B, vasopressin, and cyclin B1, as well as genes that control the circadian rhythm (*period, timeless, and clock*) (Yamashita et al. 2001; Wang and Sul 1995; Casado et al. 1999; Vallone et al. 2004; Farina et al. 1996; McDonald et al. 2001; Camara-Clayette et al. 1999). Gene ablation studies in mice have linked USF2 to iron metabolism. These mice showed lack of hepcidin expression and severe tissue iron overload (Nicolas et al. 2001). Moreover, USF1 and USF2 have been shown to regulate hepcidin gene expression through binding to E-boxes in hepcidin gene promoter (Bayele et al. 2006); these investigators also suggested that hepcidin expression might also be under pulsatile or rhythmic transcriptional control. Interestingly, TGF-β and β2m, which play a role in iron metabolism, are similarly regulated (Scholtz et al. 1996; Gobin et al. 2003). Therefore, USFs might be involved in iron homeostasis through regulation of these genes.

1.6 Aims

Hepcidin is the key regulator of systemic iron homeostasis acting as a negative regulator of intestinal iron absorption. In recent years, several proteins have been identified to act as upstream regulators of hepcidin expression, such as HFE and HJV. Despite the fact that HFE was discovered more than a decade ago, the exact role of HFE in hepcidin regulation is not clearly understood. Although hepcidin is regulated by iron, the molecules involved in this regulation, and whether HFE is involved in this regulation, remain to be clarified. Moreover, little is known about the regulation of *HJV* expression. Therefore, the aims of this study were:

- To further elucidate the mechanism of hepcidin regulation by iron *in vivo* and the role of HFE in hepcidin regulation by iron (Chapter 3).
- To study the regulation of *hepcidin* and *HJV* expression during inflammation by LPS *in vivo* and pro-inflammatory cytokines *in vitro* and the role of HFE in their regulation (Chapter 4).
- To investigate the possible regulation of *HJV* expression by USFs (Chapter 5).

Wild-type and *HFE* KO animal models were used to investigate the regulation of *hepcidin* by iron *in vivo*; the same animal models and *in vitro* studies were conducted to study the regulation of *hepcidin* and *HJV* expression during inflammation. A possible regulation of *HJV* by USFs was also examined *in vitro* and *in vivo* using the ChIP assay.

Chapter 2: General Materials and Methods

2.1 Gene expression levels by Real-Time Polymerase Chain Reaction

2.1.1 RNA extraction by TRIzol® reagent

Precautions were taken against contamination of samples with RNAses. The bench working area was cleaned with RNAse ZAP (Ambion Ltd., UK), disposable gloves were worn at all times, and sterile disposable plasticware and pipettes for RNA work only were used.

RNA extraction was carried out using the TRIzol®/chloroform extraction and isopropyl alcohol precipitation according to the manufacturer's instructions (Chomczynski and Sacchi 1987). TRIzol® reagent (Invitrogen Ltd., UK) was added to the cells or frozen tissue (1mL was used per well of six well plate or 100mg tissue) and then transferred to sterile 1.5mL microcentrifuge tubes. Samples were then incubated at room temperature for 5 minutes for complete dissociation of nucleotide/protein complexes. Chloroform (Sigma, UK) was added to the samples (200μL/ sample) and samples were shaken vigorously by hand for 15 seconds. Tubes were incubated at room temperature for 3 minutes, and then centrifuged at 12,000 x g for 15 minutes at 4^{o}C. The mixture separated into a lower red, phenol-choloroform phase, which contained DNA and protein and a colourless upper aqueous phase containing the RNA. The aqueous phase was carefully removed with a pipette and transferred to a clean microcentrifuge tube and the lower organic phase was discarded.

The RNA was precipitated from the aqueous phase with isopropyl alcohol (Sigma, UK) (500μL/ sample), by vortexing, incubating samples for 10 minutes at room temperature and centrifuging at 12,000 x g for 10 minutes at 4^{o}C. The supernatant was removed and the RNA pellet washed in 70% ethanol (1mL/sample) and centrifuged at 8000 x g for 5 minutes at 4^{o}C. The supernatant was removed and the

pellet air-dried for 10 minutes at room temperature. The RNA pellet was resuspended in DEPC- treated water (Ambion Ltd., UK).

2.1.2 RNA concentration and purity

The RNA concentration was quantified by measuring the absorbance of RNA in water at 260nm using a spectrophotometer (Beckman DU 650 Spectrophotometer, High Wycombe, UK). The concentration was calculated using the formula:
RNA concentration (μg/mL) = A_{260} x dilution x 40. The RNA had an $A_{260/280}$ ratio between 1.8 and 2.00 indicating RNA free of contamination. RNA quality was further assessed by running the RNA solution on a 2% agarose/Tris-Acetate EDTA (TAE) gel stained with ethidium bromide and visualised under UV light to show RNA integrity and to detect the presence of contaminating DNA. The RNA samples were kept at -80^{o}C until required.

2.1.3 cDNA synthesis

Complementary DNA was synthesised using the Abgene Reverse-iT 1st Strand Synthesis Kit (Abgene, UK) using the PTC-100 thermocycler (MJ Research, NV, USA). Following DNase I (Ambion Ltd., UK) treatment for 30 minutes at 37^{o}C, 1μg of total RNA was used as a template and incubated with 500nM oligo dT primer and water for 5 minutes at 70^{o}C to denature any secondary structure. First strand synthesis buffer, dNTPs, and reverse transcriptase were added. Reaction components were incubated at 47^{o}C for 60 minutes then at 70^{o}C for 10 minutes to inactivate the enzyme. cDNA was stored at -20^{o}C until required.

2.1.4 Real-Time PCR amplification

Real-time quantitative gene analysis was performed using a Lightcycler system II (Roche Diagnostics GmbH, Germany), Lightcycler version 3.5 software (Roche Molecular Biochemicals, Germany) and QuantiTect SYBR® Green PCR Kit (Qiagen, UK). QuantiTect SYBR® Green master mix contains SYBR® Green**,** HotStart Taq DNA Polymerase and a dNTP mix (including dUTP)**.** SYBR® green present in the PCR mixture binds to dsDNA, but not ssDNA, which is excited at 494nm and emits light at 521nm. Monitoring of emissions at 521nm allows indirect quantification of the dsDNA concentration within the reaction capillary. Fluorescence at 521nm is quantified within each reaction capillary following the completion of every PCR extension step. The PCR cycle at which the fluorescence reaches a threshold value is used as a measure of relative template concentration. The second derivative maximal method was used to determine threshold values of fluorescence. Cycle threshold (Ct) values were obtained for each gene of interest and the housekeeping gene. Gene expression was normalized to that of the housekeeping gene and represented as ΔCt values. For each sample the mean of the ΔCt values was calculated. SYBR green does not interfere with PCR cycling as it dissociates from the DNA product during the denaturation step of the following PCR cycle. The experiment was performed in duplicate. For each sample, the gene of interest and the housekeeping gene were run in parallel. Each PCR reaction mix contained 1μL of cDNA template, 5pmol forward and 5pmol reverse primers, 10μL 2x QuantiTect SYBR® Green PCR master mix and water to a final volume of 20μL. The primers used for real-time PCR were synthesised by Sigma-Genosys Ltd. (Poole, UK). BLAST (http://www.ncbi.nlm.nih.gov/BLAST/) searches were conducted on all primers to ensure unique specificity to the gene of interest. Primers' suitability was determined by producing a single product of the correct length after PCR cycling

and agarose gel electrophoresis. A single peak on the meltcurve analysis was also used to determine the suitability of the primers used. For the primers' sequences see Table1.

Table 2.1 Mouse and human primer sequences used for real-time PCR analysis

Primer	Accession No*	Forward 5´----------3´	Tm°	Reverse 5´----------3´	Tm°	Product length (bp)
Mouse *β-Actin*	NM_007393.2	GACGGCCAAGTCATCACTATT	65.0	CCACAGGATTCCATACCCAAGA	66.8	88
Mouse *hepcidin 1*	AF503444.1	CCTATCTCCATCAACAGATG	57.0	AACAGATACCACACTGGGAA	59.4	170
Mouse *TNF-α*	NM_013693.2	CCAGACCCTCACACTCAGATCA	66.6	CACTTGGTGGTTTGCTACGAC	64.4	58
Mouse *IL-6*	NM_031168.1	AGTTGCCTTCTTGGGACTGA	63.8	TCCACGATTTCCCAGAGAAC	64	156
Mouse *TGF-β*	NM_011577.1	CACCGGAGAGCCCTGGATA	67.4	TGTACAGCTGCCGCACACA	68.1	72
Mouse *hemojuvelin*	NM_027126.3	TGCCAGAAGGCTGTGTAAGG	65.3	TCTAAATCCGTCAAGAAGACTCG	63.4	149
Mouse *Bmp-6*	NM_007556	ATGGCAGGACTGGATCATTGC	68.4	CCATCACAGTAGTTGGCAGCG	67.8	53
Mouse *Bmp-2*	NM_007553.2	TGGAAGTGGCCCATTTAGAG	63.8	TGACGCTTTTCTCGTTTGTG	63.9	165
Mouse *Bmp-4*	NM_007554.2	ACGTAGTCCCAAGCATCACC	63.9	TCAGTTCAGTGGGGACACAA	64.3	262
Human *GAPDH*	NM_002046.3	TGGTATCGTGGAAGGACTC	60.1	AGTAGAGGCAGGGATGATG	59.2	129
Human *hepcidin*	NM_021175.2	CTGCAACCCCAGGACAGAG	66	GGAATAAATAAGGAAGGGAGG	59.3	191
Human *hemojuvelin*	NM_145277.4	GGAGCTTGGCCTCTACTGGA	65.7	ATGGTGAGCTTCCGGGTG	66.3	100

*GenBank accession numbers (http://www.ncbi.nlm.nih.gov)

2.1.5 Real time PCR cycling parameters

The real time PCR conditions were as suggested in the manufacturer's protocol (Qiagen, UK), this included an initial denaturation at 95 ^{o}C for 15 minutes, followed by PCR cycles of denaturation at 94 ^{o}C for 15 seconds, annealing at 65 ^{o}C for 20 seconds, extension at 72 ^{o}C for 30 seconds. The temperature of fluorescence acquisition was set at 2^{o}C below the product melting temperature and held for 5 seconds. Meltcurve analysis followed each RT-PCR run.

The ratio of relative abundance of the gene of interest to constitutively expressed housekeeping gene was calculated by the Lightcycler Relative Quantification software version 1.0 (RelQuant) (Roche Diagnostics GmbH, Germany).

2.1.6 Analysis of melting curve

Meltcurve analysis was performed after PCR amplification cycles. Each dsDNA has its own melting temperature based on its length and G-C content; therefore, melting curve analysis can be used to identify unwanted PCR by-products such as primer-dimers and non-specific products. This analysis involved heating the PCR products at 65 ^{o}C for 10 seconds; the temperature was then slowly increased to 95^{o}C with a ramp rate of 0.5^{o}C/second, whilst the fluorescence was monitored continuously. At 65^{o}C all DNA in the PCR product is double stranded; therefore, SYBR green binding and fluorescence emission is maximal. As the temperature is elevated, DNA is denatured, SYBR green dissociates and fluorescence is decreased. Meltcurve was produced by plotting fluorescence against temperature (Figure 2.1). Primer-dimers and other non-specific products can be identified using this method as they usually melt at lower temperatures than the desired product. Increasing the fluorescence acquisition temperature used during PCR to above the melting temperature of the primer-dimer and non-specific products, eliminates any

fluorescence due to the presence of these products. The presence of a single peak in melting curve indicates the specificity of the primers used (Figure 2.2). PCR products were also analysed by gel electrophoresis, as described in Section 2.

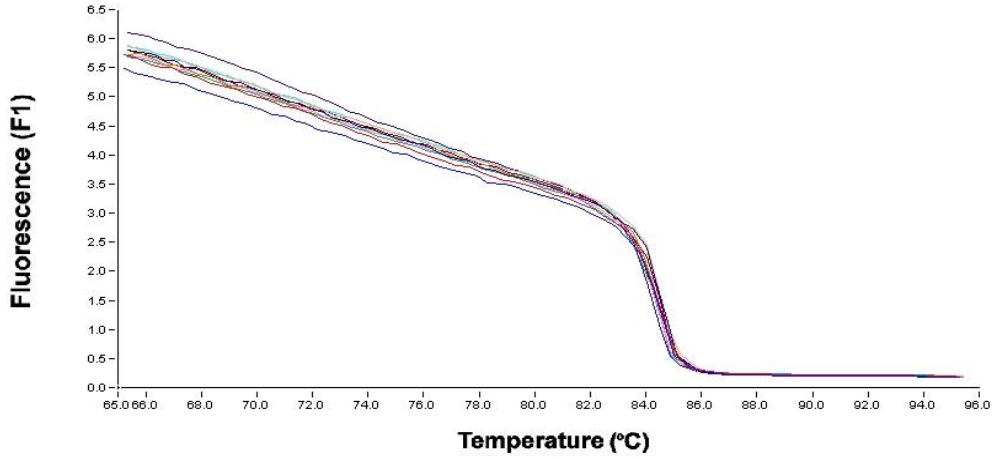

Figure 2.1 Representative graph of the meltcurve of a gene product.
At 65^{o}C all DNA in the PCR product is double stranded; therefore, SYBR green binding and fluorescence emission is maximal. As the temperature is elevated, DNA is denatured, SYBR green dissociates and fluorescence is decreased.

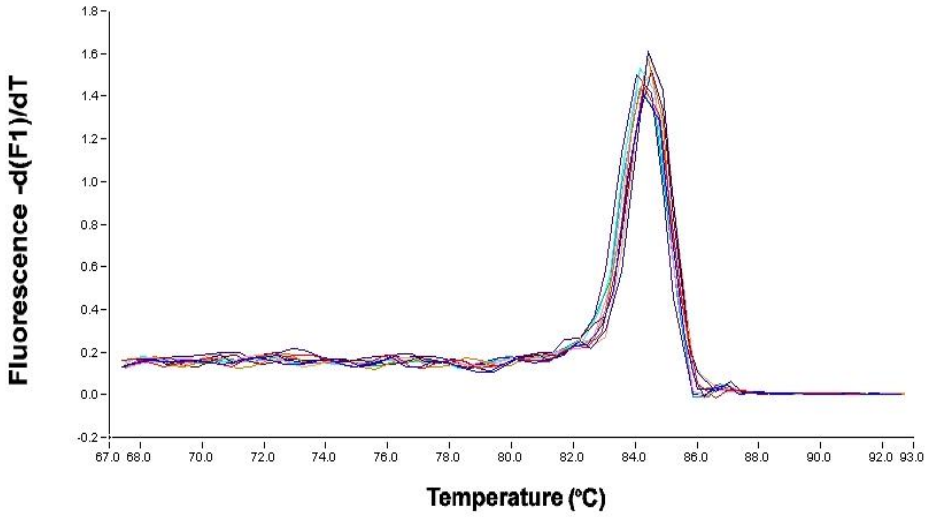

Figure 2.2 Representative graph of meltcurve peak analysis of a gene product.

A graph of meltcurve peak analysis of a gene PCR product showing a single peak that indicates specificity of the primers used for PCR amplification.

2.2 Agarose gel electrophoresis

To visually analyse DNA and RNA, samples were resolved on 1% (w/v) agarose/TAE gels containing 0.5 μg/mL ethidium bromide (Sigma, UK). Samples were run alongside the molecular weight markers (Bioline, UK) using a horizontal gel apparatus (Bio-Rad, UK). Gels were prepared by dissolving 2g agarose in 200mL of 1X TAE by microwaving. Ethidium bromide (0.5μg/mL) was then added to the cooled molten agarose and then poured into a gel cast, a comb added and the gel allowed to set for 30 minutes at room temperature before use.

Before loading, DNA or RNA was mixed with 0.6 volume of 6x loading buffer (0.25% bromophenol blue (w/v), 40% Sucrose (w/v) in water). Electrophoresis was carried out at 120 volts for 20 minutes. DNA/RNA bands were visualised under

ultraviolet illumination and images were captured using a Fluor-S MultiImager (Bio-Rad).

2.3 Generation of *HJV* promoter-reporter construct

2.3.1 Amplification of *HJV* promoter

A portion of the human *HJV* promoter extending 1.2Kb upstream of the beginning of the first *HJV* exon was amplified by PCR from placental genomic DNA as a template using the PTC-100 thermocycler (MJ Research) and Phusion High-Fidelity DNA Polymerase (New England Biolabs, UK). The following primers were used: sense 5' CATGCTAGCAAGTGACCCTCCTGCCTCAG, the *Nhe*I restriction site is underlined; antisense 5' CATCTCGAGCTGCTGTCTCACTGAGGTCA, the *Xho*I restriction site is underlined, both synthesised by Sigma-Genosys Ltd.. The PCR reaction mix contained 250ng of human genomic DNA, forward and reverse primers to a final concentration of 0.5μM, 10μL 5x Phusion HF Buffer, 500μM each of dNTPs, 1 unit of Phusion DNA polymerase, and water to a final volume of 50μL. The cycling parameters were 98^{o}C for 10 seconds (denaturation), 72^{o}C for 2 min (annealing and extension); 35 cycles of PCR were performed with a final extension for 7 min at 72^{o}C. This was followed by gel electrophoresis of the PCR product, as described in Section 2.2 The PCR product was purified from the gel as described in Section 2.3.2 below.

2.3.2 Gel extraction of PCR products

PCR products were purified from TAE gels using a Geneclean kit (BIO101, Anachem Ltd, Luton, UK). About 300mg of the product was excised from the gel using a clean scalpel and placed into a 1.5mL microcentrifuge tube with 400μL of glassmilk. Tubes were then incubated at 55^{o}C for 10 minutes to dissolve the gel. Glassmilk-DNA/gel mixture was placed into Geneclean spin filter column and

centrifuged at 12,000 x g for 1 minute to bind the DNA to the membrane and glassmilk/gel in the flowthrough was discarded. The membrane was washed with wash buffer and dried by centrifugation at 12,000x g for 2 minutes. DNA was then resuspended in 15μL elution buffer and collected by centrifuging at 12,000 x g for 1 minute. The DNA concentration was quantified using a spectrophotometer (Beckman DU 650 Spectrophotometer) and calculated using the formula:

DNA concentration (μg/mL) = A_{260} x dilution x 50

2.3.3 Restriction digestion of the PCR product

Restriction digestion of clean PCR product was performed in 1X NEB buffer 2 (10 mM Tris-HCl, 10 mM $MgCl_2$, 50 mM NaCl, 1 mM Dithiothreitol (DTT) pH 7.9, 10 units of *NheI*, 10 units of *XhoI* (New England Biolabs) and water to a final volume of 50 μL. The reaction was incubated at 37^{o}C for 24 hours followed by incubation at 65 ^{o}C for 10 minutes to inactivate the enzymes. The digested PCR product was then purified as described in Section 2.3.2

2.3.4 Ligation of the PCR product into luciferase reporter vector

The PCR product was cloned into *NheI* and *XhoI* sites of pre-digested pGL3 basic vector (Promega, UK) (Figure 2.3) to generate a *HJV* promoter-luciferase reporter construct (*HJV*P1.2-luc). Ligation reaction was carried out using 200ng of clean-digested PCR product, 100ng of digested pGL3-basic vector, NEB's 2X T4 DNA ligase buffer (100mM Tris-HCl, pH 7.5; 20mM $MgCl_2$; 20 mM DTT; 2mM ATP), 4.5 units of T4 DNA ligase. The 10μL reaction was incubated at 12^{o}C overnight.

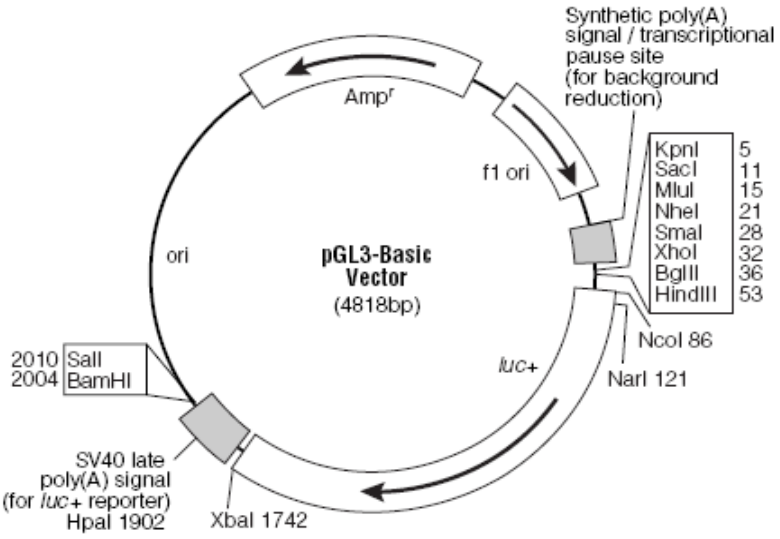

Figure 2.3 pGL3-Basic Vector circle map showing different cloning sites.
The vector contains cDNA encoding the modified firefly luciferase (*luc*+), the ampicillin resistance gene in E. coli (Amp^r), and the origin of replication in E. coli (ori). From http://www.promega.com/tbs/tm033/tm033.pdf.

2.3.5 Transformation

DH5-α competent cells (Invitrogen) were retrieved from -80^{o}C storage and immediately placed on ice until thawed. To 100μL of cells, 5μL ligation product was added. A pipette tip was used to mix the reaction by stirring, taking care not to pipette up and down. The tube was kept on ice for 30 minutes and was subsequently heat-shocked for 35 seconds in a water bath set exactly at 42^{o}C. The tube was then put on ice for 2 minutes after which 500μL of SOC medium (Invitrogen) was added and the tube incubated at 37^{o}C, 230 rpm for 60 minutes. Cells were plated out onto selection plates: LB agar with 100μg/mL ampicillin and left to grow overnight at 37^{o}C. Individual colonies were then picked up and

resuspended in 5mL LB broth at 37°C, 230 rpm overnight. Plasmid DNA was isolated using Nucleospin® plasmid miniprep columns (Macherey-Nagel, Duren, Germany), as described in Section 2.3.6 below.

2.3.6 Plasmid DNA isolation

Cells were pelleted at 11,000 x g for 30 seconds and supernatant was discarded. The pellet was resuspended in 250μL of buffer A1, after which 250μL of SDS/alkaline lysis buffer (A2) was added and the sample was inverted 6-8 times and incubated at room temperature for 2 minutes. Neutralisation buffer A3 (300μL) was added and the tube was inverted gently 6-8 times. The sample was then centrifuged at 12,000 x g for 10 minutes at room temperature. A Nucleospin® plasmid column was placed into a collection tube and the resulting supernatant was added to the column. This was centrifuged for 1 minute at 11,000 x g and the flowthrough was discarded. The Nucleospin® column was washed with 600μL washing buffer (AW) and then centrifuged at 11,000 x g for 1 minute, discarding the flow through. The column was centrifuged again for 2 minutes to dry the membrane. The column was placed into a clean microcentrifuge tube and 50μl of elution buffer AE was added to the centre of the column. This was left to stand for 2 minutes and then centrifuged at 11,000 x g for 1 minute.

2.3.7 Restriction digestion of isolated plasmid

The resulting eluent was then digested with *NheI* and *XhoI* performed in 1X NEB buffer 2 (10 mM Tris-HCl, 10 mM $MgCl_2$, 50 mM NaCl, 1 mM DTT), 10 units of *Nhe I* , 10 units of *Xho I* (New England Biolabs) and water to a final volume of 20μL. The reaction was incubated at 37°C for 2 hours. The digested samples were then run on

a 1% agarose/ethidium bromide gel in parallel with the undigested one to verify that they contained the correct size of promoter insert. The plasmid was then sent for sequencing (Wolfson Institute for Biomedical Research, UCL, UK).

2.4 Growth and propagation of HuH7 and HepG2 cells

The HuH7 and HepG2 human hepatoma cell lines were from our departmental liquid nitrogen frozen stocks (Department of Biochemistry and Molecular Biology, UCL, UK). The cells were removed from liquid nitrogen storage and left at room temperature for 1 minute to thaw. The cell-containing ampoule was then placed into a 37^{o}C water bath for 3 minutes to ensure that the cells were completely thawed. Cells were then gently added to a 75cm^{2} flask containing complete growth medium, Dulbecco's Modified Eagle's Medium (DMEM) (Invitrogen), supplemented with 10% heat-inactivated foetal bovine serum (FBS) (Invitrogen), 1X antibiotic-antimycotic mixture (Invitrogen) containing 100 units penicillin, 100μg streptomycin, and 250ng amphotericin B per mL medium. The cells were grown at 37^{o}C in a humidified atmosphere of 5% CO_2 in air.

2.5 Transfection of HuH7 and HepG2 cells and luciferase studies

Transfections were performed using Lipofectamine 2000 (Invitrogen). The day before transfection, cells were seeded onto Costar 24-well plates (Corning, USA) at densities of approximately 10^4 cells per well and the medium was changed after 24 hours until the cells reached 85% confluence. For each well to be transfected, 200ng of *HJV*P1.2-luc, mt*HJV*P1.2-luc, or 200ng of the empty pGL3Basic vector (Promega) and 50ng pSVβgal vector (Promega), which was used as an internal control to normalize transfection efficiencies, were diluted in 50μL OptiMEM 1

(Invitrogen). In addition, for each well to be transfected, 1μL of Lipofectamine2000 was diluted into 50μL OptiMEM 1. Both diluted DNA and Lipofectamine were added together and mixed gently. The mixture was then incubated at room temperature for 20 minutes to allow DNA-liposome complexes to form. Meanwhile, wells containing cells to be transfected were washed with serum-free DMEM and all remaining residual liquid was removed by aspiration. Serum-free DMEM (800μL) was then added to each well. To each well, 100μL of complex was gently added and plates were incubated at 37^{o}C overnight. The medium was then replaced with fresh DMEM with 10% FBS and antibiotics. After a further 24 hours, the medium was replaced with fresh serum-free DMEM or serum-free DMEM containing TNF-α (20ng/ml; R&D Systems, Minneapolis, MN, USA) for 24 hours. This was done in triplicate. At the end of the incubation period, the medium was removed by aspiration and the cells were washed twice with PBS (Invitrogen). Cells were lysed with 100μL 1X Reporter Lysis Buffer (Promega) ensuring that all cells were covered. Plates were then placed into the -80^{o}C freezer for a freeze-thaw cycle to ensure complete lysis of all cells. Cells were transferred to a microcentrifuge tube, and placed on ice. The tube was vortexed and then centrifuged at 12,000 x g for 15 seconds at room temperature. The supernatant was transferred to a new tube and then stored at -80^{o}C for future use.

The luciferase assay was carried out using Luciferase Assay System (Promega), 96 well plates (Nunc, Paisley, United Kingdom) and a Tropix microplate luminometer (Applied Biosystems, Foster city, CA, USA). Cell lysate (20μL) was added to each well. The luminometer was programmed to inject 100μL of the Luciferase Assay Reagent per well then to measure the light emitted for 10 seconds. The β-galactosidase assay was done using the Beta-Glo reagent (Promega). Beta-Glo (20μL) reagent was added per well and the plate was incubated for 30 minutes at

room temperature before measurement of light emission using the microplate luminometer.

2.6 Western blot analysis

2.6.1 Preparation of cell and tissue lysate

Cells were washed twice with cold PBS taking care not to disturb the monolayer. To each well, 200μL of ice-cold RIPA buffer (50mM Tris-HCl pH 8.0, 150mM NaCl, 1% NP-40, 0.5% sodium deoxycholate, 0.1% SDS) containing Complete Mini Protease Inhibitor Cocktail (Roche) and phosphatase inhibitors (Sigma) was added. Plates were kept at -80^{o}C to aid cell lysis, lysates were then transferred to sterile microcentrifuge tubes. For total tissue lysate preparation, tissues were placed in a microcentrifuge tube and homogenised in RIPA buffer with protease and phosphatase inhibitors using a Pellet Pestle ® Motor (Anachem, UK). Tubes were then kept for 30 minutes on ice. Tubes from both cell and tissue lysates were then placed into a microcentrifuge at 4^{o}C and spun for 15 minutes at 13000 x g. The supernatant was then transferred to a fresh sterile microcentrifuge tube and stored at -80^{o}C for future use. The pellet was discarded.

2.6.2 Protein quantification in cell and tissue lysates

Proteins were quantified by using the BCA Protein Assay Kit (Pierce). Standards were prepared from bovine serum albumin (BSA) (ranging from 0-2000μg/mL). The working reagent (WR) was freshly prepared by mixing 50 parts of BCA™ Reagent A with 1 part of BCA™ Reagent B.

In a 96-well microplate, 25µl of each standard or unknown sample replicate were added per well. To each well, 200µl of the WR was added and the plate was mixed thoroughly on a plate shaker for 30 seconds. The plate was then incubated at 37°C for 30 minutes followed by cooling to room temperature. Absorbance was then measured at 570nm using a plate reader (Labsystem Multiscan MS, UK).

The average absorbance of the blank replicates was subtracted from the absorbance measurements of all other individual standard and sample replicates.

A standard curve was prepared by plotting the average blank-corrected absorbance for each standard vs. its concentration in µg/ml (Figure 2.4). The standard curve was used to determine the protein concentration of each unknown sample.

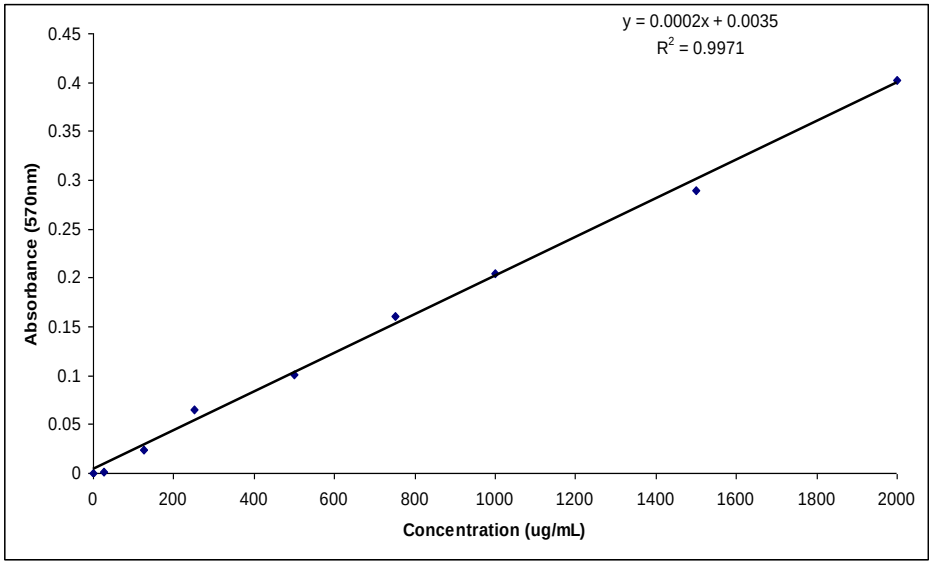

Figure 2.4 BCA protein standard curve.

The standard curve was made by plotting the average blank-corrected absorbance for each standard vs. its concentration in µg/ml. The equation used for determination of protein concentration is shown on the figure.

2.6.3 SDS-PAGE

Sodium dodecyl sulphate-polyacrylamide gel electrophoresis (SDS-PAGE) was performed using XCell *SureLock*™ and 1.5 mm gel cassettes (Invitrogen). A 12% (v/v) gel was prepared using 0.375M Tris-HCl (pH 8.8), 12% (v/v) bisacrylamide (Sigma), 0.1% (w/v) SDS, 0.0625% (w/v) ammonium persulphate and 0.0003% (v/v) TEMED. The gel solution was mixed and approximately 8ml was poured into gel cassettes. About 2mL of butanol was added to the top of the gel to exclude air and encourage a straight interface. After the gel had set (after approximately 60 minutes), the butanol was washed off with distilled water. A 4% (v/v) stacking gel was then prepared using 0.125M Tris-HCl (pH 6.8), 4% (v/v) bisacrylamide, 0.1% (w/v) SDS, 0.0625% (w/v) ammonium persulphate and 0.0003% (v/v) TEMED. The gel (about 2mL) was poured into the remaining space and lane-forming 1.5 mm plastic combs (10 tooth) (Invitrogen) were quickly inserted. The gel was left to polymerise for approximately 45 minutes. Once the gel had set, the comb was carefully removed and the apparatus was assembled according to the manufacturer's instructions for running of the gel. Reservoir buffer was prepared from 10X Glycin-Tric-SDS buffer (Sigma) by mixing 1 part of 10X buffer with 9 parts of distilled water. This was added to the gel-containing apparatus taking care to cover the wells with buffer. About 50μg of protein/sample was mixed with an equal volume of 2X loading buffer (0.5M Tris-HCl (pH 6.8), 4.4% (w/v) SDS, 20% (v/v) glycerol, 3% (v/v) DTT and 0.02% (w/v) bromophenol blue in distilled water). Samples were loaded into each well along with a Kaleidoscope Prestained Standard (Bio-Rad). The gel was run at 120V until the bromophenol dye front had migrated to about 1cm from the bottom of the gel (approximately 1 hour). Cassettes were levered apart using a spatula.

2.6.4 Immunoblotting

Protein was transferred onto a PVDF membrane (Amersham Pharmacia Biotech UK Ltd, Berkshire, UK) by semi-dry blotting for 2 hours at a constant current of 1mA/cm^3 (Trans-blot semi-dry transfer cell, Bio-Rad). Protein transfer was verified by staining the membrane with Ponceau S reagent (Sigma) for 5 minutes at room temperature. The stained proteins are bright pink in colour. Ponceau S reagent was removed by rinsing with distilled water. Membrane was blocked with PBS-T (PBS with 0.1% (v/v) Tween 20) containing 5% non-fat milk for 1 hour at room temperature to block non-specific antibody binding. The membrane was then incubated with 1:500 diluted primary antibody overnight at 4^oC on a rocking platform and then washed 3x for 10 minutes each in PBS-T. Primary antibody was probed with HRP-conjugated IgG 1:5000 diluted in PBS-T for 1 hour at room temperature, with continuous rocking. Following secondary antibody incubation, the membrane was washed 3 times with PBS-T for 10 minutes (each) at room temperature. The membrane was then subjected to enhanced chemiluminescence (ECL) detection (Amersham Life Science). Equal volumes of Reagent 1 and Reagent 2 were mixed together then added to the membrane and left for 1 minute. Membrane was then photographed by a CCD camera of a Fujifilm LAS-1000 system (Fuji photo film Co., Ltd, Japan) and images were captured.

2.6.5 Stripping and re-probing western blots

Following ECL, PVDF membranes were either placed directly into PBS-T, or stored wrapped in SaranWrap at 4^{o}C. Where re-probing with anti-actin primary antibody (Abcam, UK) was required as a loading control, antibodies were stripped from membranes by immersing them in freshly prepared stripping buffer (62.5 mM Tris-HCl, pH 6.7; 2% SDS; 100 mM 2-mercaptoethanol) at 50^{o}C for 30 minutes with occasional agitation. The membrane was then washed repeatedly in PBS-T before blocking and re-blotting following standard procedures, as described before.

2.7 Statistical analysis

Data is presented as mean ± standard error of the mean (SEM). Statistical significant differences ($p<0.05$) between two groups were determined using Student's two-tailed unpaired t-test. To test the statistically significant differences between groups in experiments with more than two groups, ANOVA followed by Bonferroni post hoc test was used. Statistical analysis was conducted with Graphpad Prism software (San Diego, CA).

Chapter 3: Regulation of Hepcidin Expression by Iron

3.1 Introduction

Hepcidin is a key regulator of systemic iron homeostasis. It mainly coordinates iron usage and storage with iron uptake (Ganz 2006). It exerts its function by binding to IREG1 on the surface of hepatocytes, macrophages, and enterocytes, and inducing its internalisation and degradation (Nemeth et al. 2004b), and subsequently leads to iron accumulation in macrophages and liver as well as a reduction in intestinal iron absorption.

Hepcidin production is stimulated by dietary or parenteral iron loading (Pigeon et al. 2001); therefore, it provides a feedback mechanism to decrease intestinal iron absorption. In contrast, hepcidin expression is decreased in response to iron deficiency, anaemia, and hypoxia (Nicolas et al. 2002b); therefore, this provides more iron to be directed to the bone marrow to sustain erythropoiesis. However, no iron responsive elements (IRE) have been identified within the hepcidin gene suggesting that hepcidin modulation by iron is not mediated by iron regulatory proteins, but by other signalling pathways.

Mutations in *hepcidin*, *hemojuvelin*, *HFE*, and *TFR2* genes are all associated with abnormally low hepcidin expression levels despite iron overload (Roetto et al. 2003; Papanikolaou et al. 2004; Nemeth et al. 2005; Piperno et al. 2007). Mutations in the *HFE* gene are associated with the first characterised form of HH. Despite the fact that HFE was discovered more than a decade ago (Feder et al. 1996), the role of HFE in hepcidin regulation is not clearly understood. HFE binds to TFR1 (Parkkila et al. 1997; Feder et al. 1998; Waheed et al. 1999) and TFR2 (Goswami and Andrews 2007; West et al. 2000; Waheed et al. 2008). In addition, mice with liver-specific disruption of *HFE* present the same phenotype as *HFE* KO mice suggesting that the liver is the main site of HFE action to regulate iron homeostasis (Vujic Spasic et al. 2008). However, these findings did not elucidate how HFE regulates hepcidin expression and iron homeostasis. Recently it has been

hypothesised that HFE is sequestered by TFR1, and that Fe-TF displaces HFE from TFR1. HFE in turn binds to TFR2 and this complex signals to regulate hepcidin expression. However, the exact mechanism remains to be fully elucidated.

Recently, Babitt *et al.* (2006) showed that the BMP-Smad signalling pathway regulates hepcidin expression. This pathway involves members of the TGF-β superfamily, as described in Chapter 1.

HJV has been shown to act as a BMP co-receptor to induce hepcidin expression. Further support for the role of BMP-Smad signalling in hepcidin regulation comes from the finding that mice with liver-targeted disruption of the *Smad-4* gene develop iron overload and express very little hepcidin; in addition, these mice fail to induce hepcidin in response to inflammatory stimulation or iron (Wang *et al.* 2005). Taken together, these findings clearly demonstrate the importance of the BMP-Smad signalling pathway in the regulation of *hepcidin* expression.

Although hepcidin is regulated by iron, the molecules involved in this regulation are not clearly identified. In particular, the involvement of HJV-BMP-Smad signalling in hepcidin regulation by iron remains to be clarified. Moreover, the role of HFE in this signalling pathway is not known. Therefore, this study is aimed to elucidate the involvement of BMP-Smad signalling in hepcidin regulation by iron. To study the effect of iron deficiency, mice were either fed with a control iron diet or an iron-deficient diet. To induce iron loading, C57Bl/6 wild-type mice were injected with an iron compound (sodium ferric gluconate). To investigate whether HFE is involved in hepcidin regulation by iron and BMP-Smad signalling pathway, *HFE* KO mice were also examined in the settings of iron deficiency and iron loading.

3.2 Methods

3.2.1 Effect of dietary iron deficiency on C57Bl/6 wild-type and *HFE* KO mice

Weanling (at the age of 3 weeks) wild-type C57Bl/6 (n=10) and *HFE* KO (of C57Bl/6 background strain; n=10) female mice were supplied by the Comparative Biology Unit at the Royal Free and UCL Medical School, London. All the experimental procedures were conducted in agreement with the UK animals (Scientific Procedures) Act, 1986. Animals were kept in a 12 hour light-dark cycle, provided with water *ad libitum*, and were fed either a control diet (RM1 diet; 180 mg Fe/kg diet; n= 5 of each genotype) or an iron-deficient diet (7.5 mg Fe/kg diet; n=5 from each genotype) for 4 weeks. At the end of the experimental period (at 7 weeks of age), mice were terminally anaesthetised with intraperitoneal pentobarbitone sodium (Sagatal, Rhone-Merieux, UK, 90 mg/Kg). The livers were collected, snap frozen in liquid N_2, and stored at -80^{o}C for real-time PCR analysis, liver iron quantification, and immunoblotting. Blood was collected by cardiac puncture and serum was separated from the blood for serum iron measurement using a commercial kit (Pointe Scientific Inc, USA) as described below.

3.2.2 Effect of parenteral iron loading on C57Bl/6 wild-type and *HFE* KO mice

Weanling C57Bl/6 and *HFE* KO female 3 week old mice were fed a normal iron RM1 diet for two weeks, after which 2.5 mg iron as sodium ferric gluconate (Ferrlecit®, Rhone-Poulenc Rorer, UK) or an equal volume of saline was administered intraperitoneally three times per week for two weeks. Three days after the last iron injection, mice were terminally anaesthetised with intraperitoneal pentobarbitone sodium. Livers were collected for hepatic iron, mRNA quantification, and immunoblotting. Blood samples were collected by cardiac puncture. Serum was

separated from clotted blood samples after centrifugation for 10 minutes at 5000 x g and used for iron measurement.

3.2.3 Liver iron quantification in wild-type and *HFE* KO mice by a modified Torrance and Bothwell method (Torrance and Bothwell 1980)

Liver samples were oven dried at 55^{o}C for at least 72 hours to ensure that the tissue was completely dry. Dried samples were then accurately weighed and placed in clean and dry 1.5mL microfuge tubes. Samples were then digested in 1 mL acid mixture (30% HCl, 10% trichloroacetic acid) at 65^{o}C for 20 hours. A blank was also prepared in the same way, but without tissue sample. After acid digestion, samples were taken out of the oven and left to cool at room temperature. The working chromogen reagent and iron standard solution were freshly prepared just before the assay. The composition of the reagents was as follows:

Working chromogen solution

20mL distilled water, 20 mL saturated sodium acetate, and 4 mL Chromogen reagent (0.1% bathophenanthroline sulfonate and 1% thioglycollic acid).

Iron Standard solution

423μl distilled water, 27μl HCl, and 50μl stock iron solution (20mM).

Blanks, standards, and samples were prepared in triplicate in plastic cuvettes with the amounts as shown in the table below:

	Working chromogen reagent (mL)	Fe Standard (μl)	Blank/Sample (μl)	Distilled water (μl)
Blank	1	0	25 from blank	225
Standard	1	125	25 from blank	100
Samples	1	0	25 from sample	225

Samples were incubated at 37^{o}C for 10 minutes, after which, the absorbance of blank, standard, and sample triplicates were measured at 535nm against water blank using a spectrophotometer (Beckman DU 650 spectrophotometer). Results are expressed per gram dry weight of tissue.

3.2.4 Measurement of serum iron and transferrin saturation

Serum iron and transferrin saturation was measured by using a commercial kit (Pointe Scientific Inc.) as instructed by the manufacturer and described below.

3.2.4.1 Measurement of serum iron

In a 96-well plate, 40μL of each sample, standard, and water blank were added per well in duplicate. Iron buffer reagent (200μL) was then added into each well and the absorbance (A1) was measured at 560nm using a plate reader. Iron colour reagent (4 μL) was added to each well and plate was incubated at 37^{o}C for 10 minutes, after which the absorbance was measured at 560nm (A2).

Total Serum iron in each sample was calculated using the following formula:

$$\frac{\text{A2 sample - A1 sample}}{\text{A2 standard - A1 standard}} \times 500 \quad (\mu g/dL)$$

3.2.4.2 Measurement of Unsaturated Iron-Binding Capacity (UIBC)

In a 96-well plate, 160μL of UIBC reagent were added to samples, standards, and blanks wells. Aliquots (40μL) from each sample, standard, and 80 μL from water as a blank were added per well in duplicate. 40 μL from standard or water were added to sample or standard wells, respectively. Absorbance was then measured at 560nm (A1). Iron colour reagent (4 μL) was added to each well, and the plate was incubated at 37^{o}C for 10 minutes, after which the absorbance was measured at 560nm (A2).

Total UIBC in each sample was calculated using the following formula

$$500 - \frac{\text{A2 sample-A1 sample}}{\text{A2 standard-A1 standard}} \times 500 \quad (\mu g/dL)$$

Total iron binding capacity was then calculated using the following formula

TIBC (μg/dL) = Serum iron + UIBC

Transferrin saturation was then calculated by the following formula using serum iron and TIBC:

TF saturation (%) = serum iron/TIBC x 100

3.3 Results

3.3.1 Effect of dietary iron deficiency on wild-type and *HFE* KO mice

3.3.1.1 Effect on liver iron content, serum iron, transferrin saturation

Liver iron levels in both wild-type and *HFE* KO mice fed an iron deficient diet for 4 weeks were significantly decreased (Figure 3.1). In addition, serum iron and transferrin saturation were also decreased in wild-type and *HFE* KO mice fed an iron deficient diet but this did not reach statistical significance (Figure 3.2). Of note, when fed on a control iron diet, serum iron and transferrin saturation were higher in *HFE* KO mice compared to wild-type animals fed on a control (RM1) diet. In addition, liver iron content was significantly higher in *HFE* KO mice fed on a RM1 diet compared to wild-type animals. When fed on an iron deficient diet, no difference was observed in liver iron, serum iron, and transferrin saturation between wild-type and *HFE* KO mice.

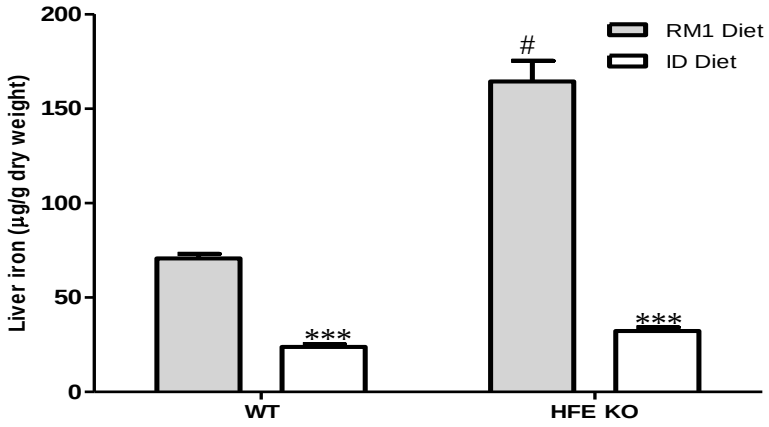

Figure 3.1 Effect of dietary iron deficiency on hepatic iron content in wild-type (WT) and *HFE* KO mice.

Mice were fed either a control (RM1) or an iron deficient (ID) diet for 4 weeks after being weaned. The liver was removed and iron was quantified. Hepatic iron content was significantly decreased by the iron deficient diet in both genotypes. Hepatic iron content was significantly higher in *HFE* KO than wild-type mice fed on an RM1 diet. Data are mean±SEM, n=5 mice per group, *** denotes significant difference from the RM1 diet group ($p<0.001$). $^{\#}$ denotes significant difference from the equivalent wild-type group ($p<0.001$).

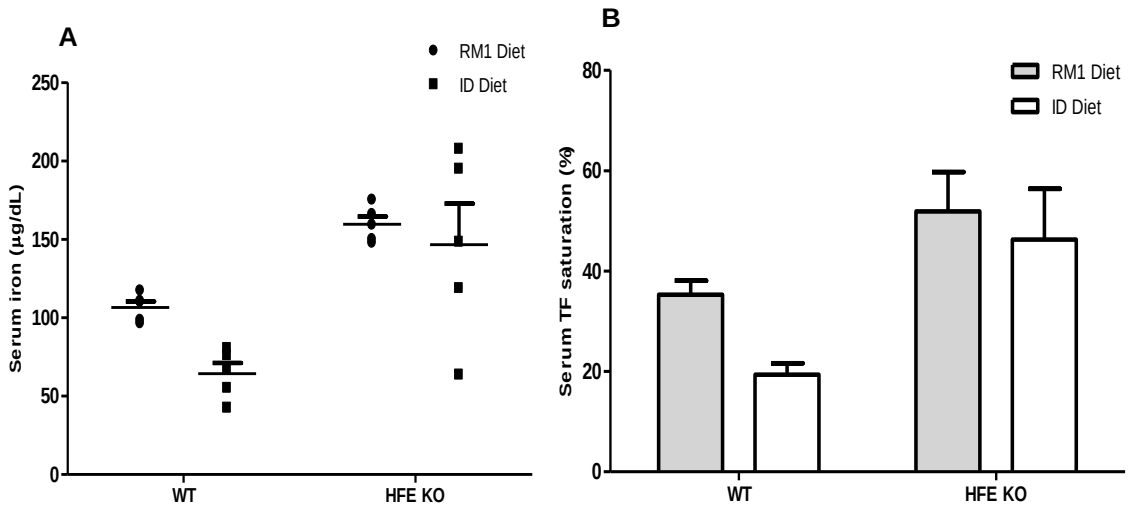

Figure 3.2 Effect of dietary iron deficiency on serum iron (A) and transferrin saturation (B) in wild-type (WT) and *HFE* KO mice.

Mice were fed either a control (RM1) or an iron deficient (ID) diet for 4 weeks after being weaned. The serum was separated from the blood and serum total iron and transferrin saturation were measured. Serum iron and transferrin saturation were decreased in WT and *HFE* KO mice fed an iron deficient diet though not significantly. Moreover, when fed on a control iron diet, *HFE* KO mice showed higher serum iron and transferrin saturation than WT mice. Data are mean±SEM, n=5 mice per group.

3.3.1.2 Effect on hepatic gene expression

3.3.1.2.1 Effect on *hepcidin 1* and *hemojuvelin* gene expression

Analysis of *hepcidin 1* and *HJV* gene expression in wild-type and *HFE* KO mice fed an iron deficient diet showed a significant decrease in *hepcidin 1* expression in both genotypes with no change in *HJV* expression (Figure 3.3). *Hepcidin 1* expression in *HFE* KO mice was lower than that of wild-type animals fed on an RM1 diet; however, it did not reach statistical significance.

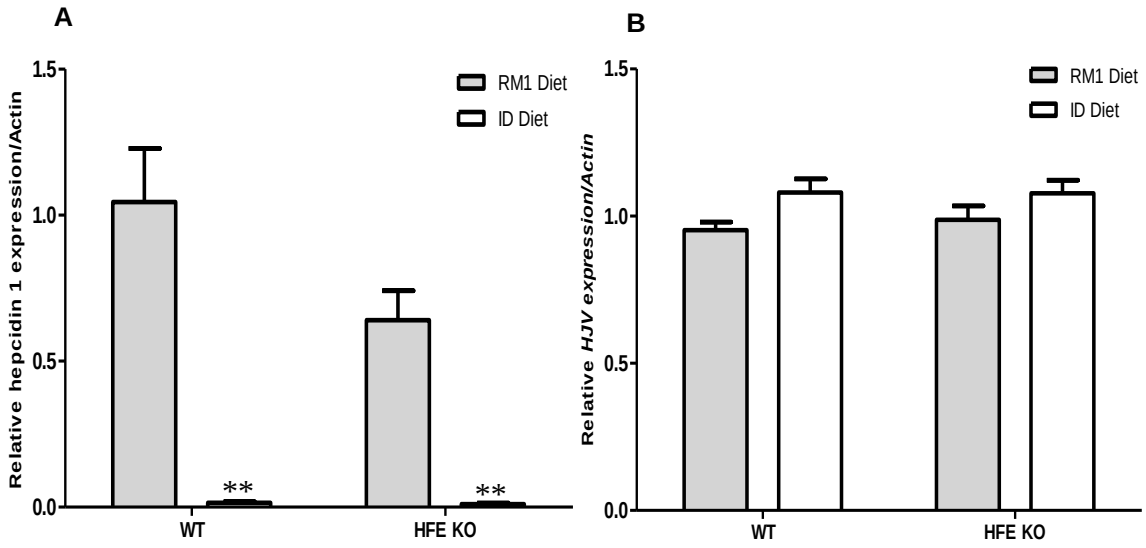

Figure 3.3 Effect of dietary iron deficiency on hepatic gene expression of *hepcidin 1* (A) and *HJV* (B) in wild-type (WT) and *HFE* KO mice.
Hepcidin1 mRNA expression significantly decreased in mice fed on an iron deficient diet with no change in *HJV* expression in both genotypes. Data are mean±SEM, n=5 mice per group, ** denotes significant difference from the RM1 diet group ($p<0.01$).

3.3.1.2.2 Effect on *BMP-2, BMP-4, and BMP-6* gene expression

To investigate the effect of iron deficiency on hepatic expression of BMPs and the role of HFE in the response, gene expression levels of *BMP-2*, -4, and -6 mRNAs were quantified in wild-type and *HFE* KO mice fed an iron deficient diet. As shown in Figure 3.4, dietary iron deficiency significantly decreased the hepatic expression of *BMP-6* in both mouse genotypes with no change in *BMP-2* and *BMP-4* expression levels. The expression of BMP 2, 4, and 6 were not significantly different between *HFE* KO and wild-type mice.

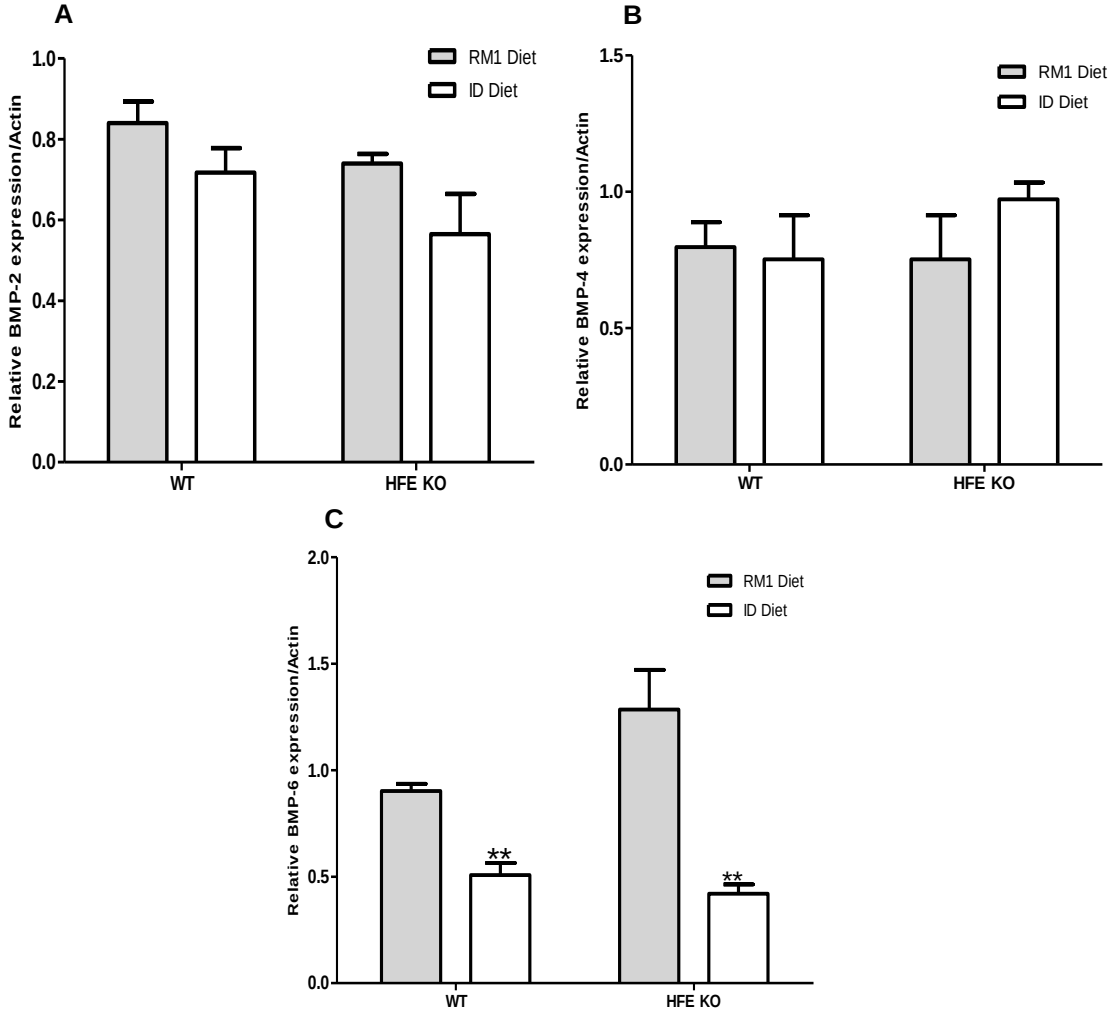

Figure 3.4 Effect of dietary iron deficiency on hepatic gene expression of *BMP-2* (A), *BMP-4* (B), and *BMP-6* (C) in wild-type (WT) and *HFE* KO mice.
Hepatic expression of *BMP-6* was significantly decreased in WT and *HFE* KO mice fed on an iron deficient diet; whereas, no change was observed in *BMP-2* and *BMP-4* expression levels Data are mean±SEM, n=5 mice per group, ** denotes significant difference from the RM1 diet group ($p<0.01$).

3.3.1.3 Effect on Smad 1, Smad 5, and Smad 8 phosphorylation in the liver

To investigate whether dietary iron deficiency affects the downstream signal of BMP, phosphorylated Smad1, 5, and 8 were quantified by Western blotting in the liver of wild-type and *HFE* KO mice fed an iron deficient diet. As shown in Figure 3.5, dietary iron deficiency caused a significant decrease in the phosphorylation of Smad 1/5/8 in wild-type and *HFE* KO mice.

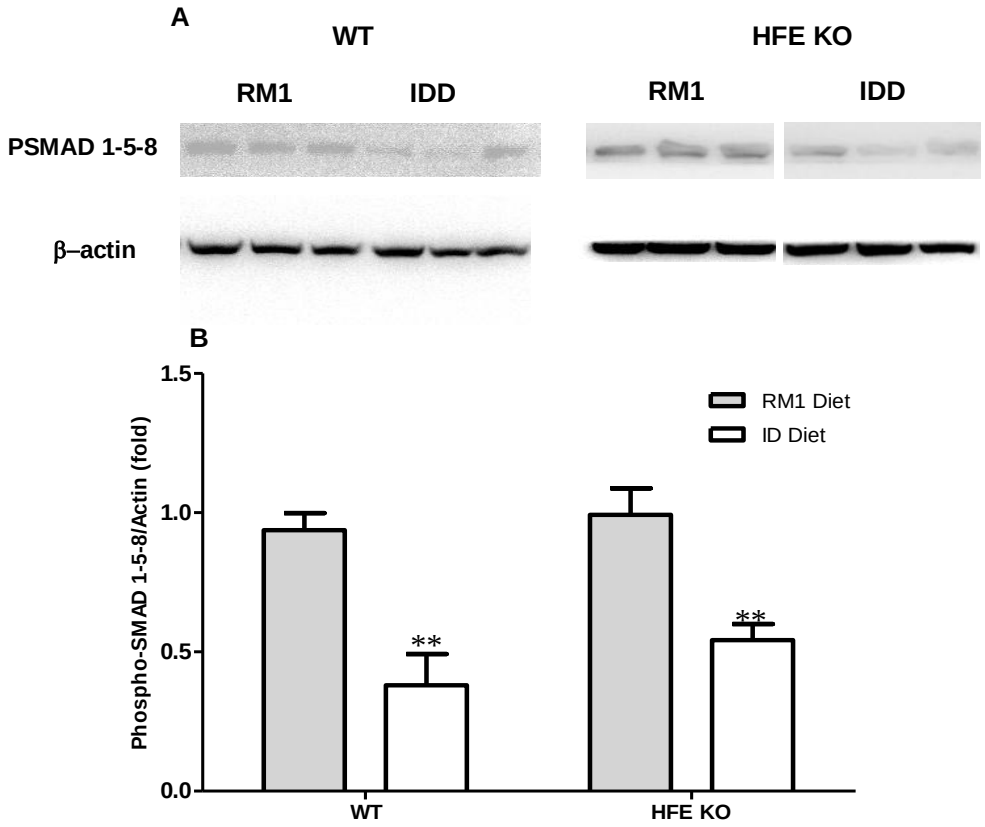

Figure 3.5 Effect of dietary iron deficiency on Smad1/5/8 phosphorylation in wild-type (WT) and *HFE* KO mice.

(A) Western blot analysis of liver lysates from control or iron-deficient WT and *HFE* KO mice using an antibody to phosphorylated Smad1/5/8, β-actin was used as loading control. (B) Chemiluminescence was quantified using Quantity One software and the ratio of phosphorylated Smad1/5/8 to β-actin was calculated. Mean ratios of four samples (± SEM) are represented on this figure, relative to the mean ratio of the control wild type mice or *HFE* KO mice. Phosphorylation of Smad1/5/8 was significantly decreased by iron deficiency in wild-type and *HFE* KO mice. Statistically significant differences relative to control mice were determined by Student *t* tests. ** denotes significant difference from the RM1 diet group ($p<0.01$).

3.3.2 Effect of parenteral iron loading on wild-type and *HFE* KO mice

3.3.2.1 Effect on liver iron content, serum iron, transferrin saturation

Parenteral Iron loading significantly increased liver iron content, serum iron, and transferrin saturation in wild-type and *HFE* KO mice (Figure 3.6 and 3.7). The serum iron was significantly higher in saline-injected (control) *HFE* KO mice compared to control wild-type animals. Moreover, no differences were observed in the liver iron and transferrin saturation between wild-type and *HFE* KO mice.

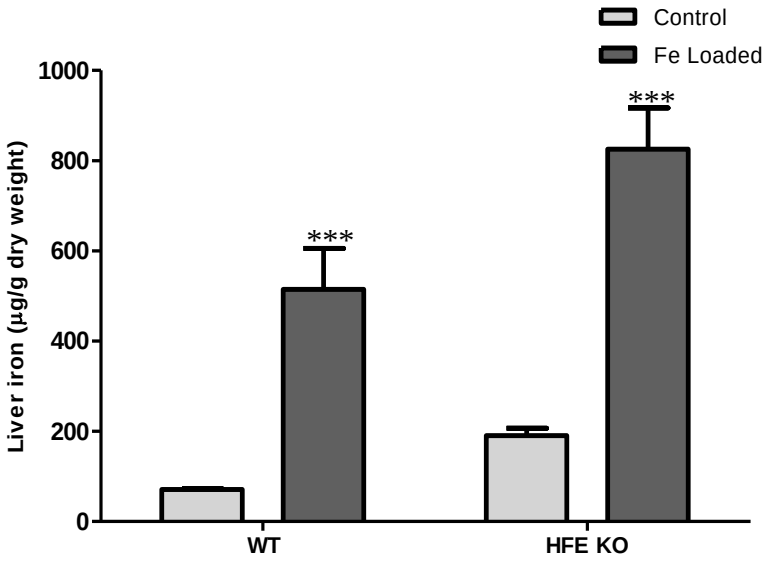

Figure 3.6 Effect of parenteral iron loading on hepatic iron content in wild-type (WT) and *HFE* KO mice.

Five week old WT or *HFE* KO mice fed on an RM1 diet were either injected with saline (control) or sodium ferric gluconate (Fe loaded) for 2 weeks. The liver was removed and iron was quantified. Hepatic iron content was significantly increased by iron loading in both genotypes. Data are mean±SEM, n=5 mice per group. *** denotes significant difference from the control group ($p<0.001$).

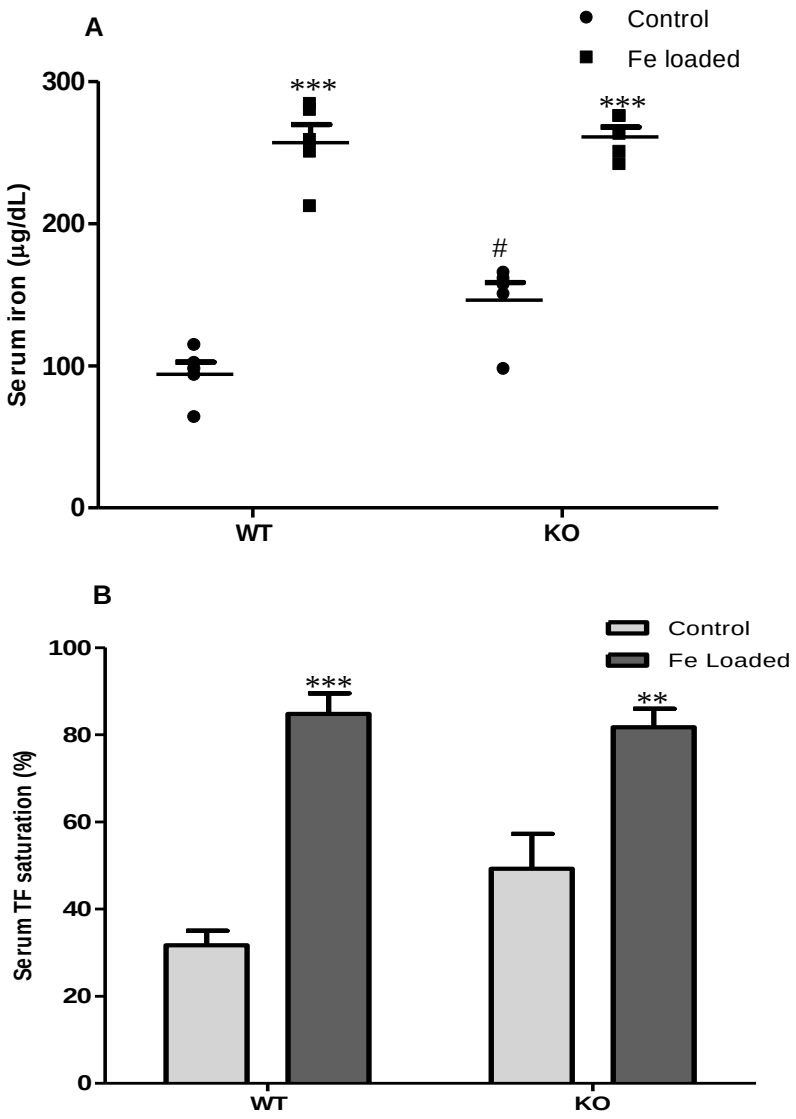

Figure 3.7 Effect of parenteral iron loading on serum iron and transferrin saturation in wild-type (WT) and *HFE* KO mice.

Five week old WT or *HFE* KO mice were either injected with saline (control) or sodium ferric gluconate (Fe loaded) for 2 weeks. The serum was separated from the blood and serum total iron and transferrin saturation were measured. Serum iron and transferrin saturation were significantly increased in iron-loaded wild-type and *HFE* KO mice. Data are Mean±SEM, n=5 mice per group. ***, ** denotes significant difference from the control group ($p<0.001$, $p<0.01$ respectively). # denotes significant difference from the equivalent wild-type group ($p<0.05$).

3.3.2.2 Effect on hepatic gene expression

3.3.2.2.1 Effect on *hepcidin 1* and *HJV* gene expression

In iron loaded wild-type and *HFE* KO mice, the hepatic expression of *hepcidin* 1 significantly increased with no change in *HJV* expression levels. Of note, in *HFE* KO mice, the iron-induced *hepcidin 1* expression was less prominent and significantly lower than that of wild-type mice as shown in Figure 3.8.

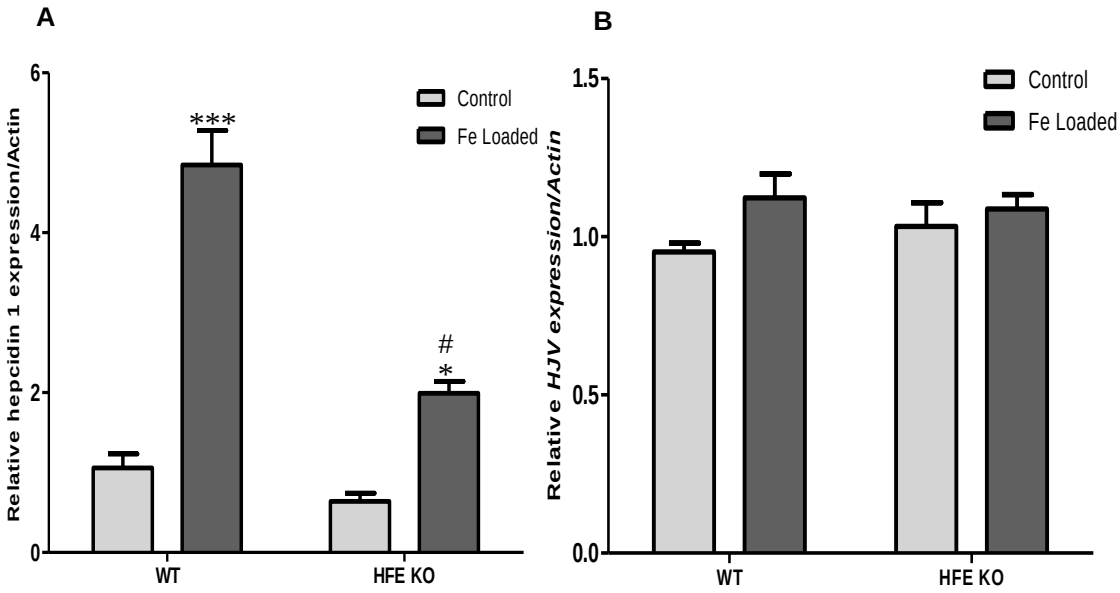

Figure 3.8 Effect of parenteral iron loading on hepatic gene expression of *hepcidin 1* (A) and *HJV* (B) in wild-type (WT) and *HFE* KO mice.

Hepcidin1 gene expression significantly increased in iron-loaded WT and *HFE* KO mice with no change in *HJV* expression in both genotypes. Of note, the iron-induced hepcidin expression was less prominent and significantly lower in *HFE* KO mice. Data are mean±SEM, n=5 mice per group, ***, * denotes significant difference from the control group ($p<0.001$, $p<0.05$ respectively) $^{\#}$ denotes significant difference from the equivalent wild-type group ($p<0.01$).

3.3.2.2.2 Effect on *BMP-2, BMP-4, and BMP-6* gene expression

To investigate the effect of iron loading on hepatic expression of BMPs and the role of HFE in the response, gene expression levels of *BMP-2, 4, and 6* were quantified in wild-type and *HFE* KO mice subjected to parenteral iron loading. As shown in Figure 3.9, iron loading significantly increased the hepatic expression of *BMP-6* in both mouse genotypes with no change in *BMP-2* and *BMP-4* expression levels.

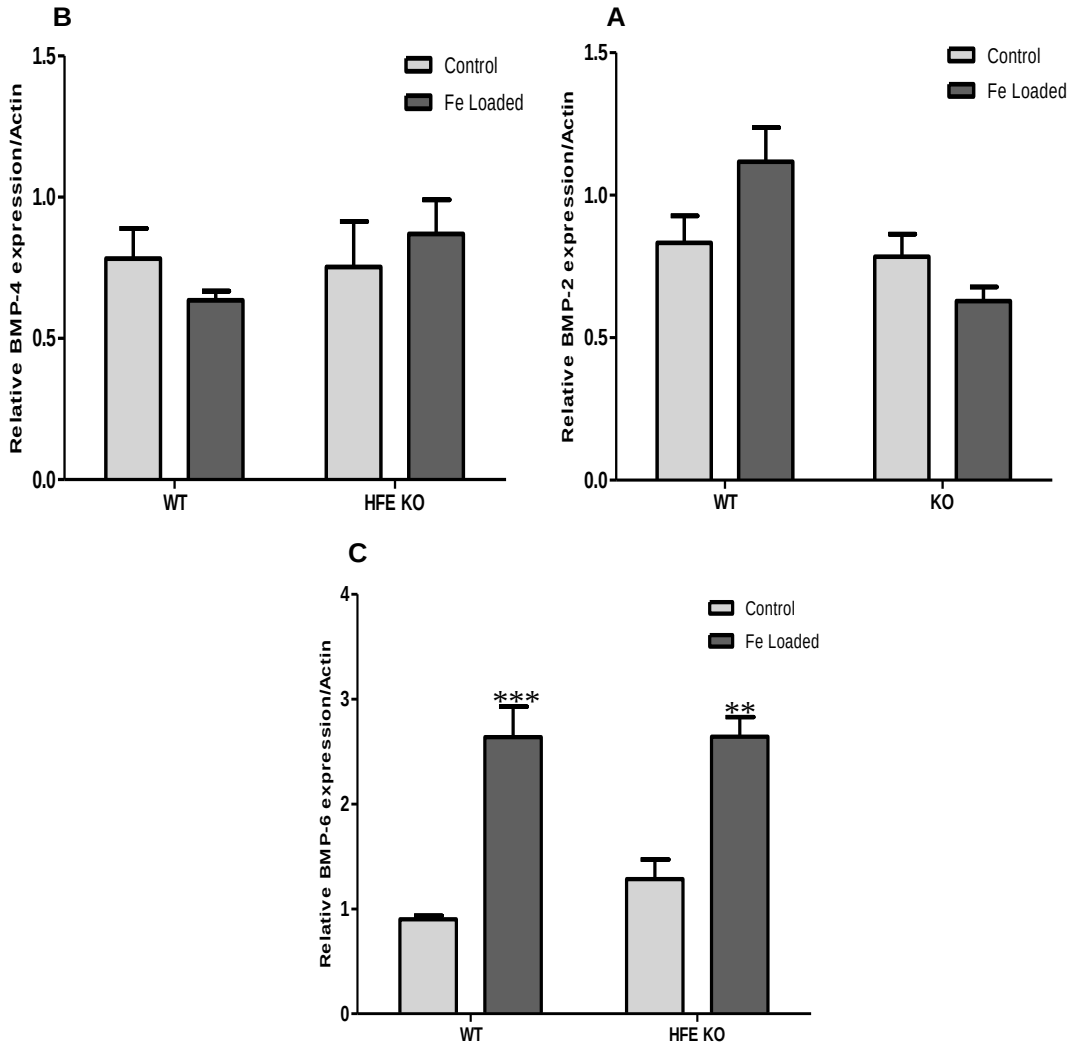

Figure 3.9 Effect of iron loading on hepatic gene expression of *BMP-2* (A), *BMP-4* (B), and *BMP-6* (C) in wild-type (WT) and *HFE* KO mice.

Hepatic expression of *BMP-6* was significantly increased in iron-loaded WT and *HFE* KO mice, whereas, no change was observed in *BMP-2* and *BMP-4* expression levels. Data are mean±SEM, n=5 mice per group, ***, ** denotes significant difference from the control group ($p<0.001$, $p<0.01$ respectively).

3.3.2.3 Effect on Smad 1/5/8 phosphorylation in the liver

To investigate whether BMP-6 induction in response to iron loading was reflected by an increase in phosphorylation of Smad 1/5/8 and whether HFE is involved, the phosphorylated Smad 1/5/8 was quantified in the liver of iron-loaded wild-type and *HFE* KO mice by western blotting. As shown in Figure 3.10, parenteral iron loading significantly increased the phosphorylation of Smad 1/5/8 in wild-type mice. In contrast, Smad1, 5, and 8 phosphorylation was not significantly induced by iron loading in *HFE* KO mice.

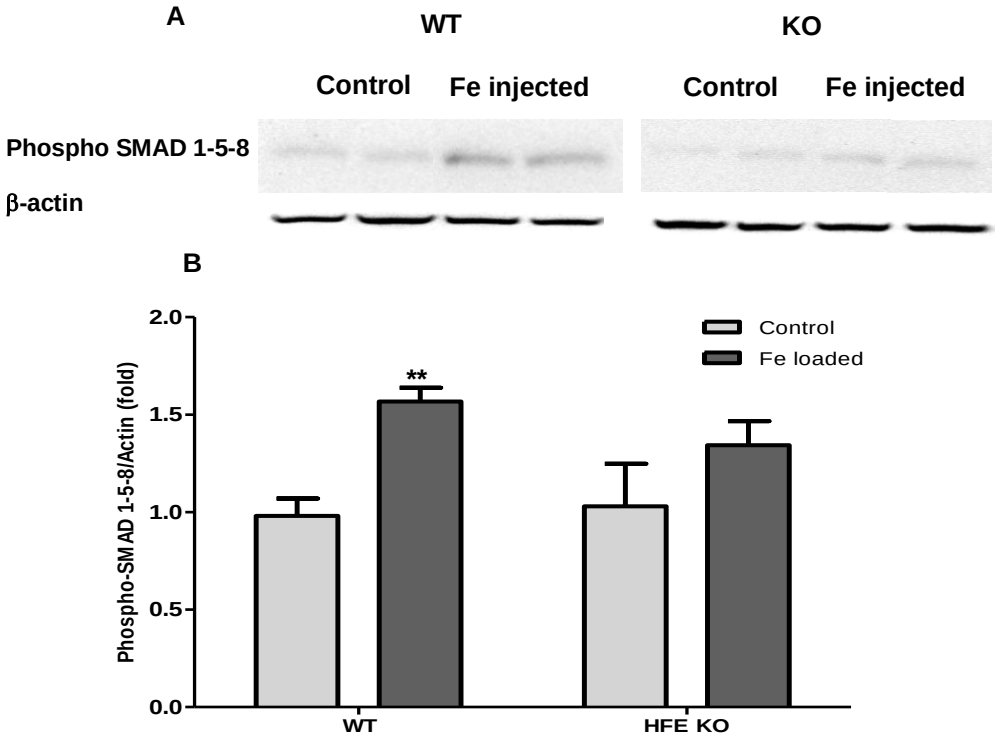

Figure 3.10 Effect of iron overload on phosphorylation of Smad 1/5/8 in the liver of wild-type (WT) and *HFE* KO mice.

(A) Western blot analysis of liver lysates from control or iron-loaded WT and *HFE* KO mice using an antibody to phosphorylated Smad1/5/8 with β-actin as a loading control. (B) Chemiluminescence was quantified using Quantity One software and the ratio of phosphorylated Smad1/5/8 to β-actin was calculated and plotted. Mean ratios of four samples (± SEM) are represented on this figure, relative to the mean ratio of the control wild type mice or *HFE* KO mice. Iron loading significantly increased the phosphorylation of Smad 1/5/8 in WT mice; whereas, Smad 1/5/8 phosphorylation was not significantly increased in iron-loaded *HFE* KO mice. Statistical significant differences relative to control mice were determined by Student *t* tests. $^{**}P < 0.01$.

3.4 Discussion

It is well known that hepcidin is regulated by iron; yet, the exact mechanism and molecules involved in this regulation are still unknown. It has been shown that BMP-Smad signalling is one of the most important pathways involved in hepcidin regulation (Babitt et al. 2006; Babitt et al. 2007). However, whether BMP-Smad signalling pathway is involved in hepcidin regulation by iron is not clear.

HFE mutations are accompanied by inappropriately low hepcidin expression levels (Piperno et al. 2007). However, the mechanism by which HFE regulates hepcidin gene expression is not clearly understood.

In this chapter, the hypothesis that regulation of hepcidin by iron status entails the BMP-Smad signalling pathway was examined. To investigate the effect of iron deficiency, C57Bl/6 mice were either fed a control or an iron-deficient diet. To study the effect of iron loading, mice were either injected with saline or iron (sodium ferric gluconate).

To explore whether HFE is involved in hepcidin regulation by iron, *HFE* KO mice were also investigated in the settings of dietary iron deficiency and parenteral iron loading. In addition, whether iron status modulates Smad signalling in these mice through phosphorylation of receptor activated smad 1/5/8 was examined. The activation of Smad1, Smad5, and Smad8 is the main BMP signalling pathway (Miyazawa et al. 2002).

My data shows that when fed on an iron-deficient diet, both wild-type and *HFE* KO mice showed a decrease in liver iron content, serum iron, and transferrin saturation. In contrast, in iron-loaded wild-type and *HFE* KO mice the liver iron, serum iron, and transferrin saturation were increased.

It was also found that hepatic gene expression of *hepcidin1* was reduced by dietary iron deficiency in wild-type and *HFE* KO mice*.* Moreover*, hepcidin 1* expression in control *HFE* KO was lower compared to wild-type mice which is inappropriate for

liver iron levels in these mice. These results of *hepcidin* 1 expression are in agreement with previous published reports (Ahmad et al. 2002; Bridle et al. 2003; Bondi et al. 2005; Latunde-Duda et al. 2004; Nicolas et al. 2002b; Vokurka et al. 2006). In contrast, no change in *HJV* expression was observed in iron-deficient wild-type and *HFE* KO mice. A similar finding was recently reported by Constante et al. (2007). These results suggest that *hepcidin 1* down-regulation during iron deficiency is not dependent on HFE, and dietary iron deficiency does not regulate hepatic *HJV* expression. Interestingly, hepatic expression of *BMP-6 mRNA,* but not *BMP-2* and *BMP-4*, and phosphorylated Smad 1/5/8 proteins were reduced by dietary iron deficiency in wild-type and *HFE* KO mice. These findings suggest that iron deficiency suppresses hepatic *BMP-6* expression and its downstream signal (pSmad 1/5/8), which in turn may cause suppression of *hepcidin 1* gene expression; however, this effect is not dependent on HFE.

In iron-loaded wild-type mice, the hepatic mRNA expression of *hepcidin1, BMP-6*, and phosphorylation of Smad 1/5/8 proteins were induced. In contrast, no change was observed in *HJV, BMP-2, and BMP-4* expression levels. Similar findings were recently reported by another group who studied dietary iron loading in different mouse strains from the one used in this study (Kautz et al. 2008).

The data suggest that parenteral iron loading induces *hepcidin 1* gene expression in accordance with previous reports (Pigeon et al. 2001; Nemeth et al. 2004a), while it has no effect on *HJV* gene expression which was shown by others (Gleeson et al. 2007; Krijt et al. 2004). In addition, the data suggests that the expression of *BMP-6* mRNA and Smad 1/5/8 phosphorylation are induced by iron loading which may subsequently induce *hepcidin 1* gene expression.

In iron-loaded *HFE* KO mice, although they showed induction of BMP-6 similar to that observed in wild-type mice, hepcidin1 induction was significantly lower than that of iron-loaded wild-type mice. Additionally, the phosphorylation of Smad 1/5/8

was not significantly increased in response to parenteral iron loading, which may explain why *hepcidin1* was inappropriately induced by iron loading in these mice. Conversely, no change was observed in the expression of *HJV, BMP-2, BMP-4* mRNAs in iron-loaded *HFE* KO mice. The data demonstrates that *BMP-6* expression was appropriately induced by iron loading in *HFE* KO mice, indicating that BMP-6 induction by iron is HFE-independent; however, the induction of Smad 1/5/8 is altered by the lack of functional HFE.

It was also found that although *HFE* KO mice showed higher *BMP-6* expression levels compared to wild-type controls, they expressed similar levels of pSmad1/5/8 and there was less *hepcidin 1* expression compared to wild-type mice. These findings further support the assumption that Smad signalling is impaired in *HFE* KO mice. This hypothesis is also supported by a recent study by Kautz et al. (2009), who showed that BMP-Smad signalling is not enhanced in *HFE* KO mice despite increased *BMP-6* expression.

Although iron injection has recently been shown to increase the phosphorylation of Smad 1/5/8 in zebra fish and mouse liver extracts (Yu et al. 2008), the precise TGF-β superfamily ligand involved in this induction is unknown. Moreover, *hepcidin* expression has been shown to be induced by different TGF-β family ligands both *in vitro* (Babitt et al. 2006; Wang et al. 2005; Truksa et al. 2006) and *in vivo* (Babitt et al. 2007; Andriopoulos et al. 2009). However, the relatively high doses of BMP ligands used in these studies may not mimic the physiological response to endogenous BMP ligands. This may also explain why some of the recent findings showed a similar *hepcidin* induction in response to BMPs in hepatocytes from both wild-type and *HFE* KO mice (Truska et al. 2006), as the relatively high doses of BMP ligands might overrule the requirement for functional HFE.

Recently, exogenous BMP-6 was shown to induce *hepcidin* expression *in vivo* (Andriopoulos et al. 2009) and *in vitro* (Babitt et al. 2007). In addition, siRNA

inhibition of endogenous BMP-6 *in vitro* reduces *hepcidin* expression levels (Babitt et al. 2007). These findings clearly demonstrate that *hepcidin* expression is not only induced by exogenous BMP-6, but it is also repressed when endogenous BMP-6 is reduced. S-HJV has been shown to interfere with BMP-Smad signalling *in vitro* and *in vivo* (Babitt et al. 2007). However, it has recently been shown that BMP-6 was selectively inhibited by S-HJV *in vivo* and *in vitro* (Andriopoulos et al. 2009). Taken together, these findings, in addition to the data shown here, converge to suggest that BMP-6 is the ligand of TGF-β that plays an important role in *hepcidin* regulation by iron *in vivo*.

My data also showed that iron-induced *hepcidin1* expression was lower in *HFE* KO mice compared with wild-type mice despite their appropriate induction of *BMP-6* expression in response to iron. Moreover, the hepatic levels of phosphorylated Smad 1/5/8 (an intracellular mediator of BMP-6 signalling) were inappropriately low for their liver iron levels and BMP-6 expression levels. Altogether, the data shown here and recently published reports (Corradini et al. 2009; Kautz et al. 2008) suggest that iron regulates hepatic expression of *BMP-6* and pSmad1/5/8 *in vivo* (i.e reduced by iron deficiency and induced by iron loading). In addition, the iron-induced downstream signal of BMP-6, which is shown here as pSmad1/5/8, is impaired in *HFE* KO mice. These results suggest that HFE may be involved in the regulation of downstream signals of BMP-6 that induce hepcidin expression in response to iron loading.

The results shown here, in conjunction with the findings of the others (Schmidt et al. 2008; Kautz et al. 2008; Corradini et al. 2009), suggest that the iron-sensing process may occur at two different levels. Iron overload increases *BMP-6* mRNA expression. It is not known how iron regulates *BMP-6 mRNA*; however, the results shown here suggest that it is not mediated by HFE. Induced BMP-6 then signals via Smad 1/5/8 to stimulate *hepcidin* expression via a common mediator, Smad-4 as mentioned before. The second mechanism of iron sensing involves HFE. It was

recently proposed that during iron loading HFE is displaced from TFR1 by holotransferrin, and then interacts with TFR2 forming a complex that acts to induce hepcidin expression (Schmidt et al. 2008; Gao et al. 2009). Based on the data shown here, it is suggested that HFE may interact with the HJV/BMP-6/Smad signalling pathway to induce *hepcidin* expression in response to iron loading. However, the exact mechanism by which HFE hinders this signalling pathway and whether TFR2 is involved needs further investigation.

3.5 Conclusion

In conclusion, the study of the regulation of hepcidin in response to dietary iron deficiency and parenteral iron loading in wild-type and *HFE* KO mice suggest that hepcidin regulation by iron status is modulated by the BMP-6/Smad signalling pathway *in vivo*. The data suggest that iron regulates the expression of BMP-6 and phosphorylation of Smads 1/5/8 in the liver which in turn may regulate hepcidin gene expression in response to different iron status. Moreover, HFE seems to be involved in the regulation of downstream signalling of BMP-6 that regulates *hepcidin* expression in response to iron loading *in vivo*. The data propose a mechanism by which HFE may be involved in iron-induced *hepcidin* expression via its interaction with HJV/BMP-6/Smad signalling. However, the exact molecular mechanism remains to be fully clarified.

Chapter 4: Regulation of Hepcidin and Hemojuvelin Expression during Inflammation

4.1 Introduction

Inflammatory stimuli are associated with profound alterations in iron homeostasis. Among the most important of these changes are the redistribution of iron into RE marcrophages and reduced intestinal iron absorption causing hypoferremia (Cartwright and Wintrobe 1952; Cartwright 1966; Lee 1983; Cortell and Conrad 1967). Similar findings have also been reported in mice exposed to endotoxins (Cartwright and Lee 1971).

The impairment of iron efflux by enterocytes and RE macrophages is believed to play an important role in host defense against infection and cancer (Weinberg 1992; Jurado 1997). However, it also limits iron availability for erythropoiesis resulting in anaemia (Moldawer et al. 1989).

Pro-inflammatory cytokines have been shown to modulate the expression of iron transport and storage proteins in a variety of cell types (Johnson et al. 2004; Ludwiczek et al. 2003; Yang et al. 2002). During inflammation, IL-6 induces hepcidin expression and hypoferremia *in vivo* (Nemeth et al. 2004a). The finding that hepcidin is modulated by inflammatory cytokines has linked hepcidin to anaemia of inflammation (Ganz 2003; Roy and Andrews 2005). Increased hepcidin, in turn, decreases intestinal iron absorption (Laftah et al. 2004; Roy et al. 2004; Roy and Andrews 2005; Yamaji et al. 2004; Chung et al. 2009).

LPS injection in humans induces IL-6 within 3 hours and increases urinary hepcidin with subsequent hypoferremia (Kemna et al. 2005). In addition, IL-6 injection in humans increases hepcidin and decreases serum iron in just 2 hours (Nemeth et al. 2004a). As mentioned in Chapter 1, IL-6 regulates hepcidin expression through phosphorylation of STAT3 that binds to the IL-6 responsive element within the hepcidin gene promoter.

LPS injection is associated with increased hepatic IL-6 expression while turpentine oil induces local irritation that results in recruitment of inflammatory cells and

induction of IL-6 in injured muscles in mice (Sheikh et al. 2006). In addition, turpentine oil injection induces hepatic expression of IL-6, IL-1β, and TNF-α in rats (Sheikh et al. 2007). Turpentine oil injections in mice result in increased hepcidin expression and hypoferremia (Nicolas et al. 2002b; Sheikh et al. 2007). However, the lack of hypoferremia in turpentine-injected *Hepcidin* KO mice suggests that the hypoferremia is hepcidin-dependent (Nicolas et al. 2002b).

Hemojuvelin, a BMP co-receptor, has been shown to be an important upstream regulator of hepcidin expression, as previously mentioned in Chapter 1. In mice lacking *HJV*, hepcidin induction in response to iron is abrogated. On the other hand, these mice retain the ability to regulate hepcidin in response to inflammation by LPS and IL-6, though to a lesser extent than wild-type animals (Niederkofler et al. 2005). Moreover, *HJV* expression is down-regulated in the liver of mice injected with LPS (Niederkofler et al. 2005). These findings suggest that HJV is not fully involved in the hepcidin response to inflammatory stimuli while it is required for hepcidin response to iron. However, it is not clear how *HJV* is regulated during inflammation.

Recently it has been shown that mice lacking hepatic Smad-4 express very low hepcidin levels. In addition, the response of hepcidin to inflammation is abrogated in these mice (Wang et al. 2005). Moreover, Verga Falzacappa et al. (2008) identified a BMP-RE that lies near the IL-6 RE in the hepcidin gene promoter. They found that this RE is not only required for the BMP response but also for IL-6 responsiveness. Taken together, these findings suggest a possible cross-talk between the BMP-Smad and IL-6 signalling pathways; however, this link remains to be clarified.

Evidence for the requirement of HFE for hepcidin induction during inflammation is conflicting. Roy et al. (2004) reported that mice lacking *HFE* do not respond to LPS with increased *hepcidin* expression as wild-type animals. In another study, the LPS response is significantly different among animals (Lee et al. 2004). A recent study by Constante et al. (2006) showed that *HFE* knockout (KO) mice are able to

regulate hepcidin by LPS as do wild-type animals. These contradictory findings on the requirement of HFE for hepcidin induction during acute inflammation suggest that the study of *HFE* KO mice during the inflammatory response requires further investigation.

This study is aimed to investigate the modulation of *hepcidin*, *HJV,* and BMP-Smad signalling and the role of HFE in their regulation during inflammation.

To investigate the effect of acute inflammation on *hepcidin* and *HJV* expression levels *in vivo*, C57Bl/6 mice were injected with LPS and sacrificed after 6 hours, the time at which maximal *hepcidin* induction and *HJV* repression have been reported (Yeh et al. 2004; Niederkofler et al. 2005; Krijt et al. 2004).

To understand the effect of inflammation on BMP-Smad signalling *in vivo*, the hepatic expression of *BMP* mRNAs and phosphorylated Smad-1/5/8 protein levels were measured in the liver of saline- and LPS-injected mice.

To investigate the role of HFE in *hepcidin, HJV,* and *BMPs* response during inflammation *in vivo*, acute inflammation was induced by LPS in C57Bl/6 *HFE* KO mice.

To investigate the direct effect of major cytokines produced during inflammation on *hepcidin* and *HJV* expression *in vitro*, HuH7 human hepatoma cells were treated with IL-6 and TNF-α. These cells were also used to study the mechanism of *HJV* suppression during inflammation.

4.2 Methods

4.2.1 Acute inflammation induced by LPS in C57Bl/6 wild-type and *HFE* KO mice

Mice were fed on an RM1 diet (190mg iron/Kg) for six weeks after being weaned (3 weeks of age). Acute inflammation was induced by a single intra-peritoneal injection of 5μg LPS/g body weight (*Escherichia coli* serotype 055:B5, Sigma, UK). Control mice were similarly injected with an equivalent volume of sterile saline solution (0.09% NaCl). The animals were sacrificed 6 hours after injection; livers were snap frozen for mRNA, protein, and iron quantification. Blood was collected by cardiac puncture and serum was separated for iron and transferrin saturation measurements using a commercial kit (Pointe Scientific, USA). Hepatic expression of phosphorylated Smad-1/5/8 was quantified by Western blotting using a commercial antibody (1:500 dilution, Cell signalling, UK). As a loading control, β-actin protein was quantified using anti-actin antibody (1:5000 dilution, Abcam).

4.2.2 Pro-inflammatory cytokines treatment of HuH7 cells

HuH7 cells were cultured in Dulbecco's modified Eagle's medium (DMEM) containing 10% FBS and antibiotics and maintained in a humidified atmosphere of 5% CO_2 at 37^{o}C. The cells were seeded in 6-well plates (Nunc, UK). Once 80-85% confluent, the medium was changed and replaced by fresh medium with vehicle (control) or medium containing recombinant human IL-6 (10ng/mL; R&D Systems, UK) or recombinant human TNF-α (20ng/mL; R&D Systems). Both cytokines were reconstituted in sterile PBS containing 0.1% bovine serum albumin. After treatment, medium was removed and cells were washed with PBS. RNA extraction, cDNA

synthesis, and RT-PCR amplification for hepcidin and HJV were carried out as described in Section 2.1.

4.2.3 Effect of TNF-α treatment on *HJV* mRNA and protein expression in HuH7 cells

HuH7 cells were seeded in 6-well plates and treated with TNF-α (20ng/mL) for 6, 12, 24, and 48 hours followed by RNA extraction, cDNA synthesis, and RT-PCR amplification of *HJV* mRNA.

To investigate the effect of TNF-α on HJV protein expression, cells were treated with TNF-α for 16 hours followed by protein extraction and immunoblotting detection of HJV protein as described in Section 2.6 using a commercial anti-HJV antibody (Santa Cruz Biotechnology, UK). β-actin was used as a loading control.

4.2.4 Effect of TNF-α treatment on luciferase activity of *HJV* promoter-reporter construct (*HJV*p1.2-luc)

A *HJV* promoter-reporter construct was generated as described in Section 2.3. This construct was used to investigate the mechanism of TNF-α down-regulation of *HJV* expression. HuH7 cells were transfected with *HJV*p1.2-luc and treated with TNF-α for 24 hours. Luciferase activity was measured as described in Section 2.5.

4.2.5 Site-directed mutagenesis of TNF-α response element (TNFRE) within *HJV* promoter

A single consensus TNFRE, **GGC (A/T) GCC**, was manually identified in the *HJV*P1.2-luc. This sequence has been shown to be responsible for down-regulation of several human genes in response to TNF-α, including osteocalcin, thrombomodulin, alkaline phosphatase, and c-myc (Li and Stashenko 1993; Ohdama et al. 1991; Weiss et al. 1988; Watt et al. 1983). As shown in Figure 4.1, this site lies 290 nucleotides upstream of the start of the *HJV* first exon.

```
TTCGTCCTTC TGAAATACTC TGCAAAGATA GGAGAGGGGC TATGAACTAC
CTCTGCTATG GATCTTATTC AAAGTCAGCT ACCTCCTAGA TACTATCTGT
AGAACCTAAA TGTAATATTC AGCATAGCAG GGATGAACAT GGTAAATGAA
AGGTATCCAA TTGCCCACTG TAATTTTTAA AGGCCAGGAG CTCAACATTA
TTGAAAATGC TGGAGGGCTG CCTGGAGTAG GCAGTGACCA CAGAGTCACA
CAAGCTGGAA TTGGATATCC AACTTGTCTG TCATATTTCT CTCCTCCCTC
CCTGACTTGG CACTCAATAC TCCATATTCT TTCTAATCCT CTAACCCTCC
CCACTCCCCC AACTCCCACA CCCTACCCCC ACCAACGTTC CTGGAATTTT
GGACTTAGCT ATTTTTAAAA CCGTCAACTC AGTAGCCACC TCCCTCCCTG
CTCAGCTGTC CAGTACTCTG GCCAGCCATA TACTCCCCCT TCCCCCCATA
CCAAACCTTC TCTGGTTCCC TGACCTCAGT GAGACAGCAG
```

Figure 4.1 Portion of the amplified sequence of the *HJV* promoter showing TNFRE.

The consensus TNF-α RE (green) lies 290 nucleotides upstream of the start of the first exon (yellow).

To test whether the identified TNFRE is functional, *HJV*P1.2-luc was subjected to site-directed mutagenesis using the QuickChange Site-Directed Mutagenesis kit (Stratagene, UK) as instructed by the manufacturer. The mutant primers were as follows: sense TGAAAATGCTGGAGGAATTCTTGGAGTAGGCAGTG and antisense CACTGCCTACTCCAAGAATTCCTCCAGCATTTTCA, and the *EcoR*I restriction site is underlined. An *EcoR*I restriction site was thereby introduced instead of TNFRE within the *HJV*P1.2-luc. After initial denaturation for 1 minute at 95^{o}C, PCR cycling parameters were 95^{o}C (1 minute), 55 ^{o}C (1 minute), and 65 ^{o}C (6 minutes), for a total of 18 cycles. Following *Dpn*I digestion of wild-type *HJV*P1.2-luc, transformation of INVαF' competent cells (Invitrogen) with the mutagenesis reaction and selection on Luria agar/ampicillin plates, plasmid DNA was purified from overnight cultures of single colonies and digested with *EcoR*I (New England Biolabs), which cuts at two sites within mutant plasmid (as there is a single *EcoR*I within the wild-type *HJV*P1.2-luc sequence in addition to the replaced TNFRE) producing an approximately 400 bp product which was used to distinguish the mutant construct from the wild-type one. The mutant construct was designated mt*HJV*P1.2-luc.

4.2.6 Effect of TNF-α treatment on luciferase activity of *HJV*p 1.2-luc and mt*HJV*P1.2-luc

HuH7 cells were transfected with *HJV*p 1.2-luc or mt*HJV*P1.2-luc and treated with TNF-α for 24 hours. Luciferase activity was then measured as described in Section 2.5.

4.3 Results

4.3.1 Effect of LPS-induced inflammation on serum iron and transferrin saturation in wild-type C57Bl/6 and *HFE* KO mice

LPS was used to induce acute inflammation in wild-type and *HFE* KO mice. Animals were treated for 6 hours. LPS treatment caused a significant decrease in serum iron in WT and *HFE* KO mice ($p<0.05$). Transferrin saturation was lower in LPS injected WT ($P<0.05$) and *HFE* KO mice; however, in the latter it did not reach statistical significance. Moreover, serum iron and transferrin saturation were not significantly higher in *HFE* KO than WT mice (Figure 4.2).

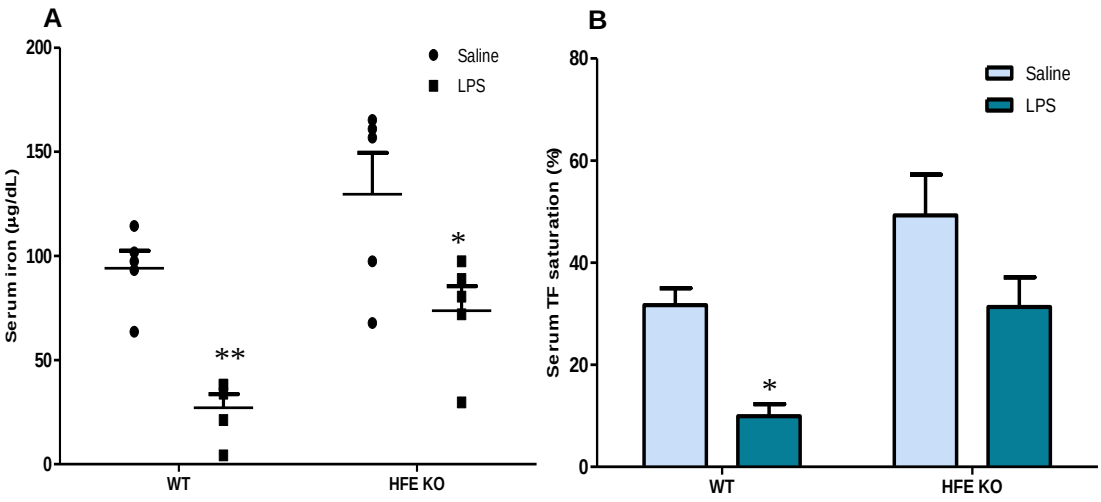

Figure 4.2 Total serum iron (A) and transferrin saturation (B) following LPS injection of wild-type (WT) and *HFE* KO mice.

C57Bl/6 WT and *HFE* KO mice 9 weeks old were injected with 5μg LPS/g body weight or an equivalent volume of saline and sacrificed after 6 hours. LPS treatment significantly decreased serum iron in both genotypes. Treatment decreased transferrin saturation in wild-type and *HFE* KO mice; however, in *HFE* KO mice it did not reach statistical significance. Data are mean±SEM of 5 mice per group. *, ** denotes significant difference from the saline–injected group ($p<0.05$, $p<0.001$ respectively).

4.3.2 Effect of LPS-induced acute inflammation on liver iron and hepatic gene expression in wild-type C57Bl/6 and *HFE* KO mice

4.3.2.1 Effect of LPS-induced acute inflammation on hepatic iron content

Liver iron content was measured in wild-type C57Bl/6 and *HFE* KO mice treated with LPS for 6 hours. Acute inflammation increased hepatic iron content in wild-type mice though not significantly and no change in liver iron was observed in LPS-injected *HFE* KO mice. In addition, liver iron was significantly higher in *HFE* KO mice compared to control and LPS-injected wild-type animals (Figure 4.3).

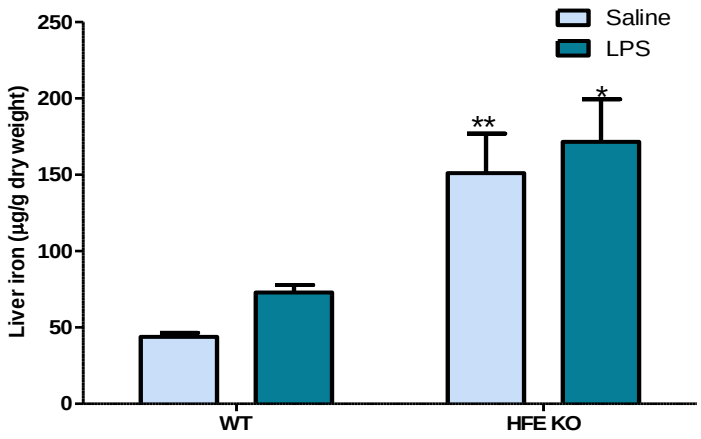

Figure 4.3 Liver iron content in WT C57Bl/6 and *HFE* KO mice in acute inflammation.

Mice were injected with LPS for 6 hours. After which, the liver was removed and iron was quantified and presented as µg/g dry weight. LPS treatment increased hepatic iron content in WT mice though not significantly with no change in hepatic iron content in LPS-injected *HFE* KO mice. Moreover, hepatic iron content was significantly higher in HFE KO mice. Data are mean±SEM of five mice per group.* denotes significant difference from LPS-injected WT mice ($p<0.05$). ** denotes significant difference from the saline–injected WT mice ($p<0.01$).

4.3.2.2 Effect of LPS-induced acute inflammation on hepatic *IL-6* and *TNF-α* gene expression

To confirm the occurrence of acute hepatic response to inflammation, hepatic *IL-6* and *TNF-α* mRNA levels were analysed by RT-PCR in saline- and LPS- injected mice. As expected, treatment with LPS significantly increased *IL-6* and *TNF-α* expression levels in the liver of wild-type and *HFE* KO mice (Figure 4.4)

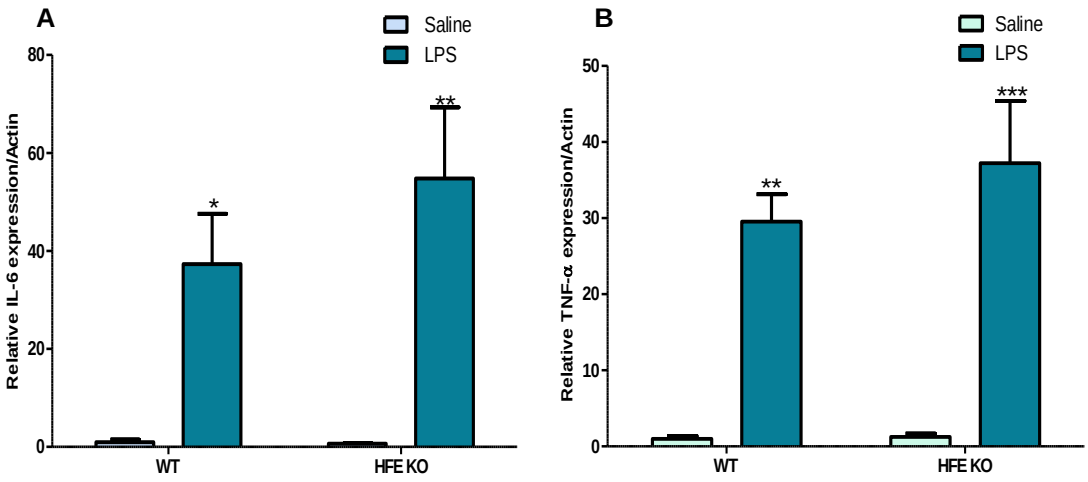

Figure 4.4 Effect of acute inflammation on hepatic IL-6 (A) and TNF-α (B) expression levels in wild-type and *HFE* KO mice.

IL-6 and TNF-α mRNA expression levels were analysed by real time PCR. LPS treatment significantly increased IL-6 and TNF-α expression in both genotypes. Data are mean±SEM of five mice per group.*p<0.05, **p<0.01, ***p<0.001 in LPS-injected mice compared to saline-injected controls.

4.3.2.3 Effect of LPS-induced acute inflammation on hepatic *hepcidin 1* gene expression

To investigate the effect of acute inflammation on hepatic *hepcidin 1* mRNA expression and the possible role of HFE in this response, gene expression levels were quantified by RT-PCR in saline- and LPS-injected wild-type and *HFE* KO mice. Treatment with LPS significantly increased *hepcidin 1* expression levels in wild-type and *HFE* KO mice, and *hepcidin1* induction was similar in both genotypes (Figure 4.5). *HFE* KO mice showed less *hepcidin 1* expression than wild-type animals though the decrease did not reach statistical significance.

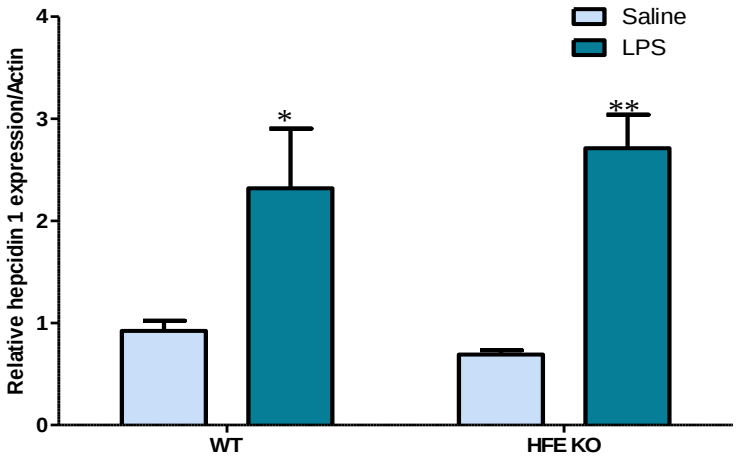

Figure 4.5 Effect of acute inflammation on hepatic *hepcidin 1* expression in wild-type and *HFE* KO mice.

Hepcidin 1 mRNA levels were analysed by RT-PCR. LPS treatment significantly increased *hepcidin 1* expression in both genotypes. Data are mean±SEM of five mice per group. *p<0.05, **p<0.01 in LPS-injected mice compared to saline-injected controls.

4.3.2.4 Effect of LPS-induced acute inflammation on hepatic *HJV* gene expression

To explore the effect of acute inflammation on hepatic *HJV* mRNA expression and the possible role of HFE in this response, hepatic *HJV* mRNA expression levels were analysed by RT-PCR in saline- and LPS- injected wild-type and *HFE* KO mice. Treatment with LPS significantly decreased *HJV* expression levels in wild-type and *HFE* KO mice (Figure 4.6).

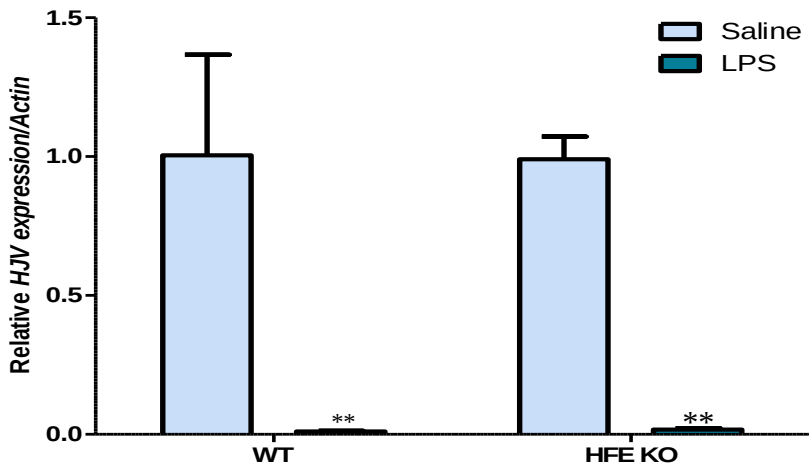

Figure 4.6 Effect of acute inflammation on hepatic *hemojuvelin* expression levels in wild-type and *HFE* KO mice.

HJV mRNA expression levels were analysed by RT-PCR. LPS treatment significantly decreased *HJV* expression in both genotypes. Data are mean±SEM of five mice per group.**p<0.01 in LPS-injected mice compared to saline-injected controls.

4.3.2.5 Effect of LPS-induced acute inflammation on hepatic *BMPs* and *TGF-β* gene expression

To further understand the possible link between inflammation and the BMP-Smad signalling pathway and whether HFE is involved, liver-expressed *BMPs (2, 4, and 6)* and *TGF-β* gene expression levels were analysed by RT-PCR in wild-type and *HFE* KO mice injected with LPS. LPS treatment significantly decreased the expression levels of *BMP2, BMP4*, and *BMP6* (Figure 4.7) in wild-type and *HFE* KO mice. On the other hand, LPS had no effect on the expression levels of *TGF-β* in either genotypes (Figure 4.7D).

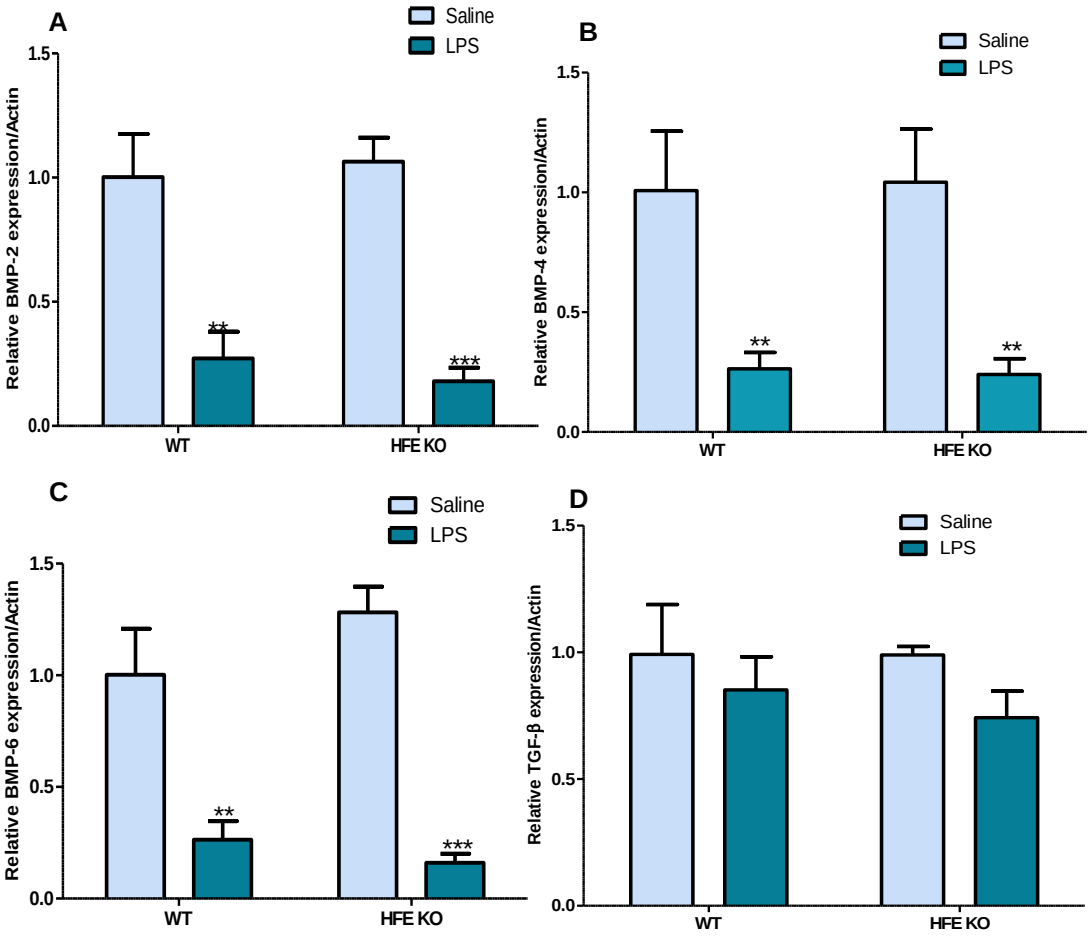

Figure 4.7 Effect of acute inflammation on hepatic *BMP-2* (A), *BMP-4* (B), BMP-6 (C), and TGF-β (D) expression in wild-type and *HFE* KO mice.
BMP-2, BMP-4, BMP-6, and TGF-β mRNA expression were analysed by RT-PCR. LPS treatment significantly decreased *BMP-2, BMP-4, BMP-6* with no change in *TGF-β* expression expression in both genotypes. Data are mean±SEM of five mice per group. **p<0.01, ***p<0.001 in LPS-injected mice compared to saline-injected controls.

4.3.3 Effect of LPS-induced acute inflammation on liver phosphosmad 1, 5, and 8 protein expression in WT C57Bl/6 and *HFE* KO mice

To examine the effect of acute inflammation on downstream signal of BMPs, protein expression levels of phosphorylated Smad 1/5/8 were analysed in wild-type and *HFE* KO mice injected with LPS. LPS treatment had no effect on pSmad 1, 5, and 8 protein expression levels in both genotypes (Figure 4.8).

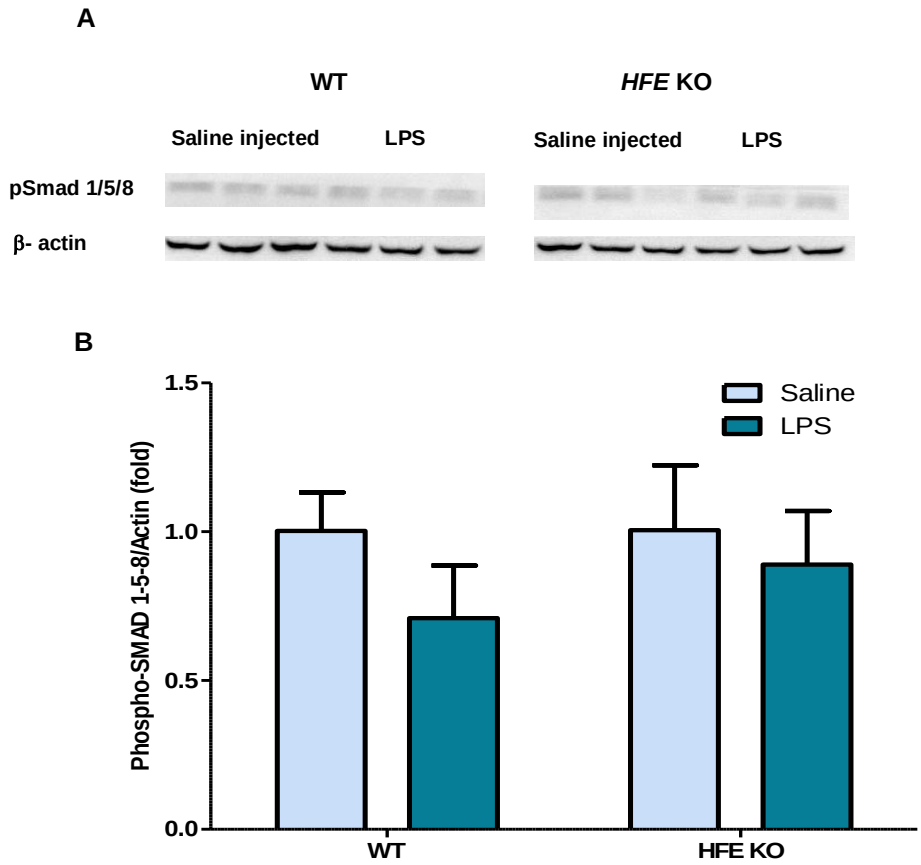

Figure 4.8 Smad1/5/8 phosphorylation is not changed by LPS injection in wild-type C57blk/6 and *HFE* KO mice.

(A) Western blotting of liver lysates from saline- or LPS-injected WT and *HFE* KO mice using an antibody to phosphorylated Smad1/5/8, β-actin was used as loading control. (B) Chemiluminescence was quantified using Quantity One software to calculate the ratio of phosphorylated Smad1/5/8 to β-actin. Mean ratios of four samples (± SEM) are represented on this figure, relative to the mean ratio of the saline-injected WT or *HFE* KO mice.

4.3.4 Effect of pro-inflammatory cytokines on *hepcidin* and *HJV* mRNA expression in HuH7 cells

HuH7 cells were used to study the effect of pro-inflammatory cytokines, IL-6 and TNF-α, on *hepcidin* and *HJV* mRNA expression *in vitro*.

4.3.4.1 Effect of IL-6 treatment on *hepcidin* and *HJV* mRNA expression

IL-6 treatment (10ng/mL for 24 hrs) of HuH7 cells significantly increased *hepcidin* mRNA expression three fold with no effect on *HJV* expression (Figure 4.9).

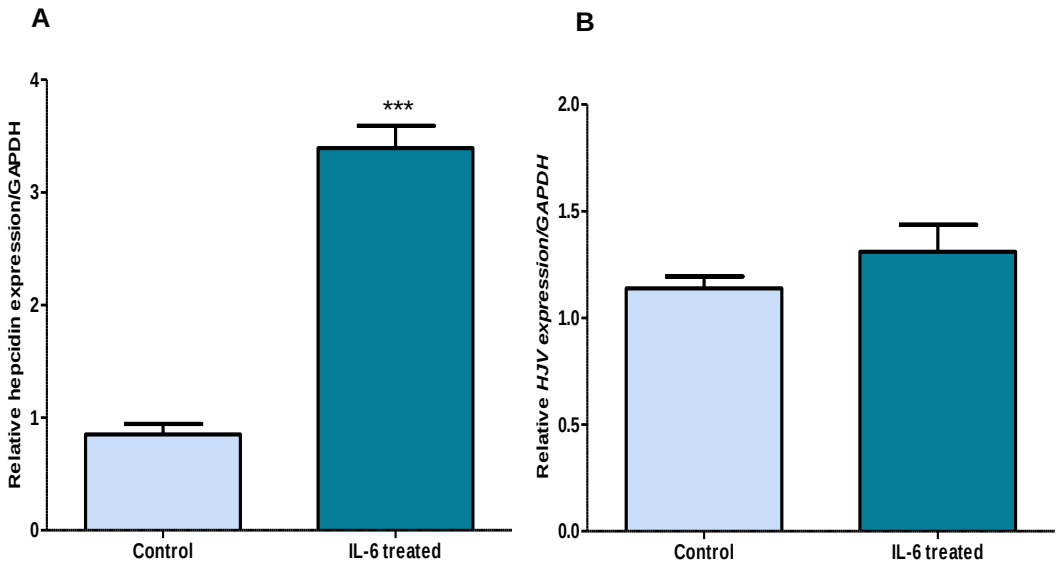

Figure 4.9 Quantitative RT-PCR analysis of *hepcidin* (A) and *HJV* (B) mRNA expression in HuH7 cells following IL-6 treatment.

HuH7 cells were incubated for 24 hours in the presence of vehicle (control) or IL-6 (10ng/mL). RT-PCR analysis of *hepcidin* and *HJV* gene expression showed that *hepcidin* mRNA levels were significantly induced by IL-6, while *HJV* mRNA expression levels remained unchanged. Data are mean± SEM of 6 samples from 3 separate experiments performed in duplicate. ***p<0.001.

4.3.4.2 Effect of TNF-α treatment on *hepcidin* and *HJV* mRNA expression

TNF-α treatment (20ng/mL for 24 hrs) of HuH7 cells significantly decreased *HJV* mRNA expression levels with no effect on *hepcidin* mRNA expression (Figure 4.10).

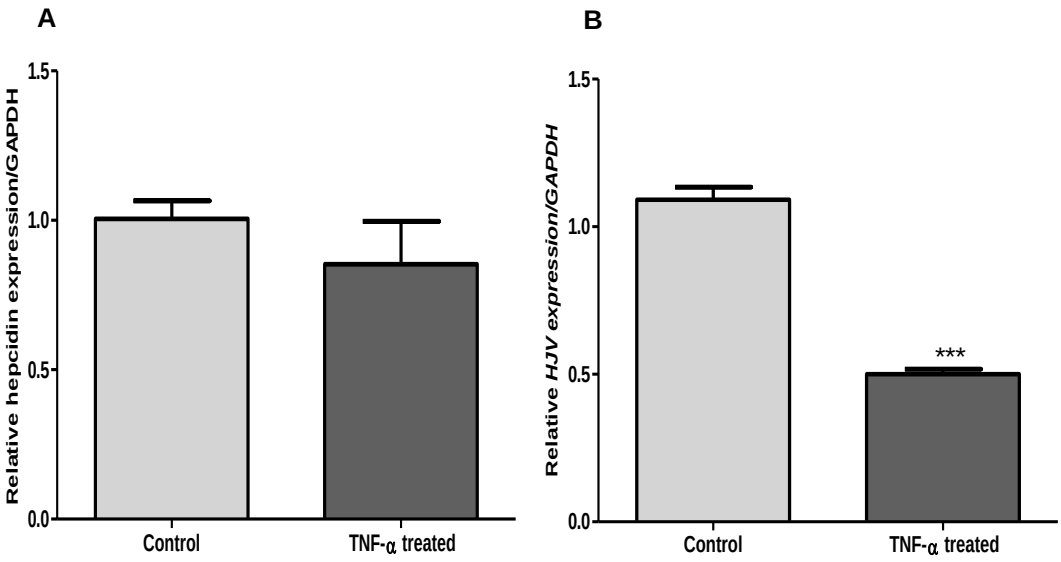

Figure 4.10 Quantitative PCR analysis of *hepcidin* (A) and *HJV* (B) expression in HuH7 cells following TNF-α treatment.

HuH7 cells were incubated for 24 hours in the presence of vehicle (control) or TNF-α (20ng/mL). Quantitative PCR analysis of *hepcidin* and *HJV* gene expression showed that *hepcidin* mRNA expression levels remained unchanged in response to TNF-α, while *HJV* mRNA expression levels were significantly repressed. Data are mean± SEM of 6 samples from 3 separate experiments performed in duplicate. ***p<0.001.

4.3.4.3 Effect of TNF-α treatment on *HJV* mRNA expression at different time points

HuH7 cells that were exposed to TNF-α (20ng/mL) for 6, 12, 24, and 48 hours demonstrated that *HJV* mRNA expression levels significantly decreased in response to TNF-α in a time-dependent manner. The maximal repression was observed after 24 hours, and *HJV* mRNA expression levels returned to normal values after 48 hours (Figure 4.11).

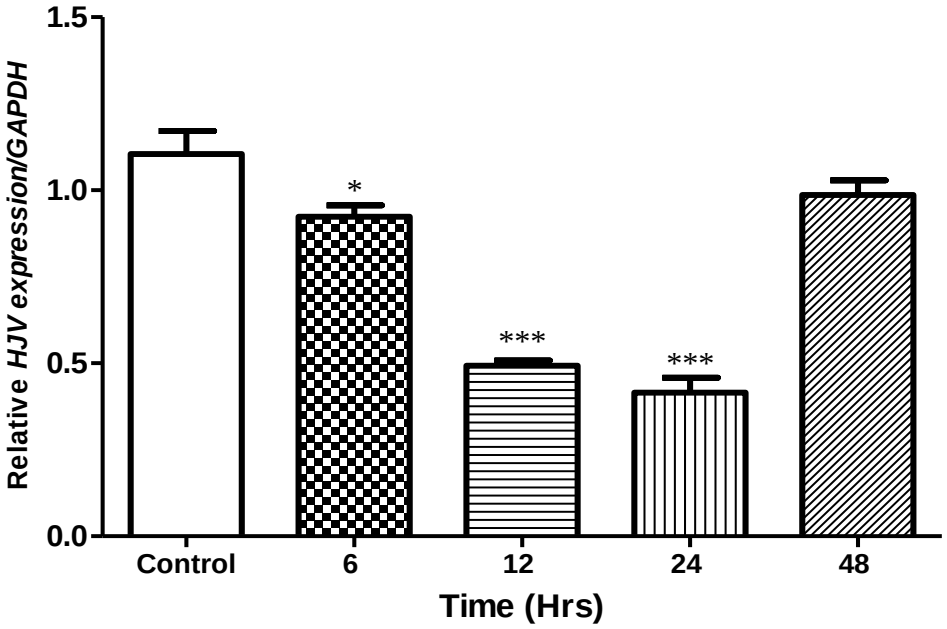

Figure 4.11 Quantitative PCR analysis of *HJV* mRNA expression in HuH7 cells following TNF-α treatment at different time points.

HuH7 cells were incubated in the presence of vehicle (control) or TNF-α (20ng/mL) for 6, 12, 24, and 48 hours. Quantitative PCR analysis of *HJV* mRNA expression showed that *HJV* mRNA expression levels decreased in response to TNF-α in a time-dependent manner reaching its maximal repression levels after 24 hours, and returning to normal expression levels after 48 hours. Data are Mean± SEM of 6 samples from 2 separate experiments in triplicate. *p<0.05, ***p<0.001.

4.3.4.4 Effect of TNF-α treatment (20ng/mL) for 16 hours on *HJV* protein expression in HuH7 cells

To explore whether the repression of *HJV* mRNA expression in response to TNF-α is mirrored by a suppression at protein levels, HuH7 cells were incubated in the presence of TNF-α for 16 hours followed by protein extraction and immunodetection of HJV protein by western blotting. As shown in figure 4.12, HJV protein levels were significantly repressed in TNF-α treated cells compared to control.

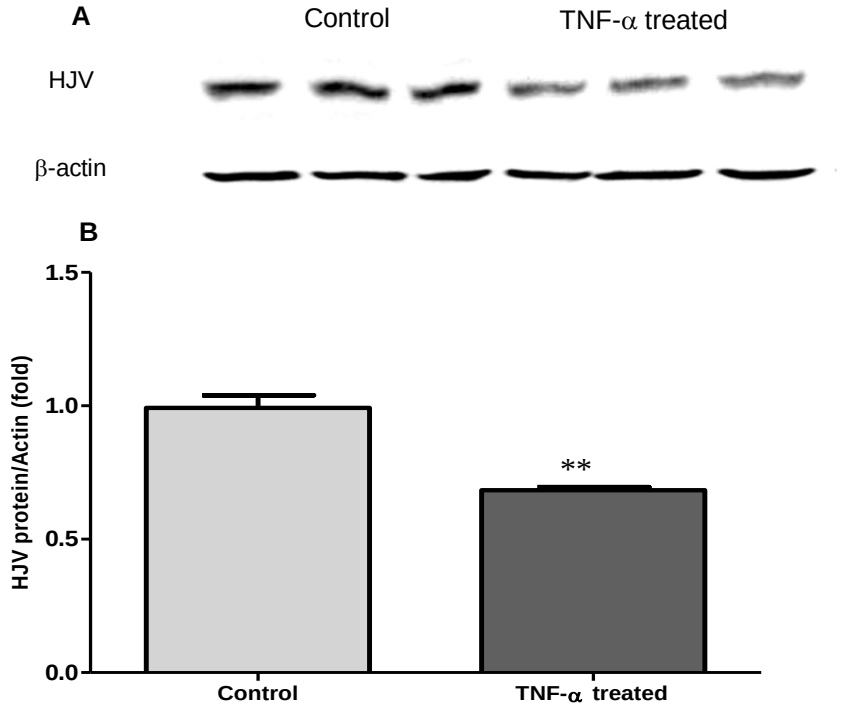

Figure 4.12 Effect of TNF-α treatment on HJV protein expression in HuH7 cells.

(A) Cell lysates from control and TNF-α treated cells (n = 6 in each group) were analyzed by Western blotting with an antibody to HJV, β-actin was used as loading control. A representative experiment is shown. (B) Chemiluminescence was quantified using Quantity One software to calculate the ratio of HJV expression to β-actin. Mean ratios of four samples (± SEM) are represented on this figure, relative to the mean ratio of the control cells. Statistical significant differences relative to control cells were determined by Student *t* tests. **p < 0.01.

4.3.4.5 Effect of TNF-α treatment on *HJV* promoter-reporter activity

In order to determine the mechanism of *HJV* suppression in response to TNF-α, 1.2 Kb of the human *HJV* promoter was cloned as a transcriptional fusion with firefly luciferase to give *HJV*P1.2-luc (Figure 4.13). The luciferase activity reported by *HJV*P1.2-luc-transfected HuH7 cells showed that the basal luciferase activity of *HJV*P1.2-luc was inhibited by 40% following TNF-α treatment (P<0.0001) (Figure 4.14), suggesting that the cloned promoter region is responsive to TNF-α.

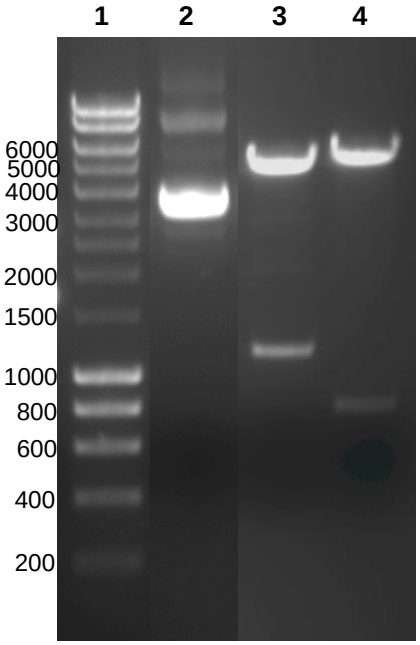

Figure 4.13 1% Agarose/ ethidium bromide gel of HJV promoter construct and restriction enzymes digest.

Lane 1 is a 10 Kb molecular weight marker, lane 2 is undigested *HJV*p1.2-luc, lane 3 is plasmid digested with *Nhe*I and *Xho*I showing 1.2 Kb insert, lane 4 is plasmid digested with *EcoR*I and *Xho*I showing the correct pattern.

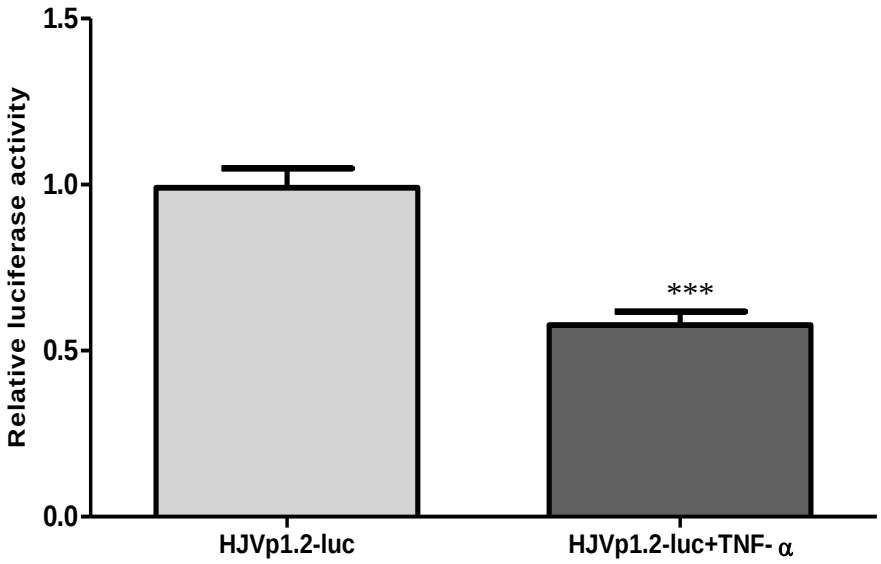

Figure 4.14 Effect of TNF-α on luciferase activity reported by *HJV*P1.2-luc transfected HuH7 cells.

Transfected HuH7 cells were incubated for 24 hours in the presence of TNF-α (20ng/ml). Luciferase activity reported by *HJV*P1.2-luc-transfected cells demonstrated that the basal luciferase activity of *HJV*P1.2-luc was significantly decreased following TNF-α treatment. Data are mean ± SEM, n=12 from 3 separate experiments. **p<0.0001.

4.3.4.6 Effect of TNF-α treatment on luciferase activity of *HJV*P1.2-luc and mt*HJV*P1.2-luc

A single consensus TNFRE was identified in the *HJV*P1.2-luc sequence. In order to ascertain whether this site is functional and responsible for TNF-α suppression of *HJV* expression, site-directed mutagenesis was performed. The TNFRE was replaced by an *EcoR*I restriction site to generate mt*HJV*P1.2-luc (Figure 4.15). As shown in Figure 4.16, the luciferase activity reported by *HJV*P1.2-luc was suppressed by 33% following TNF-α treatment ($p<0.0001$). On the other hand, mt*HJV*P1.2-luc activity did not change following TNF-α treatment. These data strongly suggest that TNF-α suppresses the transcription of *HJV* through this RE.

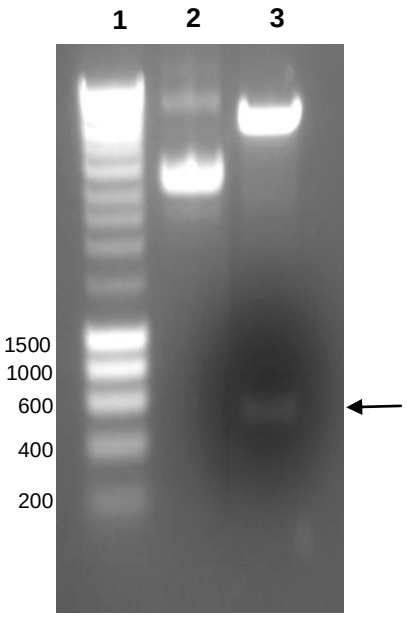

Figure 4.15 1% Agarose/ethidium bromide gel of *HJV* promoter construct with mutated TNFRE and restriction enzyme digest.

Lane 1 is a 10 Kb molecular weight marker, lane 2 is undigested mt*HJV*p1.2-luc, lane 3 is plasmid digested with *EcoRI* showing the expected band size of 400 bp (arrow).

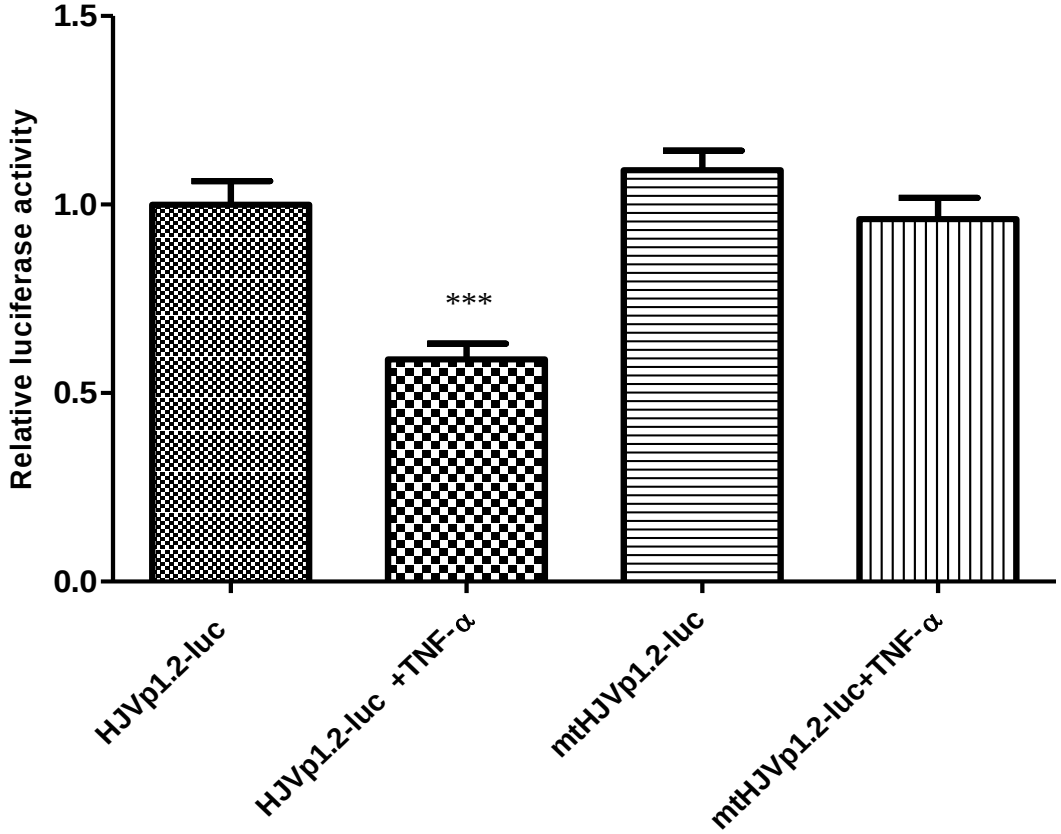

Figure 4.16 Luciferase reporter activity of *HJV*P1.2-luc and mt*HJV*Bp1.2-luc transfected Huh7 cells following TNF-α treatment.

HuH7 cells were transfected with *HJV*P1.2-luc or mt*HJV*P1.2-luc to verify that the identified TNFRE is functional. Transfected HuH7 cells were incubated for 24 hours in the presence of TNF-α (20ng/ml). The data demonstrated that the basal luciferase activity of *HJV*P1.2-luc was significantly decreased following TNF-α treatment, whereas no significant difference was observed in luciferase activity of mt*HJV*P1.2-luc following TNF-α treatment. These data suggest that this element is important for TNF-α responsiveness. Data are mean ± SEM, n=12 of 3 independent experiments. ***p<0.0001.

4.4 Discussion

The regulation of *hepcidin* and *HJV* expression in response to acute inflammation was investigated in C57Bl/6 mice. The possible interaction between inflammation and BMP/Smad signalling was also investigated in LPS-induced acute inflammation. To explore whether HFE is involved in the regulation of *hepcidin* and *HJV* expression during inflammation or the interaction between inflammation and BMP-Smad signalling, *HFE* KO mice were also examined in the setting of acute inflammation.

The direct regulation of *hepcidin* and *HJV* expression by pro-inflammatory cytokines was also examined *in vitro* using a human hepatoma cell line (HuH7). These cells were also used to study the mechanism of *HJV* regulation during inflammation using a *HJV* promoter-reporter construct.

The results showed that C57Bl/6 mice respond to LPS by increasing *hepcidin 1* expression and decreasing the expression of *HJV, BMP-2, BMP-4, and BMP-6* in the liver. *HFE* does not seem to have an effect on hepatic gene regulation during inflammation. In addition, TNF-α, but not IL-6, mediates *HJV* down-regulation during inflammation, whereas IL-6 is required to induce *hepcidin* expression in HuH7 cells. Results also showed that TNF-α-induced *HJV* suppression is possibly mediated by a novel TNF-α response element within the *HJV* promoter.

In this study, it was shown that in wild-type C57Bl/6 mice, acute inflammation significantly decreases serum iron and transferrin saturation levels and increases hepatic iron content, though not significantly. In *HFE* KO mice, LPS decreases serum iron, while it has no effect on transferrin saturation or liver iron content. Moreover, as expected, the mRNA expression of acute-phase genes *IL-6* and *TNF-*α were strongly induced in the livers of LPS-treated wild-type and *HFE* KO mice as compared with saline-treated controls.

The hypoferremia observed in LPS-injected mice in this study is due to cytokine production including IL-6 and TNF-α. IL-6 is believed to cause indirect hypoferremia through stimulation of *hepcidin* expression (Nemeth et al. 2004a), a finding confirmed in this study in IL-6-treated human hepatoma cells *in vitro*. Increased hepcidin in turn causes sequestration of iron in RE macrophages and reduces intestinal iron absorption causing hypoferremia (Roy and Andrews 2005). This effect of hepcidin occurs by binding to IREG1 inducing its internalization and degradation (Nemeth et al. 2004b). On the other hand, TNF-α-induced hypoferremia is hepcidin-independent (Laftah et al. 2004). TNF-α sequesters iron in the liver and spleen because of its ability to down-regulate *IREG1* expression in different cells including macrophages, hepatocytes, and endothelial cells (Constante et al. 2006; Ludwiczek et al. 2003; Nanami et al. 2005).

Hepatic *hepcidin 1* expression in wild-type mice was induced by LPS in this study, in accordance with previous reports (Pigeon et al. 2001; Constante et al. 2006). Contradictory reports have been published on the requirement of *HFE* in the hepcidin up-regulation during inflammation. In one report, the response to LPS is blunted (Roy et al. 2004), in another one the lack of response is because of differences from animal to animal (Lee et al. 2004), and in a study by Constante et al. (2006) they showed that *HFE* KO mice responded to LPS similarly as wild-type animals. Here it was shown that LPS injection induces *hepcidin 1* gene expression in *HFE* KO mice; the hepcidin induction in *HFE* KO was similar to that observed in wild-type mice. These results suggest that *HFE* is not required for *hepcidin* induction during acute inflammation in the mouse strain tested and are in agreement with other reports (Constante et al. 2006; Lee et al. 2004).

Hepatic *HJV* expression in wild-type and *HFE* KO mice was down-regulated by LPS. A similar finding was recently reported by Constante et al. (2007). These data

imply that the ability to down-regulate *HJV* expression during the acute phase response remains integral even in the absence of functional HFE.

It is well established that BMPs induce *hepcidin* expression through Smad signalling via a common mediator, Smad-4 (Babitt et al. 2006; 2007). However, in mice with hepatic disruption of *Smad-4*, the response of hepcidin to inflammatory stimulation is blunted (Wang et al. 2005). Moreover, a recently identified BMP-responsive element within the *hepcidin* gene promoter was found to be not only important for the BMP response but also for IL-6 responsiveness (Verga Falzacappa et al. 2008). These data suggest that there is possible cross-talk between the IL-6 and the BMP-Smad signalling pathways. Here the effect of inflammation on hepatic expression of *BMPs* was investigated. Because BMPs transmit signals through phosphorylation of Smad1, Smad5 and Smad8, the relative abundance of phosphorylated forms of these three Smads was also quantified in liver extracts of LPS- and saline- injected wild-type and *HFE* KO mice by Western blot analysis. Interestingly, it was found that *BMP-2, BMP-4, and BMP-6* mRNA expression levels were down-regulated in response to acute inflammation in wild-type and *HFE* KO mice with no change in phosphorylated Smad1/5/8 expression in the liver. In addition, no change was observed in *TGF-β* expression in response to inflammation. These findings suggest that BMPs are not required for *hepcidin* induction during inflammation, and the link between inflammation and Smad signalling is downstream of BMP ligands, possibly at the level of Smad-4, and is HFE independent. This is the first demonstration that inflammation regulates *BMPs'* expression *in vivo*; however, the exact mechanism needs further investigation.

It seems that BMP-Smad signalling needs to be switched off during inflammation in order to induce *hepcidin* expression. This is evident by selective suppression of *HJV, BMP-2, BMP-4, and BMP-6* in the liver of LPS-injected mice observed in this study. However, as mentioned previously intact Smad-4 is required for proper hepcidin response to inflammatory stimuli.

Although *BMPs* and *HJV* were suppressed in the liver of LPS-injected mice, no change in phosphorylated Smad 1/5/8 was observed in these mice. This might be due to other unidentified ligands or TGF-β whose expression does not change in response to LPS; therefore, it can maintain the basal expression levels of phosphorylated Smads.

LPS is recognized by Toll-like receptor (TLR) 4 which, upon activation, produces pro-inflammatory cytokines such as TNF-α, IL-1, and IL-6 (Hoshino et al. 1999). In this study it was shown that when HuH7 cells are exposed to IL-6, *hepcidin* mRNA expression increased 3-fold confirming the findings by other groups that IL-6 directly regulates *hepcidin* expression (Nemeth et al. 2004a; Nemeth et al. 2003). In contrast, no change in *hepcidin* expression was observed in cells treated with TNF-α. Similar findings were recently reported by Constante et al. (2007). This indicates that IL-6, but not TNF-α, mediates *hepcidin* induction during inflammation.

To test whether IL-6 and TNF-α are able to regulate *HJV* expression directly in hepatocytes, HuH7 cells were treated with the two different cytokines. Exogenous TNF-α suppressed *HJV* expression in a time-dependent fashion reaching its maximal suppression after 24 hours, whereas no response was observed in IL-6-treated cells. HJV protein suppression was also demonstrated in this study for the first time in response to TNF-α treatment in HuH7 cells. These findings indicate that TNF-α, but not IL-6, mediates *HJV* suppression during inflammation.

To further uncover the mechanism of *HJV* suppression by TNF-α during inflammation, the *HJV* promoter-reporter construct (*HJV*p1.2-luc) was used. This construct was transfected into HuH7 cells. In transfected cells, TNF-α suppressed the luciferase activity suggesting that the promoter construct is responsive to TNF-α. Next, a single consensus TNF-α responsive element (TNFRE) was identified within the cloned *HJV* promoter sequence. This sequence has been shown to be responsible for TNF-α-mediated down-regulation of different human genes such as

osteocalcin, thrombomodulin, alkaline phosphatase, and c-myc (Li and Stashenko 1993; Ohdama et al. 1991; Weiss et al. 1988; Watt et al. 1983).

To test whether this TNFRE mediates the TNF-α response, site-directed mutagenesis was carried out to disrupt this sequence. Interestingly, the mutation of the identified TNFRE abolished TNF-α responsiveness. It was concluded that the identified TNFRE is functional and may mediate TNF-α response; however, this needs further investigation.

From the results shown here, it seems that the down-regulation of *HJV* and *BMPs* in the liver during inflammation is a prerequisite for the *hepcidin* induction by cytokines during inflammation *in vivo*. This concept is supported by the recent findings that mice either lacking *HJV* or *BMP-6* retain the ability to induce hepcidin in response to inflammatory stimuli (Meynard et al. 2009; Niederkofler et al. 2005); indicating that neither *HJV* nor *BMP-6* is required for *hepcidin* response to inflammation. However, both HJV and BMP-6 have been shown to be required for *hepcidin* response to iron, in other words, they are important for iron sensing.

The prospective mechanistic explanation is as follow. The iron sensing pathway through HJV-BMP-Smad signalling is switched off during LPS-induced inflammation by the selective suppression of *HJV* (by TNF-α) and *BMP* (by an unknown mechanism) expression in the liver. This in turn stimulates cytokine-induced *hepcidin* expression.

The regulation of *HJV* and *hepcidin* by different cytokines may suggest a time-dependent control of iron homeostasis during inflammation. It is well known that LPS signalling via TLR4 causes a release of pro-inflammatory cytokines which is time-dependent. TNF-α is the first cytokine to be produced and can directly regulate *HJV* expression as shown in this study. TNF-α, in turn, causes a production of other cytokines including IL1β and IL-6. IL-6 can directly modulate *hepcidin* expression in hepatocytes as shown here and by others.

4.5 Conclusion

The results from the present study demonstrate that the pro-inflammatory cytokines TNF-α and IL-6 differently regulate *hepcidin* and *HJV* expression. TNF-α seems to suppress *HJV* transcription possibly via a novel TNFRE within the *HJV* promoter, while IL-6 induces *hepcidin* expression via STAT3 signalling. The results from the acute inflammation study in mice has shown that although *hepcidin* expression is up-regulated as a result of inflammation, *HJV* and *BMP* expression is selectively repressed in the liver suggesting a crucial requirement for the down-regulation of these genes in order to induce *hepcidin* during inflammation. However, the response observed in gene expression seems to be HFE-independent. In addition, the results also suggest that the proposed link between inflammation and BMP-SMAD signalling is downstream of HJV and BMP ligands, possibly at the level of common mediator Smad-4.

Chapter 5: Regulation of Hemojuvelin Expression by Upstream Stimulatory Factors

5.1 Introduction

Hemojuvelin (HJV) is a membrane protein that is encoded by a gene originally cloned by Papanikolaou et al. (2004). *HJV* mutations are associated with the majority of juvenile hemochromatosis. In both humans and mice, *HJV* mutations cause low or undetectable levels of hepcidin, the key iron regulatory hormone; this suggests that HJV is a potent upstream regulator of hepcidin. It has recently been shown to act as a co-receptor for BMP-Smad signalling to regulate *hepcidin* gene expression (Babitt et al. 2007).

HJV has been shown to be post-transcriptionally regulated. It has two isoforms: a secreted soluble form (s-HJV) which is generated by furin cleavage, and a membrane-bound form (m-HJV) (Kuninger et al. 2006; Lin et al. 2008; Silvestri et al. 2008a). S-HJV has been shown to repress BMP signalling by competing with m-HJV for BMP binding (Babitt et al. 2007; Lin et al. 2008). Therefore, any factor that increases s-HJV production could suppress hepcidin production. Further support for this hypothesis came from the finding that iron depletion and hypoxia, are both associated with low *hepcidin* expression, and associated with increased s-HJV production (Lin et al. 2005; Silvestri et al. 2008a).

Upstream stimulatory factors (USFs) were initially identified by Sawadogo and Roeder (1985) as a binding activity that actuate the adenovirus major late promoter. USF purification unveiled the existence of two proteins of 43kDa (USF1) and 44kDa (USF2), which are encoded by two different genes that have been characterised in mice (Henrion et al. 1995; Henrion et al. 1996, Aperlo et al. 1996). Although these genes are ubiquitously expressed in different cell types, their relative expression levels are variable among different mammalian cells (Sirito et al. 1994; Viollet et al. 1996).

USF1 and USF2 have been shown to bind to the consensus sequence CANNTG, called the E-box as homodimers or heterodimers; however, the heterodimer has

been shown to be the predominant binding species (Viollet et al., 1996). Since the demonstration of their involvement in transcriptional regulation of the adenovirus late gene promoter, USFs have been shown to regulate different genes responsible for a variety cellular processes. Among these are glucose-responsive genes, genes for glycoprotein B, actin, vasopressin, and genes controlling the circadian rhythm (Yamashita et al. 2001; Wang and Sul 1997; Casado et al. 1999; Vallone et al. 2004; Farina et al. 1996; McDonald et al. 2001; Camara-Clayette et al. 1999). More importantly, USFs have been shown to regulate the expression of *TGF-β* and *β-2 microglobulin*, which play an important role in iron metabolism (Scholtz et al. 1996; Gobin et al. 2003). In addition, our group recently showed that USFs are important for the regulation of *hepcidin* expression through binding to E-boxes within the *hepcidin* gene promoter (Bayele et al. 2006). The original link between USFs and iron metabolism was established by Nicolas et al. (2001) who found that mice with genetic ablation of *Usf2* showed massive iron overload and lacked *hepcidin* expression.

Unlike hepcidin, little is known about the regulation of *HJV* expression. In the previous chapter, it was demonstrated that *HJV* was transcriptionally down-regulated during inflammation *in vivo*, and this down-regulation was mediated via TNF-α *in vitro*. In this chapter, the aim was to investigate the possible transcriptional regulation of *HJV* by USFs by using a *HJV* promoter construct. This was achieved by deletion mapping, transactivation, DNA-binding, and chromatin-immunoprecipitation (ChIP) assays in human hepatoma cell lines, HepG2 and HuH7.

5.2 Methods

5.2.1 Overexpression of USF1 and USF2 in a human hepatoma cell line

To investigate the effect of overexpression of USFs on the endogenous *HJV* mRNA expression levels, HepG2 cells were transfected with (1μg) of USF1, USF2 expression plasmids (kindly provided by Dr. Henry Bayele), and empty pcDNA3.1 vector (Invitrogen) (control) using Lipofectamine 2000 (Invitrogen) as described in Section 2.5, for 48 hours in 6-well plates followed by RNA extraction, cDNA synthesis, and RT-PCR quantification of *HJV* mRNA as previously described in Chapter 2.

5.2.2 Effect of USFs on the activity of *HJV* promoter construct

To examine the effect of USFs on the luciferase activity of *HJV* promoter construct, HuH7 cells were either transfected with 200ng of *HJVp1.2-luc* alone or with USF1 or USF2 expression plasmids (100ng) using Lipofectamine 2000, as described in Section 2.5, for 48 hours in 24-well plates followed by measurement of luciferase activity as described before.

5.2.3 Generation of *HJV* promoter deletion constructs

PCR was used to generate different deletions within *HJV* promoter using *HJVp1.2-luc* (Section 2.3) as template. Primers used are listed in table 5.1. PCR products were then purified (Section 2.3.2), digested with *NheI* and *Xho I* (section 2.3.3), ligated into pGL3Basic vector (Section 2.3.4), and transformed into *DH5-α* competent cells (Section 2.3.5). Purified plasmids were then digested with *NheI*

and *XhoI* to verify that they contained the correct inserts. All constructs were sequenced to confirm their authenticity. To determine the basal activity of different promoter deletions, constructs (200ng each) were co-transfected with pSVβgal (50ng) into HuH7 cells for 48 hours, and reporter activities were measured as described in Section 2.5. Luciferase levels were normalized with respect to β–gal activity. Two identical E-boxes (CAGCTG) were identified in the sequence of the *HJV* promoter deletion construct with the highest basal activity.

Table 5.1 Primers used for generation of different HJV promoter deletions using PCR

Oligo name	Sense	Anti-sense
Construct 1	CATGCTAGCGGACTTAGCT ATTTTTAAAA	CATCTCGAGCTGCTGTCTCACTGAGGTCA (*XhoI* restriction site is underlined)
Construct 2	CATGCTAGC GCAGTGACCA CAGAGTCACA	
Construct 3	CATGCTAGC TGAAATACTC TGCAAAGATA	
Construct 4	CATGCTAGC GATCTGAGCT GGATAGACTG	
Construct 5	CATGCTAGC TATATTTTTG AATCTTTTTC (*NheI* restriction site is underlined)	

5.2.4 Electrophoretic mobility shift assay (EMSA)

To investigate whether USFs bind to the identified E-boxes within the *HJV* promoter, EMSA was performed using HepG2 nuclear extract or *E.coli* expressed USFs and radio-labelled E-box probes as described below.

5.2.4.1 Preparation of nuclear extract

A HepG2 nuclear extract was prepared using Nuclear Extract kit (Active Motif, USA). Cells were grown in 75cm^2 flasks until confluent, then all medium was aspirated and cells washed twice with PBS. After the second wash, 3mL of 1X Trypsin-EDTA (Invitrogen) was added to detach cells from the flask. Cells were then transferred to 15mL conical tubes and centrifuged for 5 minutes at 1000 x g. Supernatant was discarded and the cell pellet was washed twice with PBS followed by centrifugation for 5 minutes at 1000 x g. Supernatant was discarded and the pellet was kept on ice. The pellet was gently resuspended in 500μL 1X Hypotonic buffer by pipetting up and down several times, this was transferred to a pre-chilled microcentrifuge tube and incubated for 15 minutes on ice. Then 25μL of detergent was added and the tube was vortexed for 10 seconds. The suspension was then centrifuged for 30 seconds at 14,000 x g in a pre-chilled microcentrifuge at 4^{o}C. The supernatant (cytosolic fraction) was transferred into a pre-chilled microcentrifuge tube and stored at -80^{o}C for future use. The nuclear pellet was then resuspended into 50μL Complete Lysis Buffer by pipetting up and down and then vortexed for 10 seconds. Suspension was then incubated for 30 minutes on ice on a rocking platform set at 150 rpm. Tubes were then centrifuged for 10 minutes at 14,000 x g in a pre-cooled microcentrifuge. The supernatant (nuclear

fraction) was then transferred into a pre-chilled microcentrifuge tube, aliquoted and stored at -80^{o}C until ready to use.

Protein concentration was determined (as described in Section 2.6.2) in 96-well microtiter plates (Nunc, UK).

5.2.4.2 Expression and purification of recombinant USF1 and USF2

5.2.4.2.1 Expression of recombinant USFs

Recombinant USF1 and USF2 were expressed using pET25b-USF1 and pET25b-USF2 constructs as previously described (Bayele and Srai 2009). These constructs were transformed into BL21(DE3) pLysS competent cells (Novagen). To induce protein expression, 1mM (final concentration) IPTG was added to logarithmic phase cultures (OD at 600 nm around 0.4-0.6) for 3 hours at 30^{o}C. Recombinant proteins were purified with the MagneHis system (Promega) as described below.

5.2.4.2.2 Purification of recombinant USFs

To each 1ml of bacterial culture, 110µl of FastBreak^{TM} Cell Lysis Reagent was added with 1µl of DNase I, and incubated for 20 minutes at room temperature on a rotatory wheel. MagneHis^{TM} Ni-Particles were vortexed to form a uniform the suspension and 30µl was added to the cell lysate, mixed 10X by pipetting and incubated for 2 minutes at room temperature. The tube was then placed in a magnetic stand for 30 seconds to capture the MagneHis^{TM} Ni-Particles, and the supernatant was carefully removed. To the magnetic particles, 150µl of MagneHis^{TM} Binding/Wash Buffer was added and mixed with a pipette. The tube was then placed in a magnetic stand for 30 seconds, and the supernatant was carefully removed. The washing step was repeated two more times for a total of

three washes. After the third wash, 50µl of MagneHis^{TM} Elution Buffer was added, the tube was incubated for 2 minutes at room temperature and placed in a magnetic stand to capture the particles. The supernatant, containing the purified protein, was then carefully removed and analysed by running on a 10% SDS-PAGE to check the purity. The proteins were visualised by Coomassie Blue staining (0.2% Coomassie R-250, 20% methanol, 5% glacial acetic acid, 75% water) followed by destaining (20% methanol, 5% glacial acetic acid, 75% water).

5.2.4.3 Gel shift assay [Electrophoretic mobility shift assay (EMSA)]

For mobility shifts, oligonucleotides containing the wild-type, mutant *HJV* E-boxes, or consensus E-box were synthesised (Sigma) as follows E-box1 oligonucleotides sense, TCCCTCCCTGCTCAGCTGTCCAGTACTCTG and reverse complement CAGAGTACTGGACAGCTGAGCAGGGAGGGA; E-box2 sense, GAAAGGTATCCAATTGCCCACTGTAATTTT and reverse complement GACGAAAAAAGCCAGCTGTCCAGAGAAGAA; mutant E-box sense TCCCTCCCTGCTCAGCgaTCCAGTACTCTG and reverse complement CAGAGTACTGGAtcGCTGAGCAGGGAGGGA (mutated nucleotides are in lower case); consensus E-box sense, CAC CCG GTC ACG TGG CCT ACA CC and reverse complement GGTGTAGGCCACGTGACCGGGTG. Oligonucleotides were then annealed in quick ligase buffer (NEB) by heating the tubes containing oligos at 95^{o}C for 5 minutes and leaving them to cool down to room temperature. About 100pmol of each duplex was end-labeled with γ^{32}P[ATP] (111 TBq/mmol; Perkin Elmer, Wellesley, MA) and T4 polynucleotide kinase (New England Biolabs) and diluted to 1pmol/µL with Tris EDTA (pH 8.0). Approximately 1pmol of each probe was incubated with 10µg nuclear extract or 5ng from recombinant USF1 or USF2 in binding buffer (4% glycerol, 1mM MgCl2, 0.5mM EDTA, 0.5mM DTT, 10mMHEPES pH 7.9, 50mMNaCl, and 50µg/mL poly [dI-dC] _ poly[dIdC]) in a total

volume of 10μL for 20 minutes at room temperature. For competitive inhibition, a 100-fold molar excess of the cold oligonucleotides was added to the binding reaction 10 minutes before adding the labeled probe. Following incubation, 1μL from 10Xgel loading buffer (250mM Tris-HCl (pH 7.5), 0.2% (w/v) bromophenol blue and 40% (v/v) glycerol) was added to each sample. The samples were then resolved on a 4% non-denaturing polyacrylamide gel (4% (v/v) acrylamide/bisacrylamide, 3% (v/v) Glycerol, 0.05% (v/v) TEMED, 0.075% (w/v) APS) in 0.5 X TBE buffer (0.54% Tris base, 0.27% boric acid, 0.037% Disodium EDTA. $2H_2O$) pH (8.3). Gels were run at 120V until the bromophenol dye front had migrated to about 1cm from the bottom of the gel (approximately 1 hour). The gels were dried at 80°C for 6 hours using a gel dryer (Bio-Rad) and exposed to X-ray film (Fuji film) for 6 hours at - 80°C. The X-ray film was then developed in a dark room fitted with a red safety light using Compact X4 Xograph Imaging System (Xograph Healthcare Ltd, UK).

5.2.5 ChIP assay

To confirm the binding of USF to *HJV* E-boxes *in vivo*, a ChIP assay was performed using cross-linked HepG2 chromatin and USF-1 antibody as described in detail below. HepG2 cells were grown in 75cm^2 flasks to 90% confluence. DNA was cross-linked to histones by adding formaldehyde directly to the culture medium to a final concentration of 1% and incubating the cells for 10 minutes at 37^{o}C. Cells were washed twice with ice-cold PBS and scraped into conical tubes. Cells were then pelleted for 4 minutes at 2000 x g at 4^{o}C, resuspended into SDS lysis buffer (1%SDS, 10mM EDTA, 50mM Tris, pH 8.1), and incubated on ice for 10 minutes. The lysate was then sonicated with 8 sets of 30 second bursts followed by 1 minute cooling using Soniprep-15 sonicater (Sanyo MSE, UK) equipped with 2 mm tip and set to 5.5 amplitude. This procedure results in DNA fragment sizes of 200-1000bp. Samples were then centrifuged for 15 minutes at 10000 x g at 4^{o}C; the

pellet was discarded and supernatant was diluted 10-fold in ChIP dilution buffer (0.01% SDS, 1.1% Triton X-100, 1.2mM EDTA, 16.7mM Tris-HCl, pH 8.1, 167mM NaCl) and 1% of the diluted chromatin was kept as an input. To reduce nonspecific background, salmon sperm DNA and protein A-agarose beads (Sigma) were added to the sample then incubated for 30 minutes at 4^{o}C on rotatory wheel followed by centrifugation at 2000 x g for 5 minutes at 4^{o}C to collect the supernatant. Anti-USF1 antibody (10μg; Santa Cruz Biotechnology) was added to the sample and incubated overnight at 4^{o}C on rotatory wheel. As a negative control, half of the pre-cleared sample was incubated with 10μg of nonspecific immunoglobulin G (IgG) of the same isotype (Sigma). Chromatin immunoprecipitates were collected with fresh protein A agarose/salmon sperm DNA and washed sequentially for 3-5 minutes on a rotatory wheel in low-salt (0.1% SDS, 1% Triton X-100, 2mM EDTA, 20mM Tris-HCl, pH 8.1, 150mM NaCl), high-salt (0.1% SDS, 1% Triton X-100, 2mM EDTA, 20mM Tris-HCl, pH 8.1, 500mM NaCl), LiCl (0.25M LiCl, 1% NP-40, 1% sodium deoxycholate, 1mM EDTA, 10mM Tris, pH 8.1), and TE(10mM Tris-HCl, 1mM EDTA, pH 8) buffers. The immune complexes were then eluted with 1% SDS and 0.1 M NaHCO3 at room temperature for 15 minutes. To reverse cross-linking, the eluates were incubated at 65°C overnight with NaCl (0.2 M final concentration) and then with 10 mM EDTA, 40 mM Tris-HCl (pH 6.5), and 40 mg/mL proteinase K (Sigma) at 45°C for 1 hour. The DNA was extracted with a QIAquick PCR purification kit (QIAGEN) and subjected to 30 cycle-PCR amplification with the forward primer 5'-TGGAGTAGGTAGGAGGATAGAC -3' and the reverse primer 5'-TAATGTTGAGCTCCTGGCCT -3' which were specifically designed from the *HJV* promoter . The 300-bp PCR product was resolved by 2% agarose-ethidium bromide gel electrophoresis and visualized under UV. The PCR product was cloned into the pGEM-T Easy vector (Promega). The cloned PCR product was analyzed by sequencing (Wolfson Institute for Biomedical Research, UCL) and compared with the human *HJV* promoter sequence to confirm its authenticity.

5.3 Results

5.3.1 Effect of USF over-expression on *HJV* mRNA expression in HepG2 cells

To investigate the effect of over-expression of USFs on *HJV* mRNA expression, HepG2 cells were either transfected with empty vector (control), USF1 or USF2 expression plasmids followed by quantification of *HJV* mRNA expression by RT-PCR. As shown in Figure 5.1, USF1 or 2 over-expression significantly increased *HJV* mRNA expression to a similar extent.

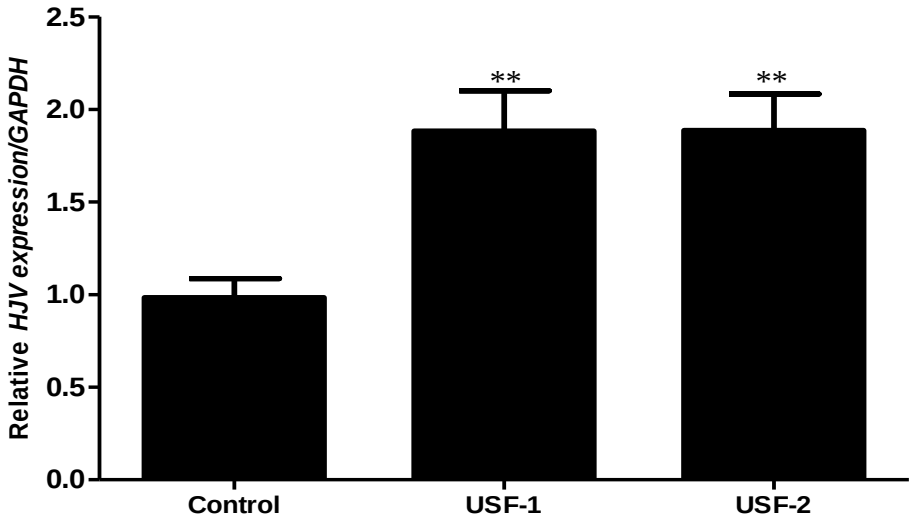

Figure 5.1 Effect of USFs overexpression on *HJV* mRNA expression in HepG2 cells.

HepG2 cells were either transfected with empty vector (control), USF1or USF2 expression plasmids followed by quantification of *HJV* mRNA by RT-PCR. Over-expression of either of the USFs significantly increased *HJV* mRNA expression. Data are mean±SEM, n=6 of three separate experiments. **p<0.01.

5.3.2 Effect of USFs on the activity of *HJV* transcription

To examine the effect of USFs on *HJV* regulation, HuH7 cells were either transfected with *HJVp1.2-luc* alone or with USF1 or USF2 expression plasmids followed by measurement of luciferase activity. Co-transfection of *HJVp1.2-luc* with exogenous USF1 and USF2 significantly increased the luciferase activity of the *HJV* promoter (Figure 5.2).

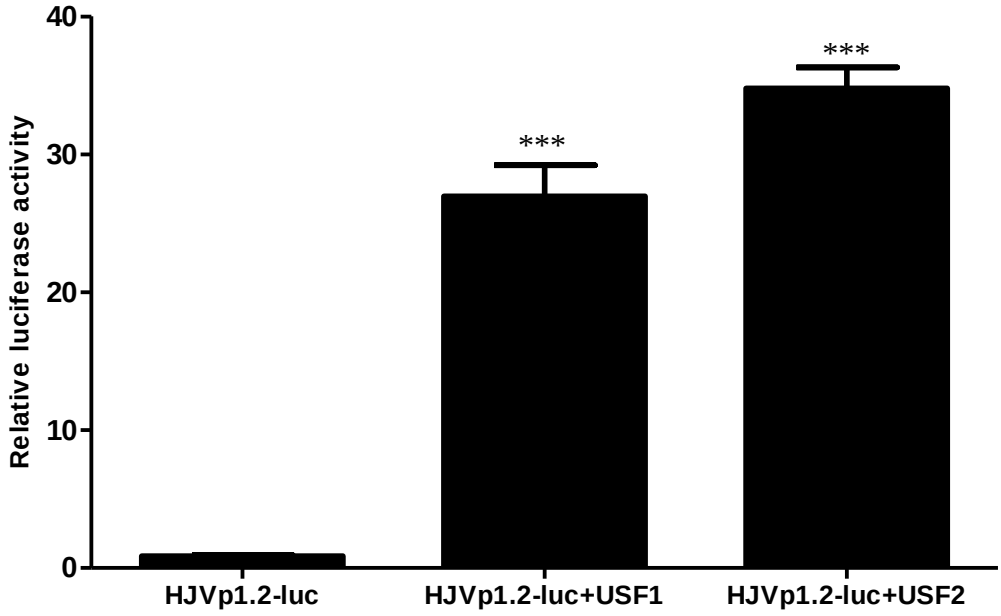

Figure 5.2 Effect of USF1 and USF2 on luciferase activity of *HJV* promoter in transfected HuH7 cells.

HuH7 cells were transfected with *HJVp1.2-luc* (200ng) alone or with USF1, USF2 expression plasmids (100ng) followed by measurement of luciferase activity. Fold activation was calculated with respect to the activity of *HJVp1.2-luc* alone. Both USFs significantly increased luciferase activity of the *HJV* promoter. Data are mean ± SEM (n=12) of 3 independent experiments. ***p<0.001.

5.3.3 Deletion mapping of HJV promoter and identification of enhancer elements

Different deletion constructs were generated from *HJVp1.2-luc* using PCR (Figure 5.4A). PCR products were then purified, ligated into pGL3Basic vector (Promega), and transformed into DH5-α competent cells (Invitrogen). Purified plasmids were then digested with *NheI* and *XhoI* to verify that they contained the correct inserts (Figure 5.3). To determine the basal activity of different deletion constructs, 200ng of each construct was co-transfected with pSVβgal (50ng) into HuH7 cells for 48 hours, and reporter activities were measured. Luciferase levels were normalized with respect to β–gal activity. As shown in Figure 5.4B some of the constructs (1, 2, and 3) showed similar activity to *HJVp1.2-luc.* Constructs 4 and 5 showed significantly higher luciferase activity than *HJVp1.2-luc.* Further inspection of the sequence of the construct 4 revealed the existence of two identical E-boxes with the sequence CAGCTG as shown in Figure 5.5.

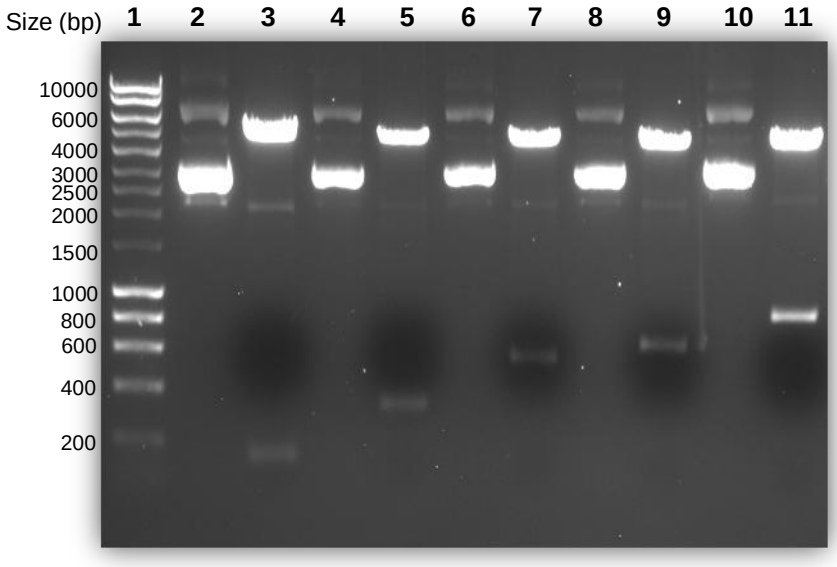

Figure 5.3 2% Agarose/Ethidium bromide gel electrophoresis of different *HJV* promoter deletion constructs.

Undigested plasmids (Lanes 2, 4, 6, 8, and 10) and *NheI-XhoI*-digested plasmids (Lanes 3, 5, 7, 9, and 11) were run on a 2%agarose/ethidium bromide gel. Inserts with correct sizes are shown in respect to a molecular weight marker (Lane1).

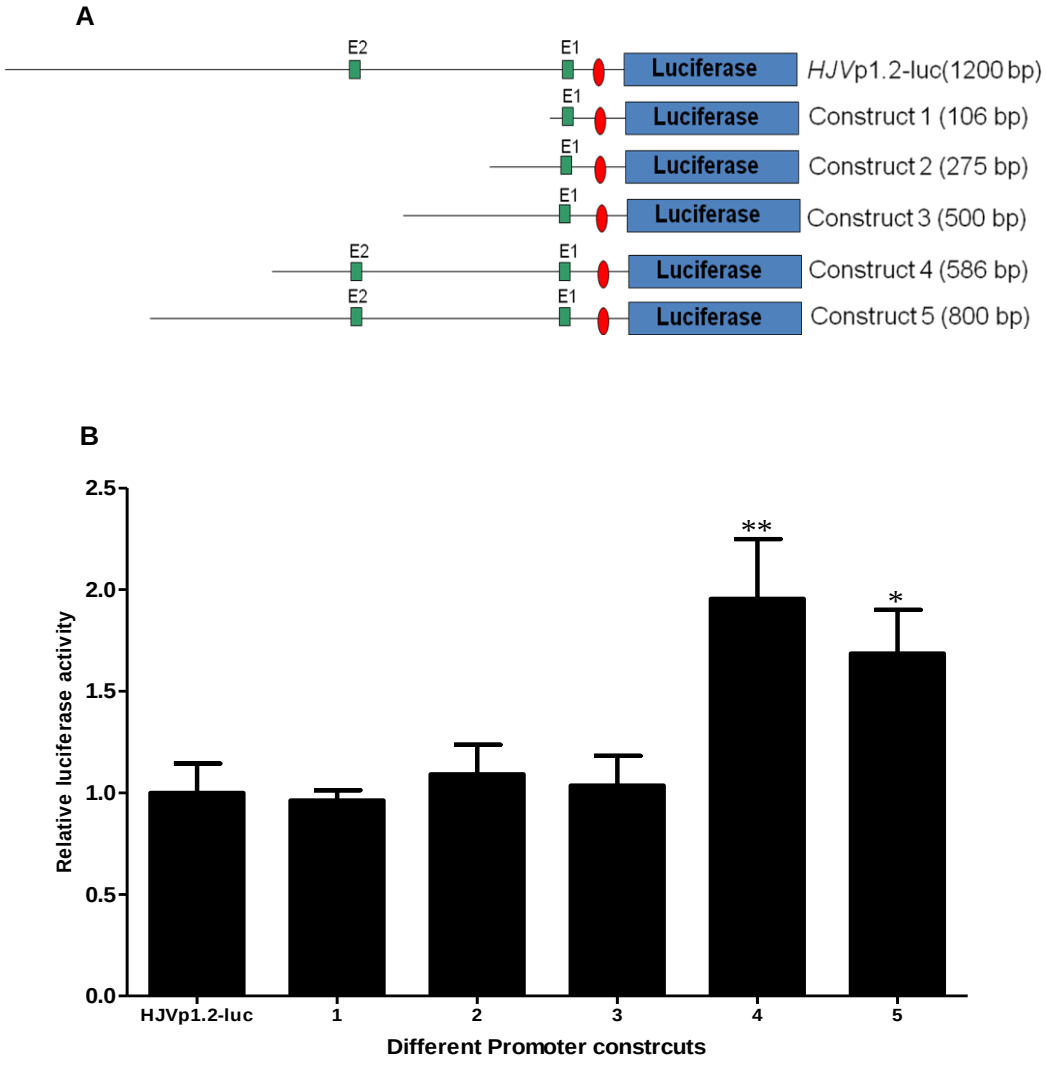

Figure 5.4 Deletion mapping of the human *HJV* gene promoter.

(A) *HJVPp1.2-luc* was subjected to deletions by PCR to generate different fragments; the size of each fragment is shown in brackets. The green boxes represent the identified E-boxes (E1, E2) with respect to the position of the beginning of the *HJV* first exon (red oval). (**B**) Basal transcriptional activity of different promoter deletion constructs from panel A. Constructs (200ng each) were co-transfected with pSVβgal (50ng) into HuH7 cells for 48 hours, and reporter activities were measured. Luciferase levels were normalized with respect to β–gal activity. Fold activation was based on the activity of *HJVp1.2-luc*, and assigned an arbitrary activation level of 1. Data are mean ±SEM, n=8 of 3 independent experiment. *p<0.05, ***p<0.*01.

gatctgagct ggatagactg aacaaaccct
catcctaagc aactcacagc tcagatttct tctctggaca gctggctttt
ttcgtccttc tgaaatactc tgcaaagata ggagaggggc tatgaactac
ctctgctatg gatcttattc aaagtcagct acctcctaga tactatctgt
agaacctaaa tgtaatattc agcatagcag ggatgaacat ggtaaatgaa
aggtatccaa ttgcccactg taatttttaa aggccaggag ctcaacatta
ttgaaaatgc tggagggctg cctggagtag gcagtgacca cagagtcaca
caagctggaa ttggatatcc aacttgtctg tcatatttct ctcctccctc
cctgacttgg cactcaatac tccatattct ttctaatcct ctaaccctcc
ccactccccc aactcccaca ccctaccccc accaacgttc ctggaatttt
ggacttagct atttttaaaa ccgtcaactc agtagccacc tccctccctg
ctcagctgtc cagtactctg gccagccata tactcccct tccccccata
ccaaaccttc tctggttccc tgacctcagt gagacagcag

Figure 5.5 The sequence of the *HJV* promoter deletion construct with the highest basal activity showing two identical E-boxes.

Spatial arrangement and nucleotide sequences of the E-boxes (blue) within the human HJV gene promoter and the start of first exon (yellow).

5.3.4 Electrophoretic mobility shift assay

To investigate whether USFs bind to *HJV* E-boxes *in vitro*, EMSA was performed using either HepG2 nuclear extract or recombinant purified USFs (Figure 5.6). The purified proteins or HepG2 nuclear extract were incubated with radio-labelled probes. As shown in Figure 5.7, E-box and consensus probes bound to nuclear protein but did not bind to mutant E-box probe. Moreover, similar binding was observed with either recombinant USf1 or USF2, which was not observed with mutant probe (Figure 5.8, 5.9). This binding was abolished when excess cold competitor was added to the binding reaction.

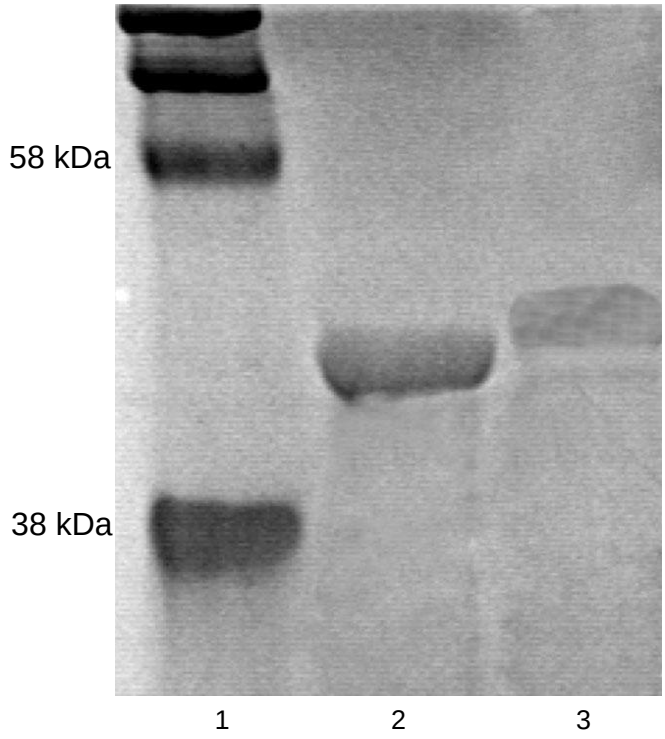

Figure 5.6 SDS-PAGE of purified recombinant USF1 and USF2.

Recombinant E-coli expressed USF1 (Lane 2) and USF2 (Lane 3) were purified from bacterial lysates using MagneHis system (Promega) and run on 10% SDS-PAGE to check protein purity. Lane 1 is molecular weight marker (Biorad) that was used to verify the sizes of purified proteins, USF1 (43 KDa) and USF2 (44 KDa).

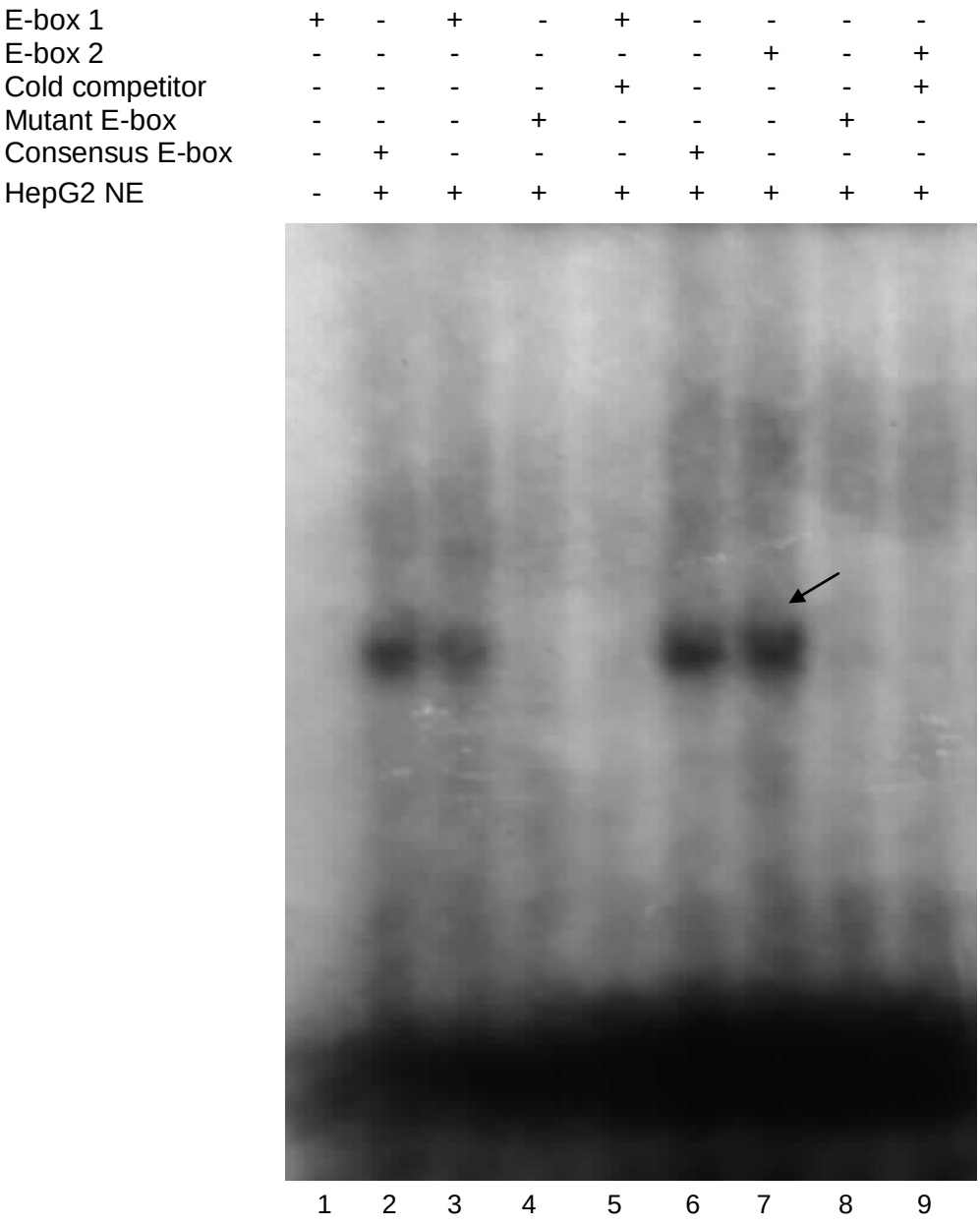

Figure 5.7 Promoter occupancy USF1/USF2 *in vitro* using EMSA.

HepG2 cell nuclear extracts (10 μg) were incubated with radio-labeled E-boxes (lane 3, 7), consensus (lane 2, 6), and mutant E-box (lane 4, 8); where indicated, excess unlabeled or cold competitor oligonucleotide (100pmol) was added to the binding reactions (lane 5, 9). Lane 1 is an E-box oligo without nuclear extract as a negative control. Arrow indicates E-box–nucleoprotein complex.

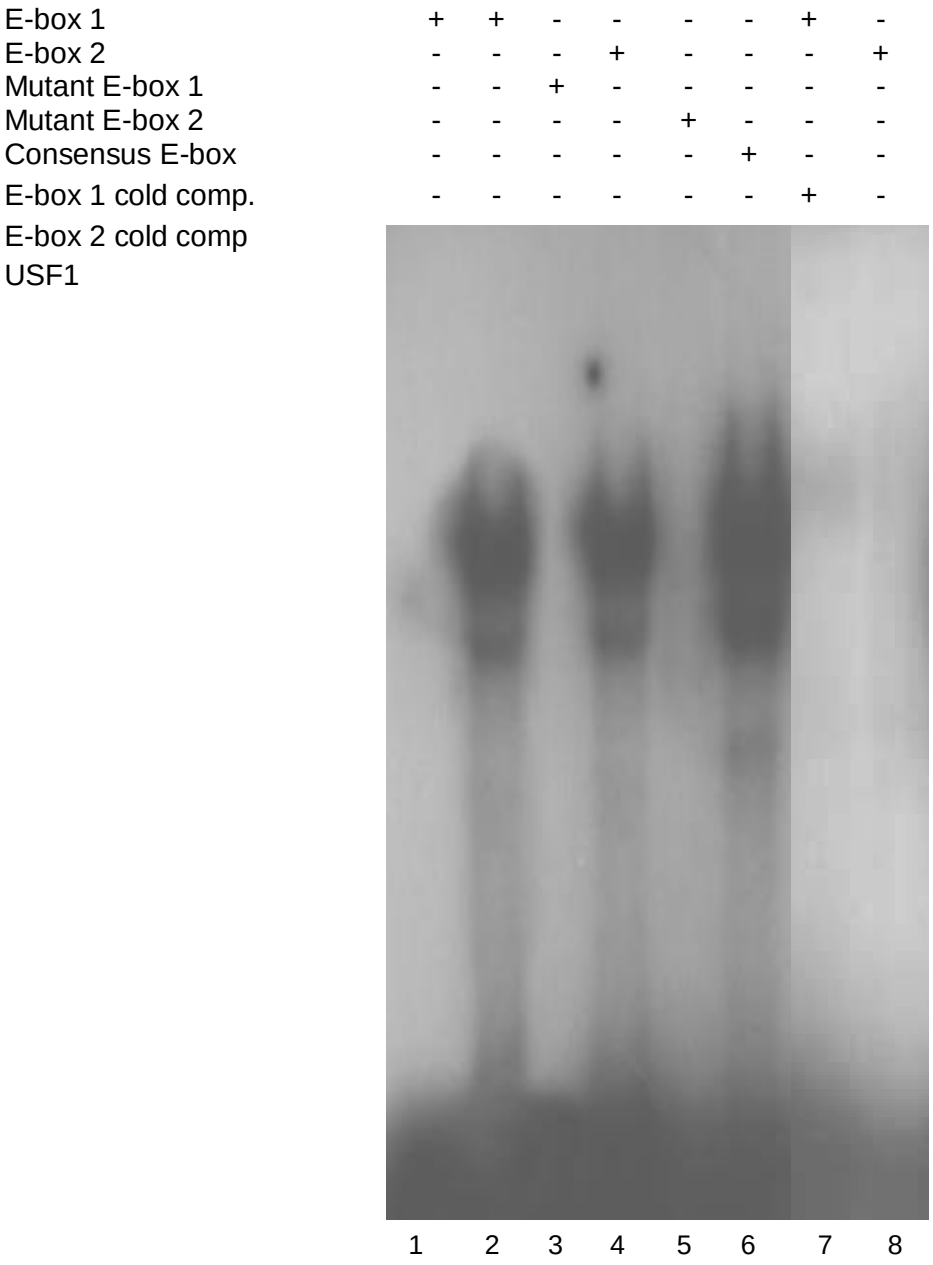

Figure 5.8 Binding of recombinant USF1 to HJV E-boxes *in vitro*.

Recombinant USF1 (10ng) was incubated with radio-labelled E-boxes (lane 2, 4), consensus (lane 6), and mutant E-box (lane 3, 5). In lanes 7 and 8, excess unlabeled or cold competitor oligonucleotide (100pmol) was included in binding reactions. Lane 1 is an E-box oligo without recombinant protein as a negative control.

E-box 1	+	+	-	-	-	+	-	-
E-box 2	-	-	+	-	-	-	-	+
Mutant E-box 1	-	-	-	-	+	-	-	-
Mutant E-box 2	-	-	-	-	-	-	+	-
Consensus E-box	-	-	-	+	-	-	-	-
E-box 1 cold comp.	-	-	-	-	-	+	-	-
E-box 2 cold comp	-	-	-	-	-	-	-	+
USF2	-	+	+	+	+	+	+	+

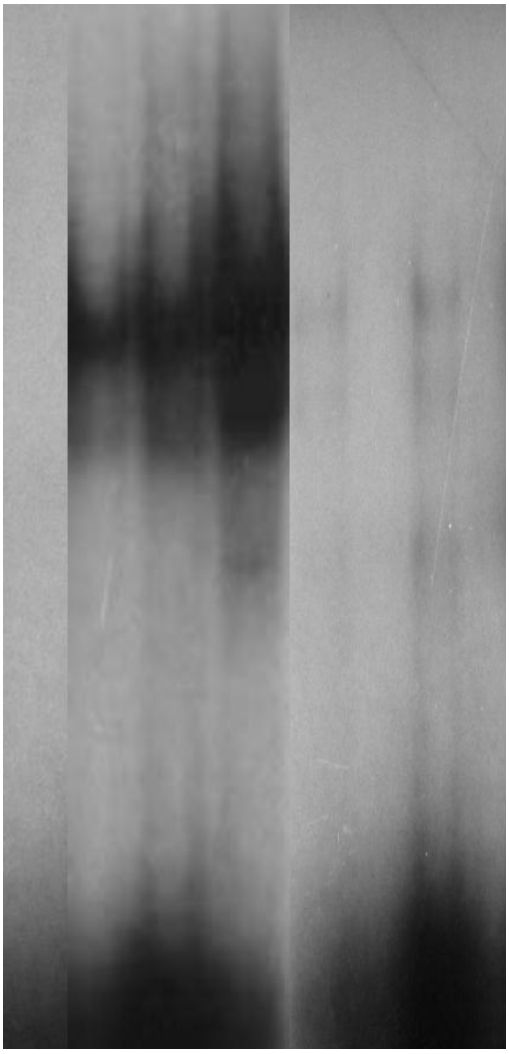

1 2 3 4 5 6 7 8

Figure 5.9 Binding of recombinant USF2 to HJV E-boxes *in vitro*.

Recombinant USF2 (10ng) was incubated with radiolabeled E-boxes (lane 2, 3), consensus (lane 4), and mutant E-box (lane 5, 7); in lanes 6 and 8, excess unlabeled or cold competitor oligonucleotide (100pmol) was included in binding reactions. Lane 1 is an E-box oligo without recombinant protein as a negative control.

5.3.5 Chromatin immunoprecipitation assay (ChIP)

To confirm the binding of USF to *HJV* E-boxes *in vivo*, ChIP assay was performed using sonicated cross-linked HepG2 chromatin (Figure 5.10) and USF1 or non-specific antibody. The immunoprecipitated chromatin was then reverse cross-linked, purified, and used for PCR to amplify a specific fragment within the *HJV* promoter containing the E-box. As shown in Figure 5.11, the expected PCR product was obtained from the chromatin immunoprecipitated with USF1 antibody but not with non-specific antibody. Input chromatin (i.e. without Immunoprecipitation), was used as a positive control.

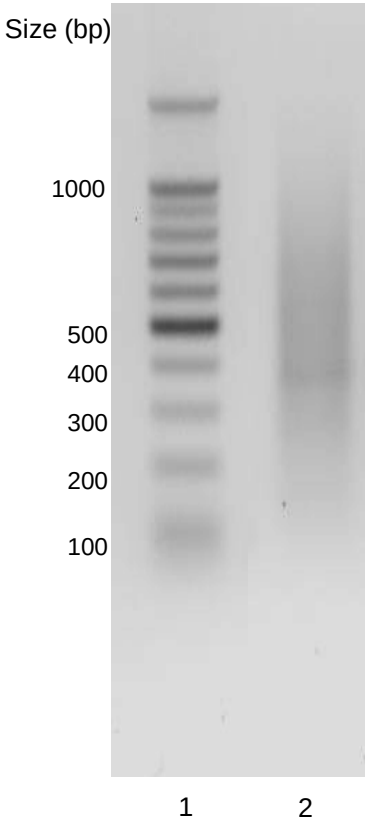

Figure 5.10 Optimisation of chromatin sonication. Agarose/ethidium bromide gel image showing sonicated HepG2 cross-linked chromatin.

Formaldehyde cross-linked HepG2 chromatin was sonicated to generate DNA fragment sizes of 200-1000bp and an aliquot was run on a 1% agarose/ethidium bromide gel (lane 2) alongside molecular weight marker (Promega) (lane1).

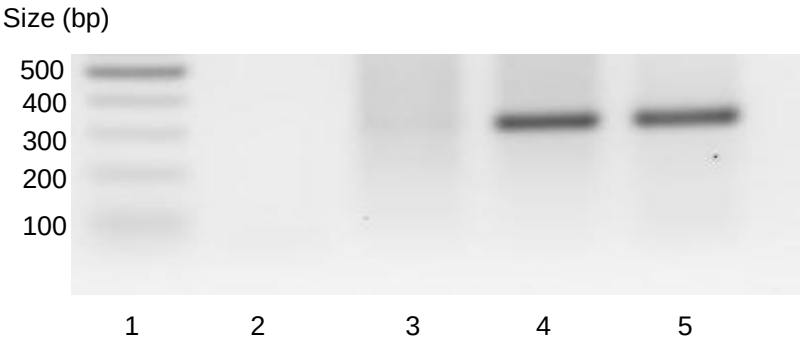

Figure 5.11 Promoter occupancy by USF1 in ChIP assay.

PCR products were run on a 2% agarose/ethidium bromide gel. PCR was performed on whole chromatin without immunoprecipitation (Input, lane 5) and on chromatin immunoprecipitated with either a non-specific antibody (lane 3), or with anti-USF1 antibody (lane 4). Lane 1 is a molecular weight marker (sizes are in base pairs) and lane 2 is a water negative control for PCR reaction.

5.4 Discussion

HJV has been shown to be an important upstream regulator of *hepcidin* gene expression by acting as a BMP co-receptor (Babitt et al. 2006). Mutations in the gene are associated with severe iron overload and low *hepcidin* expression (juvenile hemochromatosis). However, we do not know enough about the regulatory mechanisms that underlie its expression. In this study, the possible regulation of *HJV* expression by USFs was investigated. Over-expression of USF1 and USF2 in HepG2 and HuH7 cells induced *HJV* mRNA and *HJV* promoter activity. Moreover, gel mobility shift analysis demonstrated that protein complexes containing USF1 and USF2 transcription factors are able to bind the *HJV* E-boxes in a nuclear extract of HepG2 cells. Similar binding to *HJV* E-boxes was also shown using recombinant USFs. To further confirm USF binding *in vivo* using the ChIP assay, USF1 was shown to bind specifically to the *HJV* E-box.

USFs have previously been shown to regulate different genes and more importantly *β2-microglobulin*, *TGF-β*, and *hepcidin* (Scholtz et al. 1996; Gobin et al. 2003; Bayele et al. 2006); these are all important for iron homeostasis. Moreover, USF2 has originally been linked to iron metabolism through gene ablation in mice (Nicolas et al. 2001). USFs bind to the E-box, an enhancer element with the consensus sequence CANNTG (Littlewood and Evan 1995). The E-box is a widely-distributed DNA response element. Despite of its conciseness and broad distribution, the E-box is a multifaceted sequence that regulates different genes responsible for different functions including cellular differentiation, proliferation, and tissue-specific responses. Recently, the circadian clock was shown to recruit the E-box. In this regard, E-boxes possibly have a role in initiating the robust waves of gene expression characteristic of circadian transcription (Munoz et al. 2002).

In the present study, the effect of USF over-expression on the endogenous expression of *HJV* mRNA was investigated in HepG2 cells. These cells were

transfected with USF1 or USF2. Exogenous USF1 and USF2 significantly increased *HJV* mRNA expression demonstrating that USFs are important positive regulators of *HJV* expression in liver cells. In addition, co-transfection of the *HJV* promoter with exogenous USF1 and USF2 significantly enhanced reporter gene (luciferase) expression suggesting that USFs are potent positive regulators of *HJV* transcription.

By deletion mapping of the *HJV* promoter, a comparison of luciferase activity of the different constructs demonstrated that the full-length *HJV* promoter construct produced similar or less luciferase than the deletion constructs. This may be due to suppressor elements within the promoter sequence. Further inspection of the sequence of the construct with the highest luciferase activity revealed two identical E-boxes each with the sequence CAGCTG. These E-boxes have the same core sequence that is recognised by members of the basic helix-loop-helix leucine zipper (bHLH-ZIP) family of transcription factors, including USF (Bendall and Molloy 1994; Atchley and Fitch 1997). Of note, deletion constructs that contain one E-box showed the same activity as the full-length construct. In addition, the construct that encompassed both E-boxes showed higher luciferase than the full-length construct. These findings suggest the importance of the E-box elements in *HJV* basal activity.

The binding capacity of the identified E-boxes was investigated *in vitro* by EMSA. Transcription factor binding to the putative E-boxes was tested using a nuclear extract from HepG2 cells; the probes containing *HJV* E-boxes bound a nuclear protein complex. To further confirm whether the E-box bound to USFs, recombinant USF1 and USF2 were used for EMSA. Both recombinant proteins bound to E-boxes but not to the mutant E-box probe. The binding was inhibited by a 100-fold molar excess of cold or unlabelled E-box oligonucleotide. This further confirmed that the promoter occupancy by USF was specifically at the E-boxes.

To investigate the *HJV* promoter occupancy by USF *in vivo*, the ChIP assay was performed with cross-linked HepG2 chromatin. Using anti-USF1 antibody, the target region of the *HJV* promoter containing E-box was immunoprecipitated. In contrast, no immunoprecipitation was obtained when using non-specific IgG. These findings strongly demonstrate the importance of USFs in the regulation of *HJV* expression.

USF1 has been shown to regulate the transcription of hepatic lipase (HL) (Botma et al. 2005), which is also induced by glucose *in vitro* (Tu and Albers 2001) and in type two diabetes *in vivo* (Deeb et al. 2003; Rashid et al. 2003). HL plays an important role in the remodelling of HDL and LDL and the development of dyslipidaemia (Jansen et al. 2002). The *USF1* gene on chromosome 1q21 has been linked to type two diabetes and metabolic syndrome (Ng et al. 2005). Moreover, hyperglycaemic rats showed higher expression levels of USF1 and USF2 in hepatic nuclei (van Deursen et al. 2008).

Glucose has also been shown to increase the expression of USF1 and USF2 in the nuclei of non-hepatic cells (Smih et al. 2002; Bidder et al. 2002; Weigert et al. 2004), and hepatic cells (van Deursen et al. 2008). Moreover, USFs also play an important role in the gene regulation by glucose (Vallet et al. 1998; Smih et al. 2002; Bidder et al. 2002; Weigert et al. 2004; Wang et al. 2004) and insulin (Iynedjian 1998; Wang and Sul 1997; Nowak et al. 2005). These findings strongly suggest a link between these transcription factors and glucose and lipid metabolism.

Taken together, the findings shown here and recently by our group (Bayele et al. 2006) that USFs are involved in the regulation *HJV* and *hepcidin* expression further strengthen the link between these transcription factors and iron metabolism. In

addition, the findings also suggest a possible link between glucose and iron metabolism. However, this needs further investigation.

5.5 Conclusion

The results presented in this chapter clearly demonstrate the involvement of USFs in the regulation of *HJV* expression *in vitro* and *in vivo*. These findings further support the role of these transcription factors and iron homeostasis. Moreover, the role of these factors in glucose and lipid metabolism may provide a novel link between glucose, lipid, iron metabolism, and circadian transcription. However, this hypothesis needs further investigation.

Chapter 6: General Discussion

There is no doubt that the discovery of HFE and hepcidin, the iron regulatory hormone, has energised the study of iron metabolism. Outstanding progress in our understanding of hepcidin functions and regulation has been achieved since its discovery 10 years ago. It controls iron homeostasis by binding to IREG1 inducing its degradation, which in turn controls the amount of iron released from macrophages, enterocytes, and hepatocytes.

In recent years, studies of human diseases and genetically-modified mouse models have unveiled novel genes involved in hepcidin regulation and iron homeostasis, hemojuvelin being one of them. HJV has recently been identified to be an upstream regulator of *hepcidin* expression acting as a BMP-co-receptor; however, little is known about the regulation of *HJV* expression.

The studies described in this thesis were aimed to: 1) Further understand the regulation of *hepcidin* and *HJV* expression by iron and inflammation, and the role of HFE, if any, in their regulation. 2) Study the possible regulation of *HJV* expression by upstream stimulatory factors (USFs) that have previously been shown to regulate *hepcidin* expression.

6.1 Regulation of *hepcidin* expression by iron

Hepcidin is regulated by iron. However, no IREs have been identified in the *hepcidin* gene suggesting an alternative signalling pathway rather than IRP-IRE to modulate its expression by iron. BMP-Smad signalling has been shown to be one of the most important pathways involved in hepcidin regulation. However, whether this pathway is involved in hepcidin modulation by iron is not clear. HFE expression has profound effects on cellular iron status through regulation of *hepcidin* expression. However, the precise mechanism by which HFE regulates *hepcidin* expression is not clearly understood. To explore the role of HFE in the regulation of hepcidin by

iron, WT and *HFE* KO mice were either fed an iron-deficient diet or injected with iron (Chapter 3).

The data show that iron regulates hepatic expression of *hepcidin 1* and *BMP-6*, (i.e. increased by iron loading and repressed by iron deficiency), in WT and *HFE* KO mice. However, in iron-loaded *HFE* KO mice *hepcidin 1* induction was significantly lower than that of iron loaded WT mice despite increased *BMP-6* expression, which may be explained by the impaired phosphorylation of Smad-1/5/8 in these mice. Similar findings were recently reported by Corradini et al. (2009). No change in *HJV* expression was observed in response to iron deficiency or iron loading in WT or *HFE* KO mice. Similar findings were recently shown by others (Constante et al. 2007; Gleeson et al. 2007).

Recent findings showed that hepcidin is not only induced by BMP-6, but it is also repressed when endogenous BMP-6 is reduced *in vitro* (Babitt et al. 2007). In addition, s-HJV selectively inhibited BMP-6 signalling *in vivo* and *in vitro* (Andriopoulos et al. 2009). Taken together, these findings and data shown here suggest that BMP-6 is important for hepcidin regulation by iron *in vivo.* Moreover, the lack of Smad phosphorylation in iron loaded *HFE* KO mice, despite increased *BMP-6* expression, suggests that HFE is involved in the regulation of downstream signals of BMP-6 that induce *hepcidin* expression in response to iron loading *in vivo*.

The data shown here, together with the recent reports (Corradini et al. 2009; Schmidt et al. 2008; Kautz et al. 2008), suggest that the iron-sensing process may occur at two levels (Figure 6.1). Hepatic *BMP-6* expression increases in response to iron loading, via an as yet unknown HFE-independent mechanism(s). BMP-6 then signals via Smad-1/5/8 to induce *hepcidin* expression via Smad-4. From the presented data it was proposed that HFE is involved in the BMP-6 signalling and hence there is less hepcidin induction in response to iron-loading in *HFE* KO mice. During iron deficiency, hepatic *BMP-6* decreases which in turn decreases Smad-

1/5/8 phosphorylation and *hepcidin* expression. However, this process is not dependent on HFE. Other mechanisms may also contribute to *hepcidin* suppression during iron deficiency such as TMPRSS6, which is believed to sense iron deficiency, although the mechanism by which this occurs has not been identified (Du et al. 2008); generation of s-HJV (Silvestri et al. 2008a; Lin et al. 2005); and increased hepatic *HIF-1*α expression (Peyssonnaux et al. 2007). However, more recent studies failed to demonstrate transcriptional suppression of *hepcidin* by HIF-1α (Volke et al. 2009). These conflicting findings underscore the need to study the role of HIF-1α in hepcidin regulation during iron deficiency.

The second mechanism of iron sensing is thought to involve HFE and TFR2. It was recently proposed that HFE is displaced from TFR1 by holotransferrin, and then forms a complex with TFR2 to induce *hepcidin* expression (Schmidt et al. 2008; Gao et al. 2009). Moreover, recent studies suggest a possible cross-talk between TFR2 and BMP-Smad signalling. In isolated mouse hepatocytes, holotransferrin not only induced ERK1/2 phosphorylation, but also increased phosphorylation of Smad-1/ 5/8 (Ramey et al. 2009). In addition, in mice with genetic disruption of *HFE* and *TFR2*, Smad-1/5/8 phosphorylation was reduced (Wallace et al. 2009). Interestingly, Noggin, a soluble protein that prevents BMP-Smad signalling, blocked holotransferrin-induced *hepcidin* expression *in vitro* (Ramey et al. 2009) suggesting the involvement of BMP-Smad signalling in *hepcidin* induction by holotransferrin. However, how BMP-Smad and TFR2 signalling interact remains to be fully elucidated.

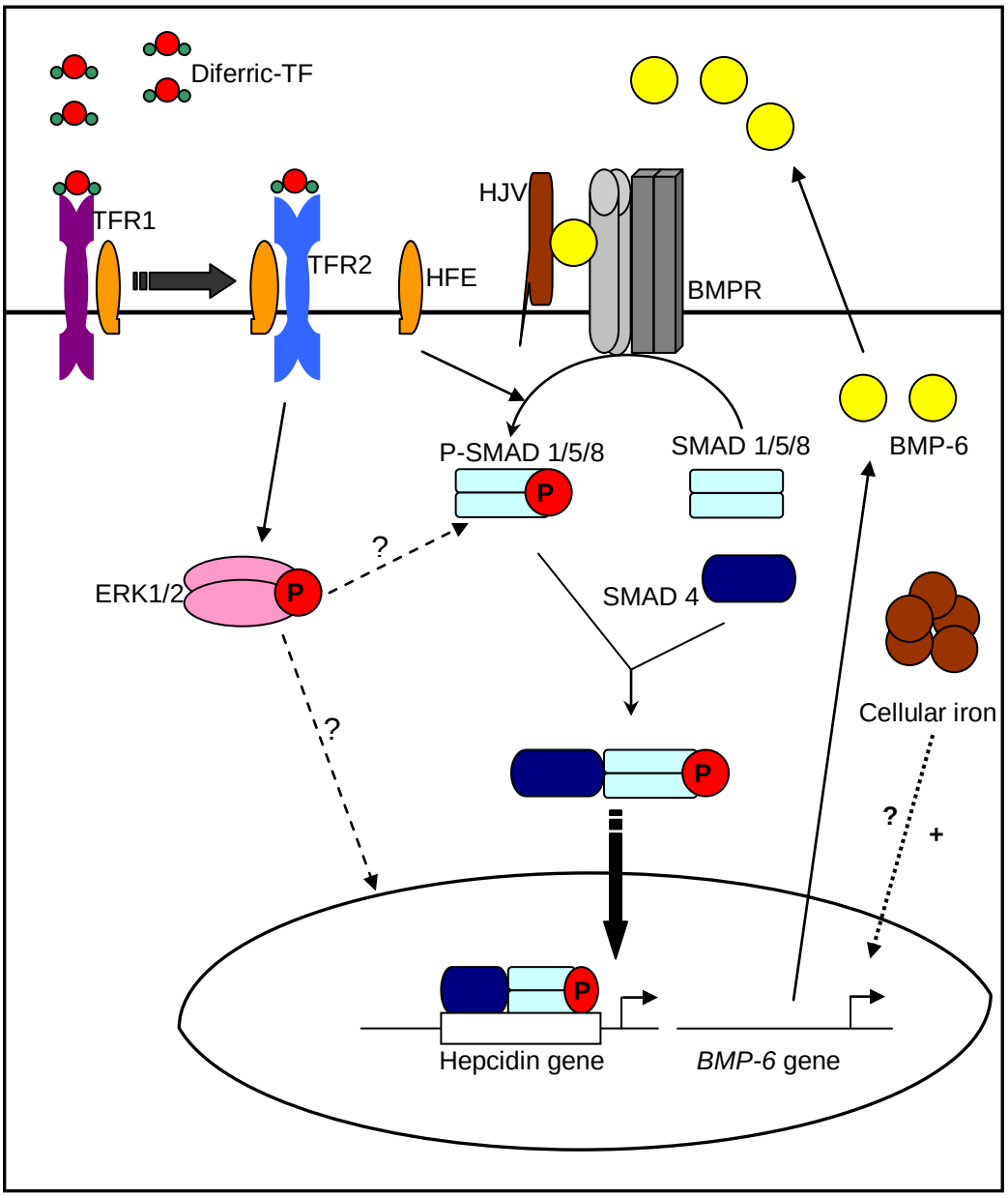

Figure 6.1 Mechanism of hepcidin induction during iron loading.

During iron overload, hepatic *BMP-6* expression is induced, which then binds to BMPR to initiate the Smad signalling cascade that activates hepcidin expression. However, HFE seems to be important for Smad-1/5/8 phosphorylation in response to iron loading. *Hepcidin* expression is also induced by binding of diferric-TF to the TFR2/HFE complex, which is believed to signal via ERK1/2. However, the exact signalling mechanism is unclear. Recent evidence suggests a possible cross-talk between TFR2/HFE and Smad signalling; though, how they interact remains to be determined.

6.2 Regulation of *hepcidin* and *HJV* expression by LPS-induced acute inflammation *in vivo* and pro-inflammatory cytokines *in vitro*

LPS is recognised by the Toll-like receptor (TLR) 4, which produces pro-inflammatory cytokines such as TNF-α, IL-1, and IL-6 (Hoshino et al. 1999). In this study (Chapter 4), WT and *HFE* KO mice respond to LPS-induced acute inflammation by inducing *hepcidin 1* expression and suppressing *HJV, BMP-2, BMP-4, and BMP-6* expression in the liver. These findings suggest that HFE does not have a role in the regulation of these genes during inflammation. This is the first demonstration that LPS-induced acute inflammation regulates hepatic *BMP* expression *in vivo*. However, the exact mechanism of this downregulation needs further investigation.

Studies in human hepatoma (HuH7) cells showed that TNF-α, but not IL-6, mediates *HJV* downregulation during inflammation, whereas IL-6 mediates *hepcidin* upregulation. A similar finding was recently reported by Constante et al. (2007). Interestingly, *in vitro* studies demonstrate for the first time that TNF-α induced *HJV* suppression is possibly mediated by a TNF-α response element within the *HJV* promoter.

Taken together, these findings suggest that the suppression of hepatic *HJV* and *BMP* expression during acute inflammation is a prerequisite for the *hepcidin* induction *in vivo*. This hypothesis is supported by the finding that mice either lacking *HJV* or *BMP-6* retain the ability to induce hepcidin in response to inflammatory stimuli (Meynard et al. 2009; Niederkofler et al. 2005). The hypothesised mechanism is as follows (Figure 6.2): iron sensing through HJV-BMP is switched off during acute inflammation by selective suppression of *HJV* and *BMP* expression in the liver. This in turn stimulates cytokine-induced *hepcidin* expression.

Recently, mice lacking either *BMP-6* (Meynard et al. 2009) or *Smad-4* (Wang et al. 2000) showed impaired *hepcidin* induction in response to LPS and IL-6, respectively. In addition, a recently identified BMP response element within the *hepcidin* gene promoter was shown to be important not only for BMP response, but also for IL-6 responsiveness (Verga Falzacappa et al. 2008). Taken together, these findings suggest a possible cross-talk between IL-6 and BMP-Smad signalling. However, the results presented here suggest that the proposed link between inflammation and BMP-Smad signalling is downstream of HJV and BMP ligands, possibly at the level of Smad-4.

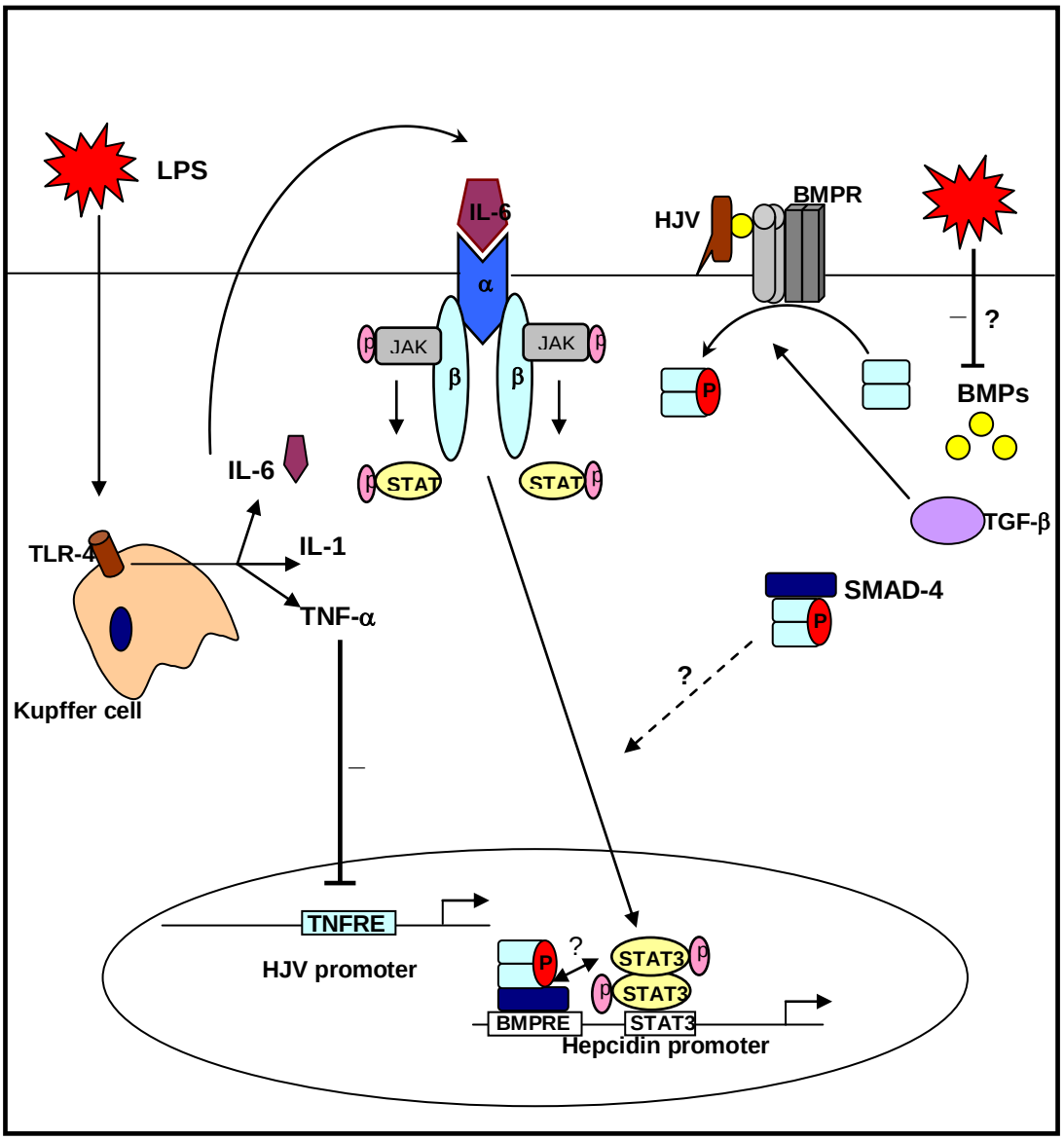

Figure 6.2 Proposed mechanism of LPS-induced cytokines in the regulation of *hepcidin* and *HJV* expression in the liver.

LPS is taken up by the Kupffer cells via TLR-4 and induces TNF-α, IL-1, and IL-6. TNF-α suppresses *HJV* expression via a TNFRE within the *HJV* promoter, while IL-6 induces *hepcidin* expression via the STAT3- pathway. LPS also represses the expression of *BMPs* (2, 4, and 6), via an as yet unknown mechanism. On the other hand, the expression of TGF-β is not affected by LPS, which could maintain basal expression levels of phosphorylated Smads. Based on these results, it was hypothesised that iron sensing through HJV-BMP-Smad pathway needs to be switched off during inflammation in order to induce *hepcidin* expression. Moreover, the proposed link between IL-6 and the Smad pathway is downstream of HJV and BMPs, probably at the level of Smad-4.

6.3 Regulation of *HJV* expression by upstream stimulatory factors

Upstream stimulatory factors have been shown to regulate the expression of plenty of genes responsible for various cellular processes. Among these are *TGF-β, β-2 microglobulin, and hepcidin* that play important roles in iron homeostasis (Scholtz et al. 1996; Gobin et al. 2003; Bayele et al. 2006). Nicolas and co workers (Nicolas et al. 2001) who showed that mice with genetic disruption of USF2 presented massive iron overload and lacked *hepcidin* expression, provided the original link between USFs and iron metabolism.

In this study (Chapter 5), it was shown that the exogenous USFs increased the expression of *HJV* mRNA as well as the reporter gene (luciferase) *in vitro* suggesting that USFs are potent positive regulators of *HJV* transcription. Moreover, the identified E-boxes within the *HJV* promoter bound a nuclear protein complex, and recombinant USF1 and 2 *in vitro* by EMSA. In addition, the binding of USF1 to *HJV* E-box was demonstrated *in vivo* by the ChIP assay. Taken together, these findings suggest that USFs are involved in the regulation of *HJV* expression via E-boxes and further strengthen the link between these transcription factors and iron metabolism.

The role of USFs in glucose and lipid metabolism (Vallet et al. 1998; Smih et al. 2002; Bidder et al. 2002; Weigert et al .2004; Wang et al. 2004; Tu and Albers 2001) suggest a possible novel link between glucose, lipid, and iron metabolism which is mediated by USFs. However, this hypothesis needs further investigation.

6.4 Conclusions

From the studies described in the thesis, it was concluded that:

- Hepcidin regulation by iron status is modulated by the BMP-6-Smad signalling pathway *in vivo.*
- HFE seems to be involved in the regulation of the downstream signalling of BMP-6 that induces *hepcidin* expression during iron loading.
- TNF-α seems to suppress *HJV* expression via a novel TNFRE within the *HJV* promoter.
- There is a crucial requirement for an HFE-independent downregulation of *HJV* and *BMP* expression during acute inflammation in order to induce *hepcidin* expression.
- The proposed link between inflammation and BMP-Smad signalling is downstream of HJV and BMPs, possibly at the level of Smad-4.
- USFs are involved in the regulation of *HJV* expression *in vivo* and *in vitro* further supporting the importance of these transcription factors in iron homeostasis.

6.5 Future Work

In the present study, it was shown that iron regulates *BMP-6* mRNA expression in the liver *in vivo,* via an as yet unknown mechanism. Therefore, further studies investigating the mechanism of *BMP-6* regulation by iron need to be performed at the promoter level to determine the presence of iron regulatory elements that could mediate iron responsiveness. This will be performed by using bioinformatics to detect the presence of iron response elements within the *BMP-6* promoter sequence. Once identified, the functionality of these response elements will be tested by reporter and gel shift assays.

The results also showed that LPS downregulates *BMP 2, 4, and 6* mRNA expression in the liver *in vivo*; however, the mechanism of this suppression needs further investigation. The effect of different pro-inflammatory cytokines, such as IL-6 and TNF-α on *BMP 2, 4, and 6* mRNA expression will be examined *in vivo* and *in vitro* to determine the mechanism of *BMP* suppression during acute inflammation.

The regulation of *HJV* and *hepcidin* expression by USFs and the involvement of these transcription factors in glucose metabolism may provide a novel link between glucose and iron metabolism. Therefore, further studies investigating the effect of glucose on *HJV* and *hepcidin* expression and the involvement of USF in this regulation need to be performed at both mRNA and promoter levels of hepcidin and HJV.

Chapter 7: References Cited

Abboud S, Haile DJ. A novel mammalian iron-regulated protein involved in intracellular iron metabolism. *J Biol Chem* 2000;275:19906–19912.

Acton RT, Barton JC, Snively BM, McLaren CE, Adams PC, Harris EL, Speechley MR, McLaren GD, Dawkins FW, Leiendecker-Foster C, Holup JL, Balasubramanyam A. Geographic and racial/ethnic differences in*HFE*mutation frequencies in the Hemochromatosis and Iron Overload Screening (HEIRS) Study. *Ethn Dis* 2006;16:815–821.

Adams Pc, Barbin YP, Khan ZA, Chkrabarti S. Expression of ferroportin in hemochromatosis liver. *Blood Cells Mol Dis* 2003;31:256-261.

Adams PC, Powell LW, Halliday JW. Isolation of a human hepatic ferritin receptor. *Hepatology* 1988;8:719–721.

Aeberli I, Hurrell RF, Zimmermann MB. Overweight children have higher circulating hepcidin concentrations and lower iron status but have dietary iron intakes and bioavailability comparable with normal weight children. *Int J Obes (Lond)* 2009;33:1111-1117.

Ahmad KA, Ahmann JR, Migas MC, Waheed A, Britton RS, Bacon BR, Sly WS, Fleming RE. Decreased liver hepcidin expression in the Hfe knockout mouse. *Blood Cells Mol Dis* 2002;29:361-366.

Aisen P, Aasa R, Redfield AG. The chromium, manganese, and cobalt complexes of transferrin. *J Biol Chem* 1969;244:4628–4633.

Aldred AR, Grimes A, Schreiber G, Mercer JF. Rat ceruloplasmin. Molecular cloning and gene expression in liver, choroid plexus, yolk sac, placenta, and testis. *J Biol Chem* 1987;262:2875–2878.

al-Refaie FN, Wickens DG, Wonke B, Kontoghiorghes GJ, Hoffbrand AV. Serum non-transferrin-bound iron in beta-thalassaemia major patients treated with desferrioxamine and L1. *Br J Haematol* 1992;82:431–436.

Anderson BF, Baker HM, Dodson EJ, Norris GE, Rumball SV, Waters JM, Baker EN. Structure of human lactoferrin at 3.2-A resolution. *Proc Natl Acad Sci USA* 1987;84:1769–1773.

Anderson GJ, Frazer DM, McKie AT, Wilkins SJ, Vulpe CD. The expression and regulation of the iron transport molecules hephaestin and IREG1: implications for the control of iron export from the small intestine. *Cell Biochem Biophys* 2002;36:137-146.

Andrews NC. Disorders of iron metabolism. *N Engl J Med* 1999;341:1986–1995.

Andriopoulos B Jr, Corradini E, Xia Y, Faasse SA, Chen S, Grgurevic L, Knutson MD, Pietrangelo A, Vukicevic S, Lin HY, Babitt JL. BMP6 is a key endogenous regulator of hepcidin expression and iron metabolism. *Nat Genet* 2009;41:482-487.

Aperlo C, Boulukos KE, Sage J, Cuzin F, Pognonec P. Complete sequencing of the murine USF gene and comparison of its genomic organization to that of mFIP/USF2. *Genomics* 1996;37:337-344.

Arosio P, Adelman TG, Drsdale JW. On ferritin heterogenecity. Further evidence for heteropolymers. *J Biol Chem* 1978;253:4451-4458.

Arosio P, Yokota M, Drysdale JW. Characterization of serum ferritin in iron overload: possible identity to natural apoferritin. *Br J Haematol* 1977;36:199-207.

Atchley WR, Fitch WM. Anatural classification of the basic helix-loop-helix class of transcription factors. *Proc Natl Acad Sci U SA* 1997;94:5172-5176.

Babitt JL, Huang FW, Wrighting DM, Xia Y, Sidis Y, Samad TA, Campagna JA, Chung RT, Schneyer AL, Woolf CJ, Andrews NC, Lin HY. Bone morphogenetic protein signaling by hemojuvelin regulates hepcidin expression. *Nat Genet* 2006;38:531–539.

Babitt JL, Huang FW, Xia Y, Sidis Y, Andrews NC, Lin HY. Modulation of bone morphogenetic protein signaling in vivo regulates systemic iron balance. *J Clin Invest* 2007;117:1933-1939.

Bacon BR, Tavill AS. Role of the liver in normal iron metabolism. *Semin Liver Dis* 1984;4:181–192.

Bailey S, Evans RW, Garratt RC, Gorinsky B, Hasnain S, Horsburgh C, Jhoti H, Lindley PF, Mydin A, Sarra R, et al. Molecular structure of serum transferrin at 3.3-A resolution. *Biochemistry* 1988;27:5804–5812.

Baker E, Baker SM, Morgan EH. Characterisation of non-transferrin-bound iron (ferric citrate) uptake by rat hepatocytes in culture. *Biochim Biophys Acta* 1998;1380:21–30.

Baker E, Page M, Morgan EH. Transferrin and iron release from rat hepatocytes in culture. *Am J Physiol Gastrointest Liver Physiol* 1985;248:G93–G97.

Baker EN, Lindley PF. New perspectives on the structure and function of transferrins. *J Inorg Biochem* 1992;47:147–160.

Bannerman RM, Bannerman CE, Kingston PJ. Hereditary iron deficiency: X-linked anaemia (SLA) in newborn and suckling mice. *Br J Haematol* 1973;25:280.

Bayele HK, McArdle H, Srai SK. Cis and trans regulation of hepcidin expression by upstream stimulatory factor. *Blood* 2006 15;108:4237-4245.

Bayele HK, Srai SK. Regulatory variation in hepcidin expression as a heritable quantitative trait. *Biochem Biophys Res Commun* 2009 19;384:22-27.

Beguin Y. Soluble transferrin receptor for the evaluation of erythropoiesis and iron status. *Clin Chim Acta* 2003;329:9-22.

Bendall AJ, Molloy PL. Base preferences for DNA binding by the bHLH-Zip protein USF: effects of $MgCl_2$ on specificity and comparison with binding of Myc family members. *Nucleic Acids Res* 1994; 22:2801-2810.

Bennett MJ, Lebrón JA, Bjorkman PJ. Crystal structure of the hereditary haemochromatosis protein HFE complexed with transferrin receptor. *Nature* 2000;403:46-53.

Beutler E, Felitti VJ, Koziol JA, Ho NJ, Gelbart T. Penetrance of the 845G->A (C282Y) *HFE* hereditary haemochromatosis mutation in the USA. *Lancet* 2002;359:211–218.

Beutler E, Hoffbrand AV, Cook JD. Iron deficiency and overload. *Hematology Am Soc Hematol Edu Program* 2003;40-61.

Bidder M, Shao JS, Charlton-Kachigian N, Loewy AP, Semenkovich CF, Towler DA. Osteopontin transcription in aortic vascular smooth muscle cells is controlled by glucose-regulated upstream stimulatory factor and activator protein-1 activities. *J Biol Chem* 2002;277:44485–44496.

Boldt DH. New perspectives on iron: an introduction. *Am J Med Sci* 1999;318:207–212.

Bomford A. Genetics of haemochromatosis. *Lancet* 2002;360:1673:1681.

Bondi A, Valentino P, Daraio F, Porporato P, Gramaglia E, Carturan S, Gottardi E, Camaschella C, Roetto A. Hepatic expression of hemochromatosis genes in two mouse strains after phlebotomy and iron overload. *Haematologica* 2005;90:1161-1167.

Bothwell TH, Charlton RW, Motulski AG. Hemochromatosis. In: Scriver CR, Beaudet AL, Sly WS and Valle D, Editors, 1995. *The Metabolic and Molecular Bases of Inherited Disease*, McGraw-Hill, New York, pp. 2237–2269.

Bothwell TH, Charlton RW. Current problems of iron overload. *Recent Results Cancer Res* 1979;69:87-95.

Botma GJ, van Deursen D, Vieira D, van Hoek M, Jansen H, Verhoeven AJM. Sterol-regulatory-element binding protein inhibits upstream stimulator factor-stimulated hepatic lipase gene expression. *Atherosclerosis* 2005;179:61–67.

Bozzini C, Campostrini N, Trombini P, Nemeth E, Castagna A, Tenuti I, Corrocher R, Camaschella C, Ganz T, Olivieri O, Piperno A, Girelli D. Measurement of urinary hepcidin levels by SELDI-TOF-MS in HFE-hemochromatosis. *Blood Cells Mol. Dis.* 2007;40:347–352.

Breuer W, Ronson A, Slotki IN, Abramov A, Hershko C, Cabantchik ZI. The assessment of serum nontransferrin-bound iron in chelation therapy and iron supplementation. *Blood* 2000;95:2975–2982.

Bridle KR, Frazer DM, Wilkins SJ, Dixon JL, Purdie DM, Crawford DH, Subramaniam VN, Powell LW, Anderson GJ, Ramm GA. Disrupted hepcidin regulation in HFE-associated haemochromatosis and the liver as a regulator of body iron homoeostasis. *Lancet* 2003;361:669-673.

Brise H, Hallberg L. Iron absorption studies. *Acta Med Scand (Suppl)* 1962;376:7-28.

Byrnes V, Barrett S, Ryan E, Kelleher T, O'Keane C, Coughlan B, Crowe J. Increased duodenal DMT-1 expression and unchanged HFE mRNA levels in HFE-associated hereditary haemochromatosis and iron deficiency. *Blood Cell Mol Dis* 2002;29:251-260.

Cairo G, Pietrangelo A. Nitric-oxide-mediated activation of iron-regulatory protein controls hepatic iron metabolism during acute inflammation. *Eur J Biochem* 1995;232:358–363.

Calzolari A, Raggi C, Deaglio S, Sposi NM, Stafsnes M, Fecchi K, Parolini I, Malavasi F, Peschle C, Sargiacomo M, Testa U.TfR2 localizes in lipid raft domains and is released in exosomes to activate signal transduction along the MAPK pathway. *J Cell Sci* 2006;119:4486-4498.

Camara-Clayette V, Rahuel C, Bertrand O, Cartron JP. The E-box of the human glycophorin B promoter is involved in the erythroid-specific expression of the GPB gene. *Biochem Biophys Res Commun* 1999;265:170-176.

Camaschella C, Roetto A, Cali A, De Gobbi M, Garozzo G, Carella M, Majorano N, Totaro A, Gasparini P. The gene TFR2 is mutated in a new type of haemochromatosis mapping to 7q22. *Nat Genet* 2000;25:14–15.

Canonne-Hergaux F, Fleming MD, Levy JE, Gauthier S, Ralph T, Picard V, Andrews NC, Gros P. The Nramp2/DMT1 iron transporter is induced in the duodenum of microcytic anaemia mk mice but is not properly targeted to the intestinal brush border. *Blood* 2000;96:3964-3970.

Canonne-Hergaux F, Gruenheid S, Ponka P, Gros P. Cellular and subcellular localization of the Nramp2 iron transporter in the intestinal brush border and regulation by dietary iron. *Blood* 1999;93:4406–4417.

Cardoso CS, de Sousa M. HFE, the MHC and hemochromatosis: paradigm for an extended function for MHC class I. *Tissue Antigens* 2003;61:263–275.

Carpenter CE, Mahoney AW. Contributions of heme and nonheme iron to human nutrition. *Crit Rev Food Sci Nutr* 1992;31:333–367.

Cartwright GE, Lee GR. The anaemia of chronic disorders. *Br J Haematol* 1971;21:147-152.

Cartwright GE, Wintrobe MM. The anemia of infection. XVII. A review. *Adv Intern Med* 1952;5:165-226.

Cartwright GE. The anemia of chronic disorders. *Semin Hematol* 1966;3:351-375.

Casado M, Vallet VS, Kahn A, Vaulont S. Essential role in vivo of upstream stimulatory factors for a normal dietary response of the fatty acid synthase gene in the liver. *J Biol Chem* 1999;274:2009-2013.

Casey JL, Hentze MW, Koeller DM, Caughman SW, Rouault TA, Klausner RD, Harford JB. Iron responsive elements: regulatory RNA sequences that control mRNA levels and translation. *Science* 1988;240:924–928.

Chen D, Zhao M, Mundy GR. Bone morphogenetic proteins. *Growth Factors* 2004;22:233-241.

Chen H, Su T, Attieh ZK, Fox TC, McKie AT, Anderson GJ, Vulpe CD. Systemic regulation of Hephaestin and Ireg1 revealed in studies of genetic and nutritional iron deficiency. *Blood* 2003;102:1893-1899.

Chen J, Chloupkova M, Gao J, Chapman-Arvedson TL, Enns CA. HFE modulates transferrin receptor 2 levels in hepatoma cells via interactions that differ from transferrin receptor 1/HFEinteractions. *J Biol Chem* 2007;282:36862–36870.

Choi SO, Cho YS, Kim HL, Park JW. ROS mediate the hypoxic repression of the hepcidin gene by inhibiting C/EBPα and STAT-3. *Biochem Biophys Res Commun* 2007;356:312–317.

Chomczynski P, Sacchi N. Single-step method of RNA isolation by acid guanidinium thiocyanate-phenol-chloroform extraction. *Anal Biochem* 1987;162:156-159.

Chua AC, Graham RM, Trinder D, Olynyk JK. The regulation of cellular iron metabolism. *Crit Rev Clin Lab Sci* 2007;44:413-459.

Chua ACG, Drake SF, Herbison CE, Olynyk JK, Leedman PJ, Trinder D. Limited iron export by hepatocytes contributes to hepatic iron-loading in the Hfe knockout mouse. *J Hepatol* 2006a;44:176–182.

Chua ACG, Herbison CE, Drake SF, Graham RM, Olynyk JK, Trinder D. Iron uptake by transferrin receptor 1 is regulated by HFE in hepatocytes. *Hepatology* 2006b;44: 432A.

Chua ACG, Ingram HA, Raymond KN, Baker E. Multidentate pyridinones inhibit the metabolism of nontransferrin-bound iron by hepatocytes and hepatoma cells. *Eur J Biochem* 2003;270:1689–1698.

Chua ACG, Olynyk JK, Leedman PJ, Trinder D. Nontransferrin-bound iron uptake by hepatocytes is increased in the Hfe knockout mouse model of hereditary hemochromatosis. *Blood* 2004;104:1519–1525.

Chung B, Chaston T, Marks J, Srai SK, Sharp PA. Hepcidin decreases iron transporter expression in vivo in mouse duodenum and spleen and in vitro in THP-1 macrophages and intestinal Caco-2 cells. *J Nutr* 2009 Aug;139:1457-1462.

Chung B, Matak P, McKie A, Sharp P. Leptin increases the expression of the iron regulatory hormone hepcidin in HuH7 human hepatoma cells. J Nutr 2007;137:2366-2370.

Collins JF, Franck CA, Kowdley KV, Ghishan FK. Identification of differentially expressed genes in response to dietary iron deprivation in rat duodenum. *Am J Physiol Gastrointest Liver Physiol* 2005;288:G964-G971.

Conrad ME, Umbreit JN, Moore EG. Iron absorption and transport. *Am J Med Sci* 1999; 318:213–229.

Conrad ME, Weintraub LR, Sears DA, Crosby WH. Absorption of haemoglobin iron. *Am J Physiol* 1966;211:1123-1130.

Constante M, Jiang W, Wang D, Raymond VA, Bilodeau M, Santos MM. Distinct requirements for Hfe in basal and induced hepcidin levels in iron overload and inflammation. *Am J Physiol Gastrointest Liver Physiol* 2006;291:G229-G237.

Constante M, Wang D, Raymond VA, Bilodeau M, Santos MM. Repression of repulsive guidance molecule C during inflammation is independent of Hfe and involves tumor necrosis factor-alpha. *Am J Pathol* 2007;170:497-504.

Cook JD, Berry WE, Hershko C, Fillet G, Finch CA. Iron kinetics with emphasis on iron overload. *Am J Pathol* 1973;72:337-343.

Coppin H, Darnaud V, Kautz L, Meynard D, Aubry M, Mosser J, Martinez M, Roth MP. Gene expression profiling of Hfe−/− liver and duodenum in mouse strains with differing susceptibilities to iron loading: identification of transcriptional regulatory targets of Hfe and potential hemochromatosis modifiers. *Genome Biol.* 2007;8:R221.

Corradini E, Garuti C, Montosi G, Ventura P, Andriopoulos B Jr, Lin HY, Pietrangelo A, Babitt JL. Bone morphogenetic protein signaling is impaired in an HFE knockout mouse model of hemochromatosis. *Gastroenterology* 2009;137:1489-1497.

Cortell S, Conrad ME. Effect of endotoxin on iron absorption. *Am J Physiol* 1967 Jul;213:43-47.

Craven CM, Alexander J, Eldridge M, Kushner JP, Bernstein S, Kaplan J. Tissue distribution and clearance kinetics of non-transferrin-bound iron in the hypotransferrinemic mouse: a rodent model for hemochromatosis. *Proc Natl Acad Sci USA* 1987;84:3457–3461.

Dautry-Varsat A, Ciechanover A, Lodish HF. pH and the recycling of transferrin during receptor-mediated endocytosis. *Proc Natl Acad Sci USA* 1983;80:2258–2262.

Davidsson L, Lonnerdal B, Sandstrom B, Kunz C, Keen CL. Identification of transferrin as the major plasma carrier protein for manganese introduced orally or intravenously or after in vitro addition in the rat. *J Nutr* 1989;119:1461–1464.

Davies M, Parry JE, Sutcliffe RG. Examination of different preparations of human placental plasma membrane for the binding of insulin, transferrin and immunoglobulins. *J Reprod Fertil* 1981;63:315–324.

De Domenico I, McVey WD, Musci G, Kaplan J. Iron overload due to mutations in ferroportin. *Haematologica* 2006;91:92–95.

De Domenico I,Ward DM, Langelier C, Vaughn MB, Nemeth E, Sundquist WI, Ganz T, Musci G, Kaplan J. The molecular mechanism of hepcidin-mediated ferroportin down-regulation. *Mol. Biol. Cell* 2007;18:2569–2578.

De Gobbi M, Roetto A, Piperno A, Mariani R, Alberti F, Papanikolaou G, Politou M, Lockitch G, Girelli D, Fargion S, Cox TM, Gasparini P, Cazzola M, Camaschella C. Natural history of juvenile haemochromatosis. *Br J Haematol* 2002;117:973–979.

Deeb SS, Zambon A, Carr MC, Ayyobi AF, Brunzell JD. Hepatic lipase and dyslipidemia: interactions among genetic variants, obesity, gender, and diet. *J Lipid Res* 2003;44:1279–1286.

Delatycki MB, Allen KJ, Gow P, MacFarlane J, Radomski C, Thompson J, Hayden MR, Goldberg YP, Samuels ME. A homozygous HAMP mutation in a multiply consanguineous family with pseudodominant juvenile hemochromatosis. *Clin Genet* 2004; 65:378–383.

Demaeyer EM. Epidemiology, treatment and prevention of iron deficiency and iron deficiency anaemia. *Rev Epidemiol Sante Publique* 1980;28:235-249.

Donovan A, Brownlie A, Zhou Y, Shepard J, Pratt SJ, Moynihan J, Paw BH, Drejer A, Barut B, Zapata A, Law TC, Brugnara C, Lux SE, Pinkus GS, Pinkus JL, Kingsley PD, Palis J, Fleming MD, Andrews NC, Zon LI. Positional cloning of zebrafish ferroportin1 identifies a conserved vertebrate iron exporter. *Nature* 2000;403:776–781.

Donovan A, Lima CA, Pinkus JL, Zon LI, Robine S, Andrews NC. The iron exporter ferroportin/Slc40a1 is essential for iron homeostasis. *Cell Metab* 2005;1:191-200.

Drakesmith H, Schimanski LM, Ormerod E, Merryweather-Clarke AT, Viprakasit V, Edwards JP, Sweetland E, Bastin JM, Cowley D, Chinthammitr Y, Robson KJ, Townsend AR. Resistance to hepcidin is conferred by hemochromatosis-associated mutations of ferroportin. *Blood* 2005;106:1092–1097.

Du X, She E, Gelbart T, Truksa J, Lee P, Xia Y, Khovananth K, Mudd S, Mann N, Moresco EM, Beutler E, Beutler B: The serine protease TMPRSS6 is required to sense iron deficiency. *Science* 2008;320:1088–1092.

Duthie HL. The relative importance of the duodenum in the intestinal absorption of iron. *Br J Haematol* 1964;10:59-68.

Edwards JA, Hoke JE. Defect of intestinal mucosal iron uptake in mice with hereditary microcytic anemia. *Proc Soc Exp Biol Med* 1972;141:81-84.

Enns CA, Suomalainen HA, Gebhardt JE, Schroder J, Sussman HH. Human transferrin receptor: expression of the receptor is assigned to chromosome 3. *Proc Natl Acad Sci USA* 1982;79:3241–3245.

Enns CA, Sussman HH. Physical characterization of the transferrin receptor in human placentae. *J Biol Chem* 1981;256:9820–9823.

Fahmy M, Young SP. Modulation of iron metabolism in monocyte cell line U937 by inflammatory cytokines: changes in transferrin uptake, iron handling and ferritin mRNA. *Biochem J* 1993;296:175–181.

Farina A, Gaetano C, Crescenzi M, Puccini F, Manni I, Sacchi A, Piaggio G. The inhibition of cyclin B1 gene transcription in quiescent NIH3T3 cells is mediated by an E-box. *Oncogene* 1996;13:1287-1296.

Feder JN, Gnirke A, Thomas W, Tsuchihashi Z, Ruddy DA, Basava A, Dormishian F, Domingo R Jr, Ellis MC, Fullan A, Hinton LM, Jones NL, Kimmel BE, Kronmal GS, Lauer P, Lee VK, Loeb DB, Mapa FA, McClelland E, Meyer NC, Mintier GA, Moeller N, Moore T, Morikang E, Prass CE, Quintana L, Starnes SM, Schatzman RC, Brunke KJ, Drayna DT, Risch NJ, Bacon BR, Wolff RK. A novel MHC class I-like gene is mutated in patients with hereditary haemochromatosis. *Nat Genet* 1996;13:399-408.

Feder JN, Penny DM, Irrinki A, Lee VK, Lebron JA, Watson N, Tsuchihashi Z, Sigal E, Bjorkman PJ, Schatzman RC. The hemochromatosis gene product complexes with the transferrin receptor and lowers its affinity for ligand binding. *Proc Natl Acad Sci USA* 1998;95:1472–1477.

Feder JN, Tsuchihashi Z, Irrinki A, Lee VK, Mapa FA, Morikang E, Prass CE, Starnes SM,Wolff RK, Parkkila S, Sly WS, Schatzman RC. The hemochromatosis founder mutation in HLA-H disrupts beta2-microglobulin interaction and cell surface expression. *J Biol Chem* 1997;272:14025–14028.

Fernandes A, Preza GC, Phung Y, De Domenico I, Kaplan J, Ganz T, Nemeth E. The molecular basis of hepcidin-resistanct hereditary hemochromatosis. *Blood* 2009;114:437-443.

Ferring-Appel D, Hentze MW, Galy B. Cell-autonomous and systemic context-dependent functions of iron regulatory protein 2 in mammalian iron metabolism. *Blood* 2009 15;113:679-87.

Finberg KE, Heeney MM, Campagna DR, Aydinok Y, Pearson HA, Hartman KR, Mayo MM, Samuel SM, Strouse JJ, Markianos K, Andrews NC, Fleming MD: Mutations in TMPRSS6 cause iron-refractory iron deficiency anemia (IRIDA). *Nat Genet* 2008;40:569–571.

Flanagan JM, Peng H, Wang L, Gelbart T, Lee P, Johnson Sasu B, Beutler E. Soluble transferrin receptor-1 levels in mice do not affect iron absorption. *Acta Haematol* 2006;116:249-254.

Fleming MD, Romano MA, Su MA, Garrick LM, Garrick MD, Andrews NC. Nramp2 is mutated in the anemic Belgrade (b) rat: evidence of a role for Nramp2 in endosomal iron transport. *Proc Natl Acad Sci USA* 1998;95:1148–1153.

Fleming MD, Trenor CC 3rd, Su MA, Foernzler D, Beier DR, Dietrich WF, Andrews NC. Microcytic anaemia mice have a mutation in Nramp2, a candidate iron transporter gene. *Nat Genet* 1997;16:383–386.

Fleming RE, Ahmann JR, Migas MC, Waheed A, Koeffler HP, Kawabata H, Britton RS, Bacon BR, Sly WS.Targeted mutagenesis of the murine transferrin receptor–2 gene produces hemochromatosis. *Proc. Natl. Acad. Sci. USA 2002;*99:10653–10658.

Fleming RE, Migas MC, Holden CC, Waheed A, Britton RS, Tomatsu S, Bacon BR, Sly WS. Transferrin receptor 2: continued expression in mouse liver in the face of iron overload and in hereditary hemochromatosis. *Proc Natl Acad Sci USA* 2000;97:2214–2219.

Fleming RE, Sly WS. Mechanisms of iron accumulation in hereditary hemochromatosis. *Annu Rev Physiol* 2002;64:663-680.

Fleming RE. Hepcidin activation during inflammation: make it STAT. *Gastroenterology* 2007;132:447-449.

Folgueras AR, de Lara FM, Pendas AM, Garabaya C, Rodriguez F, Astudillo A, Bernal T, Cabanillas R, Lopez-Otin C, Velasco G: Membrane-bound serine protease matriptase-2 (Tmprss6) is an essential regulator of iron homeostasis. *Blood* 2008;112:2539–2545.

Forth W, Rummel W. Iron absorption. *Physiol Rev* 1973; 53: 724–792.

Frazer DM, Wilkins SJ, Becker EM, Vulpe CD, McKie AT, Trinder D, Anderson GJ. Hepcidin expression inversely correlates with the expression of duodenal iron transporters and iron absorption in rats. *Gastroenterology* 2002;123:835:844.

Frazer DM, Wilkins SJ, Millard KN, McKie AT, Vulpe CD, Anderson GJ. Increased hepcidin expression and hypoferraemia associated with an acute phase response are not affected by inactivation of HFE. *Br J Haematol* 2004;126:434–436.

Galy B, Ferring-Appel D, Kaden S, Grone HJ, Hentze MW. Iron regulatory proteins are essential for intestinal function and control key iron absorption molecules in the duodenum. *Cell Metab* 2008;7:79-85.

Gambaro K, Aberdam E, Virolle T, Aberdam D, Rouleau M. BMP-4 induces a Smad-dependent apoptotic death of mouse embryonic stem cell-derived neural precursors. *Cell Death Differ* 2006;13:1075-1087.

Ganz T, Nemeth E. Iron imports. IV. Hepcidin and regulation of body iron metabolism. *Am J Physiol Gastrointest Liver Physiol* 2006;290:G199-G203.

Ganz T. Hepcidin, a key regulator of iron metabolism and mediator of anemia of inflammation. *Blood* 2003; 102:783-788.

Ganz T. Hepcidin-a regulator of intestinal iron absorption and iron recycling by macrophages. *Best Pract Res Clin Haematol* 2005;18:171–182.

Ganz T. Molecular pathogenesis of anemia of chronic disease. *Pediatr Blood Cancer* 2006; 46:554-557.

Gao J, Chen J, Kramer M, Tsukamoto H, Zhang AS, Enns CA. Interaction of the hereditary hemochromatosis protein HFE with transferrin receptor 2 is required for transferrin-induced hepcidin expression. *Cell Metab* 2009;9:217-227.

Gao J, Zhao N, Knutson MD, Enns CA. The hereditary hemochromatosis protein, HFE, inhibits iron uptake via down-regulation of Zip14 in HepG2 cells. *J Biol Chem* 2008 1;283:21462-1468.

Gehrke SG, Kulaksiz H, Herrmann T, Riedel HD, Bents K, Veltkamp C, Stremmel W. Expression of hepcidin in hereditary hemochromatosis: evidence for a regulation in response to the serum transferrin saturation and to non-transferrin-bound iron. *Blood* 2003 1;102:371-376.

Gerlach M, Ben-Shachar D, Riederer P, Youdim MB. Altered brain metabolism of iron as a cause of neurodegenerative diseases? *J Neurochem* 1994;63:793–807.

Gleeson F, Ryan E, Barrett S, Russell J, Crowe J. Hepatic iron metabolism gene expression profiles in HFE associated hereditary hemochromatosis. *Blood Cells Mol Dis* 2007;38:37-44.

Gobin SJ, Biesta P, Van den Elsen PJ. Regulation of human beta 2-microglobulin transactivation in hematopoietic cells. *Blood* 2003;101:3058-3064.

Goswami T, Andrews NC. Hereditary hemochromatosis protein, HFE, interaction with transferring receptor 2 suggests a molecular mechanism for mammalian iron sensing. *J Biol Chem* 2006;281:28494–28498.

Graham RM, Morgan EH, Baker E. Characterisation of citrate and iron citrate uptake by cultured rat hepatocytes. *J Hepatol* 1998a;29:603–613.

Graham RM, Morgan EH, Baker E. Ferric citrate uptake by cultured rat hepatocytes is inhibited in the presence of transferrin. *Eur J Biochem* 1998b;253:139–145.

Green R, Charlton R, Seftel H, Bothwell T, Mayet F, Adams B, Finch C, Layrisse M. Body iron excretion in man: a collaborative study. *Am J Med* 1968;45:336–353.

Greenberg AS, Obin MS. Obesity and the role of adipose tissue in inflammation and metabolism. Am J Nutr 2006;83:461S-465S.

Griffiths WJ, Cox TM. Co-localization of the mammalian hemochromatosis gene product (HFE) and a newly identified transferrin receptor (TfR2) in intestinal tissue and cells. *J Histochem Cytochem* 2003;51:613–624.

Grohlich D, Morley CG, Miller RJ, Bezkorovainy A. Iron incorporation into isolated rat hepatocytes. *Biochem Biophys Res Commun* 1977;76:682–690.

Grootveld M, Bell JD, Halliwell B, Aruoma OI, Bomford A, Sadler PJ. Non-transferrin-bound iron in plasma or serum from patients with idiopathic hemochromatosis. Characterization by high performance liquid chromatography and nuclear magnetic resonance spectroscopy. *J Biol Chem* 1989;264:4417–4422.

Gross CN, Irrinki A, Feder JN, Enns CA. Co-trafficking of HFE, a nonclassical major histocompatibility complex class I protein, with the transferrin receptor implies a role in intracellular iron regulation. *J Biol Chem* 1998;273:22068-22074.

Guillem F, Lawson S, Kannengiesser C, Westerman M, Beaumont C, Grandchamp B: Two nonsense mutations in the TMPRSS6 gene in a patient with microcytic anemia and iron deficiency. *Blood* 2008;112:2089–2091.

Gunshin H, Allerson CR, Polycarpou-Schwarz M, Rofts A, Rogers JT, Kishi F, HentzeMW, Rouault TA, Andrews NC, Hediger MA. Iron-dependent regulation of the divalent metal ion transporter. *FEBS Lett* 2001;509:309–316.

Gunshin H, Fujiwara Y, Custodio AO, Direnzo C, Robine S, Andrews NC. Slc11a2 is required for intestinal iron absorption and erythropoiesis but dispensable in placenta and liver. *J Clin Invest* 2005;115:1258–1266.

Gunshin H, Mackenzie B, Berger UV, Gunshin Y, Romero MF, Boron WF, Nussberger S, Gollan JL, Hediger MA. Cloning and characterization of a mammalian proton-coupled metal-ion transporter. *Nature* 1997;388:482–488.

Gunshin H, Starr CN, Direnzo C, Fleming MD, Jin J, Greer EL, Sellers VM, Galica SM, Andrews NC. Cybrd1 (duodenal cytochrome b) is not necessary for dietary iron absorption in mice. *Blood* 2005;106:2879–2883.

Guo B, Phillips JD, Yu Y, Leibold EA. Iron regulates the intracellular degradation of iron regulatory protein 2 by the proteasome. *J Biol Chem* 1995 15;270:21645-21651.

Halliwell B. Free redicals and antioxidants: a personal view. *Nutr Rev* 1994;52:253-265.

Han O, Failla ML, Hill AD, Morris ER, Smith JC Jr. Reduction of Fe(III) is required for uptake of nonheme iron by Caco-2 cells. *J Nutr* 1995;125:1291-1299.

Harris ZL, Durley AP, Man TK, Gitlin JD. Targeted gene disruption reveals an essential role for ceruloplasmin in cellular iron efflux. *Proc Natl Acad Sci USA* 1999;96:10812–10817.

Harrison PM, Arosio P. The ferritins: molecular properties, iron storage function and cellular regulation. *Biochem Biophys Acta* 1996;1275:161-203.

Hayashi H, Abdollah S, Qiu Y, Cai J, Xu YY, Grinnell BW, Richardson MA, Topper JN, Gimbrone MA Jr, Wrana JL, Falb D. The MAD-related protein Smad7 associates with the TGFbeta receptor and functions as an antagonist of TGFbeta signaling. *Cell* 1997 27;89:1165-1173.

Heinrich PC, Behrmann I, Haan S, Hermanns HM, Muller-Newen G, Schaper F. Principles of interleukin (IL)-6-type cytokine signalling and its regulation. *Biochem J* 2003;374:1–20.

Hellman NE, Gitlin JD. Ceruloplasmin metabolism and function. *Ann Rev Nutr* 2002;22:439-485.

Henrion AA, Martinez A, Mattei MG, Kahn A, Raymondjean M. Structure, sequence, and chromosomal location of the gene for USF2 transcription factors in mouse. *Genomics* 1995;25:36-43.

Henrion AA, Vaulont S, Raymondjean M, Kahn A. Mouse USF1 gene cloning: comparative organization within the c-myc gene family. *Mamm Genome* 1996;7:803-809.

Hentze MW, Caughman SW, Casey JL, Koeller DM, Rouault TA, Harford JB, Klausner RD. A model for the structure and functions of iron-responsive elements. *Gene* 1988;72:201–208.

Higa Y, Oshiro S, Kino K, Tsunoo H, Nakajima H. Catabolism of globin-haptoglobin in liver cells after intravenous administration of hemoglobin-haptoglobin to rats. *J Biol Chem* 1981;256:12322-12328.

Holmström P, Dzikaite V, Hultcrantz R, Melefors O, Eckes K, Stål P, Kinnman N, Smedsrød B, Gafvels M, Eggertsen G. Structure and liver cell expression pattern of the HFE gene in the rat. *J Hepatol* 2003;39:308-314.

Hoshino K, Takeuchi O, Kawai T, Sanjo H, Ogawa T, Takeda Y, Takeda K, Akira S. Cutting edge: Toll-like receptor 4 (TLR4)-deficient mice are hyporesponsive to lipopolysaccharide: evidence for TLR4 as the Lps gene product. *J Immunol* 1999;162:3749-3752.

Huang FW, Pinkus JL, Pinkus GS, Fleming MD, Andrews NC. A mouse model of juvenile hemochromatosis. *J Clin Invest* 2005;115:2187–2191.

Huang TS, Melefors O, Lind MI, Soderhall K. An atypical iron-responsive element (IRE) within crayfish ferritin mRNA and an iron regulatory protein 1 (IRP1)-like protein from crayfish hepatopancreas. *Insect Biochem Mol Biol* 1999;29:1-9.

Hubert N, Hentze MW. Previously uncharacterized isoforms of divalent metal transporter (DMT)-1: implications for regulation and cellular function. *Proc Natl Acad Sci USA* 2002;99:12345–12350.

Hunter HN, Fulton DB, Ganz T, Vogel HJ. The solution structure of human hepcidin, a peptide hormone with antimicrobial activity that is involved in iron uptake and hereditary hemochromatosis. *J Biol Chem* 2002;277:37597–37603.

Hvidberg V, Maniecki MB, Jacobsen C, Hojrup P, Moller HJ, Moestrup SK. Identification of the receptor scavenging hemopexin-heme complexes. *Blood* 2005;106:2572-2579.

Imamura T, Takase M, Nishihara A, Oeda E, Hanai J, Kawabata M, Miyazono K. Smad6 inhibits signalling by the TGF-beta superfamily. *Nature* 1997; 389:622-626.
Imlay JA, Linn S. DNA damage and oxygen radical toxicity. *Science* 1988;240:1302-1309.

Ivan M, Kondo K, Yang H, Kim W, Valiando J, Ohh M, Salic A, Asara JM, Lane WS, Kaelin WG Jr. HIFalpha targeted for VHL-mediated destruction by proline hydroxylation: implications for O2 sensing. *Science* 2001;292:464-468.

Iynedjian PB. Identification of upstream stimulatory factor as transcriptional activator of the liver promoter of the glucokinase gene. *Biochem J* 1998;333:705–712.

Jaakkola P, Mole DR, Tian YM, Wilson MI, Gielbert J, Gaskell SJ, Kriegsheim Av, Hebestreit HF, Mukherji M, Schofield CJ, Maxwell PH, Pugh CW, Ratcliffe PJ. Targeting of HIF-alpha to the von Hippel-Lindau ubiquitylation complex by O2-regulated prolyl hydroxylation. *Science* 2001;292:468–472.

Jacolot S, Le Gac G, Scotet V, Quere I, Mura C, Ferec C. *HAMP* as a modifier gene that increases the phenotypic expression of the *HFE* pC282Y homozygous genotype. *Blood* 2004;103:2835–2840.

Jansen H, Verhoeven AJM, Sijbrands EJG. Hepatic lipase: a pro- or anti-atherogenic protein? *J Lipid Res* 2002;43:1352–1362.

Jing SQ, Trowbridge IS. Identification of the intermolecular disulfide bonds of the human transferring receptor and its lipid-attachment site. *EMBO J* 1987;6:327–331.

Johnson D, Bayele H, Johnston K, Tennant J, Srai SK, Sharp P. Tumour necrosis factor alpha regulates iron transport and transporter expression in human intestinal epithelial cells. *FEBS Lett* 2004;573:195-201.

Johnson G, Jacobs P, Purves LR. Iron binding proteins of iron-absorbing rat intestinal mucosa. *J Clin Invest* 1983;71:1467-1476.

Johnson MB, Enns CA. Diferric transferrin regulates transferrin receptor 2 protein stability. *Blood* 2004;104:4287–4293.

Jordan JB, Poppe L, Haniu M, Arvedson T, Syed R, Li V, Kohno H, Kim H, Schnier PD, Harvey TS, Miranda LP, Cheetham J, Sasu BJ. Hepcidin revisited, disulfide connectivity, dynamics, and structure. *J Biol Chem* 2009 4;284:24155-24167.

Jordanov J, Courtois-Verniquet F, Neuburger M, Douce R. Structural investigations by extended X-ray absorption fine structure spectroscopy of the iron center of mitochondrial aconitase in higher plant cells. *J Biol Chem* 1992;262;16775-16778.

Jurado RL. Iron, infections, and anemia of inflammation. *Clin Infect Dis* 1997;25:888 895.

Kattamis A, Papassotiriou I, Palaiologou D, Apostolakou F, Galani A, Ladis V, Sakellaropoulos N, Papanikolaou G. The effects of erythropoetic activity and iron burden on hepcidin expression in patients with thalassemia major. *Haematologica* 2006;91:809-812.

Kautz L, Meynard D, Besson-Fournier C, Darnaud V, Al Saati T, Coppin H, Roth MP. BMP/Smad signaling is not enhanced in Hfe-deficient mice despite increased Bmp6 expression. *Blood* 2009 ;114:2515-2520.

Kautz L, Meynard D, Monnier A, Darnaud V, Bouvet R, Wang RH, Deng C, Vaulont S, Mosser J, Coppin H, Roth MP. Iron regulates phosphorylation of Smad1/5/8 and gene expression of Bmp6, Smad7, Id1, and Atoh8 in the mouse liver. *Blood* 200815;112:1503-1509.

Kawabata H, Fleming RE, Gui D, Moon SY, Saitoh T, O'Kelly J, Umehara Y, Wano Y, Said JW, Koeffler HP. Expression of hepcidin is downregulated in TfR2 mutant mice manifesting a phenotype of hereditary hemochromatosis. *Blood* 2005*;*105:376–381.

Kawabata H, Germain RS, Vuong PT, Nakamaki T, Said JW, Koeffler HP. Transferrin receptor 2-alpha supports cell growth both in iron-chelated cultured cells and in vivo. *J Biol Chem* 2000;275:16618–16625.

Kawabata H, Yang R, Hirama T, Vuong PT, Kawano S, Gombart AF, Koeffler HP. Molecular cloning of transferrin receptor 2. A new member of the transferrin receptor-like family. *J Biol Chem* 1999;274:20826–20832.

Kemna E, Pickkers P, Nemeth E, van der Hoeven H, Swinkels D. Time-course analysis of hepcidin, serum iron, and plasma cytokine levels in humans injected with LPS. *Blood* 2005;106:1864-1866.

Klomp LW, Gitlin JD. Expression of the ceruloplasmin gene in the human retina and brain: implications for a pathogenic model in aceruloplasminemia. *Hum Mol Genet* 1996;5:1989–1996.

Knutson MD. Iron-sensing proteins that regulate hepcidin and enteric iron absorption. *Annu Rev Nutr* 2010 ;30:149-171.

Koschinsky ML, Funk WD, van Oost BA, MacGillivray RT. Complete cDNA sequence of human preceruloplasmin. *Proc Natl Acad Sci USA* 1986;83:5086–5090.

Krause A, Neitz S, Magert HJ, Schulz A, Forssmann WG, Schulz-Knappe P, Adermann K. LEAP-1, a novel highly disulfide-bonded human peptide, exhibits antimicrobial activity. *FEBS Lett* 2000;480:147–150.

Krijt J, Vokurka M, Chang KT, Necas E. Expression of Rgmc, the murine ortholog of hemojuvelin gene, is modulated by development and inflammation, but not by iron status or erythropoietin. *Blood* 2004 15;104:4308-4310.

Kristiansen M, Graversen JH, Jacobsen C, Sonne O, Hoffman HJ, Law SK, Moestrup SK. Identification of the haemoglobin scavenger receptor. *Nature* 2001;409:198–201.

Kulaksiz H, Theilig F, Bachmann S, Gehrke SG, Rost D, Janetzko A, Cetin Y, Stremmel W. The iron-regulatory peptide hormone hepcidin: expression and cellular localization in the mammalian kidney. *J Endocrinol* 2005;184:361–370.

Kuninger D, Kuns-Hashimoto R, Kuzmickas R, Rotwein P. Complex biosynthesis of the muscle-enriched iron regulator RGMc. *J Cell Sci* 2006;15:3273-83.

Laftah AH, Ramesh B, Simpson RJ, Solanky N, Bahram S, Schumann K, Debnam ES, Srai SK. Effect of hepcidin on intestinal iron absorption in mice. *Blood* 2004;103:3940-3944.

Lago F, Dieguez C, Gomez-Reino J, Gualillo O. The emerging role of adipokines as mediators of inflammation and immune responses. Cytokine Growth Factors Rev 2007;18:313-325.

Lanzara C, Roetto A, Daraio F, Rivard S, Ficarella R, Simard H, Cox TM, Cazzola M, Piperno A, Gimenez-Roqueplo AP, Grammatico P, Volinia S, Gasparini P,

Camaschella C. Spectrum of hemojuvelin gene mutations in 1q-linked juvenile hemochromatosis. *Blood* 2004;103:4317-4321.

Latunde-Dada GO, Vulpe CD, Anderson GJ, Simpson RJ, McKie AT. Tissue-specific changes in iron metabolism genes in mice following phenylhydrazine-induced haemolysis. *Biochim Biophys Acta* 2004 14;1690:169-176.

Le Gac G, Mons F, Jacolot S, Scotet V, Ferec C, Frebourg T. Early onset hereditary hemochromatosis resulting from a novel *TFR2* gene nonsense mutation (R105X) in two siblings of north French descent. *Br J Haematol* 2004*;*125:674–678.

Lebron JA, Bennett MJ, Vaughn DE, Chirino AJ, Snow PM, Mintier GA, Feder JN, Bjorkman PJ.Crystal Structure of the hemochromatosis protein HFE and characterization of its interaction with transferrin receptor. *Cell* 1998;93:111-123.

Lebron JA, West AP Jr, Bjorkman PJ. The hemochromatosis protein HFE competes with transferrin for binding to the transferrin receptor. *J Mol Biol* 1999;294:239–245.

Lee GR. The anemia of chronic disease. *Semin Hematol* 1983;20:61-80.

Lee P, Peng H, Gelbart T,Wang L, Beutler E. Regulation of hepcidin transcription by interleukin-1 and interleukin-6. *Proc Natl Acad Sci U S A.* 2005;102:1906-1910.

Lee P. Role of matriptase-2 (TMPRSS6) in iron metabolism. *Acta Haematol* 2009;122:87-96.

Lee PL, Gelbart T,West C, Halloran C, Beutler E. Seeking candidate mutations that affect iron homeostasis. *Blood Cells Mol Dis* 2002*;*29:471–487.

Lee PL, Peng H, Gelbart T, Beutler E. The IL-6- and lipopolysaccharide-induced transcription of hepcidin in *HFE*, transferrin receptor-2, and β2 microglobulin deficient hepatocytes. *Proc Natl Acad Sci USA 2004;*101:9263–9265.

Lesbordes-Brion JC, Viatte L, Bennoun M, Lou DQ, Ramey G, Houbron C, Hamard G, Khan A, Vaulont. Targeted disruption of the hepcidin1 gene results in severe hemochromatosis. *Blood* 2006 15;108:1402–1405.

Levi S, Luzzago A, Cesareni G, Cozzi A, Franceschinelli F, Albertini A, Arosio P. Mechanism of ferritin iron uptake: activity of the H-chain and deletion mapping of the ferro-oxidase site. A study of iron uptake and ferro-oxidase activity of human liver, recombinant H-chain ferritins, and of two H-chain deletion mutants. *J Biol Chem* 1988;263:18086:18092.

Levi S, Yewdall SJ, Harrison PM, Santamrogio P, Cozzi A, Rovida E, Albertini A, Arosio P. Evidence of H- and L-chains have co-operative roles in the iron-uptake mechanism of human ferritin. *Biochem J* 1992;288:591-596.

Levy JE, Jin O, Fujiwara Y, Kuo F, Andrews NC. Transferrin receptor is necessary for development of erythrocytes and the nervous system. *Nat Genet* 1999;21:396–399.

Li YP, Stashenko P. Characterization of tumor necrosis factor-responsive element which down-regulates the human osteocalcin gene. *Mol Cell Biol* 13; 3714-3721.

Lieu PT, Heiskala M, Peterson PA, Yang Y. The roles of iron in health and disease. *Mol Aspects Med* 2001;22:1–87.

Lin L, Goldberg YP, Ganz T. Competitive regulation of hepcidin mRNA by soluble and cell-associated hemojuvelin. *Blood* 2005;106:2884-2889.

Lin L, Nemeth E, Goodnough JB, Thapa DR, Gabayan V, Ganz T. Soluble hemojuvelin is released by proprotein convertase-mediated cleavage at a conserved polybasic RNRR site. *Blood Cells Mol Dis* 2008;40:122-131.

Lin L, Valore EV, Nemeth E, Goodnough JB, Gabayan V, Ganz T. Iron transferrin regulates hepcidin synthesis in primary hepatocyte culture through hemojuvelin and BMP2/4. *Blood* 2007 15;110:2182-2189.

Lin Q, Luo X, Sawadogo M. Archaic structure of the gene encoding transcription factor USF. *J Biol Chem* 1994;269:23894-23903.

Linder MC, Schaffer KJ, Hazegh-Azam M, Zhou CY, Tran TN, Nagel GM. Serum ferritin: does it differ from tissue ferritin? *J Gastroenterol Hepatol* 1996;11:1033-1036.

Littlewood TD, Evan GI. Transcription factors 2: helix-loop-helix. *Protein Profile* 1995;2:621-702.

Liuzzi JP, Aydemir F, Nam H, Knutson MD, Cousins RJ. Zip14 (Slc39a14) mediates non-transferrin-bound iron uptake into cells. *Proc Natl Acad Sci USA* 2006;103:13612–13617.

Loreal O, Gosriwatana I, Guyader D, Porter J, Brissot P, Hider RC. Determination of non-transferrin-bound iron in genetic hemochromatosis using new HPLC-based method. *J Hepatol* 2000;32:727-733.

Lou DQ, Nicolas G, Lesbordes JC, Viatte L, Grimber G, Szajnert M, Khan A, Vaulont S Functional differences between hepcidin-1 and -2 in transgenic mice. *Blood* 2004;103:2816–2821.

Ludwiczek S, Aigner E, Theurl I, Weiss G. Cytokine-mediated regulation of iron transport in human monocytic cells. *Blood* 2003;101:4148-4154.

Mack U, Powell LW, Halliday JW. Detection and isolation of a hepatic membrane receptor for ferritin. *J Biol Chem* 1983;258:4672-4675.

Manis J. Intestinal iron-transport defect in the mouse with sex-linked anemia. *Am J Physiol* 1971 Jan;220:135-139.

Mann S, Bannister JV, Williams RJ. Structure and composition of ferritin cores isolated from human spleen, limpet (Patella vulgata) hemolymph and bacterial (Pseudomonas aeruginosa) cells. *J Mol Biol* 1986;188:225-232.

Mastrogiannaki M, Matak P, Keith B, Simon MC, Vaulont S, Peyssonnaux C. HIF-2alpha, but not HIF-1alpha, promotes iron absorption in mice. *J Clin Invest* 2009;119:1159-1166.

Matsunaga E, Tauszig-Delamasure S, Monnier PP, Mueller BK, Strittmatter SM, Mehlen P, Chédotal A. RGM and its receptor neogenin regulate neuronal survival. *Nat Cell Biol* 2004;6:749-755.

Matthes T, Aguilar-Martinez P, Pizzi-Bosman L, Darbellay R, Rubbia-Brandt L, Giostra E, Michel M, Ganz T, Beris P. Severe hemochromatosis in a Portuguese family associated with a new mutation in the 5' UTR of the *HAMP* gene. *Blood* 2004;104:2181–2183.

McDonald MJ, Rosbash M, Emery P. Wild-type circadian rhythmicity is dependent on closely spaced E boxes in the Drosophila timeless promoter. *Mol Cell Biol* 2001;21:1207-1217.

McKie AT, Barrow D, Latunde-Dada GO, Rolfs A, Sager G, Mudaly E, Mudaly M, Richardson C, Barlow D, Bomford A, Peters TJ, Raja KB, Shirali S, Hediger MA, Farzaneh F, Simpson RJ. An iron-regulated ferric reductase associated with the absorption of dietary iron. *Science* 2001;291:1755–1759.

McKie AT, Marciani P, Rolfs A, Brennan K, Wehr K, Barrow D, Miret S, Bomford A, Peters TJ, Farzaneh F, Hediger MA, Hentze MW, Simpson RJ. A novel duodenal iron-regulated transporter, IREG1, implicated in the basolateral transfer of iron to the circulation. *Mol Cell* 2000;5:299–309.

Melis MA, Cau M, Congiu R, Sole G, Barella S, Cao A, Westerman M, Cazzola M, Galanello R: A mutation in the TMPRSS6 gene, encoding a transmembrane serine protease that suppresses hepcidin production, in familial iron deficiency anemia refractory to oral iron. *Haematologica* 2008;93:1473–1479.

Merle U, Theilig F, Fein E, Gehrke S, Kallinowski B, Riedel HD, Bachmann S, Stremmel W, Kulaksiz H. Localization of the iron-regulatory proteins hemojuvelin and transferrin receptor 2 to the basolateral membrane domain of hepatocytes. *Histochem Cell Biol* 2007;127:221–226.

Merryweather-Clarke AT, Cadet E, Bomford A, Capron D, Viprakasit V, Miller A, McHugh PJ, Chapman RW, Pointon JJ, Wimhurst VLC, Livesey KJ, Tanphaichitr V, Rochette J, Robson KJH. Digenic inheritance of mutations in *HAMP* and *HFE* results in different types of haemochromatosis. *Hum Mol. Genet* 2003;12:2241–2247.

Meynard D, Kautz L, Darnaud V, Canonne-Hergaux F, Coppin H, Roth MP. Lack of the bone morphogenetic protein BMP6 induces massive iron overload. *Nat Genet* 2009;41:478-481.

Miranda CJ, Makui H, Andrews NC, Santos MM. Contributions of β2-microglobulin-dependent molecules and lymphocytes to iron regulation: insights from HfeRag1(−/−) and β2mRag1(−/−) double knock-out mice. *Blood 2004;*103:2847–2849.

Miret S, Simpson RJ, McKie AT. Physiology and molecular biology of dietary iron absorption. *Annu Rev Nutr* 2003;23:283–301.

Miyajima H, Nishimura Y, Mizoguchi K, Sakamoto M, Shimizu T, Honda N. Familial apoceruloplasmin deficiency associated with blepharospasm and retinal degeneration. *Neurology* 1987;37:761–767.

Miyazawa K, Shinozaki M, Hara T, Furuya T, Miyazono K. Two major Smad pathways in TGF-beta superfamily signalling. *Genes Cells* 2002;7:1191–1204.

Moldawer LL, Marano MA, Wei H, Fong Y, Silen ML, Kuo G, Manogue KR, Vlassara H, Cohen H, Cerami A, Lowry SF. Cachectin/tumor necrosis factor-alpha alters red blood cell kinetics and induces anemia in vivo. *FASEB J* 1989;3:1637-1643.

Monnier PP, Sierra A, Macchi P, Deitinghoff L, Andersen JS, Mann M, Flad M, Hornberger MR, Stahl B, Bonhoeffer F, Mueller BK. RGM is a repulsive guidance molecule for retinal axons. *Nature* 2002;419:392-395.

Montosi G, Donovan A, Totaro A, Garuti C, Pignatti E, Cassanelli S, Trenor CC, Gasparini P, Andrews NC, Pietrangelo A. Autosomal-dominant hemochromatosis is associated with a mutation in the ferroportin (*SLC11A3*) gene. *J Clin Invest* 2001;108:619–623.

Moore CV, Dubach R, Minnich V, Roberts HK. Absorption of ferrous and ferric radioactive iron by human subjects and by dogs. *J Clin Invest* 1944;23:755–767.

Morgan EH, Baker E. Iron uptake and metabolism by hepatocytes. *Fed Proc* 1986;45:2810–2816.

Morgan EH, Smith GD, Peters TJ. Uptake and subcellular processing of ^{59}Fe-^{125}I-labelled transferrin by rat liver. *Biochem J* 1986;237:163–173.

Morgan EH. Effect of pH and iron content of transferrin on its binding to reticulocyte receptors. *Biochim Biophys Acta* 1983;762:498–502.

Morgan EH. Iron metabolism and transport. In Zakim D, Boyer TD, Eds. *Hepatology: A Textbook of Liver Disease*. Pp 526–554. New York: W. B. Saunders Company Ltd., 1996.

Morgan EH. Transferrin biochemistry, physiology and clinical significance. *Molec Aspects Med* 1981;4:1–123.

Morton AG, Tavill AS. The control of hepatic iron uptake: correlation with transferrin synthesis. *Br J Haematol* 1978;39:497–507.

Munoz E, Brewer M, Baler R. Circadian Transcription. Thinking outside the E-Box. *J Biol Chem* 2002 27;277:36009-36017.

Nakao A, Afrakhte M, Morén A, Nakayama T, Christian JL, Heuchel R, Itoh S, Kawabata M, Heldin NE, Heldin CH, ten Dijke P. Identification of Smad7, a TGFbeta-inducible antagonist of TGF-beta signalling. *Nature* 1997 9;389:631-635.

Nanami M, Ookawara T, Otaki Y, Ito K, Moriguchi R, Miyagawa K, Hasuike Y, Izumi M, Eguchi H, Suzuki K, Nakanishi T. Tumor necrosis factor-alpha-induced iron sequestration and oxidative stress in human endothelial cells. *Arterioscler Thromb Vasc Biol* 2005;25:2495-2501.

Neilands JB. Iron and its role in microbial physiology. In Neilands JB, Ed. *Microbial Iron Metabolism: A Comprehensive Treatise*. Pp 3–34. London: Academic Press, 1974.

Nemeth E, Ganz T. Hepcidin and iron-loading anemias. *Haematologica* 2006; 91;727-732.

Nemeth E, Ganz T. The role of hepcidin in iron metabolism. *Acta Haematol* 2009;122:78-86.

Nemeth E, Preza GC, Jung CL, Kaplan J, Waring AJ, Ganz T. The N-terminus of hepcidin is essential for its interaction with ferroportin: structure-function study. *Blood* 2006;107:328-333.

Nemeth E, Rivera S, Gabayan V, Keller C, Taudorf S, Pedersen BK, Ganz T. IL-6 mediates hypoferremia of inflammation by inducing the synthesis of the iron regulatory hormone hepcidin. *J Clin Invest* 2004a;113:1271–1276.

Nemeth E, Roetto A, Garozzo G, Ganz T, Camaschella C. Hepcidin is decreased in *TFR2* hemochromatosis. *Blood* 2005*;*105:1803–1806.

Nemeth E, Tuttle MS, Powelson J, Vaughn MB, Donovan A,Ward DM, Ganz T, Kaplan J. Hepcidin regulates cellular iron efflux by binding to ferroportin and inducing its internalization. *Science* 2004b;306:2090–2093.

Nemeth E, Valore EV, Territo M, Schiller G, Lichtenstein A, Ganz T. Hepcidin, a putative mediator of anemia of inflammation, is a type II acute-phase protein. *Blood* 2003;101:2461– 2463.

Ng MC, Miyake K, So WY, Poon EW, Lam VK, Li JK, Cox NJ, Bell GI, Chan JC.The linkage and association of the gene encoding upstream stimulatory factor 1 with type 2 diabetes and metabolic syndrome in the Chinese population. *Diabetologia* 2005;48:2018–2024.

Nicolas G, Bennoun M, Devaux I, Beaumont C, Grandchamp B, Kahn A, Vaulont S. Lack of hepcidin gene expression and severe tissue iron overload in upstream stimulatory factor 2 (USF2) knockout mice. *Proc Natl Acad Sci USA* 2001;98:8780–8785.

Nicolas G, Bennoun M, Porteu A, Mativet S, Beaumont C, Grandchamp B, Sirito M, Sawadogo M, Khan A, Vaulont S. Severe iron deficiency anemia in transgenic mice expressing liver hepcidin. *Proc Natl Acad Sci USA* 2002a*;*99:4596–45601.

Nicolas G, Chauvet C, Viatte L, Danan JL, Bigard X, Devaux I, Beaumont C, Kahn A, Vaulont S. The gene encoding the iron regulatory peptide hepcidin is regulated by anemia, hypoxia, and inflammation. *J Clin Invest* 2002b;110:1037-1044.

Nicolas G, Viatte L, Lou DQ, Bennoun M, Beaumont C, Kahn A, Andrews NC, Vaulont S. Constitutive hepcidin expression prevents iron overload in a mouse model of hemochromatosis. *Nat Genet.* 2003;34:97–101.

Nicolas G,Viatte L, Bennoun M, Beaumont C, Kahn A,Vaulont S. Hepcidin, a new iron regulatory peptide. *Blood Cells Mol Dis* 2002c;29:327–335.

Niederkofler V, Salie R, Arber S. Hemojuvelin is essential for dietary iron sensing, and its mutation leads to severe iron overload. *J Clin Invest* 2005;115:2180-2186.

Njajou OT, Vaessen N, Joosse M, Berghuis B, van Dongen JW, Breuning MH, Snijders PJ, Rutten WP, Sandkuijl LA, Oostra BA, van Duijn CM, Heutink P. A mutation in SLC11A3 is associated with autosomal dominant hemochromatosis. *Nat Genet* 2001;28:213–214.

Nowak M, Helleboid-Chapman A, Jakel H, Martin G, Duran-Sandoval D, Staels B, Rubin EM, Pennacchio LA, Taskinen MR, Fruchart-Najib J, Fruchart JC. Insulin-mediated down-regulation of apolipoprotein A5 gene expression through the phosphatidylinositol 3-kinase pathway: role of upstream stimulatory factor. *Mol Cell Biol 2005*;25:1537–1548.

Nunez MT, Alvarez X, Smith M, Tapia V, Glass J. Role of redox systems on Fe3+ uptake by transformed human intestinal epithelial (Caco-2) cells. *Am J Physiol* 1994;267:C1582-C1588.

Ohdama S,Takano S, Ohashi k, Miyake S, Aoki N. Pentoxifylline prevents tumor necrosis factor-induced suppression of endothelial cell surface thrombomodulin. *Thrombosis Res* 1991; 62: 745-755.

Ohgami RS, Campagna DR, Greer EL, Antiochos B, McDonald A, Chen J, Sharp JJ, Fujiwara Y, Barker JE, Fleming MD. Identification of a ferrireductase required for efficient transferrin-dependent iron uptake in erythroid cells. *Nat Genet* 2005;37:1264–1269.

Ohgami RS, Campagna DR, McDonald A, Fleming MD. The Steap proteins are metalloreductases. *Blood* 2006;108:1388–1394.

Origa R, Galanello R, Ganz T, Giagu N, Maccioni L, Faa G, Nemeth E. Liver iron concentrations and urinary hepcidin in beta-thalassemia. *Haematologica* 2007;92:583-588.

Osterloh K, Aisen P. Pathways in the binding and uptake of ferritin by hepatocytes. *Biochim Biophys Acta* 1989;1011:40–45.

Oudit GY, Sun H, Trivieri MG, Koch SE, Dawood F, Ackerley C, Yazdanpanah M, Wilson GJ, Schwartz A, Liu PP, Backx PH. L-type Ca2+ channels provide a major pathway for iron entry into cardiomyocytes in iron-overload cardiomyopathy. *Nat Med* 2003;9:1187–1194.

Pak M, Lopez MA, Gabayan V, Ganz T, Rivera S. Suppression of hepcidin during anemia requires erythropoietic activity. *Blood* 2006;108:3730–3735.

Papanikolaou G, Samuels ME, Ludwig EH, MacDonald ML, Franchini PL, Dube MP, Andres L, MacFarlane J, Sakellaropoulos N, Politou M, Nemeth E, Thompson J, Risler JK, Zaborowska C, Babakaiff R, Radomski CC, Pape TD, Davidas O, Christakis J, Brissot P, Lockitch G, Ganz T, Hayden MR, Goldberg YP. Mutations in HFE2 cause iron overload in chromosome 1q-linked juvenile hemochromatosis. *Nat Genet* 2004;36:77–82.

Papanikolaou G, Tzilianos M, Christakis JI, Bogdanos D, Tsimirika K, MacFarlane J, Goldberg YP, Sakellaropoulos N, Ganz T, Nemeth E. Hepcidin in iron overload disorders. *Blood* 2005;105:4103-4105.

Park CH, Valore EV, Waring AJ, Ganz T. Hepcidin, a urinary antimicrobial peptide synthesized in the liver. *J Biol Chem* 2001;276:7806–7810.

Parkes JG, Randell EW, Olivieri NF, Templeton DM. Modulation by iron loading and chelation of the uptake of non-transferrin-bound iron by human liver cells. *Biochim Biophys Acta* 1995;1243:373–380.

Parkkila S,Waheed A, Britton RS, Bacon BR, Zhou XY, Tomatsu S, Fleming RE, Sly WS. Association of the transferrin receptor in human placenta with HFE, the protein defective in hereditary hemochromatosis. *Proc Natl Acad Sci USA* 1997;94:13198–13202.

Parmley RT, Barton JC, Conrad ME, Austin RL, Holland RM. Ultrastructural cytochemistry and radioautography of haemoglobin-iron absorption. *Exp Mol Pathol* 1981;34:131-144.

Parmley RT, Barton JC, Conrad ME. Ultrastructural location of transferrin receptor and iron binding sites on human placenta and duodenal microvilli. *Br J Haematol* 1985;60: 81-89.

Paterson S, Armstrong NJ, Iacopetta BJ, McArdle HJ, Morgan EH. Intravesicular pH and iron uptake by immature erythroid cells. *J Cell Physiol* 1984;120:225–232.

Peters TJ, Raja KB, Simpson RJ, Snape S. Mechanisms and regulation of intestinal iron absorption. *Ann NY Acad Sci* 1988;526:141–147.

Peyssonnaux C, Zinkernagel AS, Schuepbach RA, Rankin E, Vaulont S, Haase VH, Nizet V, Johnson RS. Regulation of iron homeostasis by the hypoxia-inducible transcription factors (HIFs). *J Clin Invest* 2007;117:1926-1932.

Philpott CC. Molecular aspects of iron absorption: insights into the role of HFE in hemochromatosis. *Hepatology* 2002;35:993-1001.

Pietrangelo A, Rocchi E, Casalgrandi G, Rigo G, Ferrari A, Perini M, Ventura E, Cairo G. Regulation of transferrin, transferrin receptor, and ferritin genes in human duodenum. *Gastroenterology* 1992;102:802–809.

Pietrangelo A. The ferroportin disease. *Blood Cells Mol Dis* 2004;32:131-138.

Pigeon C, Ilyin G, Courselaud B, Leroyer P, Turlin B, Brissot P, Loréal O. A new mouse liver–specific gene, encoding a protein homologous to human antimicrobial peptide hepcidin, is over-expressed during iron overload. *J Biol Chem* 2001;276:7811–7819.

Piperno A, Girelli D, Nemeth E, Trombini P, Bozzini C, Poggiali E, Phung Y, Ganz T, Camaschella C. Blunted hepcidin response to oral iron challenge in HFE-related hemochromatosis. *Blood* 2007*;*110:4096–4100.

Ponka P, Beaumont C, Richardson DR. Function and regulation of transferrin and ferritin. *Semin Hematol* 1998;35:35-54.

Ponka P, Lok CN. The transferrin receptor: role in health and disease. *Int J Biochem Cell Biol* 1999;31:1111–1137.

Pootrakul P, Josephson B, Huebers HA, Finch CA. Quantitation of ferritin iron in plasma, an explanation for non-transferrin iron. *Blood* 1988;71:1120-1123.

Raffin SB,Woo CH, Roost KT, Price DC, Schmid R. Intestinal absorption of hemoglobin iron-heme cleavage by mucosal heme oxygenase. *J Clin Invest* 1974;54:1344–1352.

Raja KB, Simpson RJ, Peters TJ. Investigation of a role for reduction in ferric iron uptake by mouse duodenum. *Biochim Biophys Acta* 1992;1135:141–146.

Rajagopalan S, Deitinghoff L, Davis D, Conrad S, Skutella T, Chedotal A, Mueller BK, Strittmatter SM. Neogenin mediates the action of repulsive guidance molecule. *Nat Cell Biol* 2004;6:756-762.

Ramey G, Deschemin JC, Vaulont S. Cross-talk between the mitogen-activated protein kinase and bone morphogenetic protein/hemojuvelin pathways is required for the induction of hepcidin by holotransferrin in primary mouse hepatocytes. *Haematologica* 2009;94:765-772.

Ramey G, Faye A, Durel B, Viollet B, Vaulont S. 2007. Iron overload in Hepc1(−/−) mice is not impairing glucose homeostasis. *FEBS Lett* 2007*;*581:1053–1057.

Ramsay AJ, Reid JC, Velasco G, Quigley JP, Hooper JD. The type II transmembrane serine protease matriptase-2--identification, structural features, enzymology, expression pattern and potential roles. *Front Biosci* 2008 1;13:569-579.

Randell EW, Parkes JG, Olivieri NF, Templeton DM. Uptake of non-transferrin-bound iron by both reductive and nonreductive processes is modulated by intracellular iron. *J Biol Chem* 1994;269:16046–16053.

Rashid S, Watanabe T, Sakaue T, Lewis GF. Mechanisms of HDL lowering in insulin resistant, hypertriglyceridemic states: the combined effect of HDL triglyceride enrichment and elevated hepatic lipase activity. *Clin Biochem* 2003;36:421–429.

Richardson DR, Chua ACG, Baker E. Activation of an iron uptake mechanism from transferring in hepatocytes by small-molecular-weight iron complexes: implications for the pathogenesis of iron-overload disease. *J Lab Clin Med* 1999;133:144–151.

Richardson DR, Ponka P. The molecular mechanisms of the metabolism and transport of iron in normal and neoplastic cells. *Biochem Biophys Acta* 1997;1331:1-40.

Rideau A, Mangeat B, Matthes T, Trono D, Beris P. Molecular mechanism of hepcidin deficiency in a patient with juvenile hemochromatosis. *Haematologica* 2007;92:127–128.

Riedel HD, Remus AJ, Fitscher BA, Stremmel W. Characterization and partial purification of a ferrireductase from human duodenal microvillus membranes. *Biochem J* 1995;309:745–748.

Rivera S, Liu L, Nemeth E, Gabayan V, Sorensen OE, Ganz T. Hepcidin excess induces the sequestration of iron and exacerbates tumor-associated anemia. *Blood* 2005;105:1797–1802.

Robb A, Wessling-Resnick M. Regulation of transferrin receptor 2 protein levels by transferrin. *Blood* 2004;104:4294–4299.

Rochette J, Pointon JJ, Fisher CA, Perera G, Arambepola M, Arichchi DS, De Silva S, Vandwalle JL, Monti JP, Old JM, Merryweather-Clarke AT, Weatherall DJ, Robson KJ. Multicentric origin of hemochromatosis gene (*HFE*) mutations. *Am J Hum Genet* 1999;64:1056–1062.

Roetto A, Papanikolaou G, Politou M, Alberti F, Girelli D, Christakis J, Loukopoulos D, Camaschella C.Mutant antimicrobial peptide hepcidin is associated with severe juvenile hemochromatosis. *Nat. Genet* 2003;33:21–22.

Roetto A, Totaro A, Piperno A, Piga A, Longo F, Garozzo G, Calì A, De Gobbi M, Gasparini P, Camaschella C. New mutations inactivating transferring receptor 2 in hemochromatosis type 3. *Blood 2001;*97:2555–2560.

Rouault TA, Stout CD, Kaptain S, Harford JB, Klausner RD. Structural relationship between an iron-regulated RNA-binding protein (IRE-BP) and aconitase: functional implications. *Cell* 1991 8;64:881-883.

Roy CN, Andrews NC. Anemia of inflammation: the hepcidin link. *Curr Opin Hematol* 2005;12:107-111.

Roy CN, Custodio AO, de Graaf J, Schneider S, Akpan I, Montross LK, Sanchez M, Gaudino A, Hentze MW, Andrews NC, Muckenthaler MU. An Hfe-dependent pathway mediates hyposideremia in response to lipopolysaccharide-induced inflammation in mice. *Nat Genet* 2004;36:481-485.

Sahlstedt L, von BL, Ebeling F, Ruutu T, Parkkinen J. Effective binding of free iron by a single intravenous dose of human apotransferrin in haematological stem cell transplant patients. *Br J Haematol* 2002;119:547-553.

Salahudeen AA, Thompson JW, Ruiz JC, Ma HW, Kinch LN, Li Q, Grishin NV, Bruick RK. An E3 ligase possessing an iron-responsive hemerythrin domain is a regulator of iron homeostasis. *Science* 2009 30;326:722-726.

Sanchez M, Galy B, Muckenthaler MU, Hentze MW. Iron-regulatory proteins limit hypoxia-inducible factor-2alpha expression in iron deficiency. *Nat Struct Mol Biol* 2007;14:420-426.

Santos M, Schilham MW, Rademakers LH, Marx JJ, de Sousa M, Clevers H. Defective iron homeostasis in beta 2-microglobulin knockout mice recapitulates hereditary hemochromatosis in man. *J Exp Med* 1996;184:1975–1985.

Sawadogo M, Roeder RG. Interaction of a gene-specific transcription factor with the adenovirus major late promoter upstream of the TATA box region. *Cell* 1985;43:165-175.

Sawadogo M. Multiple forms of the human gene-specific transcription factor USF. II. DNA binding properties and transcriptional activity of the purified HeLa USF. *J Biol Chem* 1988;263:11994-2001.

Schalinske KL, Anderson SA, Tuazon PT, Chen OS, Kennedy MC, Eisenstein RS. The iron-sulfur cluster of iron regulatory protein 1 modulates the accessibility of RNA binding and phosphorylation sites. *Biochemistry* 1997 1;36:3950-3958.

Schmidt PJ, Toran PT, Giannetti AM, Bjorkman PJ, Andrews NC. The transferrin receptor modulates Hfe-dependent regulation of hepcidin expression. *Cell Metab* 2008;7:205-214.

Scholtz B, Kingsley-Kallesen M, Rizzino A. Transcription of the transforming growth factor-beta2 gene is dependent on an E-box located between an essential cAMP response element/activating transcription factor motif and the TATA box of the gene. *J Biol Chem* 1996;271:32375-32380.

Searle J, Kerr JFR, Halliday JW, Powell LW. Iron storage disease In: MacSween RNM, Anthony PP, Scheuer PJ, Burt AD, Portmann BC, Eds. *Pathology of the Liver*. 3rd ed. Pp 219-241. London: Churchill Livingstone, 1994.

Semenza GL, and Wang GL. A nuclear factor induced by hypoxia via de novo protein synthesis binds to the human erythropoietin gene enhancer at a site required for transcriptional activation. *Mol Cell Biol* 1992;12:5447–5454.

Semenza GL. Hypoxia-inducible factor 1 (HIF-1) pathway. *Sci. STKE* 2007, cm8.

Shah YM, Matsubara T, Ito S, Yim SH, Gonzalez FJ. Intestinal hypoxia-inducible transcription factors are essential for iron absorption following iron deficiency. *Cell Metab* 2009;9:152-164.

Sham RL, Phatak PD, West C, Lee PL, Andrews C, Beutler E. Autosomal dominant hereditary hemochromatosis associated with a novel ferroportin mutation and unique clinical features. *Blood Cells Mol Dis* 2005;34:157–161.

Shayeghi M, Latunde-Dada GO, Oakhill JS, Laftah AH, Takeuchi K, Halliday N, Khan Y,Warley A, McCann FE, Hider RC, Frazer DM, Anderson GJ, Vulpe CD, Simpson RJ, McKie AT. Identification of an intestinal heme transporter. *Cell* 2005;122:789–801.

Sheikh N, Dudas J, Ramadori G. Changes of gene expression of iron regulatory proteins during turpentine oil-induced acute-phase response in the rat. *Lab Invest* 2007;87:713-725.

Sheikh N, Tron K, Dudas J, Ramadori G. Cytokine-induced neutrophil chemoattractant-1 is released by the noninjured liver in a rat acute-phase model. *Lab Invest* 2006;86:800-814.

Sheth S, Brittenham GM. Genetic disorders affecting proteins of iron metabolism: clinical implications. *Annu Rev Med* 2000;51:443–464.

Siah CW, Trinder D, Olynyk JK. Iron overload. *Clin Chim Acta* 2005;358:24–36.

Sibille JC, Ciriolo M, Kondo H, Crichton RR, Aisen P. Subcellular localization of ferritin and iron taken up by rat hepatocytes. *Biochem J* 1989;262:685-688.

Silvestri L, Guillem F, Pagani A, Nai A, Oudin C, Silva M, Toutain F, Kannengiesser C, Beaumont C, Camaschella C, Grandchamp B: Molecular mechanisms of the defective hepcidin inhibition in TMPRSS6 mutations associated with iron-refractory iron deficiency anemia. *Blood* 2009;113:5605– 5608.

Silvestri L, Pagani A, Camaschella C. Furin mediated release of soluble hemojuvelin: a new link between hypoxia and iron homeostasis. *Blood* 2008a;111(2):924-931.

Silvestri L, Pagani A, Fazi C, Gerardi G, Levi S, Arosio P, Camaschella C. Defective targeting of hemojuvelin to plasma membrane is a common pathogenetic mechanism in juvenile hemochromatosis. *Blood* 2007;109:4503-4510.

Silvestri L, Pagani A, Nai A, De Domenico I, Kaplan J, Camaschella C: The serine protease matriptase-2 (TMPRSS6) inhibits hepcidin activation by cleaving membrane hemojuvelin. *Cell Metab* 2008b;8:502–511.

Sirito M, Lin Q, Maity T, Sawadogo M. Ubiquitous expression of the 43- and 44-kDa forms of transcription factor USF in mammalian cells. *Nucleic Acids Res* 1994;22:427-433.

Sirito M, Walker S, Lin Q, Kozlowski MT, Klein WH, Sawadogo M. Members of the USF family of helix-loop-helix proteins bind DNA as homo- as well as heterodimers. *Gene Expr* 1992;2:231-240.

Smih F, Rouet P, Lucas S, Mairal A, Sengenes C, Lafontan M, Vaulont S, Casado M, Langin D.Transcriptional regulation of adipocyte hormone-sensitive lipase by glucose. *Diabetes* 2002;51:293–300.

Smith A, Hunt RC. Hemopexin joins transferrin as representative members of a distinct class of receptor-mediated endocytic transport systems. *Eur J Cell Biol* 1990;53:234–245.

Smith A, Morgan WT. Haem transport to the liver by haemopexin. Receptor-mediated uptake with recycling of the protein. *Biochem J* 1979;182:47-54.

Smith A, Morgan WT. Hemopexin-mediated transport of heme into isolated rat hepatocytes. *J Biol Chem* 1981;256:10902–10909.

Smith A, Morgan WT. Transport of heme by hemopexin to the liver: evidence for receptor-mediated uptake. *Biochem Biophys Res Commun* 1978;84:151-157.

Stadtman ER, Wittenberger ME. Inactivation of Escherichia coli glutamine synthetase by xanthine oxidase, nicotinate hydroxylase, horseradish peroxidase, or glucose oxidase: effects of ferredoxin, putidaredoxin, and menadione. *Arch Biochem Biophys* 1985;239:379-387.

Stopa M, Anhuf D, Terstegen L, Gatsios P, Gressner AM, Dooley S. Participation of Smad2, Smad3, and Smad4 in transforming growth factor beta (TGF-beta)-induced activation of Smad7. The TGF-beta response element of the promoter requires functional Smad binding element and E-box sequences for transcriptional regulation. *J Biol Chem* 2000 22;275:29308-29317.

Stubbe J. Ribonucleotide reductases. *Adv Enzymol Relat Areas Mol Biol* 1990;63: 349–419.

Su MA, Trenor CC, Fleming JC, Fleming MD, Andrews NC. The G185R mutation disrupts function of the iron transporter Nramp2. *Blood* 1998;92:2157–2163.

Syed BA, Beaumont NJ, Patel A, Naylor CE, Bayele HK, Joannou CL, Rowe PS, Evans RW, Srai SK. Analysis of the human hephaestin gene and protein: comparative modelling of the N-terminus acto-domain based upon ceruloplasmin. *Protein Eng* 2002;15:205-214.

Tabuchi M, Yoshimori T, Yamaguchi K, Yoshida T, Kishi F. Human NRAMP2/DMT1, which mediates iron transport across endosomal membranes, is localised to late endosomes and lysosomes in Hep-2 cells. *J Biol Chem* 2000;275:22220-22228.

Tandy S, Williams M, Leggett A, Lopez-Jimenez M, Dedes M, Ramesh B, Srai SK, Sharp P. Nramp2 expression is associated with pH-dependent iron uptake across the apical membrane of human intestinal Caco-2 cells. *J Biol Chem* 2000;275:1023–1029.

Tanno T, Bhanu NV, Oneal PA, Goh SH, Staker P, Lee YT, Moroney JW, Reed CH, Luban NL, Wang RH, Eling TE, Childs R, Ganz T, Leitman SF, Fucharoen S, Miller JL. High levels of GDF15 in thalassemia suppress expression of the iron regulatory protein hepcidin. *Nat Med* 2007;13:1096-1101.

Tanno T, Porayette P, Sripichai O, Noh SJ, Byrnes C, Bhupatiraju A, Lee YT, Goodnough JB, Harandi O, Ganz T, Paulson RF, Miller JL. Identification of TWSG1 as a second novel erythroid regulator of hepcidin expression in murine and human cells. *Blood* 2009 2;114:181-186.

Theil EC. Ferritin: at the crossroads of iron and oxygen metabolism. *J Nutr* 2003;133:15495-15535.

Theil EC. Ferritin: structure, function, and regulation. *Adv Inorg Biochem* 1983;5:1-38.

Theil EC. The ferritin family of iron storage proteins. *Adv Enzymol Relat Areas Mol Biol* 1990;63:421-449.

Thorstensen K, Romslo I. Uptake of iron from transferrin by isolated rat hepatocytes. A redoxmediated plasma membrane process? *J Biol Chem* 1988;263:8844–8850.

Thorstensen K. Hepatocytes and reticulocytes have different mechanisms for the uptake of iron from transferrin. *J Biol Chem* 1988;263:16837–16841.

Tolosano E, Altruda F. Hemopexin: structure, function, and regulation. DNA *Cell Biol* 2002;21:297–306.

Tomatsu S, Orii KO, Fleming RE, Holden CC, Waheed A, Britton RS, Gutierrez MA, Velez-Castrillon S, Bacon BR, Sly WS. Contribution of the H63D mutation in HFE to murine hereditary hemochromatosis. *Proc Natl Acad Sci USA*. 2003;100:15788-15793.

Torrance JD, Bothwell TH. Tissue iron stores. In Cook JD Ed. Methods in hematology (Iron). Pp 90-115. New York: Churchill Livingstone, 1980.

Torti FM, Torti SV. Regulation of ferritin genes and protein. *Blood* 2002;99:3505–3516.

Trinder D, Batey RG, Morgan EH, Baker E. Effect of cellular iron concentration on iron uptake by hepatocytes. *Am J Physiol Gastrointest Liver Physiol* 1990;259:G611–G617.

Trinder D, Morgan E, Baker E. The mechanisms of iron uptake by fetal rat hepatocytes in culture. *Hepatology* 1986;6:852–858.

Trinder D, Morgan E. Inhibition of uptake of transferrin-bound iron by human hepatoma cells by nontransferrin-bound iron. *Hepatology* 1997;26:691–698.

Trinder D, Morgan E. Mechanisms of ferric citrate uptake by human hepatoma cells. *Am J Physiol Gastrointest Liver Physiol* 1998;275:G279–G286.

Trinder D, Oates PS, Thomas C, Sadleir J, Morgan EH. Localisation of divalent metal transporter 1 (DMT1) to the microvillus membrane of rat duodenal enterocytes in iron deficiency, but to hepatocytes in iron overload. *Gut* 2000;46:270–276.

Trinder D, Zak O, Aisen P. Transferrin receptor-independent uptake of differic transferrin by human hepatoma cells with antisense inhibition of receptor expression. *Hepatology* 1996;23:1512–1520.

Truksa J, Gelbart T, Peng H, Beutler E, Beutler B, Lee P. Suppression of the hepcidin-encoding gene Hamp permits iron overload in mice lacking both hemojuvelin and matriptase-2/TMPRSS6. *Br J Haematol* 2009;147:571-581.

Truksa J, Peng H, Gelbart T, Lee P, Beutler E. Bone morphogenetic proteins 2, 4, and 9 stimulate murine hepcidin 1 expression independently of Hfe, transferrin receptor 2 (Tfr2), and IL-6. *Proc Natl Acad Sci USA* 2006;103:10289–10293.

Truksa J, Peng H, Lee P, Beutler E. Different regulatory elements are required for response of hepcidin to IL-6 and bone morphogenetic proteins BMP 4 and 9. *Br J Haematol* 2007;139:138–147.

Tsunoo H, Sussman HH. Characterization of transferrin binding and specificity of the placental transferrin receptor. *Arch Biochem Biophys* 1983;225:42–54.

Tu AY, Albers JJ.Glucose regulates the transcription of human genes relevant to HDL metabolism. *Diabetes* 2001;50:1851–1856.

Unger A, Hershko C. Hepatocellular uptake of ferritin in the rat. *Br J Haematol* 1974;28:169-179.

Uppsten M, Davis J, Rubin H, Uhlin U. Crystal structure of the biologically active form of class Ib ribonucleotide reductase small subunit from Mycobacterium tuberculosis. *FEBS Lett* 2004;569:117-122.

Vallet VS, Casado M, Henrion AA, Bucchini D, Raymondjean M, Kahn A, Vaulont S. Differential roles of upstream stimulatory factors 1 and 2 in the transcriptional response of liver genes to glucose. *J Biol Chem* 1998;273:20175–20179.

Vallone D, Gondi SB, Whitmore D, Foulkes NS. E-box function in a period gene repressed by light. *Proc Natl Acad Sci USA* 2004;101:4106-4111.

van Deursen D, Jansen H, Verhoeven AJ. Glucose increases hepatic lipase expression in HepG2 liver cells through upregulation of upstream stimulatory factors 1 and 2. *Diabetologia* 2008;51:2078-2087.

Van Wyk CP, Linder-Horowitz M, Munro HN. Effect of iron loading on non-heme iron compounds in different liver cell populations. *J Biol Chem* 1971;246:1025–1031.

Varga AC, Wrana JL. The disperate role of BMP in stem cell biology. *Oncogene* 2005;24:5713-5721.

Vashisht AA, Zumbrennen KB, Huang X, Powers DN, Durazo A, Sun D, Bhaskaran N, Persson A, Uhlen M, Sangfelt O, Spruck C, Leibold EA, Wohlschlegel JA. Control of iron homeostasis by an iron-regulated ubiquitin ligase. *Science* 2009 30;326:718-21.

Velasco G, Cal S, Quesada V, Sanchez LM, Lopez-Otin C: Matriptase-2, a membranebound mosaic serine proteinase predominantly expressed in human liver and showing degrading activity against extracellular matrix proteins. *J Biol Chem* 2002;277:37637–37646.

Verga Falzacappa MV, Casanovas G, Hentze MW, Muckenthaler MU. A bone morphogenetic protein (BMP)-responsive element in the hepcidin promoter controls HFE2-mediated hepatic hepcidin expression and its response to IL-6 in cultured cells. *J Mol Med* 2008;86:531-540.

Verga Falzacappa MV, Vujic Spasic M, Kessler R, Stolte J, Hentze MW, Muckenthaler MU. STAT-3 mediates hepatic hepcidin expression and its inflammatory stimulation. *Blood* 2007;109:353-358.

Viollet B, Lefrançois-Martinez AM, Henrion A, Kahn A, Raymondjean M, Martinez A. Immunochemical characterization and transacting properties of upstream stimulatory factor isoforms. *J Biol Chem* 1996;271:1405-1415.

Vokurka M, Krijt J, Sulc K, Necas E. Hepcidin mRNA levels in mouse liver respond to inhibition of erythropoiesis. *Physiol Res* 2006*;*55:667–674.

Volke M, Gale DP, Maegdefrau U, Schley G, Klanke B, Bosserhoff AK, Maxwell PH, Eckardt KU, Warnecke C. Evidence for a lack of a direct transcriptional suppression of the iron regulatory peptide hepcidin by hypoxia-inducible factors. *PLoS One* 200918;4:e7875.

Vujic Spasic M, Kiss J, Herrmann T, Galy B, Martinache S, Stolte J, Gröne HJ, Stremmel W, Hentze MW, Muckenthaler MU. Hfe acts in hepatocytes to prevent hemochromatosis. *Cell Metab* 2008;7:173-178.

Vulpe CD, Kuo YM, Murphy TL, Cowley L, Askwith C, Libina N, Gitschier J, Anderson GJ. Hephestin, a ceruloplasmin homologue implicated in intestinal iron transport, is defective in the sla mouse. *Nat Genet* 1999;21:195–199.

Waheed A, Britton RS, Grubb JH, Sly WS, Fleming RE. HFE association with transferrin receptor 2 increases cellular uptake of transferrin-bound iron. *Arch Biochem Biophys* 2008 1;474:193-197.

Waheed A, Parkkila S, Saarnio J, Fleming RE, Zhou XY, Tomatsu S, Britton RS, Bacon BR, Sly WS. Association of HFE protein with transferrin receptor in crypt enterocytes of human duodenum. *Proc Natl Acad Sci USA* 1999;96:1579-1584.

Waheed A, Parkkila S, Zhou XY, Tomatsu S, Tsuchihashi Z, Feder JN, Schatzman RC, Britton RS, Bacon BR, Sly WS. Hereditary hemochromatosis: effects of C282Y and H63D mutations on association with beta2-microglobulin, intracellular processing, and cell surface expression of the HFE protein in COS-7 cells. *Proc Natl Acad Sci USA* 1997;94:12384–12389.

Wallace DF, Summerville L, Crampton EM, Frazer DM, Anderson GJ, Subramaniam VN. Combined deletion of Hfe and transferrin receptor 2 in mice leads to marked dysregulation of hepcidin and iron overload. *Hepatology* 2009;50:1992-2000.

Wallace DF, Summerville L, Lusby PE, Subramaniam VN. First phenotypic description of transferrin receptor 2 knockout mouse, and the role of hepcidin. *Gut* 2005;54:980–986.

Wallen KE, Hotamisligil GS. Obesity-induced inflammatory changes in adipose tissue. *J Clin Invest* 2003;112:1785-1788.

Wang D, Sul HS. Upstream stimulatory factor binding to the E-box at –65 is required for insulin regulation of the fatty acid synthase promoter. *J Biol Chem* 1997;272:26367–26374.

Wang GL, Jiang BH, Rue EA, Semenza GL. Hypoxia-inducible factor 1 is a basic-helix-loop-helix-PAS heterodimer regulated by cellular O2 tension. *Proc Natl Acad Sci USA* 1995;92:5510–5514.

Wang GL, Semenza GL. Characterization of hypoxia-inducible factor 1 and regulation of DNA binding activity by hypoxia. *J Biol Chem* 1993;268:21513–21518.

Wang RH, Li C, Xu X, Zheng Y, Xiao C, Zerfas P, Cooperman S, Eckhaus M, Rouault T, Mishra L, Deng CX. A role of SMAD4 in iron metabolism through the positive regulation of hepcidin expression. *Cell Metab* 2005;2:399-409.

Wang S, Skorczewiski J, Feng X, Mei L, Murphy-Ullrich JE. Glucose up-regulates thrombospondin 1 gene transcription and transforming growth factor-β activity through antagonism of cGMP-dependent protein kinase repression via upstream stimulatory factor 2. *J Biol Chem* 2004;279:34311–34322

Wassell J. Haptoglobin: function and polymorphism. *Clin Lab* 2000;46:547-552.

Watt R, Nishikura K, Sorrentino J, Ar-Rushdi A, Croce CM, Rovera G. The structure and nucleotide sequence of the 5' end of the human c-myc oncogene. *Proc Natl Acad Sci USA* 1983; 80: 6307-6311.

Wei Y, Miller SC, Tsuji Y, Torti SV, Torti FM. Interleukin 1 induces ferritin heavy chain in human muscle cells. *Biochem Biophys Res Commun* 1990;169:289–296.

Weigert C, Brodbeck K, Sawadogo M, Häring HU, Schleicher ED. Upstream stimulatory factor (USF) proteins induce human TGF-β1 gene activation via the glucose-response element –1013/−1002 in mesangial cells. *J Biol Chem* 2004;279:15908–15915.

Weinberg ED. Iron depletion: a defense against intracellular infection and neoplasia. *Life Sci* 1992;50:1289-1297.

Weinstein DA, Roy CN, Fleming MD, Loda MF, Wolfsdorf JI, Andrews NC. Inappropriate expression of hepcidin is associated with iron refractory anemia: implications for the anemia of chronic disease. *Blood* 2002;100:3776–3781.

Weiss MJ, Henthorn PS, Ray K, Lamb B, Kadesch T, Harris H. Structure of the human liver/bone/kidney alkaline phosphatase gene. *J Biol Chem* 1988; 263: 12002-12010.

Wessling-Resnick, M. Biochemistry of iron uptake. *Crit Rev Biochem Mol Biol* 1999;34:285-314.

West AP, Jr., Bennett MJ, Sellers VM, Andrews NC, Enns CA, Bjorkman PJ. Comparison of the interactions of transferrin receptor and transferrin receptor 2 with transferrin and the hereditary hemochromatosis protein HFE. *J Biol Chem* 2000;275:38135–38138.

Wheby MS, Jones LG, Crosby WH. Studies on iron absorption. Intestinal regulatory mechanisms. *J Clin Invest* 1964;43:1433-1442.

Winfield ME. Electron transfer within and between haemoprotein molecules. *J Mol Biol* 1965;12:600-611.

Worwood M, Dawkins S, Wagstaff M, Jacobs A. The purification and properties of ferritin from human serum. *Biochem J* 1976;157:97-103.

Wright TL, Brissot P, Ma WL, Weisiger RA. Characterization of non-transferrin-bound iron clearance by rat liver. *J Biol Chem* 1986;261:10909–10914.

Wright TL, Fitz JG,Weisiger RA. Non-transferrin-bound iron uptake by rat liver. Role of membrane potential difference. *J Biol Chem* 1988;263:1842–1847.

Wrighting DM, Andrews NC. Interleukin-6 induces hepcidin expression through STAT3. *Blood* 2006;108:3204–3209.

Wyllie Jc, Kaufman N. An electron microscope study of haem uptake by rat duodenum. *Lab Invest* 1982;47:471-476.

Xia Y, Babitt JL, Sidis Y, Chung RT, Lin HY: Hemojuvelin regulates hepcidin expression via a selective subset of BMP ligands and receptors independently of neogenin. *Blood* 2008;111:5195–5204.

Yamaji S, Sharp P, Ramesh B, Srai SK. Inhibition of iron transport across human intestinal epithelial cells by hepcidin. *Blood* 2004;104:2178-2180.

Yamashita H, Takenoshita M, Sakurai M, Bruick RK, Henzel WJ, Shillinglaw W, Arnot D, Uyeda K. A glucose-responsive transcription factor that regulates carbohydrate metabolism in the liver. *Proc Natl Acad Sci USA* 2001;98:9116-9121.

Yang F, Friedrichs WE, deGraffenried L, Herbert DC,Weaker FJ, Bowman BH, Coalson JJ. Cellular expression of ceruloplasmin in baboon and mouse lung during development and inflammation. *Am J Respir Cell Mol Biol* 1996;14:161–169.

Yang F, Liu XB, Quinones M, Melby PC, Ghio A, Haile DJ. Regulation of reticuloendothelial iron transporter MTP1 (Slc11a3) by inflammation. *J Biol Chem* 2002;277:39786–39791.

Yang F, Lum JB, McGill JR, Moore CM, Naylor SL, van Bragt PH, Baldwin WD, Bowman BH. Human transferrin: cDNA characterization and chromosomal localization. *Proc Natl Acad Sci USA* 1984;81:2752–2756.

Yang F, Naylor SL, Lum JB, Cutshaw S, McCombs JL, Naberhaus KH, McGill JR, Adrian GS, Moore CM, Barnett DR, Bowman BH. Characterization, mapping, and expression of the human ceruloplasmin gene. *Proc Natl Acad Sci USA* 1986;83:3257–3261.

Yeh KY, Yeh M, Glass J. Hepcidin regulation of ferroportin 1 expression in the liver and intestine of the rat. *Am J Physiol Gastrointest Liver Physiol* 2004;286:G385-G394.

Yoshida K, Furihata K, Takeda S, Nakamura A, Yamamoto K, Morita H, Hiyamuta S, Ikeda S, Shimizu N, Yanagisawa N. A mutation in the ceruloplasmin gene is associated with systemic hemosiderosis in humans. *Nat Genet* 1995;9:267–272.

Young SP, Fahmy M, Golding S. Ceruloplasmin, transferrin and apotransferrin facilitate iron release from human liver cells. *FEBS Lett* 1997;411:93–96.

Yu PB, Hong CC, Sachidanandan C, Babitt JL, Deng DY, Hoyng SA, Lin HY, Bloch KD, Peterson RT. Dorsomorphin inhibits BMP signals required for embryogenesis and iron metabolism. *Nat Chem Biol* 2008;4:33–41.

Zhang AS, Anderson SA, Meyers KR, Hernandez C, Eisenstein RS, Enns CA. Evidence that inhibition of hemojuvelin shedding in response to iron is mediated through neogenin. *J Biol Chem* 2007 27;282:12547-12556.

Zhang AS, West AP Jr, Wyman AE, Bjorkman PJ, Enns CA. Interaction of hemojuvelin with neogenin results in iron accumulation in human embryonic kidney 293 cells. *J Biol Chem* 2005;280:33885-33894.

Zhang AS, Xiong S, Tsukamoto H, Enns CA. Localization of iron metabolism-related mRNAs in rat liver indicate that HFE is expressed predominantly in hepatocytes. *Blood* 2004;103:1509–1514.

Zhang DL, Hughes RM, Ollivierre-Wilson H, Ghosh MC, Rouault TA. A ferroportin transcript that lacks an iron-responsive element enables duodenal and erythroid precursor cells to evade translational repression. *Cell Metab* 2009;9:461-473.

Zhang Y, Pronenca R, Maffei M, Barone M, Leopold L, Friedman JM. Positional cloning of the mouse obese gene and its human homologue. *Nature* 1994;372;425-432.

Zimmer M, Ebert BL, Neil C, Brenner K, Papaioannou I, Melas A, Tolliday N, Lamb J, Pantopoulos K, Golub T, Iliopoulos O. Small-molecule inhibitors of HIF-2a translation link its 5'UTR iron-responsive element to oxygen sensing. *Mol Cell* 2008 26;32:838-848.

Zoller H, Koch RO, Theurl I, Obrist P, Pietrangelo A, Montosi G, Haile DJ, Vogel W, Weiss G. Expression of the duodenal iron transporters divalent-metal transporter 1 and ferroportin 1 in iron deficiency and iron overload. *Gastroenterology* 2001;120:1412–1419.

Zoller H, Pietrangelo A, Vogel W, Weiss G. Duodenal metal-transporter (DMT-1, NRAMP-2) expression in patients with hereditary haemochromatosis. *Lancet* 1999;353:2120–2123.